Chuan-Feng Chen · Yun Shen

Helicene Chemistry

From Synthesis to Applications

Springer

Helicene Chemistry

Chuan-Feng Chen · Yun Shen

Helicene Chemistry

From Synthesis to Applications

Springer

Chuan-Feng Chen
Beijing National Laboratory for Molecular
    Sciences, CAS Key Laboratory
    of Molecular Recognition and Function,
    Institute of Chemistry
Chinese Academy of Sciences
Beijing
China

Yun Shen
Beijing National Laboratory for Molecular
    Sciences, CAS Key Laboratory
    of Molecular Recognition and Function,
    Institute of Chemistry
Chinese Academy of Sciences
Beijing
China

Preface

Compared with other chiral molecules, helicenes, comprised of *ortho*-fused aromatics, bear helicity and π-conjugated structures. Because of the highly contorted π-surfaces with superior chiroptical properties, synthetic challenges for the diversity of the skeletons, interesting interaction behaviors between themselves or with other (chiral) molecules, the helicene chemistry has been attracting more and more attention. Since the first report in 1903, it has been developed for more than 110 years. In 1950s, the helical structure was unambiguously demonstrated by X-ray crystallographic analysis. Moreover, the optical resolution was achieved and the relationship between the absolute configuration and chiroptical property was established. Some practical synthetic methods have been discovered, especially in the last three decades, such as metal-mediated [2+2+2] triynes cycloisomerization, Diels–Alder addition, and oxidative photocyclization. Some reactions render the preparation in gram scale, and some reactions could afford helicenes even in >99 % ee. Due to the advances in preparation, different applications have been discovered, including environmental-stimulus responsive molecular switches, asymmetric catalysis, molecular recognition, and organic electronic devices. Previously, we composed a review, *Helicenes: Synthesis and Applications*, in which the structures and properties were briefly introduced, nearly all the synthetic methods and applications developed before 2012 were summarized. However, since then, more than 350 peer-reviewed journal papers have been published, but there are only a few mini-reviews on specific topics among them. This motivated us to prepare this book *Helicene Chemistry: From Synthesis to Applications* to describe the recent progress. Moreover, we hope this book could be a primer for beginners who plan to enter this research area and also a useful manual for researchers and graduate students working in this area.

This book is composed of three parts. In Part I, we would like to make an introduction to helicenes. In Chap. 1, the nomenclature and the historical development are introduced. In Chap. 2, the structural features are presented in detail with crystal structures. The properties are classified by π-conjugated system and the helicity. The photophysical and electronic behaviors, chiroptical characteristics and

racemization process are discussed in different sections. In addition, other properties and helicenes with charges or open shells are listed at last. In Part II, the practical synthetic methods are summarized. For the nonselective methods, the widely accepted ones, such as oxidative photocyclization (Chap. 3), Diels–Alder addition and Friedel–Crafts-type reactions (Chap. 4), metal-mediated reactions (Chap. 5), and other methods (Chap. 6) are examined with advantages and disadvantages. The recent development of asymmetric synthesis is reviewed in Chap. 7 in three categories: (1) enantioselective approaches, (2) diastereoselective methods, and (3) strategies based on enantioenriched substrates. The reactivity of helicene skeletons, the direct C–H functionalization, the useful transformation of functional groups, and the helicene-based organometallics are discussed in Chap. 8. In Part III, selected hot research topics in the past 4 years are presented. In Chap. 9, the helicene-based organocatalysts and helical ligands used in the asymmetric catalysis are introduced. The chiral recognition, helicene-based sensors, and responsive switches are summarized in Chap. 10. And the applications of helicenes in biological realm are presented in Chap. 11. The circularly polarized luminescence and the organic electronic devices are discussed in Chap. 12. At last, the assembly behaviors of helicenes at interfaces and in organogels, LB films, and liquid crystals are reviewed. We sincerely hope the results selected and presented here will attract more chemists' attention and advance the development of helicene chemistry.

Finally, we would like to thank June Tang, from Springer for her kind invitation and help during the preparation of the book. We also thank Han-Xiao Wang and Wei-Bin Lin from our research group for literature analysis.

Beijing, China   Chuan-Feng Chen
                                                                                                        Yun Shen

Contents

Abbreviations

A	Adenine
Ac	Acetyl
acac	Acetylacetonyl
AFM	Atomic force microscopy
AIBN	2,2′-azobis(2-methylpropionitrile)
BCP	2,9-dimethyl-4,7-diphenyl-1,10-phenanhroline
BINAP	2,2′-bis(diphenylphosphino)-1,1′-binaphthyl
BINAPO	[1,1′-binaphthalene]-2,2′-diylbis(diphenylphosphine oxide)
BINOL	1,1′-bi-2-naphthol
B_{max}	The maximum brightness
BP	Benzophenone
Bphen	Bathophenanthroline
CAN	Ceric ammonium nitrate
CBP	4,4′-N,N′-dicarbazolebiphenyl
CD	Cyclodextrin (only for alpha-CD, beta-CD, gamma-CD)
CD	Circular dichroism
CE	Cotton effect
CIE	Commission Internationale de l′Eclairage
CLSM	Confocal laser scanning microscopy
cod	1,5-cyclooctadiene
Cp	Cyclopentadienyl
CP	Circularly polarized
CPL	Circularly polarized luminescence
Cy	Cyclohexyl
dba	Dibenzylideneacetone
DBU	1,5-diazabicyclo[5,4,0]-5-undecene
DCE	1,2-dichloroethane
DCM	Dichrolomethane
DDQ	2,3-dichloro-5,6-dicyano-1,4-benzoquinone
DFT	Density functional theory

DIPA	Diisopropylamine
DMA	*N,N*-dimethylacetamide
DMAP	*N,N*-4-dimethylaminopyridine
DME	1,2-dimethoxyethane
DMF	*N,N*-dimethylformamide
dmso	Dimethyl sulfoxide
DNA	Deoxyribonucleic acid
DNT	1-methyl-2,4-dinitrobenzene
dppb	1,4-bis(diphenylphosphino)butane
dppf	1,1-bis(diphenylphosphino)ferrocene
dppm	1,1-bis(diphenylphosphino)methane
dppp	1,3-bis(diphenylphosphino)propane
ee	Enantiomeric excess
EL	Electroluminescence
ENDOR	Electron nuclear double resonance
EPR	Electron paramagnetic resonance
ESR	Electron spin resonance
F8BT	Poly[9,9-dioctylfluorene-co-benzothiadiazole]
FVP	Flash vacuum pyrolysis
G	Guanine
g_{lum}	Dissymmetric factor
HAT-CN	Dipyrazino[2,3-*f*:2′,3′-*h*]quinoxaline-2,3,6,7,10,11-hexacarbonitrile
HELIXOL	2,2′-dihydroxyhelicene
HELOL	2,2′-bihelicenyl-1,1′-diol
HOMO	Highest occupied molecular orbital
HPLC	High performance liquid chromatography
I_D	Drain current
ITO	Indium-tin oxide
LAH	Lithium aluminum hydride
LB	Langmuir–Blodgett
LDA	Lithium diisopropylamide
LLC	Lyotropic liquid crystalline
LUMO	Lowest unoccupied molecular orbital
m-CPBA	Meta-chloroperbenzoic acid
MOM	Methoxymethyl
MS	Molecular sieve
MW	Microwave
N/D	Not determined
NA	Not available
NBS	*N*-bromosuccinimide
NEXAFS	Near edge X-ray absorption fine structure
Nf	Nonafluorobutanesulfonyl
NIR	Near infrared
NIS	*N*-iodosuccinimide
NMP	*N*-methyl-2-pyrrolidinone

NMR	Nuclear magnetic resonance
NP	Nanoparticle
NPB	4,4′-bis(1-naphthyl-*N*-phenylamino)-biphenyl
NR	No reaction
NT	1-methyl-4-nitrobenzene
OFET	Organic field-effect transistor
OLED	Organic light-emitting diode
OPV	Organic photovoltaic
OR	Optical rotation
PA	Picric acid
PAH	Polycyclic aromatic hydrocarbon
p-BQ	*p*-benzoquinone
PEDOT	Poly(3,4-ethylene dioxylthiophene)
PLED	Polymer light-emitting diode
PMMA	Polymethylmethacrylate
PPA	Polyphosphoric acid
PSS	Photostationary state (Chapter 10)
PSS	Poly(styrenesulfonate) (Chapter 12)
p-Tol	*p*-tolyl
Py	Pyridyl
rt	Room temperature
SOMO	Singly occupied molecular orbital
STM	Scanning tunneling microscope
T	Thymine
TAPA	2-(2,4,5,7-tetranitro-9-fluorenylideneaminooxy)propionic acid
TBAF	Tetra-*N*-butylammonium fluoride
TBBD	*N4,N4,N4′,N4′*-tetra([1,1′-biphenyl]-4-yl)-[1,1′-biphenyl]-4, 4′-diamine
TBDMS	Tert-butyldimethylsilyl
TCTA	Tris(4-(9*H*-carbazoyl-9-yl)phenyl)amine
T_d	Decomposition temperature
TEA	Triethyl amine
Tf	Trifluoromethanesulfonyl
TFA	Trifluoroacetic acid
TFAA	Trifluoroacetic anhydride
T_g	Glass transition temperature
THF	Tetrahydrofuran
tht	Tetrahydrothiophene
TIPS	Triisopropylsilyl
T_m	Melting temperature
TMEDA	*N,N,N′,N′*-tetramethylethylenediamine
TMP	Lithium 2,2,6,6,-tetramethylpiperidide
TMS	Trimethylsilyl
TNT	2-methyl-1,3,5-trinitrobenzene
TPBi	1,3,5-tris(1-phenyl-1*H*-benzo[d]imidazol-2-yl)benzene

TS	Transition state
Ts	p-toluenesulfonyl
UV–vis	Ultraviolet–visible
VAZO	1,1′-azobis(cyclohexanecarbonitrile)
V_g	Gate voltage
$\eta_{c,max}$	The maximum current efficiency
$\eta_{p,max}$	The maximum power efficiency
μ	Carrier mobility
μ_e	Electron mobility
μ_h	Hole mobility

Part I
What Are Helicenes?

Chapter 1
Introduction to Helicene Chemistry

Abstract In this chapter, a brief introduction to helical structure and helicene is first given followed by the nomenclature. The historical development is discussed in detail, and some landmarks such as the first reported helicene, the demonstration of helical structure by X-ray analysis, the first large-scale synthesis by Diels-Alder addition, and the contributions of leading research groups at different times are highlighted. This book is aimed to become a primer for beginners who want to enter this area and also a useful manual for researchers and graduate students. Literatures from 2012 to early 2016 are covered and important discoveries before 2012 are emphasized as well. At last, helicene-related books or review articles published before 2016 are summarized. If readers are interested in a specific topic, more details could be obtained from them.

Keywords Helicene · Helicene chemistry · Historical overview · Nomenclature · Objectives and literature coverage

1.1 Introduction

Helical structures are very common in our daily life and microscopic world. For example, at macroscopic level, the beautiful Sunflower Galaxy (Messier 63) photographed by Hubble Telescope (Fig. 1.1) [1], the violent tornadoes formed by rotating air, the transitory whirlpools generated by boat paddle, the vines entwined with trees, at microscopic level, the famous DNA double helix in a cell, the foldamers in supramolecular chemistry, they all bear different types of helical forms. From an energy standpoint, the helical structures stabilize the systems to some degree.

If benzene rings are added one by one to a benzene molecule at the ortho-positions as shown in Fig. 1.2, it would be easy to predict that molecules with more than three rings would cause great steric hindrance. Therefore, the skeletons spiral up and come into helical shapes to decrease the van der Waals interaction.

Fig. 1.2 Structures of
molecules with different
numbers of benzene rings
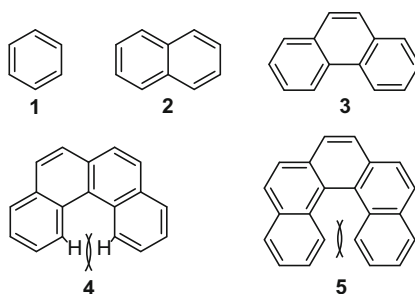
Such are helicenes [3–10], one type of polycyclic aromatic compounds with non-
planar screw-shaped structures composed by ortho-fused aromatic rings.

The nomenclature was proposed by Newman and Lednicer in 1956 [3]. For
hexahelicene (Fig. 1.3), "A systematic name is phenanthro[3, 4-c]phenanthrene.
However, a proposal to create the systematic name **helicene** for nuclei of the
continuously coiled type is at present being considered by American and
International Nomenclature committees. The prefixes, penta, hexa and hepta, etc.,
would be used for five, six and seven, etc., ring compounds."

This proposal was accepted quickly and widely used in the literatures after
1950s. Another simple method was also accepted: [*n*]helicene, where *n* means the
number of aromatics ring in the helical skeleton, and other rings fused to the
backbone should not be counted [4, 6–10]. This method would be adopted in this
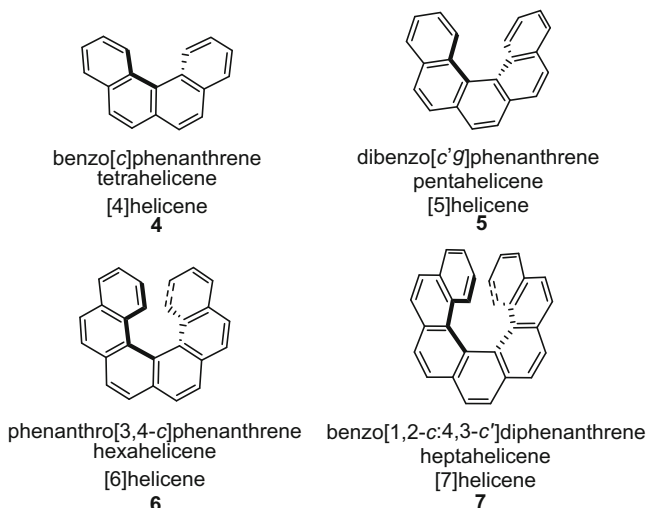
benzo[c]phenanthrene
tetrahelicene
[4]helicene
4

dibenzo[c'g]phenanthrene
pentahelicene
[5]helicene
5

phenanthro[3,4-c]phenanthrene
hexahelicene
[6]helicene
6

benzo[1,2-c:4,3-c']diphenanthrene
heptahelicene
[7]helicene
7

Fig. 1.3 Nomenclature of helicenes

book when the name of a helicene is referred to. In addition to the carbohelicenes that are formed all by benzene rings, if heteroatoms, like O, N, S, P, Si, present on the backbones (generally named heterohelicenes), they are named oxa-, aza-, thia-, phospha-, sila[n]helicenes (or silahelicenes), respectively [4–7, 11, 12].

Besides the structures mentioned above, two helicene moieties connected by a single bond are named bihelicenyls; two helicenes fused together are called double helicenes; and the helicenes where an aliphatic chain or other fragments that form a bridge to link the terminal rings are helicenophanes [4, 6, 7, 13, 14].

1.2   A Historical Overview

Although the systematical nomenclature was proposed in 1956, the first two helicenes (Fig. 1.4), 1,1-dinaphto-2,2-imin **8** and 1,1-dinaphto-2,2-*ortho*-diazin **9**, could date back to 1903, when Meisenheimer and Witte studied the reduction of 2-nitronaphthalene [15].

Before 1950s, reports on helicene were rare, where the names usually appeared as dibenzonaphthalene, tribenzonaphthalene, benzophenanthrene, dibenzophenanthrene, tribenzophenanthrene, etc. [16]. The research mainly focused on the synthetic methods. According to the key step, namely the step to construct helicene backbone, three strategies were developed, including Pschorr reaction, Friedel–Crafts acylation, and Diels–Alder addition.

Fig. 1.4 The first two
helicenes and numbering

7-aza[5]helicene
8

7,8-diaza[5]helicene
9
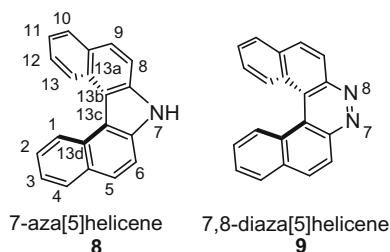
Scheme 1.1 Synthesis of [4]
helicene
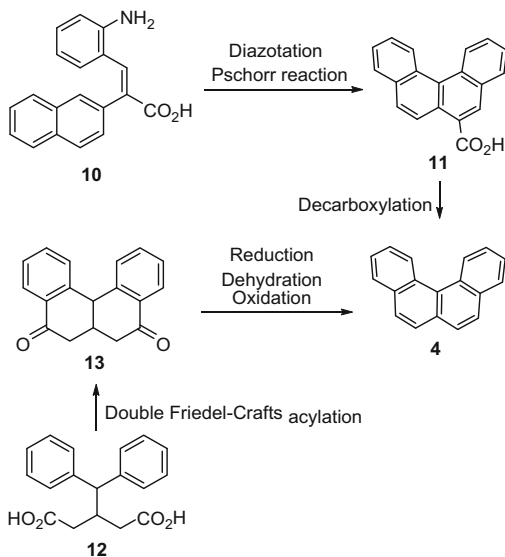
In 1912, Weitzenböck and Lieb prepared the first carbo[4]helicene from
2-naphthylacetic acid and 2-nitrobenzaldehyde [17]. By condensation and reduc-
tion, diarylethene **10** could be obtained, which was diazotized and treated with
copper powder followed by decarboxylation to give helicene **4** (Scheme 1.1).
Utilizing similar procedure, Weitzenböck and Klingler synthesized the first carbo[5]
helicene **5** in 1918 [18]. Friedel-Crafts acylation was used as well, by which
Newman and Joshel prepared [4]helicene from 3-benzhydrylglutaric acid **12**
(Scheme 1.1) [19]. In addition, by virtue of Diels-Alder reaction between
tetrahydro-1,1′-dinaphthyl **14** and maleic anhydride, Clar synthesized [5]helicene **5**
via the following route with decarboxylation, reduction, dehydration, and oxidation
(Scheme 1.2) [20]. Based on these synthetic methods, several derivatives of
helicenes had been prepared during these 50 years [21–33].

The next landmark was in 1952, McIntosh et al. for the first time demonstrated
that [5]helicene had a helical structure by X-ray crystallographic analysis, resulted
from the steric hinderance between two terminal rings which prevented the skeleton

Scheme 1.2 Synthesis of [5] helicene
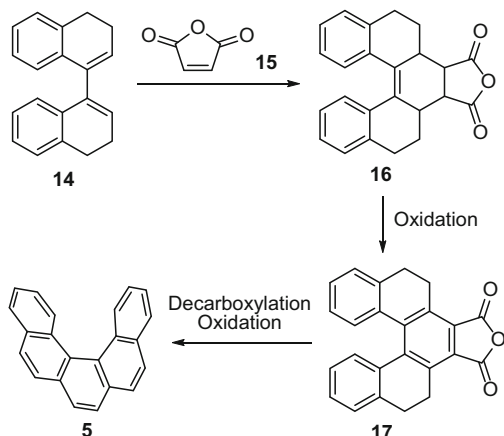
**Fig. 1.5** Two partially resolved helicene acids
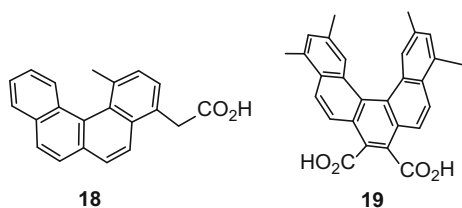
from assuming a coplanar configuration and had little effect on the benzene ring structures [34]. This screw-shaped structure rendered the molecule chiral.

Before this, Newman et al. [35] and Bell et al. [36] tested and verified the optical activity of helicene molecules in 1948 and 1949, respectively. Helicene acid **18** ($[\alpha]_D$ = +1.4 ± 0.2°, c, 1 in CHCl$_3$) [35] was partially resolved by crystallization of the diastereomers formed by the reaction with l-menthol (Fig. 1.5); enantioenriched helicene diacid **19** ($[\alpha]_D$ = −47.2°, acetone) [36] was obtained by crystallization of the morphine salts. Both two groups found that the compounds displayed no optical activity after several hours at room temperature, which were thermally unstable and underwent racemization very fast.

The successful resolution of [6]helicene became a milestone achieved by Newman and co-workers by forming charge transfer complexes in 1955 [37] and 1956 [3]. This strategy opened the door of the chiroptical properties of helicenes. At this point, people started to know helicenes.

During 1966–1967, Mallory et al. [38], Carruthers [39], Scholz et al. [40], and Martin et al. [41] independently reported the first examples of helicenes synthesized by photochemical strategy, namely the oxidative cyclization of diarylethenes (Scheme 1.3). This greatly accelerated the development of helicene chemistry. Based on this method, helicenes bearing five to fourteen benzene rings with different functional groups had been obtained, and the spectral properties including UV,

hv
cyclohexane

64%

20   **4**

hv, I₂
benzene

66%

**21**   **7**
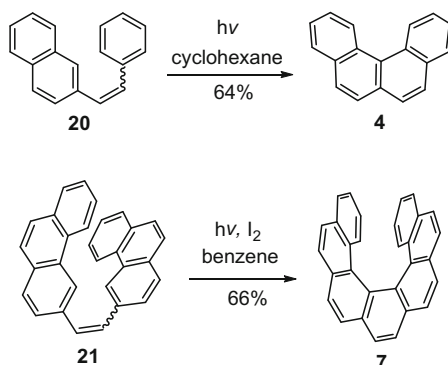
NMR, ORD, CD were systematically studied during the next two decades
[40, 42–44]. Martin group made a great contribution to the exploration of this
strategy [4]; Wynberg group expanded this method to heterohelicenes [11];
Laarhoven group carefully studied the mechanism of the photochemical procedure
[6]. Katz and co-workers improved this method by adding propylene oxide to
promote the effectiveness of the reaction, which became a standard reaction con-
dition afterwards [45].

Another breakthrough was made by Katz and collaborator in 1990, utilizing the
Diels-Alder reaction between the *p*-benzoquinone and diene to prepare the helicene
quinone in large scale (Scheme 1.4) [46]. It resolved the problem that helicenes
could not be prepared in quantity through photochemical procedures. From then on,
the applications of helicene molecules began to be disclosed.

Compared with planar acenes, helicenes are not only π-conjugated systems, but
also optically active [7, 10]. Therefore, the applications could be classified into two
categories: one is based on the π-conjugated structure, like LB films [47], liquid
crystals [48], optoelectronic material [49], functional polymers [50], and the other one
is related to the helicity, including asymmetric catalysis [51–54], chiral recognition
[55], chiroptical switches [56], nanoscience [57], and biological applications [58].

Meanwhile, the synthetic methods were greatly developed. For example, Starý
and Stará groups developed intramolecular [2+2+2] cycloisomerization of triynes to
construct helicene backbones (Scheme 1.5) [59]. When chiral ligands were used,
asymmetric synthesis could be achieved with high enantioselectivity. Tanaka group
utilized intermolecular [2+2+2] cycloaddition with chiral ligands and realized the

Scheme 1.4 Synthesis of [5]
helicene bisquinone

22   +   23   toluene, reflux, 33h   →   **24**
   17%   2.93 g
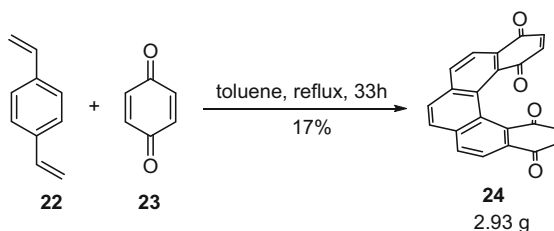
Scheme 1.5 Synthesis of [7] helicene by intramolecular [2+2+2] cycloisomerization
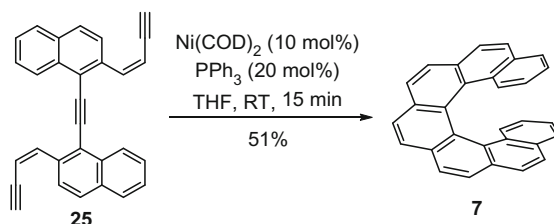

enantioselective synthesis of long helicenes (Scheme 1.6) [60, 61]. Carreño and Urbano groups utilized chiral *p*-benzoquinone to prepare helicene quinones with high stereoselectivity (Scheme 1.7) [62]. Crassous, Autschbach, Réau, and colleagues had synthesized a variety of organometallic helicenes, which displayed optimized chiroptical properties (Fig. 1.6) [63].

Helicenes, as a member of polycyclic aromatic hydrocarbons (PAHs) for more than a century have been attracting more and more attentions to their physical properties, chemical reactivity, and synthetic challenges. The records of papers about helicenes are summarized in Fig. 1.7, which was obtained from *ISI Web of Knowledge*® website using *helicene** as the search term. It is obvious that the number of publications increased rapidly, especially after 2010. Undoubtedly,
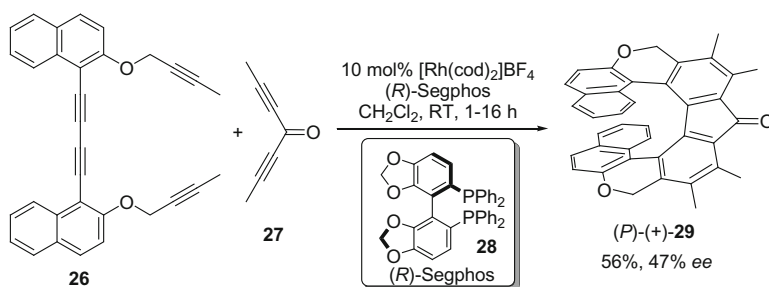
Scheme 1.6 Asymmetric synthesis of [9]helicene-like molecule
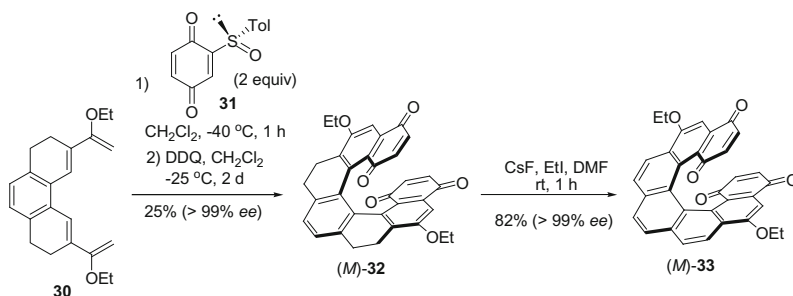
Scheme 1.7 Asymmetric synthesis of [7]helicene bisquinone
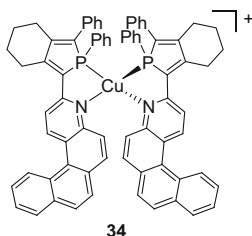
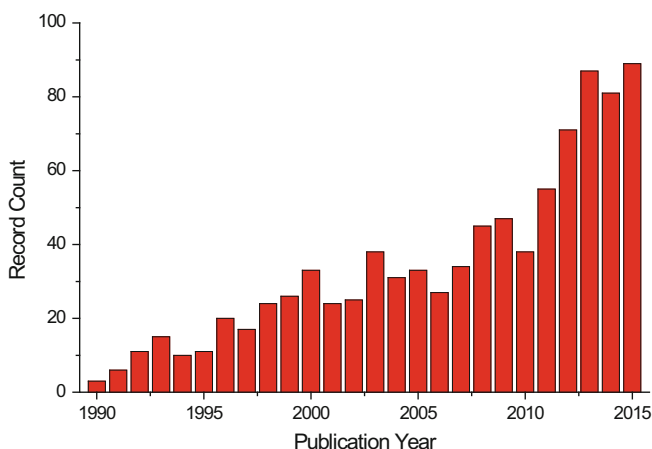**Fig. 1.6** Organometallic helicenes

Fig. 1.7 Statistics of the literature published from 1990, retrieved on Oct. 21st, 2015

enormous progress has been witnessed in the past 20 years, and this active research field will get considerable development in the near future.

1.3   Objectives and Literature Coverage

This book is prepared to be a primer for beginners who plan to enter this research area and also a useful manual for researchers and graduate students working in this area. Therefore, besides the general physical and chemical properties, we will focus on the practical synthetic methods as well, which have been widely accepted and used to prepare helicene in large scale via simple procedures. In addition, the frontiers of applications will be discussed in detail with regard to the helicity and the π-conjugated skeletons. The contents is based on the peer-reviewed journal papers from a thorough search of the literatures published between 2012 and early 2016, and important discoveries before 2012 will also be discussed here to give readers an overview of the progress of helicene chemistry.

1.4   Books and Reviews on Helicene Chemistry

So far, dozens of book chapters and reviews have been published, and they are listed in Tables 1.1 and 1.2, respectively. Readers, if interested in a specific area, could find the related books or review articles to get more information.

Table 1.1   Book chapters on helicenes

Title	Author(s)	Year	Notes	Ref.
Polycyclic Hydrocarbons (Vol. I)	Clar, E.	1964	[4]-, [5]-, [6]helicenes and their derivatives prepared before 1964 via non-photochemical strategies	[16]
Photocyclization of Stilbenes and Related Molecules	Mallory, F. B., Mallory, C. W.	1984	Helicenes prepared by photochemical methods before 1980	[64]
Fascinating Molecules in Organic Chemistry	Vögtle, F.	1992	The properties and synthesis of helicenes	[65]
Classics in Hydrocarbon Chemistry: Syntheses, Concepts, Perspectives.	Hopt, H.	2000	The synthesis of helicenes	[66]
Cyclophane Chemistry for 21st Century	Sato, K., Arai, S.	2002	The synthesis of azahelicenes	[13]
Cotrimerizations of Acetylenic Addition Reactions	Agenet, N. et al.	2006	The synthesis of helicenes and helicene-like molecules by metal-mediated [2+2+2] triyne cycloisomerization	[67]
Functional Organic Materials: Syntheses, Strategies, and Applications	Rajca, A., Miyasaka, M.	2007	A review of helicenes including the synthesis and chiroptical properties	[68]
Dynamic Stereochemistry of Chiral Compounds: Principles and Applications	Wolf, C.	2008	Stereoselective synthesis of helicenes	[69]
Strained Hydrocarbons	Starý, I., Stará, I. G.	2009	A brief review of physicochemical properties, synthesis, and the applications of helicenes	[70]
Aromatic Ring Assemblies, Polycyclic Aromatic Hydrocarbons, and Conjugated Polyenes	Starý, I., Stará, I. G.	2010	A comprehensive review of synthetic methods	[59]
Transition-Metal-Mediated Aromatic Ring Construction	Tanaka, K.	2013	The synthesis of helicenes by metal-mediated reactions, especially the [2+2+2] cycloaddition	[71]
Helical Phosphorus Derivatives: Synthesis and Applications	Virieux, D. et al.	2015	The synthesis of phosphahelicenes and applications in asymmetric catalysis	[53]
Organic Photoredox Chemistry in Flow	Gilmore, K. et al.	2015	The synthesis of helicenes by continuous flow methods	[72]

Table 1.2 Reviews on helicenes

Title	Author(s)	Journal name, year, starting page	Ref.
Some Observations on the Chemical, Photochemical, and Spectral Properties of Thiophenes	Wynberg, H.	Acc Chem Res, 1971, 65	[11]
Helicenes	Martin, R. H.	Angew Chem Int Ed Engl, 1974, 649	[4]
Chemistry of Heterochemistry	Kawazura, H., Yamada, K.	J Syn Org Chem Jpn, 1976, 111	[5]
Carbohelicenes and Heterohelicenes	Laarhoven, W. H., Prinsen, W. J. C.	Top Curr Chem, 1984, 63	[6]
Helical Molecules in Organic Chemistry	Meurer, K. P., Vögtle, F.	Top Curr Chem, 1985, 1	[73]
Synthesis and Properties of Helicenes	Oremek, G. et al.	Chem–Ztg, 1987, 69	[74]
Carbohelicenes, Heterohelicenes and Related Systems—Some Aspects of Synthesis and Reactions	Osuga, H., Suzuki, H.	J Syn Org Chem Jpn, 1994, 1020	[75]
Structure/Chiroptics Relationships of Planar Chiral and Helical Molecules	Vögtle, F. et al.	Eur J Org Chem, 1998, 1491	[76]
Syntheses of Functionalized and Aggregating Helical Conjugated Molecules	Katz, T. J.	Angew Chem Int Ed, 2000, 1921	[77]
Recent Developments in the Synthesis of Helicene-like Molecules	Urbano, A.	Angew Chem Int Ed, 2003, 3986	[78]
Unlocking the Potential of Thiaheterohelicenes: Chemical Synthesis as the Key	Collins, S. K., Vachon, M. P.	Org Biomol Chem, 2006, 2518	[79]
Photochemical Reactions as Key Steps in Organic Synthesis	Hoffmann, N.	Chem Rev, 2008, 1052	[80]
Azahelicenes and Other Similar Tri and Tetracyclic Helical Molecules	Dumitrascu, F. et al.	ARKIVOC, 2010, 1	[12]
Photochemical Oxidative Cyclisation of Stilbenes and Stilbenoids—The Mallory-Reaction	Jørgensen, K. B.	Molecules, 2010, 4334	[81]
Advances in the Synthesis of Helicenes	Dou, G.-L. Shi, D.-Q.	Chin J Org Chem, 2011, 1989	[82]
Helicenes: Synthesis and Applications	Shen, Y., Chen, C.-F.	Chem Rev, 2012, 1463	[7]
One Hundred Years of Helicene Chemistry. Part 1: Non-stereoselective Syntheses of Carbohelicenes	Gingras, M.	Chem Soc Rev, 2013, 968	[9]
One Hundred Years of Helicene Chemistry. Part 2: Stereoselective Syntheses and Chiral Separations of Carbohelicenes	Gingras, M., et al.	Chem Soc Rev, 2013, 1007	[10]
One Hundred Years of Helicene Chemistry. Part 3: Applications and Properties of Carbohelicenes	Gingras, M.	Chem Soc Rev, 2013, 1051	[8]

Table 1.2 (continued)

Title	Author(s)	Journal name, year, starting page	Ref.
Applications of Helical-Chiral Pyridines as Organocatalysts in Asymmetric Synthesis	Peng, Z., Takenaka, N.	Chem Rec, 2013, 28	[51]
Metal-Catalyzed Annulation Reactions for π-Conjugated Polycycles	Jin, T. et al.	Chem Eur J, 2014, 3554	[83]
Helicene-based Transition Metal Complexes: Synthesis, Properties and Applications	Crassous, J. et al.	Chem Sci, 2014, 3680	[84]
Cationic Triangulenes and Helicenes: Synthesis, Chemical Stability, Optical Properties and Extended Applications of These Unusual Dyes	Lacour, J. et al.	Chem Soc Rev, 2014, 2824	[85]
Helical-Chiral Small Molecules in Asymmetric Catalysis	Narcis, M. J., Takenaka, N.	Eur J Org Chem, 2014, 21	[52]
Photochemical Reactions Applied to the Synthesis of Helicenes and Helicene-like Compounds	Hoffmann, N.	J Photochem Photobio C: Photochem Rev, 2014, 1	[86]
Synthesis, Double-Helix Formation, and Higher-Assembly Formation of Chiral Polycyclic Aromatic Compounds: Conceptual Development of Polyketide Aldol Synthesis	Yamaguchi, M. et al.	Chem Rec, 2014, 15	[55]
Helicene-like Chiral Auxiliaries in Asymmetric Catalysis	Marinetti, A. et al.	Dalton Trans., 2014,15263	[54]
Enantioselective Helicene Synthesis by Rhodium-Catalyzed [2+2+2] Cycloadditions	Tanaka, K. et al.	Bull Chem Soc Jpn, 2015, 375	[61]
Circularly Polarized Luminescence from Simple Organic Molecules	de la Moya, S. et al.	Chem Eur J, 2015, 13488	[87]
Cyclophanes Containing Large Polycyclic Aromatic Hydrocarbons	Bodwell, G. J. et al.	Chem Soc Rev, 2015, 6494	[14]
Recent Advances in Stereoselective [2+2+2] Cycloadditions	Amatore, M., Aubert, C.	Eur J Org Chem, 2015, 265	[60]

References

1. Jones KG (1991) Messier's nebulae and star clusters, 2nd edn. Cambridge University Press, Cambridge
2. A galactic sunflower. http://www.spacetelescope.org/images/potw1536a/. Accessed 21 Oct 2015
3. Newman MS, Lednicer D (1956) The synthesis and resolution of hexahelicene. J Am Chem Soc 78(18):4765–4770
4. Martin RH (1974) Helicenes. Angew Chem Int Ed Engl 13(10):649–659
5. Kawazura H, K-i Yamada (1976) Chemistry of heterohelicenes. J Synth Org Chem Jpn 34 (2):111–117
6. Laarhoven WH, Prinsen WJC (1984) Carbohelicenes and heterohelicenes. Top Curr Chem 125:63–130
7. Shen Y, Chen C-F (2012) Helicenes: synthesis and applications. Chem Rev 112(3):1463–1535
8. Gingras M (2013) One hundred years of helicene chemistry. Part 3: applications and properties of carbohelicenes. Chem Soc Rev 42(3):1051–1095

9. Gingras M (2013) One hundred years of helicene chemistry. Part 1: non-stereoselective syntheses of carbohelicenes. Chem Soc Rev 42(3):968–1006

10. Gingras M, Felix G, Peresutti R (2013) One hundred years of helicene chemistry. Part 2: stereoselective syntheses and chiral separations of carbohelicenes. Chem Soc Rev 42(3):1007–1050

11. Wynberg H (1971) Some observations on chemical, photochemical, and spectral properties of thiophenes. Acc Chem Res 4(2):65–73

12. Dumitrascu F, Dumitrescu DG, Aronb I (2010) Azahelicenes and other similar tri and tetracyclic helical molecules. Arkivoc 1:1–32

13. Sato K, Arai S (2002) Cyclophane chemistry for the 21st century. Research Signpost, Kerala

14. Ghasemabadi PG, Yao T, Bodwell GJ (2015) Cyclophanes containing large polycyclic aromatic hydrocarbons. Chem Soc Rev 44(18):6494–6518

15. Meisenheimer J, Witte K (1903) Reduction von 2-nitronaphtalin. Ber Dtsch Chem Ges 36 (4):4153–4164

16. Clar E (1964) Polycyclic hydrocarbons, vol 1, 1st edn. Springer-Verlag, Berlin Heidelberg, London. doi:10.1007/978-3-662-01665-7

17. Weitzenböck R, Lieb H (1912) Eine neue synthese des chrysens. Monatshefte für Chemie und verwandte Teile anderer Wissenschaften 33(5):549–565

18. Weitzenböck R, Klingler A (1918) Synthese der isomeren Kohlenwasserstoffe 1, 2–5, 6-dibenzanthracen und 3, 4–5, 6-dibenzphenanthren. Monatshefte für Chemie und verwandte Teile anderer Wissenschaften 39(5):315–323

19. Newman MS, Joshel LM (1938) A new synthesis of 3,4-benzphenanthrene. J Am Chem Soc 60(2):485–488

20. Clar E (1932) Über die Konstitution des perylens; die Synthesen des 2.3, 10.11-Dibenz- und des 1.12-Benz-peryles und Betrachtungen über die Konstitution des Benzanthrons und Phenanthrens (Zur Kenntnis mehrkerniger aromatischer Kohlenwasserstoffe und ihrer Abkömmlinge, XIV. Mitteil.). Ber Dtsch Chem Ges (A and B Series) 65(5):846–859

21. Cook JW (1931) CCCL.-Polycyclic aromatic hydrocarbons. Part VI. 3: 4-Benzphenanthrene and its quinone. J Chem Soc (Resumed) (0):2524–2528

22. Hewett CL (1936) 133. Polycyclic aromatic hydrocarbons. Part XIV. A new synthesis of 3: 4-benzphenanthrene. J Chem Soc (Resumed) (0):596–599

23. Hewett CL (1938) 241. Polycyclic aromatic hydrocarbons. Part XVIII. A general method for the synthesis of 3: 4-benzphenanthrene derivatives. J Chem Soc (Resumed) (0):1286–1291

24. Hewett CL (1938) 34. Polycyclic aromatic hydrocarbons. Part XVI. 1: 2: 3: 4-Dibenzphenanthrene. J Chem Soc (Resumed) (0):193–196

25. Hewett CL (1940) 60. Polycyclic aromatic hydrocarbons. Part XXII. J Chem Soc (Resumed) (0):293–303

26. Szmuszkovicz J, Modest EJ (1948) Condensation of phenylcycloalkenes with maleic anhydride. I. Synthesis of 7-Methoxy-3,4-benzphenanthrene. J Am Chem Soc 70(7):2542–2543

27. Bachmann WE, Edgerton RO (1940) The synthesis of 3,4-Benzphenanthrene and 1-Methylpyrene. J Am Chem Soc 62(11):2970–2973

28. Bergmann F, Szmuszkowicz J (1947) 1,2,3,4-Dibenzphenanthrene and its derivatives. III. Synthesis of 1,2-Dimethyl-3,4-benzphenanthrene1. J Am Chem Soc 69(6):1367–1370

29. Beyer H (1938) Über polycyclische systeme, I. Mitteil.: Die Kondensation des chrysens mit bernsteinsäure-anhydrid. Ber Dtsch Chem Ges (A and B Series) 71(4):915–922

30. Weidlich HA (1938) Synthese kondensierter Ringsysteme (I. Mitteil.). Ber Dtsch Chem Ges (A and B Series) 71(6):1203–1209

31. Fuchs W, Niszel F (1927) Über die Tautomerie der Phenole, IX.: Die Naphtho-carbazol-Bildung aus Naphtholen. Ber Dtsch Chem Ges (A and B Series) 60 (1):209–217

32. Dischendorfer O (1939) Über die Kondensation von Glyoxal und β-Naphthol. Monatsh Chem/Chemical Monthly 73(1):45–56

33. Newman MS (1940) A new synthesis of coronene. J Am Chem Soc 62:1683–1687

34. McIntosh AO, Robertson JM, Vand V (1952) Crystal Structure of 3.4; 5.6 Dibenzphenanthrene. Nature 169(4295):322–323

35. Newman MS, Wheatley WB (1948) Optical Activity of the 4,5-Phenanthrene Type—4-(1-Methylbenzo[C]Phenanthryl)-Acetic Acid and 1-Methylbenzo[C]Phenanthrene. J Am Chem Soc 70(5):1913–1916

36. Bell F, Waring DH (1949) 567. The symmetrical dianthryls. Part III. J Chem Soc (Resumed) (0):2689–2693

37. Newman MS, Lutz WB, Lednicer D (1955) A new reagent for resolution by complex formation—the resolution of phenanthro-[3,4-c]phenanthrene. J Am Chem Soc 77(12):3420–3421

38. Mallory FB, Mallory CW, Halpern EJ (1966) Paper presented at the first middle atlantic regional meeting of the American Chemical Society, Philadelphia, Pa, Feb. 3

39. Carruthers W (1967) Photocyclisation of some stilbene analogues. Synthesis of dibenzo[a,l] pyrene. J Chem Soc C: Org (0):1525–1527

40. Scholz M, Mühlstädt M, Dietz F (1967) Chemie angeregter zustände. I. Mitt. Die richtung der photocyclisierung naphthalinsubstituierter äthylene. Tetrahedron Lett 8(7):665–668

41. Flammang-Barbieux M, Nasielski J, Martin RH (1967) Synthesis of heptahelicene (1) benzo [c] phenanthro [4, 3-g]phenanthrene. Tetrahedron Lett 8(8):743–744

42. Laarhove Wh, Brus GJM (1971) Polarographic data and deviations from coplanarity of helicene molecules. J Chem Soc B-Phy Org 7:1433–1434

43. Martin RH, Baes M (1975) Helicenes—photosyntheses of [11]Helicene, [12]Helicene and [14]Helicene. Tetrahedron 31(17):2135–2137

44. Moradpour A, Kagan H, Baes M, Morren G, Martin RH (1975) Photochemistry with circularly polarized light—III: Synthesis of helicenes using bis(arylvinyl) arenes as precursors. Tetrahedron 31(17):2139–2143

45. Liu LB, Yang BW, Katz TJ, Poindexter MK (1991) Improved methodology for photocyclization reactions. J Org Chem 56(12):3769–3775

46. Liu LB, Katz TJ (1990) Simple preparation of a helical quinone. Tetrahedron Lett 31 (28):3983–3986

47. Nuckolls C, Katz TJ, Verbiest T, Van Elshocht S, Kuball HG, Kiesewalter S, Lovinger AJ, Persoons A (1998) Circular dichroism and UV-visible absorption spectra of the Langmuir-Blodgett films of an aggregating helicene. J Am Chem Soc 120(34):8656–8660

48. Lovinger AJ, Nuckolls C, Katz TJ (1998) Structure and morphology of helicene fibers (vol 120, p 264, 1998). J Am Chem Soc 120(8):1944–1944

49. Yang Y, da Costa RC, Fuchter MJ, Campbell AJ (2013) Circularly polarized light detection by a chiral organic semiconductor transistor. Nat Photon 7(8):634–638

50. Dai YJ, Katz TJ, Nichols DA (1996) Synthesis of a helical conjugated ladder polymer. Angew Chem Int Ed Engl 35(18):2109–2111

51. Peng Z, Takenaka N (2013) Applications of helical-chiral pyridines as organocatalysts in asymmetric synthesis. Chem Rec 13(1):28–42

52. Narcis MJ, Takenaka N (2014) Helical-chiral small molecules in asymmetric catalysis. Eur J Org Chem 1:21–34

53. Virieux D, Sevrain N, Ayad T, Pirat J-L (2015) Chapter Two—helical phosphorus derivatives: synthesis and applications. In: Eric FVS, Christopher AR (eds) Advances in heterocyclic chemistry, vol 116. Academic Press, pp 37–83

54. Aillard P, Voituriez A, Marinetti A (2014) Helicene-like chiral auxiliaries in asymmetric catalysis. Dalton Trans 43(41):15263–15278

55. Yamaguchi M, Shigeno M, Saito N, Yamamoto K (2014) Synthesis, double-helix formation, and higher-assembly formation of chiral polycyclic aromatic compounds: conceptual development of polyketide aldol synthesis. Chem Rec 14(1):15–27

56. Wigglesworth TJ, Sud D, Norsten TB, Lekhi VS, Branda NR (2005) Chiral discrimination in photochromic helicenes. J Am Chem Soc 127(20):7272–7273

57. Fasel R, Parschau M, Ernst KH (2006) Amplification of chirality in two-dimensional enantiomorphous lattices. Nature 439(7075):449–452

58. Shinohara K, Sannohe Y, Kaieda S, Tanaka K, Osuga H, Tahara H, Xu Y, Kawase T, Bando T, Sugiyama H (2010) A Chiral Wedge Molecule Inhibits Telomerase Activity. J Am Chem Soc 132(11):3778–3782

59. Stará IG, Starý I (2010) Aromatic ring assemblies, polycyclic aromatic hydrocarbons, and conjugated polyenes, vol 45b

60. Amatore M (2015) Aubert C (2015) recent advances in stereoselective [2+2+2] cycloadditions. Eur J Org Chem 2:265–286

61. Tanaka K, Kimura Y, Murayama K (2015) Enantioselective helicene synthesis by rhodium-catalyzed [2+2+2] cycloadditions. Bull Chem Soc Jpn 88(3):375–385

62. Carreno MC, Hernandez-Sanchez R, Mahugo J, Urbano A (1999) Enantioselective approach to both enantiomers of helical bisquinones. J Org Chem 64(4):1387–1390

63. Shen WT, Graule S, Crassous J, Lescop C, Gornitzka H, Reau R (2008) Stereoselective coordination of ditopic phospholyl-azahelicenes: a novel approach towards structural diversity in chiral pi-conjugated assemblies. Chem Commun (Camb) 7:850–852

64. Mallory FB, Mallory CW (2004) Photocyclization of stilbenes and related molecules. In: Organic Reactions. John Wiley & Sons, Inc.

65. Vögtle F (1992) Fascinating molecules in organic chemistry

66. Hopf H (2000) Classics in hydrocarbon chemistry: syntheses, concepts, perspectives. Wiley-VCH, Weinheim

67. Agenet N, Buisine O, Slowinski F, Gandon V, Aubert C, Malacria M (2004) Cotrimerizations of acetylenic compounds. In: Organic reactions. John Wiley & Sons, Inc.

68. Rajca A, Miyasaka M (2007) Synthesis and characterization of novel chiral conjugated materials. In: Functional organic materials. Wiley-VCH Verlag GmbH & Co. KGaA, pp 547–581

69. Wolf C (2007) Dynamic stereochemistry of chiral compounds: principles and applications. RSC, Cambridge

70. Smith PJ, Liebman JF, Hopf H, Starý I, Stará IG, Halton B (2009) Strained aromatic molecules. In: Strained hydrocarbons. Wiley-VCH Verlag GmbH & Co. KGaA, pp 147–204

71. Tanaka K (2013) Synthesis of helically chiral aromatic compounds via [2+2+2] cycloaddition. In: Transition-metal-mediated aromatic ring construction. John Wiley & Sons, Inc., pp 281–298

72. Plutschack M, Correia C, Seeberger P, Gilmore K (2015) Organic photoredox chemistry in flow. In: Topics in organometallic chemistry. Springer Berlin Heidelberg, pp 1–34

73. Meurer KP, Vogtle F (1985) Helical molecules in organic chemistry. Top Curr Chem 127:1–76

74. Oremek G, Seiffert U, Janecka A (1987) Synthesis and properties of helicenes. Chem Ztg 111(2):69–75

75. Osuga H, Suzuki H (1994) Carbohelicenes, heterohelicenes and related systems—some aspects of synthesis and reactions. J Synth Org Chem Jpn 52(12):1020–1031

76. Grimme S, Harren J, Sobanski A, Vogtle F (1998) Structure/chiroptics relationships of planar chiral and helical molecules. Eur J Org Chem 8:1491–1509

77. Katz TJ (2000) Syntheses of functionalized and aggregating helical conjugated molecules. Angew Chem Int Ed 39(11):1921–1923

78. Urbano A (2003) Recent developments in the synthesis of helicene-like molecules. Angew Chem Int Ed 42(34):3986–3989

79. Collins SK, Vachon MP (2006) Unlocking the potential of thiaheterohelicenes: chemical synthesis as the key. Org Biomol Chem 4(13):2518–2524

80. Hoffmann N (2008) Photochemical reactions as key steps in organic synthesis. Chem Rev 108(3):1052–1103

81. Jørgensen KB (2010) Photochemical oxidative cyclisation of stilbenes and stilbenoids—the mallory-reaction. Molecules 15(6):4334–4358

82. Dou G-L, Shi D-Q (2011) Advances in the synthesis of helicenes. Chin J Org Chem 31(12):1989–1996

83. Jin T, Zhao J, Asao N, Yamamoto Y (2014) Metal-catalyzed annulation reactions for π-conjugated polycycles. Chem Eur J 20(13):3554–3576
84. Saleh N, Shen C, Crassous J (2014) Helicene-based transition metal complexes: synthesis properties and applications. Chem Sci 5(10):3680–3694
85. Bosson J, Gouin J, Lacour J (2014) Cationic triangulenes and helicenes: synthesis, chemical stability, optical properties and extended applications of these unusual dyes. Chem Soc Rev 43 (8):2824–2840
86. Hoffmann N (2014) photochemical reactions applied to the synthesis of helicenes and helicene-like compounds. J Photochem Photobio C: Photochem Rev 19:1–19
87. Sánchez-Carnerero EM, Agarrabeitia AR, Moreno F, Maroto BL, Muller G, Ortiz MJ, de la Moya S (2015) Circularly Polarized Luminescence from Simple Organic Molecules. Chem Eur J 21(39):13488–13500

Chapter 2
Structures and Properties of Helicenes

Abstract Structural features of helicenes are briefly introduced, and the crystal structures of several helicenes and heterohelicenes are then discussed. Since helicenes are a kind of polycyclic aromatic hydrocarbons with helical chirality, they exhibit specific physical properties and optical properties, especially the excellent luminescent properties. For example, some helicenes display high fluorescence quantum yields in both solution and solid states. The unique helicity of helicenes also makes them show high specific optical rotation, electronic circularly dichroism, and vibrational circular dichroism. Besides, the determination of absolute configuration of optically pure helicenes and the thermal racemization of helicenes are further discussed. Three empirical rules are proposed for the hinderance of racemization. In addition, other related properties of helicenes including the solubility, basicity of azahelicenes, elasticity of thiahelicenes are also introduced. Finally, the preparation and properties of helicenes with charges and open shells, such as radical anions, radical cations, and helicene cations are described.

Keywords Absolute configuration · Helicene radical anions · Helicene radical cations · Helicene cations · Helicity · Optical property · Racemization · Structural feature · π-system

2.1 Structural Features

Compared with other planar polyarenes, helicenes, composed by aromatic rings, are twisted to give helical structures to decrease the steric hindrance between two terminal rings [1]. Therefore, the ends spiral upward or downward, forming a pair of enantiomers. As shown in Fig. 2.1a, according to the specification [2], if a helix spirals downward anticlockwise (left handed) along the helical axis, this type of helix, the helicity or the helical chirality, could be denoted by *M*; while if a helix spirals downward clockwise (right handed), it could be denoted by *P*. The molecule [6]helicene with left handedness is shown in Fig. 2.1b. And if we add more benzene rings to the scaffold, it could be predicted that a cylindrical helix would be
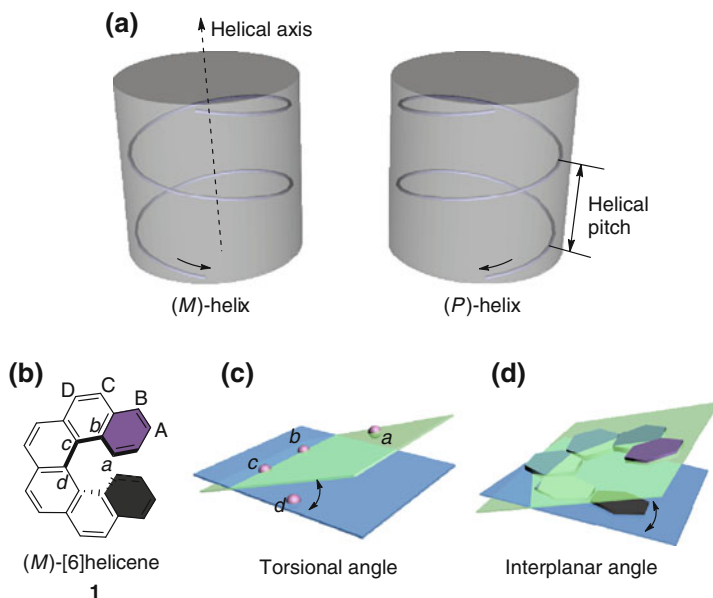
Fig. 2.1 **a** A pair of (*M*)- and (*P*)-helixes; **b** molecular structure of (*M*)-[6]helicene; and schematic representation of **c** torsional angle and **d** interplanar angle

generated like a spring. When such a helix spirals for 360°, the distance between two ends is the helical pitch, which is greatly influenced by the structure of the helicene [3]. From the point of view of atomic arrangement, helicenes have two apparent helixes: one is formed by atoms in the inner rim, like a, b, c, d, and the other is composed by outer atoms, like A, B, C, D. Both of them have constant helical pitch, but the latter is slightly larger than the former [3].

The six-membered aromatic rings, like benzene or pyridine, have larger internal angles (about 60°) than that of five-membered rings (about 45° for thiophene, 32° for furan, and 35° for pyrrole) [4], so more rings are required to cover a complete 360° rotation if five-membered rings are present. For example, carbo[6]helicene needs nearly six rings [5], whereas thia[7]helicene needs three benzene rings and four thiophenes [4].

Torsional angle (Fig. 2.1c) and interplanar angle (Fig. 2.1d) are used to describe the extent of distortion of the helical skeleton. The former is dihedral angle between the four adjacent inner carbon atoms, like a, b, c, d; the latter is the angle between the two terminal benzene rings, as shown in purple and black in Fig. 2.1b, d. Several crystal structures of helicenes are depicted in Fig. 2.2, and some important structural parameters from X-ray crystallographic analysis are summarized in Table 2.1.

The torsional angle is greatly influenced by the extent of steric hindrance of the functional groups at C(1) position of the helicene framework. For [4]helicenes, **3** has bigger torsional angles than **2**, because the methyl groups is much more bulky

Fig. 2.2 Crystal structures of
several helicenes (*gray* carbon
atoms; *red* oxygen atoms;
blue nitrogen atoms; *yellow*
silicon atoms; hydrogen
atoms were omitted for
clarity.)
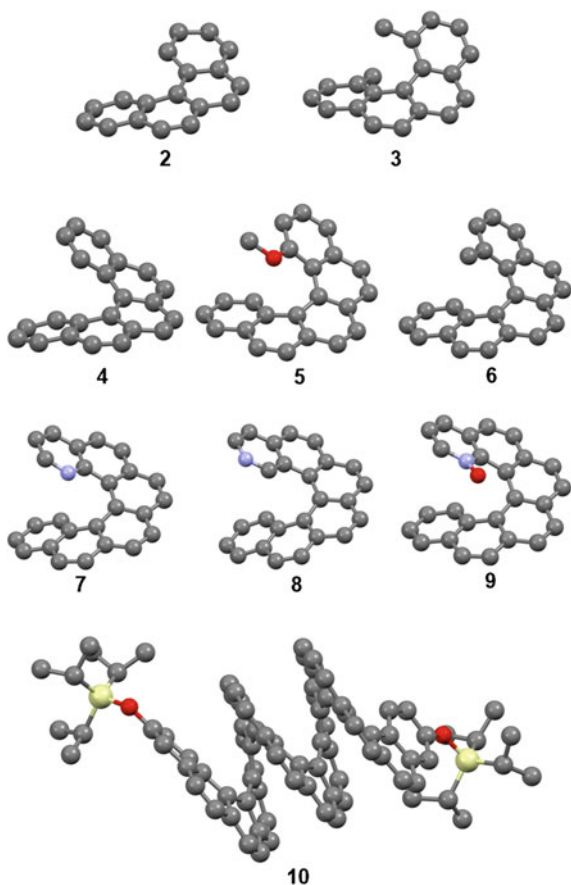
than H atoms, twisting the helical structure more and enlarging the interplanar angle
between the terminal rings; for [5]helicenes, methyl group is bigger than methoxy
group, which itself is bigger than H atom, so the total torsional angle is **6** > **5** > **4**;
for [6]helicenes, the extent of the steric hindrance is O > H > lone pair of electrons,
thus **9** has the most distorted structure as expected, and **7** has a lesser twisted one
than **8**. However, the interplanar angle is not decided by the torsional angle, but by
the mean planes where the terminal rings located, so it is difficult to predict the
trend, which is affected by the functional groups incorporated and the length of
helical skeleton [1]. Generally, it increases from the frameworks bearing four
benzene rings to that with six benzene rings and decreases as the helical structures
lengthened further [12].

By virtue of the distortion, benzene rings in the helical structures are deformed
from the planar hexagon: (1) the lengths of the bonds in the inner helix are length-
ened; (2) the lengths of that in the outer helix are shortened. For the bond lengths
between the *sp2*-hybridized carbons, C(*sp2*)–C(*sp2*) single bond is ca. 1.48 Å; C

Table 2.1 Comparison of X-ray data of **2–10**

Helicene	Space group	Bond length (Å)[a]		Torsional angle (°)	Interplanar angle (°)	Ref.
		Inner helix	Outer helix			
2	$P2_12_12_1$	1.428, 1.453, 1.439, 1.437	1.363,1.332, 1.352, 1.414	17.11, 20.13	24.87	[6]
3[b]	*Pbna*	1.439, 1.352	1.382, 1.367	30.91	47.97	[6]
4	$P2_1/c$	1.340, 1.453, 1.369, 1.433, 1.380	1.289, 1.327, 1.239, 1.294, 1.322	20.26, 26.39, 19.29 (65.94 in total)	46.03	[7]
5	$P2_1/n$	1.414, 1.453, 1.448, 1.454, 1.429	1.365, 1.348, 1.354, 1.351, 1.366	25.57, 28.06, 17.52 (71.15 in total)	43.76	[8]
6	*Pbca*	1.415, 1.450, 1.439, 1.456, 1.430	1.363, 1.349, 1.362, 1.351, 1.366	14.51, 30.44, 31.38 (76.33 in total)	51.68	[8]
7	*Pbca*	1.369[c], 1.452, 1.438, 1.444, 1.455, 1.406	1.369[c], 1.342, 1.347, 1.343, 1.342, 1.352	14.63[c], 27.01, 26.86, 14.18 (82.68 in total)	47.98	[9]
8	$P2_1/c$	1.409[c], 1.450, 1.447, 1.445, 1.449, 1.412	1.354[c], 1.336. 1.348. 1.348, 1,368, 1.353	15.68[c], 25.61, 27.12, 16.29 (84.70 in total)	52.92	[9]
9	$P2_1/c$	1.394[c], 1.449, 1.438, 1.438, 1.455, 1.405	1.358[c], 1.338, 1.330, 1.324, 1.337, 1.354	24.80[c], 24.09, 24.63, 19.63 (93.15 in total)	41.75	[10]
10	$P2_1/c$	1.423, 1.458, 1.449, 1.443, 1.448, 1.445, 1.441, 1.449, 1.436, 1.446, 1.448, 1.446, 1.452, 1.452, 1.462, 1.412	1.365, 1.333, 1.341, 1.361, 1.369, 1.357, 1.345, 1.349, 1.368, 1.363, 1.366, 1.359, 1.346, 1.355, 1.356, 1.372	14.94, 27.73, 27.43, 22.35, 27.26, 28.05, 23.34, 25.62, 27.29, 25.34, 23.93, 26.94, 26.63, 14.24	A/H: 8.30, B/I: 8.86, C/J: 3.27, D/K: 10.01, E/L: 9.81, F/M: 5.83, G/N: 7.60, H/O: 10.34, I/P: 12.01[d]	[11]

[a]Bond lengths are listed by the order of that in inner or outer helix; [b]the molecule is resolved as a symmetric structure; [c]parameters related with the heteroaromatic rings; [d]the rings in [16]helicene **10** was named in order alphabetically from A to P

$(sp2)$=C$(sp2)$ double bond is ca. 1.32 Å; while C$(sp2)$–C$(sp2)$ bond in benzene ring is 1.393 Å [13]. According to this, the C$(sp2)$–C$(sp2)$ bond length of helicene in the inner helix ($\sim$1.44 Å) is close to the value of C$(sp2)$–C$(sp2)$ single bond; while that in outer helix ($\sim$1.35 Å) is approaching the average value of C$(sp2)$=C$(sp2)$ double bond. Therefore, it will be much more reasonable if we draw the bonds in the inner helix as single bonds in the Kekulé structure of a helicene. In comparison with the rings in the helical skeleton, the two terminal ones distort least and are the most aromatic indicated by the DFT calculation [14]. Although helicenes have a C_2-symmetric axis theoretically, this is hardly found in the crystal structures. Each ring is twisted to different degrees, where the inner bond lengths and the torsional angles are different.

We would like to discuss the properties of helicenes in two sections according to two different characteristics: the π-systems and helicity.

2.2   The π-systems

As a member of polycyclic aromatic hydrocarbons (PAHs), the local aromaticity does not lose so much because the π-electrons could be delocalized via the twisted structure [15–18]. However, the extent of π-conjugation is not as good as planar PAHs. Table 2.2 lists the physical properties of some helicenes. As the number of the benzene rings increases, from [4]helicene to [16]helicene, the wavelength of the maximum absorption does not change so much, and the color of them is all yellowish or yellow. This indicates that the carbohelicenes have big HOMO–LUMO gaps (E_{gap}), which could not be reduced by fusing benzene rings to the helical skeletons. The band gaps of carbo[n]helicenes, thia[n]helicenes with alternating benzene and thiophene rings, and carbon–sulfur [n]helicenes are estimated by density functional theory (DFT) studies in gas phase: by virtue of ineffective conjugation, carbon–sulfur helicenes (4.1 eV) have the largest energy gap, while the thiahelicenes (2.5 eV) show smaller gap than that of carbohelicenes (2.9 eV) [19]. Experimental studies show that replacing one or two rings of all thiophene [7] helicene will increase the electron delocalization, and carbon–sulfur [11]helicene just has an energy gap of 3.4 eV [20, 21].

This optical property could be modified by two general strategies: (1) extending the conjugated area and (2) constructing the pull–push structures by incorporation with donor/acceptor substituents. Introducing pyrene moiety to the helicene structure could not reduce the band gap significantly [27, 28], but helicene **11** displays a Stokes shift of 296 nm resulting from the intramolecular excimer behavior upon radiation [29]. Extending the π-conjugated area of double [6]helicene, the energy gap of **12** is greatly reduced with the λ_{max} of 525 nm in the absorption spectrum [30]. Compared with former method, constructing pull–push structures is more practical, because the electron-donating or electron-withdrawing groups could be easily introduced [31–33]. Incorporation of antiaromatic core to the skeleton would also decrease the energy gap. For example, **17** with an antiaromatic *as*-indacene core even displays the gap of 1.48 eV [34] (Table 2.3).
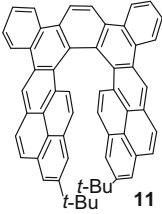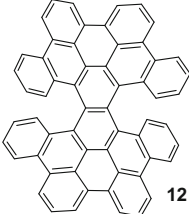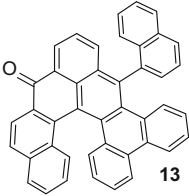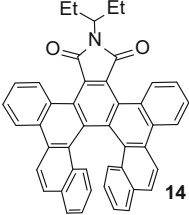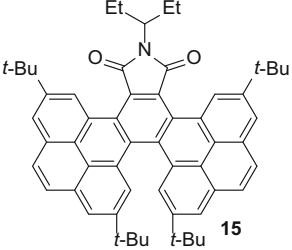
In addition, highly luminescent helicene-like molecules were reported. Tetrahydrohelicene **18** (Fig. 2.3) shows highly luminescent property with

Table 2.2 Physical properties of helicenes

[n]Helicene n	Formula	Formula weight (g/mol)	Melting point (°C, racemic)	Color	λ_{max} (nm)	Ref.
4	$C_{18}H_{12}$	228.2940	68	Off-white	372	[22]
5	$C_{22}H_{14}$	278.3540	177–189	Yellowish	395	[23]
6	$C_{26}H_{16}$	328.4140	231–233	Pale yellow	413	[24]
7	$C_{30}H_{18}$	378.4740	245–255	Yellow	*ca.* 425	[25]
8	$C_{34}H_{20}$	428.5340	330–331	Yellow	<400	[26]
9	$C_{38}H_{22}$	478.5940	359–360	Yellow	398	[11, 26]
16	$C_{66}H_{36}$	829.0140	N/D	Yellow	N/D	[11]
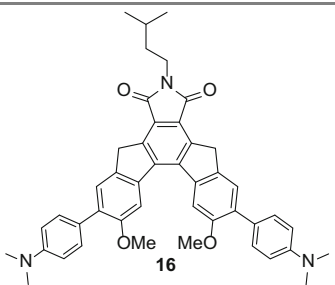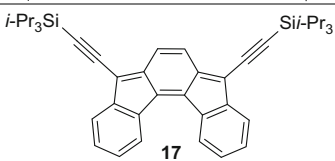
N/D Not determined

Table 2.3 Carbohelicenes with modified optical properties

Helicenes	Color	$\lambda_{\max}$ (nm)	E_{gap} (eV)[a]	Ref.
11	Yellow	396	/	[29]
12	Orange	525	/	[30]
13	Orange-red	496	/	[31]
14	Orange	470	2.38	[32]
15	Red	510	2.21	[32]

(continued)

Table 2.3 (continued)

Helicenes	Color	λ_{max} (nm)	E_{gap} (eV)[a]	Ref.
16	Red	440	2.35[b]	[33]
17	Dark green	647	1.48	[34]

[a]Calculation based on the λ_{max} of UV-vis spectra, $E_{gap} = 1240$ (eV · nm)/λ_{max} (nm); [b]calculation based on the electrochemical method (vs. Fc/Fc$^+$), $E_{gap} = E_{HOMO} - E_{LUMO}$

Fig. 2.3 Helicene-like molecules with high fluorescence quantum yields

19a R = *n*-Pr
19b R = *n*-Bu
19c R = *n*-Pen
19d R = *n*-Hex
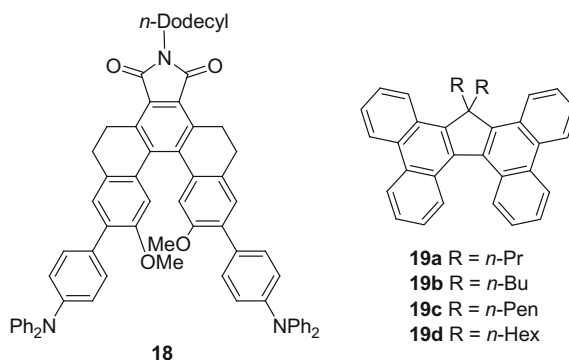
fluorescence quantum yields 85.3 % in CH$_2$Cl$_2$ solution and 61.8 % in film state [35]. Helicene-like **19a–d** show quantum yields higher than 85 % both in CH$_2$Cl$_2$ solution and film state, and **19c** has nearly 100 % quantum yield in film state [36]. The study reveals that the π–π interaction between the helical cores in aggregation is prevented by the alkyl substituent, resulting in little quenching of the solid fluorescence.

Helicenes, as good electron donors, could form charge transfer complexes with electron acceptors like other PAHs. This phenomenon was first utilized in the optical resolution of helicenes. For example, (*S*)-TAPA had stronger interaction with (*M*)-helicenes and (*R*)-TAPA preferentially interacted with (*P*)-helicenes. Therefore, the enantiomers could be separated by recrystallization [24, 37]. Also,
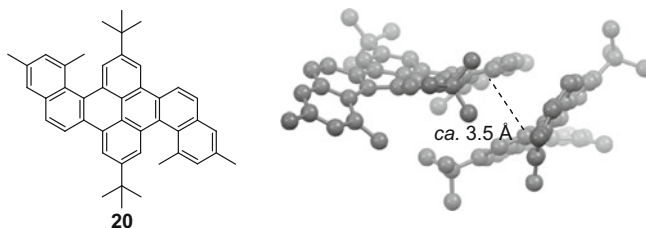
Fig. 2.4 Crystal packing of double helicene **20**
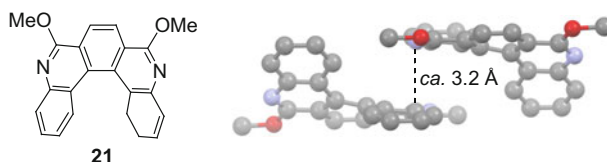
Fig. 2.5 Crystal packing of diaza[5]helicene **21**

other electron deficient molecules were used, like TCNQ [38], TAPM [39], TABA [40, 41], DNBA, TND, and NIPA [42]. Some of them were grafted to the stationary phases to achieve the optical resolution by HPLC [40, 41]. Recently, riboflavin derivatives were chemically bonded to the silica gel as stationary phase for HPLC to separate helicenes [43].

Moreover, the face-to-face π–π interactions were found between the helicene aggregates. Hu, Yamato, and co-workers prepared double [4]helicene **20** with a pyrene core in the middle. X-ray analysis showed that the racemic aggregation was composed by (*P*,*P*)- and (*M*,*M*)-enantiomers (Fig. 2.4), and each lateral dimethyl naphthalene stacking on the pyrene core of the other enantiomer with a distance about 3.5 Å [28]. In addition, Dehaen group found that the π–π interactions were enhanced in the presence of pyridine rings in the skeleton [44]. The terminal benzene ring was located upon the pyridine ring of its enantiomer and the distance between the layers was *ca.* 3.2 Å (Fig. 2.5). Nozaki group synthesized λ^5-phospha [7]helicene **22** and discovered the unusual one-way chirality (Fig. 2.6) [45]. First, the aggregation of each column was achieved by the intermolecular face-to-face π–π interactions of the helicenes bearing the same helicity with a distance of 3.35 Å; second, the columns of different helicity were alternately aligned in the crystal. This phenomenon resulted from the dipole moments of enantiomers differentiated by helicity: the column formed by (*P*)-**22** had opposite dipole moment with the one formed by (*M*)-**22**.
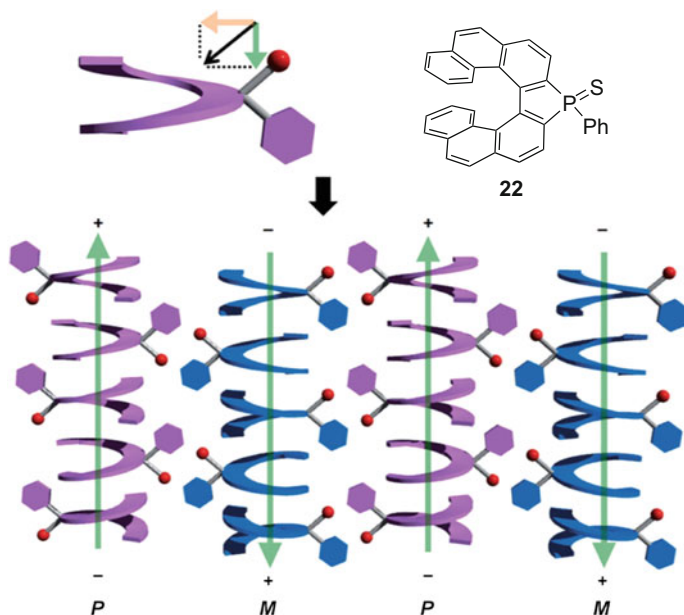
Fig. 2.6 Schematic representation of one-way chirality. Reprinted with the permission from Ref. [45]. Copyright 2012 John Wiley and Sons

2.3 The Helicity

Helicenes have very high specific optical rotation (OR) (Table 2.4), of which [13] helicene exhibits the ability near 10^4. Based on enormous studies of the absolute configuration, an empirical rule has been established: levorotatory helicenes (with negative $[\alpha]_\lambda^T$) possess M-helicity, while dextrorotatory helicenes (with positive $[\alpha]_\lambda^T$) bare P-helicity [1, 3, 4, 12, 46, 47].

Table 2.4 Specific rotation of carbohelicenes

(−)-[n]Helicene n	λ (nm)	Temperature (°C)	Solvent	c (g/100 mL)	[α] (°)	Ref.
5	578	26	Iso-octane	/	−1670	[48]
6	579	24	Chloroform	0.098	−3460 ± 10	[24]
7	579	25	Chloroform	0.06	−5900 ± 200	[49]
8	579	25	Chloroform	0.043	−6900 ± 200	[49]
9	579	25	Chloroform	0.0607	−8100 ± 200	[49]
10	579	25	/	/	−8940 ± 100	[12]
11	579	25	/	/	−9310 ± 100	[12]
13	579	25	/	/	−9620 ± 100	[12]
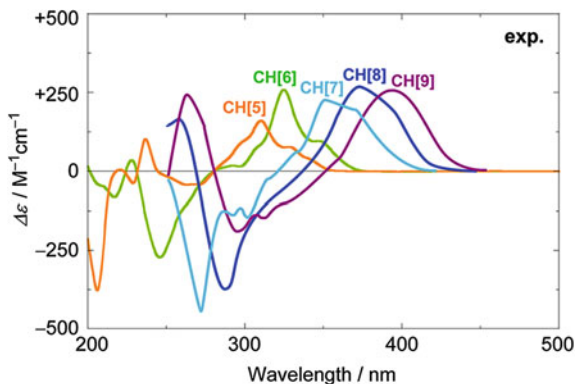
The electronic circularly dichroism (ECD) spectra of some (+)-helicenes are depicted in Fig. 2.7, which show that all the levorotatory helicenes have positive Cotton effect (CE) at the maximum absorption wavelength, and then negative CE at the shorter wavelength [50]. Autschbach group used time-dependent DFT to calculate the OR of [6]helicenes and [7]helicene by introducing system-specific range-separation parameters with tuned precision [51]. Inoue, Mori, and co-workers studied the ECD and OR of [n]helicenes by coupled cluster (CC) and DFT calculations [50, 52, 53]. The experimental results were nicely reproduced (RI-CC2/TZVPP//DFT-D2-B97-D/TZVP level) and the anisotropy factor (g) of the ^1B_a and ^1B_b bands were both proportional to $1/n$ [50]. As for [6]helicenes with different functional groups, they found that the electronic and steric effects greatly affected the spectral behaviors: (1) the more the structure deformed, the weaker the CE intense of ^1B_b band was; (2) the effect of methylation was nearly additive (the intensity 3,3′-dimethyl[6]helicene > 3-methyl[6]helicene > [6]helicene); (3) positive (C atoms) and negative (N, O atoms) induce effects were discovered [52].

Moreover, the vibrational circular dichroism (VCD) spectra were also used to determine the absolute configuration [54]. Compared with ECD spectra, which are related to the excited states displaying overlapped transitions, VCD spectra are associated with the ground states (Fig. 2.8) providing the fine vibration pattern [54]. However, larger quantities of enantiopure samples were needed for the test than that of ECD [54]. Recently, Raman optical activity (ROA), the other form of vibrational optical activity, was measured experimentally and interpreted by electron–phonon coupling analysis (Fig. 2.9) [55]. The strongest ROA band of [7]helicene dropped in the range of 1350–1400 cm^{-1}, which was associated with the bending of the H-C-C planes and the stretching of the C–C bonds.

For the determination of absolute configuration, crystal structure gave the direct evidence [5]. If suitable crystal for X-ray crystal analysis testing could not be obtained, it could be deduced experimentally via the chiroptical features mentioned above. However, this deduction must be made very carefully since it is based on the assumption that similar molecules with same helicity exhibit similar chiroptical properties, like [6]helicene and 2-bromo[6]helicene. In comparison with the known
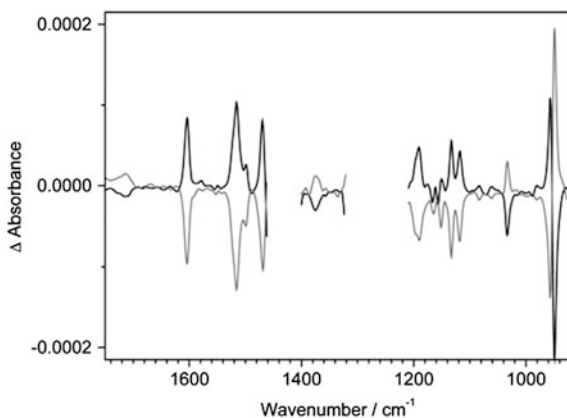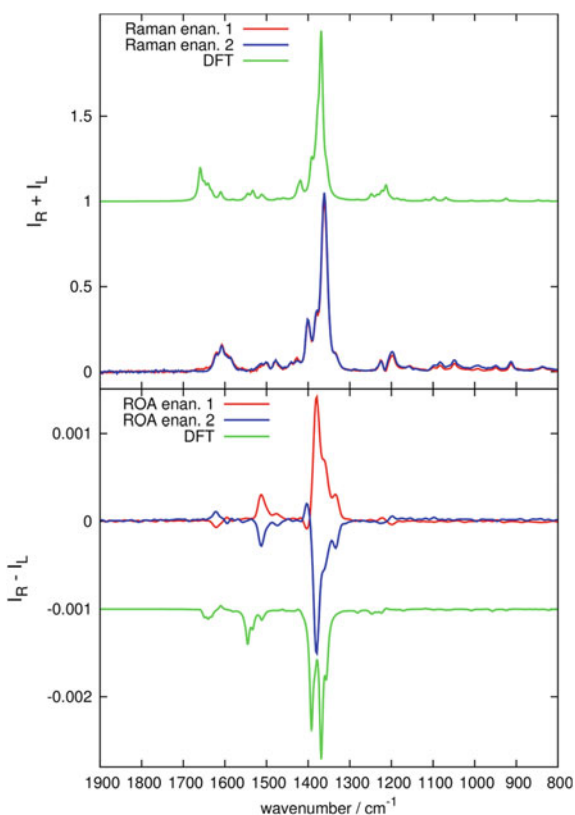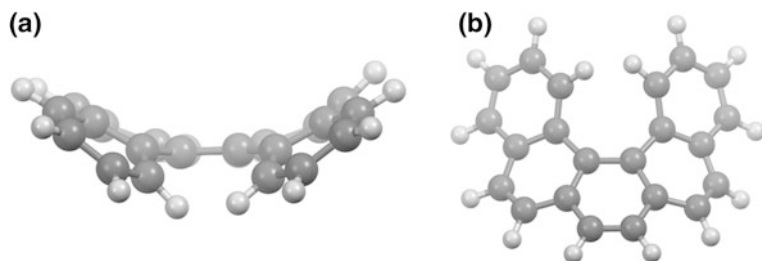
Fig. 2.10 **a** *Side view* and **b** *top view* of the TS of [5]helicene

helicenes, the absolute configuration could be safely established (the results deduced from OR and CD spectra should be consistent with each other) [56].

Although helicenes are composed by aromatic rings, the helical skeleton is not as rigid as it is shown: a helicene molecule could complete the conversion from one helicity to the other via structural deformation. The racemization phenomenon was elucidated by computational studies [57–59]. For example, the transition state (TS) of [5]helicene was calculated and depicted in Fig. 2.10 [58]. In TS, [5]helicene was deformed into a bowl-like structure with a C_s symmetry, and the molecule in such a state was achiral by excitation. With the release of the strain, this state had equal possibility to transform to the ground states (C_2 symmetry) with P- or M-helicity. A similar process with a saddle-shaped structure (C_s symmetry) was captured via [6+6] photocycloaddition (Scheme 2.1) [60]. For longer helicenes, two or more TSs might be involved when the racemization happened.

Some parameters of thermal racemization of helicenes are listed in Table 2.5. By comparison, three empiric rules could be found

(1) the longer the helicene is, the higher the barrier (E_a) is (Entries 1, 3, and 7–9);
(2) the substituents at the most steric hindered positions, namely C(1) and C(1′), could greatly increase the activation energy (Entries 1 and 3 versus Entries 2, 4, and 5); and the smaller the functional group at C(1) is, the more unstable the helicene is (Entries 1, 2, and 11); however, the effect of substitutions at other positions is not so obvious (Entries 4–6);
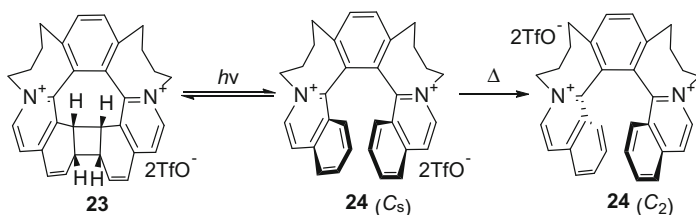
Scheme 2.1 The [6+6] cycloaddition of helquat **24**

Table 2.5 Experimental results of racemization of helicenes

Entry	Helicenes[a]	E_a (kcal/mol)	T (K)	$t_{1/2}$ (min)	Ref.
1	[5]	24.6	293	62.7 (57 °C)	[48]
2	1-Me[5]	38.7	473	/	[62]
3	[6]	36.2	300	13.4 (221.7 °C)	[63]
4	1-Me[6]	43.8	542	231	[64]
5	1,1′-DiMe[6]	44.0	543	444	[64]
6	2,2′-DiMe[6]	39.5	513	222	[64]
7	[7]	41.7	542	13.4 (295 °C)	[63]
8	[8]	42.4	543	3.1 (293.2 °C)	[63]
9	[9]	43.5	543	12.3 (293.5)	[63]
10	Thia[6][b]	22	298	13	[65]
11	1-Aza[5]	21.7	298	/	[66]

[a][n]=[n]helicene, Me=methyl; [b]3,6,9-trithia[6]helicene

(3)   if five-membered rings are incorporated in a helicene, the barrier of racem-
ization is lower than the corresponding carbohelicene (Entries 3 and 10).
Therefore, such optically pure helicenes should be kept at low temperature.

For example, [5]helicene underwent racemization very fast at room temperature,
and thia[6]helicene even just had a half-life of 13 min at room temperature. If
optically stable helicenes need to be synthesized, it would be better that the
molecular design start from [6]helicene or C(1)-substituted [5]helicene. Protonated
azahelicenes exhibited similar energy barrier to the related carbohelicenes [61].
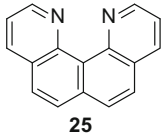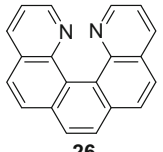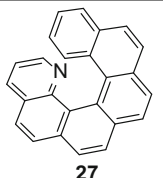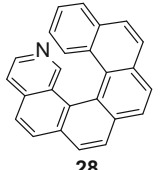
2.4   Other Properties

Helicenes has better solubility than that of planar PAHs. The common solvents are
methylene chloride, chloroform, ethyl acetate, toluene, and phenyl chloride. In
addition, the solubility could be improved by the functional groups, like alkyl and
alkoxy groups [67].

Azahelicenes could perform like bases. For example, **25–28** (Table 2.6) showed
strong basicity, and only **27** was weaker than pyridine, in which the nitrogen atom
was shielded by the helical backbone [61]. Diaza[4]helicene **25** could form linear
hydrogen bond between two nitrogen atoms like proton sponge [68]. However,
because of the helical structure, **26** and 1,16-diaza[6]helicene did not have such
properties [69].

Tanaka and co-workers synthesized a series of thia[7]helicenes in which the
terminal rings were connected by an alkyl chain [70]. The interplanar angle became
bigger as the chain was lengthened. However, the amount of increase became
smaller as the bridge was lengthened further, because the skeleton might come to a
stretched state. According to the theoretical studies, the stiffness of the spring could

Table 2.6 The experimental pK_a values of azahelicenes

Entry	Molecule	pK_a (in MeCN)	Ref.
1	Pyridine	12.56	[61]
2	**25**	12.8	[68]
3	**26**	14.87, 4.7 (MeOH)	[61]
4	**27**	11.65, 4.94 (MeOH)	[61]
5	**28**	13.06, 5.68 (MeOH)	[61]

be improved by adjusting the length and electron density of helicenes [71], while the elasticity of helicenes decreased as it became longer [72].

Recently, Zhang and co-workers studied the deformation capacity of carbohelicenes (Fig. 2.11) by DFT calculations and found that the maximum reversible tensile strain varied in the range of 78–222 % [73]. The replacement of hexagons
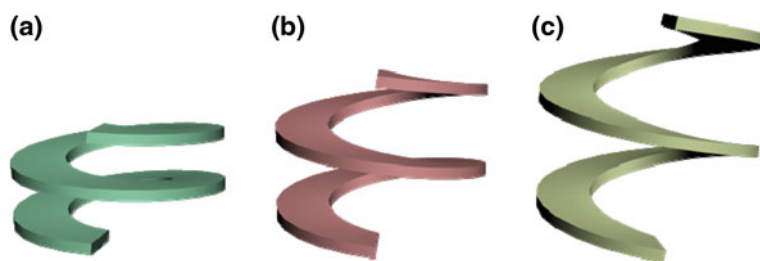
Fig. 2.11 Schematic representation of the deformation of a helicene molecule like a spring: **a** compressed; **b** optimal; **c** stretched
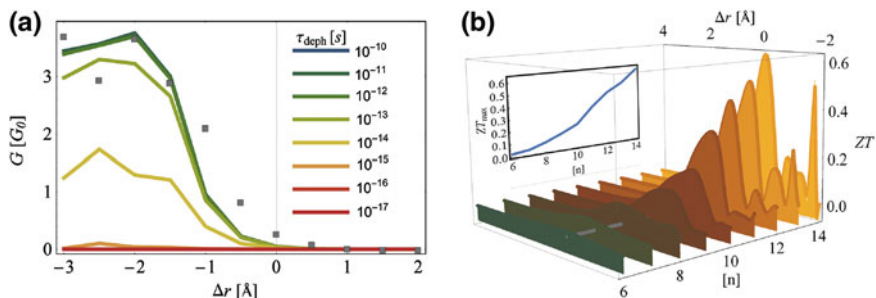
Fig. 2.12 **a** Conductance as a function of the change Δr in the inter-electrode distance measured from the relaxed configuration; **b** *ZT* as a function of Δr for a series of homologous diaza[*n*] helicenes (from 2,15-diaza[6]helicene to 2,31-diaza[14]helicene). *Inset* maximal thermoelectric FOM, ZT_{max}, as a function of helicene length. Reprinted with the permission from ref. [74] which is Open Access licensed under a Creative Commons Attribution 4.0 International License

with pentagons or heptagons greatly influenced the bonding pattern of the internal chain. For helicene formed by hexagon, there was only C–C single bond internally, while other structures form the internal chain with alternate C–C single and C=C double bonds.

Vacek, Dubi, and co-workers using DFT and tight-binding calculation to study the mechanic tuning of conductance and thermopower in helicene molecular junctions (HMJs) (Fig. 2.12) [74]. First, the HMJs could be mechanically tuned from an insulating state (for example, $\Delta r = 2$ Å, 'OFF') to a metallic state ($\Delta r = -2$ Å, 'ON'). Second, the thermoelectric figure of merit *ZT* could be tuned by helicene length and the Δr. This resulted from the deformation of helicenes followed by the changes in the tunneling matrix elements.

Yan and co-workers discovered the U-shaped relationship between the pitch of the helicene (*d*) and the current (*I*) under a certain bias voltage (Fig. 2.13) [75]. The DFT calculation revealed that the structural deformation induced the change of

Fig. 2.13 *I−V* behaviors of aza[12]helicene contacted with carbon chain electrodes. Current varies with *d* under the bias of 2.0 V. Reprinted with the permission from Ref. [75] which is Open Access licensed under a Creative Commons Attribution 4.0 International License
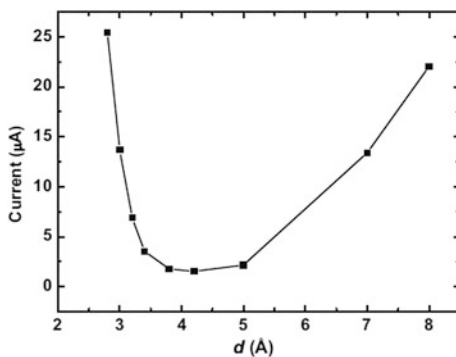
the extent of overlap between the orbitals, resulting in such a relationship between the HOMO–LUMO gap with d. This is an intrinsic characteristic of helicenes, which is independent of the electrode material or the heteroatoms in the skeletons used in the study.

2.5 Helicenes with Open Shell and Charges

Since helicenes are composed by aromatic rings, although they are twisted, these molecules are difficult to be reduced or oxidized. Kurreck group prepared the helicene radical anions by the reaction between the [6]helicene and alkali metals, which was confirmed by ESR, ENDO, and TRIPLE measurements [76]. The introduction of heteroatoms, like O and N atoms, increased the diversity of electronic structures.

Helicene bisquinones **29a–d** could be reduced to radical anions by electrochemical method, which exhibited the absorption in NIR or IR region (Fig. 2.14 and Table 2.7) [77, 78]. Such small energy gap resulted from the transannular delocalization of electrons like a Möbius system. This result was reexamined and confirmed again by ab initio calculations [79].

Rajca, Lapkowski, and co-workers prepared a thia[7]helicene radical cation **30**$^{\bullet+}$· PF$_6^-$ via the oxidation of **30** by electrochemical method, which was stable at room temperature with a half-life about 15–20 min [80]. To compare with the
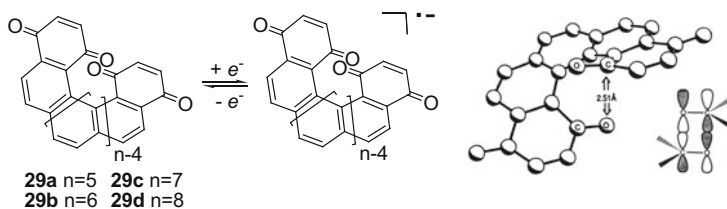
Fig. 2.14 Reduction of helicene bisquinones, geometry of **29**$^{\bullet-}$ and the proposed transannular interaction. Reprinted with the permission from Ref. [78]. Copyright 1993 American Chemical Society

Table 2.7 The reduction of helicene bisquinones

Entry	Radical anions	λ_{max} (nm)	ΔE (mV)	Ref.
1	**29a**$^{\bullet-}$	1400, 590, 420	470	[77, 78]
2	**29b**$^{\bullet-}$	1825, 680, 340	380	[77, 78]
3	**29c**$^{\bullet-}$	2200, 580	310	[77, 78]
4	**29d**$^{\bullet-}$	2200, 800, 530	270	[77, 78]
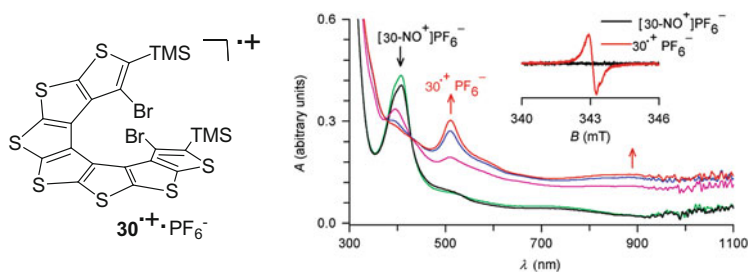
Fig. 2.15 Thia[7]helicene radical cation $30^{\bullet+}$ (*left*) and UV-vis-NIR/EPR spectroscopic monitoring of chemical oxidation of [7]helicene *rac*-**30** with [NO][PF$_6$] (*right*). EPR spectra are obtained after the UV-vis-NIR spectra corresponding to [**30**-NO]$^+$PF$_6^-$ and $30^{\bullet+}$PF$_6^-$. Reprinted with the permission from Ref. [80]. Copyright 2010 American Chemical Society

radical cation, [**30**-NO]$^+$PF$_6^-$ was synthesized by chemical oxidation with [NO] [PF$_6$] (Fig. 2.15). The salt $30^{\bullet+} \cdot$PF$_6^-$ showed a broad absorption band around the wavelength of 900 nm. Based on the CD spectra, it was proved that **30** could not be oxidized into a planar quasi-[8]circulene structure.

Arai, Sato, and co-workers prepared several azoniahelienes (**31–33**, Fig. 2.16) by oxidative photocyclization [81, 82]. They were all yellow solid, and exhibited similar absorption properties to related carbohelicenes. Teplý group prepared the helquats molecules (Fig. 2.16) [83], which could be prepared in large scale and resolved by crystallization [84, 85]. The advantage of such molecules is the good solubility in aqueous phase which renders the helicenes applicable in water.

Another kind of helicene cations has a carbocation on the skeleton. This was systematically studied by Lacour group [86]. This species was highly stable. Compared with carbohelicenes, the absorption of the helicene cation exhibited a bathochromic shift to even 700 nm and the band gap was greatly reduced (Table 2.8) [87]. According to the chemical shift of carbocation (similar to the carbon atom in benzene), the electron was delocalized well through the whole skeleton.
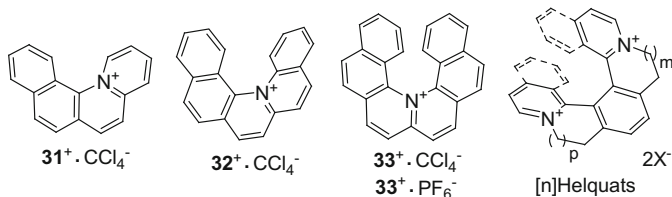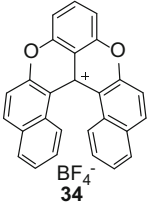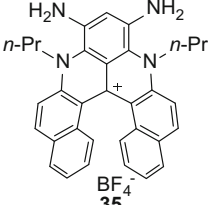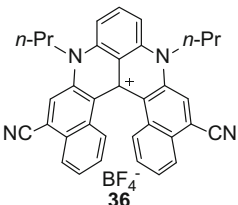
Fig. 2.16 Some helicene cations

Table 2.8 Some properties of helicene cations [87]

Entry	Cations	λ_{max} (nm)	Color	δ (C$^+$, ppm)
1		575	Red	161.5
2		700	Green	148.3
3		690	Green	141.6

References

1. Shen Y, Chen C-F (2012) Helicenes: synthesis and applications. Chem Rev 112(3):1463–1535
2. Cahn RS, Ingold C, Prelog V (1966) Specification of molecular chirality. Angew Chem Int Ed 5(4):385–415
3. Meurer KP, Vogtle F (1985) Helical molecules in organic-chemistry. Top Curr Chem 127:1–76
4. Wynberg H (1971) Some observations on chemical, photochemical, and spectral properties of thiophenes. Acc Chem Res 4(2):65–73
5. Lightner DA, Hefelfin DT, Frank GW, Powers TW, Truebloo KN (1971) Absolute configuration of hexahelicene. Nature-Phys Sci 232(32):124–125
6. Hirshfeld FL, Sandler S, Schmidt GMJ (1963) 398. The structure of overcrowded aromatic compounds. Part VI. The crystal structure of benzo[c]phenanthrene and of 1,12-dimethylbenzo[c]phenanthrene. J Chem Soc (Resumed) (0):2108–2125
7. Kuroda R (1982) Crystal and molecular structure of [5]helicene: crystal packing modes. J Chem Soc, Perkin Trans 2(7):789–794
8. Yamamoto K, Okazumi M, Suemune H, Usui K (2013) Synthesis of [5]helicenes with a substituent exclusively on the interior side of the helix by metal-catalyzed cycloisomerization. Org Lett 15(8):1806–1809
9. Misek J, Teply F, Stara IG, Tichy M, Saman D, Cisarova I, Vojtisek P, Stary I (2008) A straightforward route to helically chiral N-heteroaromatic compounds: practical synthesis of racemic 1,14-diaza[5]helicene and optically pure 1-and 2-aza[6]helicenes. Angew Chem Int Ed 47(17):3188–3191

10. Takenaka N, Sarangthem RS, Captain B (2008) Helical chiral pyridine *n*-oxides: a new family of asymmetric catalysts. Angew Chem Int Ed 47(50):9708–9710
11. Mori K, Murase T, Fujita M (2015) One-step synthesis of [16]helicene. Angew Chem Int Ed 54(23):6847–6851
12. Laarhoven WH, Prinsen WJC (1984) Carbohelicenes and Heterohelicenes. Top Curr Chem 125:63–130
13. Allen FH, Kennard O, Watson DG, Brammer L, Orpen AG, Taylor R (1987) Tables of bond lengths determined by X-ray and neutron diffraction. Part 1. Bond lengths in organic compounds. J Chem Soc, Perkin Trans 2(12):S1–S19
14. Wolstenholme DJ, Matta CF, Cameront TS (2007) Experimental and theoretical electron density study of a highly twisted polycyclic aromatic hydrocarbon: 4-methyl-[4]helicene. J Phys Chem A 111(36):8803–8813
15. Obenland S, Schmidt W (1975) Photoelectron-spectra of polynuclear aromatics. 4. Helicenes. J Am Chem Soc 97(23):6633–6638
16. Deb BM, Kavu G (1980) An indo-mo study of the spectral properties and trans-annular interaction in [6]-helicene. Can J Chem Rev Can Chim 58(3):258–262
17. Schulman JM, Disch RL (1999) Aromatic character of [n]helicenes and [n]phenacenes. J Phys Chem A 103(33):6669–6672
18. Portella G, Poater J, Bofill JM, Alemany P, Sola M (2005) Local aromaticity of [n]acenes, [n]phenacenes, and [n]helicenes (n = 1–9). J Org Chem 70(7):2509–2521
19. Tian YH, Park G, Kertesz M (2008) Electronic structure of helicenes, C2S helicenes, and thiaheterohelicenes. Chem Mater 20(10):3266–3277
20. Rajca A, Pink M, Xiao SZ, Miyasaka M, Rajca S, Das K, Plessel K (2009) Functionalized thiophene-based [7]helicene: chirooptical properties versus electron delocalization. J Org Chem 74(19):7504–7513
21. Miyasaka M, Pink M, Olankitwanit A, Rajca S, Rajca A (2012) Band gap of carbon-sulfur [n]helicenes. Org Lett 14(12):3076–3079
22. Johnson WS, Woroch E, Mathews FJ (1947) Cyclization studies in the benzoquinoline and naphthoquinoline series. II. J Am Chem Soc 69(3):566–571
23. Clar E, Stewart DG (1952) Aromatic hydrocarbons. LXIII. Resonance restriction and the absorption spectra of aromatic hydrocarbons1. J Am Chem Soc 74(24):6235–6238
24. Newman MS, Lednicer D (1956) The synthesis and resolution of hexahelicene. J Am Chem Soc 78(18):4765–4770
25. Flammang-Barbieux M, Nasielski J, Martin RH (1967) Synthesis of heptahelicene (1) benzo [c] phenanthro [4, 3-g] phenanthrene. Tetrahedron Lett 8(8):743–744
26. Martin RH, Flammang M, Cosyn JP, Gelbcke M (1968) 1. Synthesis of octa- and nonahelicenes. 2. New syntheses of hexa- and heptahelicenes. 3. Optical rotation and ORD of heptahelicene. Tetrahedron Lett (31):3507–3510
27. Bédard A-C, Vlassova A, Hernandez-Perez AC, Bessette A, Hanan GS, Heuft MA, Collins SK (2013) Synthesis, crystal structure and photophysical properties of pyrene-helicene hybrids. Chem Eur J 19(48):16295–16302
28. Hu J-Y, Paudel A, Seto N, Feng X, Era M, Matsumoto T, Tanaka J, Elsegood MRJ, Redshaw C, Yamato T (2013) Pyrene-cored blue-light emitting [4]helicenes: synthesis, crystal structures, and photophysical properties. Org Biomol Chem 11(13):2186–2197
29. Buchta M, Rybáček J, Jančařík A, Kudale AA, Buděšínský M, Chocholoušová JV, Vacek J, Bednárová L, Císařová I, Bodwell GJ, Starý I, Stará IG (2015) Chimerical pyrene-based [7] helicenes as twisted polycondensed aromatics. Chem Eur J 21(24):8910–8917
30. Fujikawa T, Segawa Y, Itami K (2015) Synthesis, structures, and properties of π-extended double helicene: a combination of planar and nonplanar π-systems. J Am Chem Soc 137 (24):7763–7768
31. Dougherty KJ, Kraml CM, Byrne N, Porras JA, Bernhard S, Mague JT, Pascal RA Jr (2015) Helical mesobenzanthrones: a class of highly luminescent helicenes. Tetrahedron 71 (11):1694–1699

32. Bock H, Subervie D, Mathey P, Pradhan A, Sarkar P, Dechambenoit P, Hillard EA, Durola F (2014) Helicenes from Diarylmaleimides. Org Lett 16(6):1546–1549

33. Li Y-Y, Lu H-Y, Li M, Li X-J, Chen C-F (2014) Dihydroindeno[2,1-c]fluorene-based imide dyes: synthesis, structures, photophysical and electrochemical properties. J Org Chem 79 (5):2139–2147

34. Fix AG, Deal PE, Vonnegut CL, Rose BD, Zakharov LN, Haley MM (2013) Indeno[2,1-c] fluorene: a new electron-accepting scaffold for organic electronics. Org Lett 15(6):1362–1365

35. Li M, Niu Y, Zhu X, Peng Q, Lu H-Y, Xia A, Chen C-F (2014) Tetrahydro[5]helicene-based imide dyes with intense fluorescence in both solution and solid state. Chem Commun (Camb) 50(23):2993–2995

36. Kitamura C, Tanigawa Y, Kobayashi T, Naito H, Kurata H, Kawase T (2012) 17,17-Dialkyltetrabenzo[a, c, g, i]fluorenes with extremely high solid-state fluorescent quantum yields: relationship between crystal structure and fluorescent properties. Tetrahedron 68(6):1688–1694

37. Newman MS, Lutz WB, Lednicer D (1955) A new reagent for resolution by complex formation—the resolution of phenanthro-[3,4-C]phenanthrene. J Am Chem Soc 77(12):3420–3421

38. Tanaka H, Nakagawa H, Yamada K, Kawazura H (1981) An NMR-study on the association stabilities of thiaheterohelicenes against 7,7,8,8-tetracyanoquinodimethan—effect of the staggered configuration of helicene. Bull Chem Soc Jpn 54(12):3665–3668

39. Balan A, Gottlieb HE (1981) Diastereoisomeric charge-transfer complexes—measurement of thermodynamic constants by H-1 nuclear magnetic-resonance spectroscopy. J Chem Soc, Perkin Trans 2(2):350–352

40. Mikes F, Boshart G, Gilav E (1976) Resolution of optical isomers by high-performance liquid-chromatography, using coated and bonded chiral charge-transfer complexing agents as stationary phases. J Chromatogr 122:205–221

41. Mikes F, Boshart G, Gil-Av E (1976) Helicenes—resolution on chiral charge-transfer complexing agents using high-performance liquid-chromatography. J Chem Soc, Chem Commun 3:99–100

42. Ermer O, Neudörfl J (2001) Comparative supramolecular chemistry of coronene and hexahelicene: helix alignment in crystalline complexes with trimesic acid (=benzene-1,3,5-tricarboxylic Acid) and π-acceptor compounds. Helv Chim Acta 84 (6):1268–1313

43. Kumano D, Iwahana S, Iida H, Shen C, Crassous J, Yashima E (2015) Enantioseparation on riboflavin derivatives chemically bonded to silica gel as chiral stationary phases for HPLC. Chirality 27(8):507–517

44. Waghray D, Zhang J, Jacobs J, Nulens W, Basarić N, Meervelt LV, Dehaen W (2012) Synthesis and structural elucidation of diversely functionalized 5,10-diaza[5]helicenes. J Org Chem 77(22):10176–10183

45. Nakano K, Oyama H, Nishimura Y, Nakasako S, Nozaki K (2012) λ5-Phospha[7]helicenes: synthesis, properties, and columnar aggregation with one-way chirality. Angew Chem Int Ed 51(3):695–699

46. Martin RH (1974) Helicenes. Angew Chem Int Ed Engl 13(10):649–659

47. Gingras M, Felix G, Peresutti R (2013) One hundred years of helicene chemistry. Part 2: stereoselective syntheses and chiral separations of carbohelicenes. Chem Soc Rev 42(3):1007–1050

48. Goedicke C, Stegemeyer H (1970) Resolution and racemization of pentahelicene. Tetrahedron Lett 11(12):937–940

49. Martin RH, Marchant MJ (1974) Resolution and optical-properties ([alpha]max, ORD and CD) of hepta-helicene, octa-helicene and nonahelicene. Tetrahedron 30(2):343–345

50. Nakai Y, Mori T, Inoue Y (2012) Theoretical and experimental studies on circular dichroism of carbo[n]helicenes. J Phys Chem A 116(27):7372–7385

51. Srebro M, Autschbach J (2012) Tuned range-separated time-dependent density functional theory applied to optical rotation. J Chem Theory Comput 8(1):245–256

52. Nakai Y, Mori T, Inoue Y (2013) Circular dichroism of (di)methyl- and diaza[6]helicenes. A combined theoretical and experimental study. J Phys Chem A 117(1):83–93
53. Nakai Y, Mori T, Sato K, Inoue Y (2013) Theoretical and experimental studies of circular dichroism of mono- and diazonia[6]helicenes. J Phys Chem A 117(24):5082–5092
54. Burgi T, Urakawa A, Behzadi B, Ernst K-H, Baiker A (2004) The absolute configuration of heptahelicene: aVCD spectroscopy study. New J Chem 28(3):332–334
55. Johannessen C, Blanch EW, Villani C, Abbate S, Longhi G, Agarwal NR, Tommasini M, Lightner DA (2013) Raman and ROA Spectra of (−)- and (+)-2-Br-hexahelicene: experimental and DFT studies of a π-conjugated chiral system. J Phys Chem B 117(7):2221–2230
56. Shen Y, Lu H-Y, Chen C-F (2014) Dioxygen-triggered transannular dearomatization of benzo[5]helicene diols: highly efficient synthesis of chiral π-extended diones. Angew Chem Int Ed 53(18):4648–4651
57. Grimme S, Peyerimhoff SD (1996) Theoretical study of the structures and racemization barriers of [n]helicenes (n = 3–6, 8). Chem Phys 204(2–3):411–417
58. Janke RH, Haufe G, Wurthwein EU, Borkent JH (1996) Racemization barriers of helicenes: A computational study. J Am Chem Soc 118(25):6031–6035
59. Lindner HJ (1975) Atomisierungsenergien gespannter konjugierter kohlenwasserstoffe—I: Razemisierungsenergien von helicenen. Tetrahedron 31(3):281–284
60. Severa L, Ončák M, Koval D, Pohl R, Šaman D, Císařová I, Reyes-Gutiérrez PE, Sázelová P, Kašička V, Teplý F, Slavíček P (2012) A chiral dicationic [8]circulenoid: photochemical origin and facile thermal conversion into a helicene congener. Angew Chem Int Ed 51(48):11972–11976
61. Vacek Chocholoušová J, Vacek J, Andronova A, Míšek J, Songis O, Šámal M, Stará IG, Meyer M, Bourdillon M, Pospíšil L, Starý I (2014) On the physicochemical properties of pyridohelicenes. Chem Eur J 20(3):877–893
62. Scherübl H, Fritzsche U, Mannschreck A (1984) Liquid chromatography on triacetylcellulose, 6. Synthesis, chromatographic enrichment of enantiomers, and barriers to enantiomerization of helical phenanthrenes. Chem Ber 117(1):336–343
63. Martin RH, Marchant MJ (1974) Thermal racemization of hepta-helicene, octa-helicene, and nonahelicene—kinetic results, reaction path and experimental proofs that racemization of hexahelicene and heptahelicene does not involve an intramolecular double diels-alder reaction. Tetrahedron 30(2):347–349
64. Borkent JH, Laarhoven WH (1978) Thermal racemization of methyl-substituted hexahelicenes. Tetrahedron 34(16):2565–2567
65. Wynberg H, Groen MB (1969) Racemization of two hexaheterohelicenes. J Chem Soc D: Chem Commun 17:964–965
66. Caronna T, Mele A, Famulari A, Mendola D, Fontana F, Juza M, Kamuf M, Zawatzky K, Trapp O (2015) A combined experimental and theoretical study on the stereodynamics of monoaza[5]helicenes: solvent-induced increase of the enantiomerization barrier in 1-aza-[5]helicene. Chem Eur J 21(40):13919–13924
67. Katz TJ, Liu LB, Willmore ND, Fox JM, Rheingold AL, Shi SH, Nuckolls C, Rickman BH (1997) An efficient synthesis of functionalized helicenes. J Am Chem Soc 119(42):10054–10063
68. Zirnstein MA, Staab HA (1987) Quino[7,8-h]quinoline, a new type of "proton sponge". Angew Chem Int Ed Engl 26(5):460–461
69. Staab HA, Diehm M, Krieger C (1994) Synthesis, structure and basicity of 1,16-diaza[6]helicene. Tetrahedron Lett 35(45):8357–8360
70. Osuga H, Tanaka K (2002) Synthesis and properties of heterohelicenes as "molecular springs". J Synth Org Chem Jpn 60(6):593–603
71. Jalaie M, Weatherhead S, Lipkowitz KB, Robertson D (1997) Modulating force constants in molecular springs. Electronic J Theo Chem 2(1):268–272
72. Rulisek L, Exner O, Cwiklik L, Jungwirth P, Stary I, Pospisil L, Havlas Z (2007) On the convergence of the physicochemical properties of [n]helicenes. J Phys Chem C 111(41):14948–14955

73. Sestak P, Wu J, He J, Pokluda J, Zhang Z (2015) Extraordinary deformation capacity of smallest carbohelicene springs. Phys Chem Chem Phys 17(28):18684–18690

74. Vacek J, Chocholousova JV, Stara IG, Stary I, Dubi Y (2015) Mechanical tuning of conductance and thermopower in helicene molecular junctions. Nanoscale 7(19):8793–8802

75. Guo Y-D, Yan X-H, Xiao Y, Liu C-S (2015) U-shaped relationship between current and pitch in helicene molecules. Sci Rep 5:16731

76. Fey HJ, Kurreck H, Lubitz W (1979) Endor studies of [6]helicene anion radical. Tetrahedron 35(7):905–907

77. Yang BW, Liu LB, Katz TJ, Liberko CA, Miller LL (1991) Electron delocalization in helical quinone anion radicals. J Am Chem Soc 113(23):8993–8994

78. Liberko CA, Miller LL, Katz TJ, Liu LB (1993) The electronic-structure of helicene bisquinone anion radicals. J Am Chem Soc 115(6):2478–2482

79. Sargent AL, Almlof J, Liberko CA (1994) Electron delocalization in helical bis(quinone) anion-radicals. J Phys Chem 98(24):6114–6117

80. Zak JK, Miyasaka M, Rajca S, Lapkowski M, Rajca A (2010) Radical cation of helical, cross-conjugated beta-oligothiophene. J Am Chem Soc 132(10):3246–3247

81. Arai S, Ishikura M, Yamagishi T (1998) Synthesis of polycyclic azonia-aromatic compounds by photo-induced intramolecular quaternization: Azonia derivatives of benzo[c]phenanthrene, [5]helicene and [6]helicene. J Chem Soc, Perkin Trans 1(9):1561–1567

82. Sato K, Yamagishi T, Arai S (2000) Synthesis of novel azonia[5]helicenes containing terminal thiophene rings. J Heterocycl Chem 37(4):1009–1014

83. Adriaenssens L, Severa L, Salova T, Cisarova I, Pohl R, Saman D, Rocha SV, Finney NS, Pospisil L, Slavicek P, Teply F (2009) Helquats: a facile, modular, scalable route to novel helical dications. Chem Eur J 15(5):1072–1076

84. Vávra J, Severa L, Švec P, Císařová I, Koval D, Sázelová P, Kašička V, Teplý F (2012) Preferential crystallization of a helicene-viologen hybrid—an efficient method to resolve [5] helquat enantiomers on a 20 g scale. Eur J Org Chem 3:489–499

85. Vávra J, Severa L, Císařová I, Klepetářová B, Šaman D, Koval D, Kašička V, Teplý F (2013) Search for conglomerate in set of [7]helquat salts: multigram resolution of helicene-viologen hybrid by preferential crystallization. J Org Chem 78(4):1329–1342

86. Bosson J, Gouin J, Lacour J (2014) Cationic triangulenes and helicenes: synthesis, chemical stability, optical properties and extended applications of these unusual dyes. Chem Soc Rev 43 (8):2824–2840

87. Torricelli F, Bosson J, Besnard C, Chekini M, Bürgi T, Lacour J (2013) Modular synthesis, orthogonal post-functionalization, absorption, and chiroptical properties of cationic [6] helicenes. Angew Chem Int Ed 52(6):1796–1800

Part II
How to Prepare Helicenes?

In this part, we will introduce some practical synthetic methods for helicenes, including those do not need special substrates, strategies which are widely utilized, and efficient methods to construct long helicenes. Also, the content herein will focus on the preparation of the helical backbones, namely the constructions of six- or five-membered rings, whereas the asymmetric synthesis will be summarized in the subsequent chapter, followed by the transformation of functional groups. Given the similar methods might be used for carbohelicenes and heterohelicenes, we would like to organize them together according to different methods rather than separate them into two categories. In addition, some special properties of specific helicenes will also be emphasized.
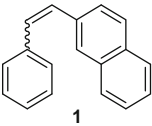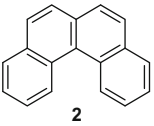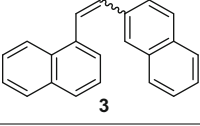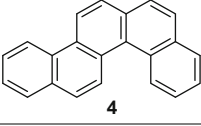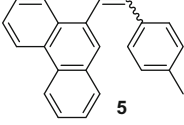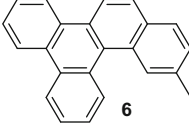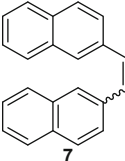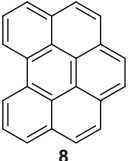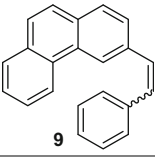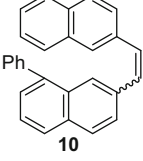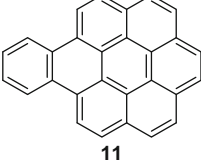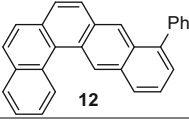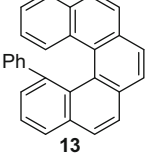
Chapter 3
Oxidative Photocyclization

Abstract Oxidative photocyclization is the most widely used method to the synthesis of carbohelicenes, in particular the long carbohelicenes. It is also an efficient way to the synthesis of heterohelicenes including azahelicenes and thiahelicenes. In this chapter, we first introduce the synthesis of various carbohelicenes by different oxidative photocyclization strategy starting from the stilbene precursors. With two aryl groups in the stilbene precursors bearing heteroaromatic rings, azahelicenes and thiahelicenes can be regioselectively synthesized by the similar oxidative photocyclization. Based on this methodology, optically active helicenes can also be obtained after resolution, which makes these molecules applicable. Although this methodology has been widely utilized, it is difficult to be used for large-scale preparation because the photocyclization needs highly diluted solution (usually ca. 10^{-3} M) to prevent the [2+2] intermolecular cycloaddition. Recently, chemists found a solution—the continuous flow strategy—to solve the problem of large-scale preparation. Under the optimal condition, the helicene can be prepared at the rate of 60 mg/h.

Keywords Carbohelicene · Continuous flow strategy · Heterohelicene · Oxidative photocyclization · Regioselectivity
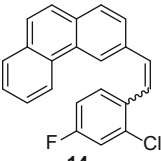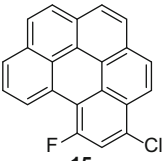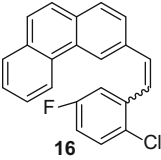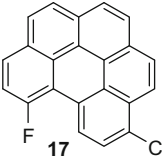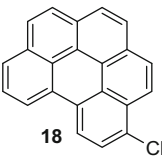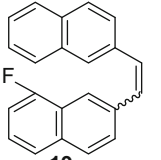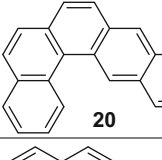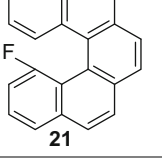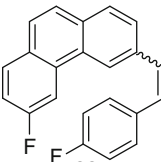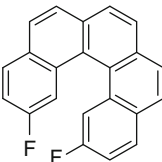
This method was first reported in 1960s [1–3], and the general two-step procedure has been developed thereafter: (1) the preparation of the stilbene precursors by the reactions between aldehyde and *P*-ylides [4–6] or Heck-type cross-coupling reactions between the aryl halides and aryl ethenes [7], (2) radiation of the stilbene solutions in the presence of oxidants or sensitizers. Herein, we will focus on the second step and selected photochemical reactions listed in Table 3.1 for carbohelicenes and Table 3.2 for heterohelicenes. To simplify the description, we would like to discuss the procedures by [*n* + *m*] or [*n* + *m* + *p* + …], in which the plus sign, '+', denotes a 1,2-disubstituted ethylene moiety and the numbers stand for the number of aromatic rings contributing to the helical skeletons in the substituted aryl group, like *n, m, p,* etc.

Table 3.1 Synthesis of carbohelicenes by photocyclization

Entry	Precursor	Condition[a]	Product[b]	Yield (%)[c]	Ref.
1	**1**	A	**2**	74	[1, 8]
2	**3**	B	**4**	76	[1, 8]
3	**5**	C	**6**	95	[9]
4	**7**	D	**8**	89	[3]
5	**9**	E	8	88	[10]
6	**10**	C	**11**	42	[11]
			12	10	
			13	7	
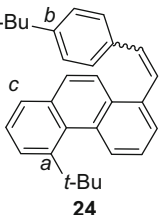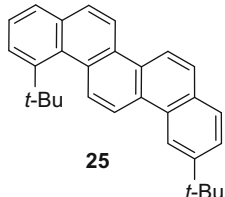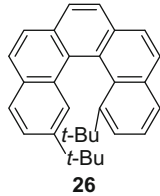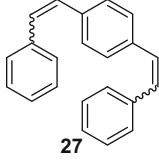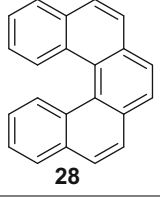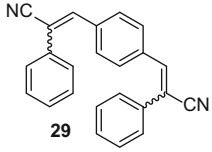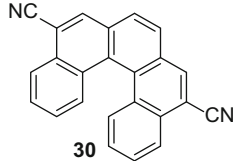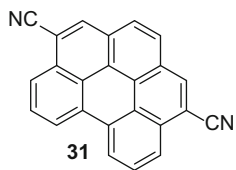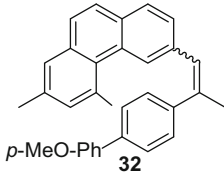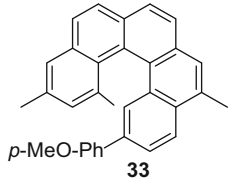
Table 3.1 (continued)

Entry	Precursor	Condition[a]	Product[b]	Yield (%)[c]	Ref.
7	**14**	**B**	**15**	44	[12]
8	**16**	**E**	**17** **18**	1:2	[12]
9	**19**	**E**	**20** **21**	1:1	[12]
10	**22**	**C**	**23**	64	[13]
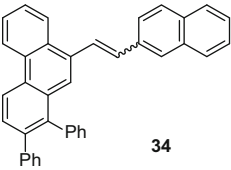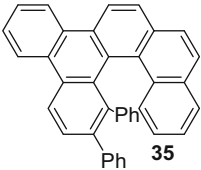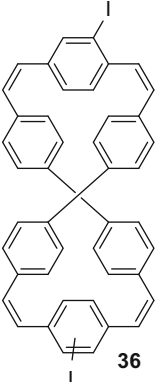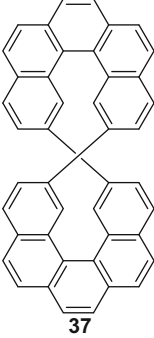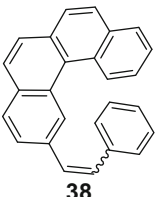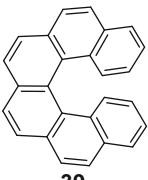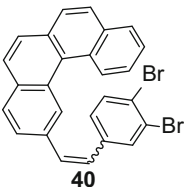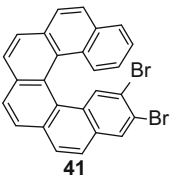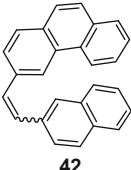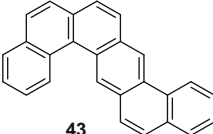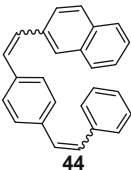
Table 3.1 (continued)

Entry	Precursor	Condition[a]	Product[b]	Yield (%)[c]	Ref.
11	*t*-Bu **24**	B	*t*-Bu **25** *t*-Bu	71	[14]
			t-Bu *t*-Bu **26**	21	
12	**27**	B	**28**	N.D.[d]	[15]
			8	16	
13	NC CN **29**	B	NC CN **30**	83	[15]
			NC CN **31**	N.D.[d]	
14	*p*-MeO-Ph **32**	C	*p*-MeO-Ph **33**	52	[11]
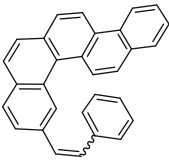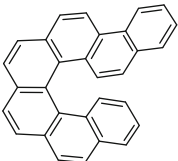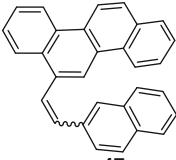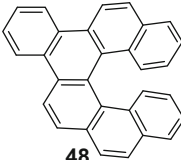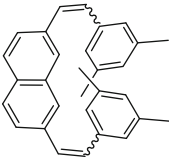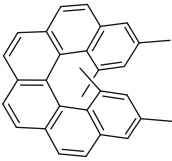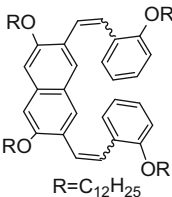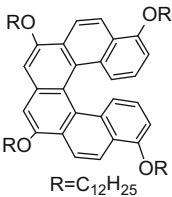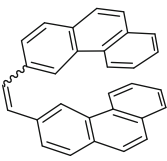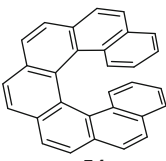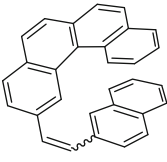
(continued)

Table 3.1 (continued)

Entry	Precursor	Condition[a]	Product[b]	Yield (%)[c]	Ref.
15	**34**	B	**35**	70	[16]
16	**36**	B	**37**	70	[17]
17	**38**	B	**39**	85	[18, 19]
18	**40**	B	**41**	62	[20]
19	**42**	C	**39**	22	[9]
			43	55	
20	**44**	B	**39**	55	[21]
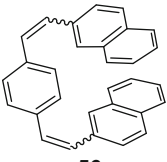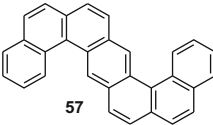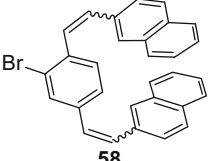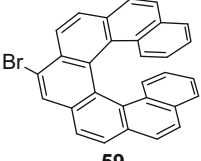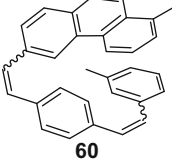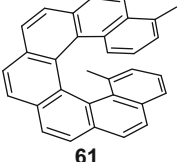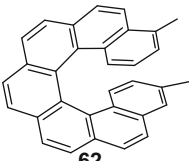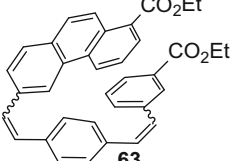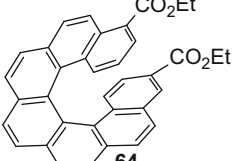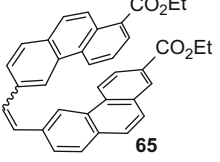
Table 3.1 (continued)

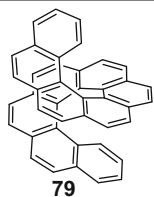| Entry	Precursor	Condition[a]	Product[b]	Yield (%)[c]	Ref.
21	**45**	C	**46**	65	[9, 22]
22	**47**	C	**48**	90	[9, 22]
23	**49**	B	**50**	80	[23]
24	RO OR RO OR R=C₁₂H₂₅ **51**	F	RO OR RO OR R=C₁₂H₂₅ **52**	82	[24]
25	**53**	C	**54**	50	[9, 22]
26	**55**	B	**54**	20	[25]
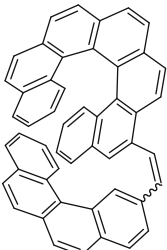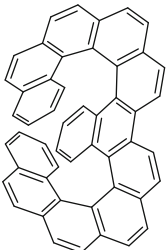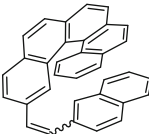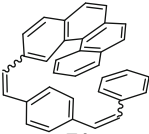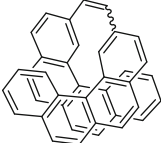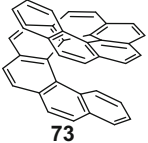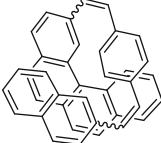
(continued)

Table 3.1 (continued)

Entry	Precursor	Condition[a]	Product[b]	Yield (%)[c]	Ref.
27	**56**	**B**	**54**	20	[21]
			57	20	
28	**58**	**G**		75	[26]
29		**H**	**59**	87	[27]
30	**60**	**B**	**61**	7	[28]
			62	7	
31	**63**	**B**	**64**	20	[28]
32	**65**	**B**	**64**	35	[28]
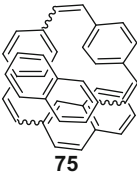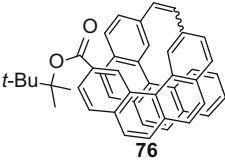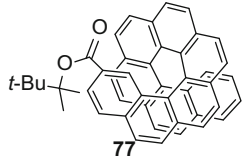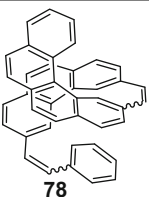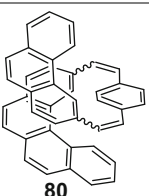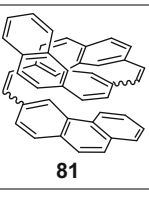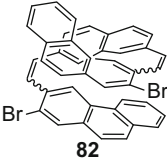
(continued)

Table 3.1 (continued)

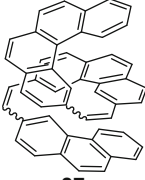| Entry	Precursor	Condition[a]	Product[b]	Yield (%)[c]	Ref.
33	**66**	I	**67**	26	[29]
34	**68**	B	**69**	85	[19]
35	**70**	B	**69**	80 40	[30] [31]
36	**71**	B	**69**	30	[19]
37	**72**	B	**73**	50 48	[30] [22, 25]
38	**74**	B	**73**	50	[19]
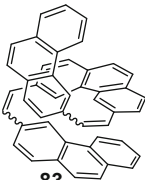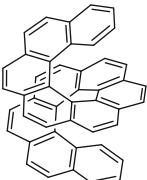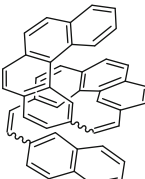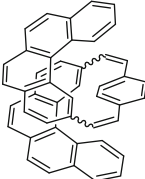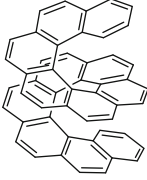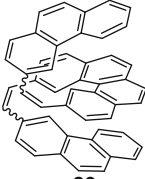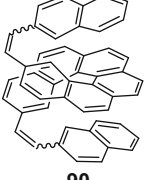
(continued)

Table 3.1 (continued)

Entry	Precursor	Condition[a]	Product[b]	Yield (%)[c]	Ref.
39	**75**	J	**73**	67	[32]
40	**76**	B	**77**	8	[33]
41	**78**	B	**79**	20	[19]
42	**80**	B	**79**	30	[19]
43	**81**	C	**79**	70	[34, 35]
44	**82**	I	**79**	81	[36]
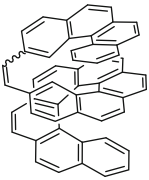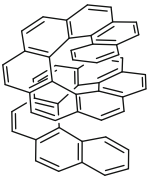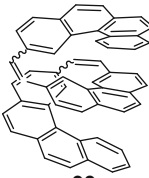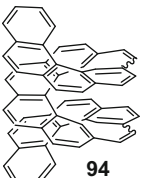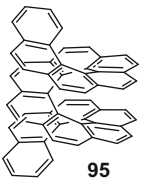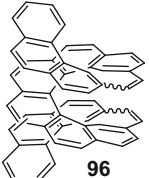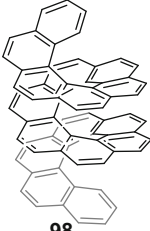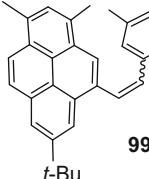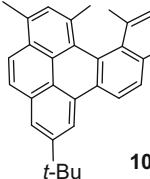
(continued)

Table 3.1 (continued)

Entry	Precursor	Condition[a]	Product[b]	Yield (%)[c]	Ref.
45	**83**	B	**84**	54	[37]
46	**85**	B	**84**	80	[19]
47	**86**	B	**84**	84	[37]
48	**87**	B	**88**	30	[19]
49	**89**	B	**88**	32	[37]
50	**90**	B	**88**	42	[37]
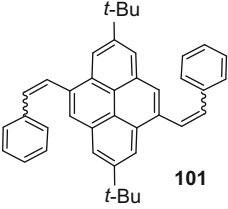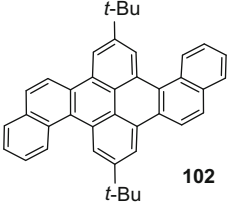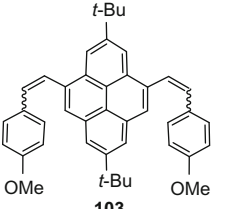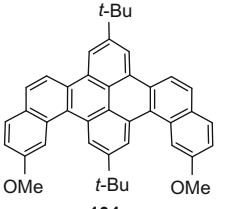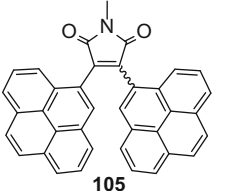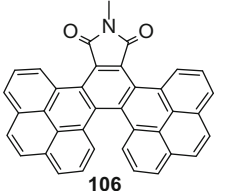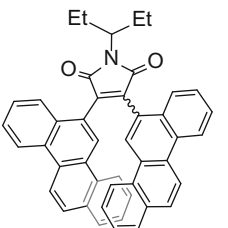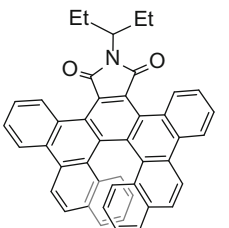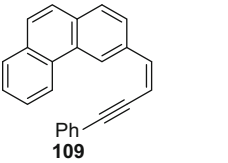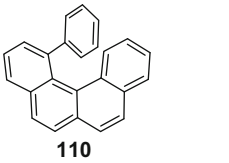
(continued)

Table 3.1 (continued)

Entry	Precursor	Condition[a]	Product[b]	Yield (%)[c]	Ref.
51	**91**	B	**92**	29	[38]
52	**93**	B	**92**	52 40	[38] [19]
53	**94**	B	**95**	10	[37]
54	**96**	B	**95**	45	[37]
55	**97**	K	**98**	7	[32]
56	**99** t-Bu	L	**100** t-Bu	40	[39]

(continued)

Table 3.1 (continued)

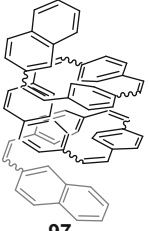| Entry	Precursor	Condition[a]	Product[b]	Yield (%)[c]	Ref.
57	*t*-Bu ... **101** ... *t*-Bu	**M**	*t*-Bu ... **102** ... *t*-Bu	81	[40]
58	*t*-Bu ... OMe *t*-Bu OMe **103**	**M**	*t*-Bu ... OMe *t*-Bu OMe **104**	70	
59	**105**	**N**	**106**	60	[41]
60	Et Et **107**	**N**	Et Et **108**	68	[41]
61	Ph **109**	**B**	**110**	60 50	[42] [43]
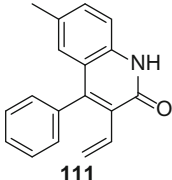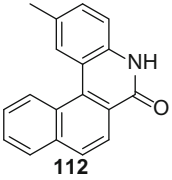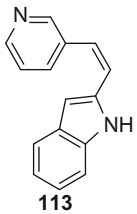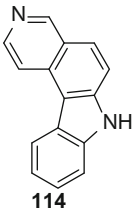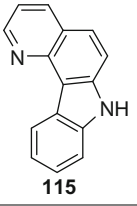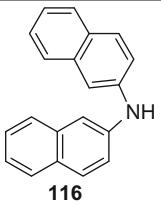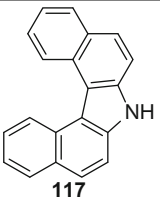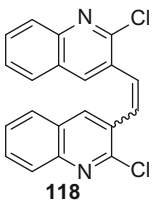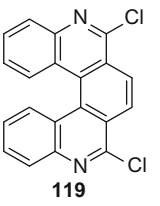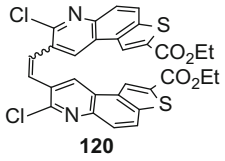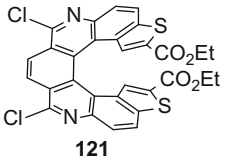
[a] Conditions: **A**, *h*v, C₆H₁₂, I₂; **B**, *h*v, benzene, I₂; **C**, *h*v, benzene, I₂, N₂; **D**, *h*v, benzene, air; **E**, *h*v, benzene, I₂, air; **F**, *h*v, benzene, I₂ (2 equiv), N₂; **G**, *h*v, benzene, I₂ (0.2 equiv), 2 h; **H**, *h*v, benzene, I₂ (2 equiv), propylene oxide, Ar, 1.2 h; **I**, *h*v, toluene, I₂; **J**, *h*v, toluene, I₂ (3 equiv), propylene oxide (50 equiv), Ar, 90 °C, 8 h; **K**, *h*v, toluene, I₂ (6 equiv), propylene oxide (100 equiv), Ar, 90 °C, 48 h; **L**, *h*v, toluene, I₂; **M**, *h*v, benzene, I₂, propylene oxide, RT, 12 h; **N**, *h*v, toluene, I₂, O₂, reflux, 16–64 h

[b] If more than one compound were listed in one Entry, all of them were separated from the raw product

[c] If more than one yield were listed, this reaction was examined by different groups
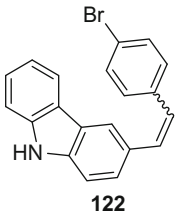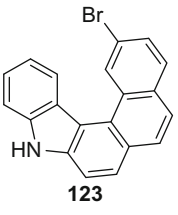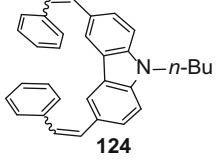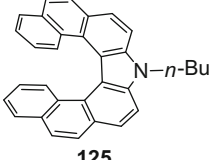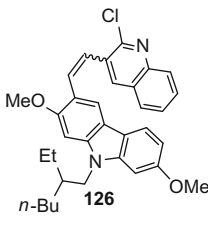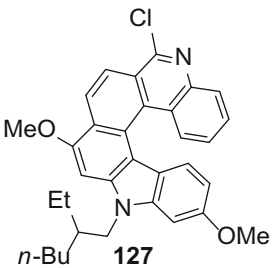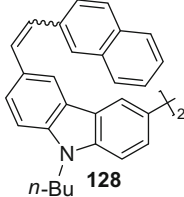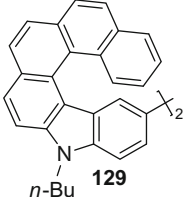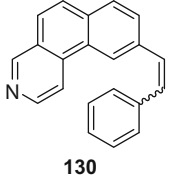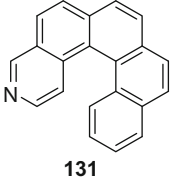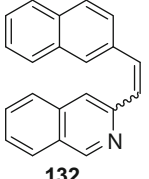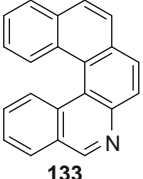
[d] N.D., not detected

Table 3.2 Synthesis of heterohelicenes by photocyclization

Entry	Precursor	Condition[a]	Product[b]	Yield (%)	Ref.
1	**111**	A	**112**	55	[47]
2	**113**	B	**114**	54	[48]
			115	32	
3	**116**	C	**117**	18	[49]
4	**118**	D	**119**	57	[50]
5	**120**	E	**121**	56	[51]
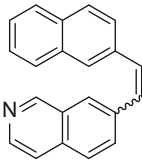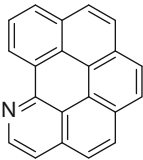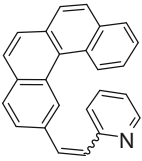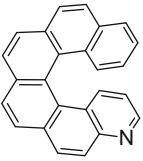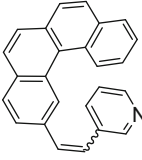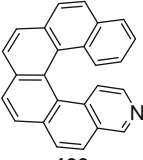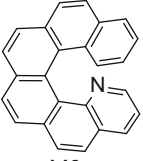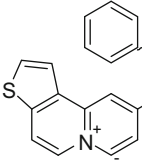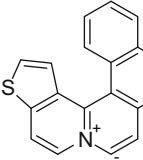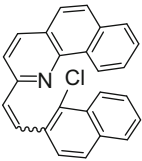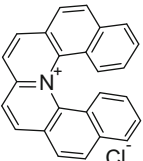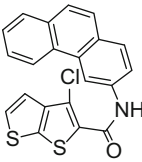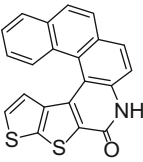
(continued)

Table 3.2 (continued)

Entry	Precursor	Condition[a]	Product[b]	Yield (%)	Ref.
6	**122**	F	**123**	76	[52]
7	**124**	F	**125**	44	[7]
8	**126**	F	**127**	53	[53]
9	**128**	F	**129**	32	[54]
10	**130**	A	**131**	95	[55]
11	**132**	G	**133**	40	[56]
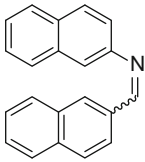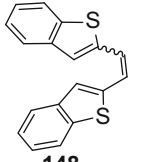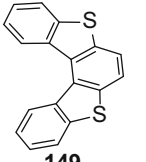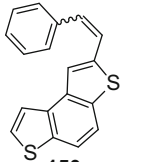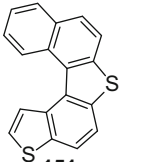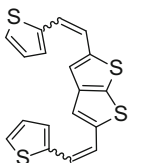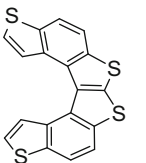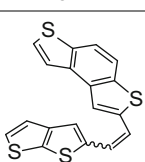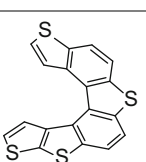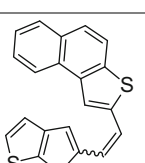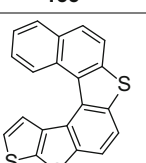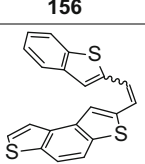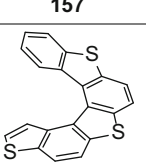
(continued)

Table 3.2 (continued)

Entry	Precursor	Condition[a]	Product[b]	Yield (%)	Ref.
12	**134**	G	**135**	98	[55]
13	**136**	H	**137**	18	[57]
14	**138**	I	**139**	50	[58]
			140	7	
15	**141** ClO$_4^-$	J	**142** ClO$_4^-$	81	[59]
16	**143**	K	**144**	40	[60]
17	**145**	L	**146**	80	[61]
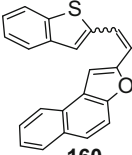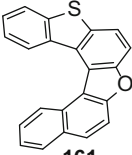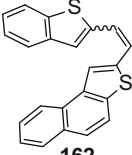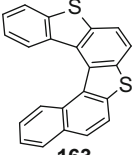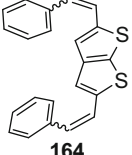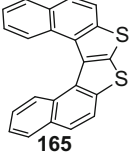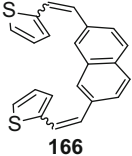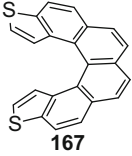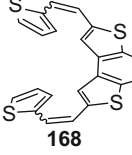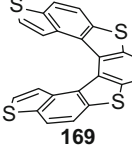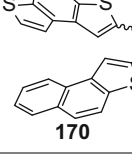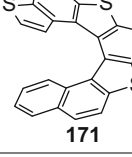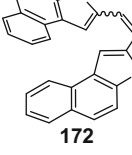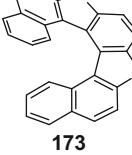
(continued)

Table 3.2 (continued)

Entry	Precursor	Condition[a]	Product[b]	Yield (%)	Ref.
18	**147**	A	/	N.R.[c]	[55]
19	**148**	A	**149**	57	[62]
20	**150**	A	**151**	50	[63]
21	**152**	A	**153**	51	[64]
22	**154**	A	**155**	69	[64]
23	**156**	A	**157**	60	[64]
24	**158**	A	**159**	40	[62]
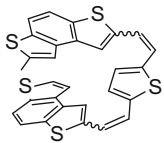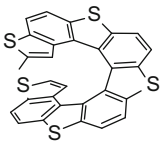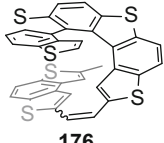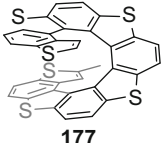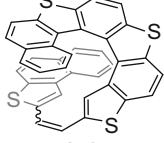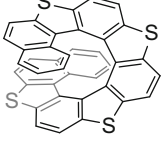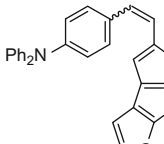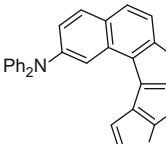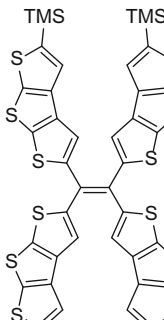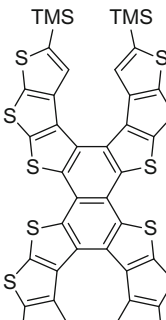
Table 3.2 (continued)

Entry	Precursor	Condition[a]	Product[b]	Yield (%)	Ref.
25	**160**	A	**161**	40	[62]
26	**162**	A	**163**	73	[62]
27	**164**	A	**165**	50	[64]
28	**166**	A	**167**	50	[64]
29	**168**	A	**169**	26	[62]
30	**170**	A	**171**	49	[62]
31	**172**	A	**173**	66	[62]
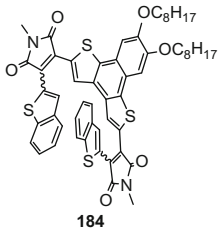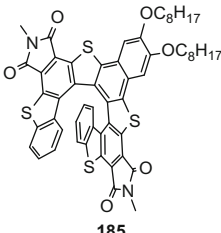
(continued)

Table 3.2 (continued)

Entry	Precursor	Condition[a]	Product[b]	Yield (%)	Ref.
32	**174**	A	**175**	18	[65]
33	**176**	A	**177**	22	[65]
34	**178**	A	**179**	14	[62]
35	**180**	A	**181**	38	[66]
36	**182**	A	**183**	70	[67]

(continued)

Table 3.2 (continued)

Entry	Precursor	Condition[a]	Product[b]	Yield (%)	Ref.
37	**184**	**M**	**185**	37	[68]

[a] Conditions: **A**, $h\nu$, benzene, I_2; **B**, $h\nu$, EtOH, I_2; **C**, $h\nu$, C_6H_{12}, air; **D**, $h\nu$, toluene, I_2, 10 h; **E**, $h\nu$, toluene, I_2, propylene oxide, 15 h; **F**, $h\nu$, THF/toluene, I_2; **G**, $h\nu$, EtOAc, 36 h; **H**, $h\nu$, benzene, I_2, air; **I**, $h\nu$, I_2, cyclohexane, propylene oxide; **J**, $h\nu$, MeOH, I_2; **K**, $h\nu$, MeCN, I_2; **L**, $h\nu$, benzene, I_2, Et_3N, heat; M, $h\nu$, toluene, I_2, 8–9 h

[b] If more than one compound were listed in one Entry, all of them were separated from the raw product

[c] N.R., no reaction

Since the first studies reported by Mallory group [1] and Dietz group [3] for [4]helicene independently and Martin group for [7]helicene [2], this method, i.e., oxidative photochemical strategy has been widely used and [4–8] and [16]carbohelicene had been synthesized (Table 3.1).

[4]Helicene could be easily prepared by [1+2] procedure in high yield using iodine as the oxidant either in benzene or cyclohexane (Entries 1–3) [1, 8, 9].

However, for [5]helicenes, great attentions need to be paid to the design of precursors. Dietz group first reported the oxidative cyclization of 1,2-di (naphthalen-2-yl)ethene **7** and 3-styrylphenanthrene **9**, which produced benzo[g, h,i]perylene **8** instead of [5]helicene via [2+2] (Entry 4) and [3+1] (Entry 5) strategy [3, 10]. Other groups [12, 15, 44] reexamined the similar reactions and obtained same results (Entries 7, 12). During the reactions, the scaffold of [5]helicene was obtained initially, which was transformed into benzo[g,h,i]perylene core immediately. Upon these studies, [5]helicene was found to be easier to be oxidized than its stilbene precursor. As an obstacle for the second cyclization, introducing functional groups like methyl (Entry 14) and phenyl (Entry 15) at C(1) position seemed to be a good choice. Nevertheless, in some cases, rearrangement or elimination happened. For example, Laarhoven and Tinnemans discovered that stilbene precursor **10** could yield benzo[a]coronene **11** by rearrangement and oxidation (Entry 6); Mallory group [12] reported an unusual fluorine atom rearrangement via a biradical intermediate giving **17** and **18** under the reaction conditions (Entry 8). To prevent the overannulation, Matsuda and coworkers found that the introduction of cyano groups to ethylene moieties could eliminate the degeneracy of unoccupied molecular orbitals (UMO) and stop the reaction after the first photocyclization [15]. According to their experimental and theoretical studies, they also indicated that if the contribution of the C_2-symmetric UMO in the excited state was smaller than

34 %, the oxidative cyclization of terminal rings could not occur; while if the contribution of the C_2-symmetric UMO in the excited state was larger than 42 %, the overannulation proceeded. For example, [5]helicene was not detected in the photochemical reaction of **27** (Entry 12), whereas dicyano [5]helicene **30** could be prepared even in 83 % yield from **29** (Entry 13). This phenomenon was also observed by Frimer and coworkers for the preparation of [5]helicene dianhydride [45]. In addition, the strain that the structure bore could also help to avoid the overannulation, like helicenophane **37** (Entry 16) [17]. Recently, Mallory and coworkers discovered an unusual rearrangement reaction of **24**, which produced [5] phenacene **25** and [5]helicene **26** (Entry 11) [14]. The two tert-butyl groups at C(*a*) and C(*b*) were necessary for this; the bigger the substituent was at C(*c*) position, the higher the yield was for the helicene product.

For [6]helicene, several strategies had been investigated as [1+4] (Entries 17, 18, and 21) [18, –20, 9, 22], [2+3] (Entries 19 and 22) [9, 22], [1+1+2] (Entry 20) [21], and [1+2+1] (Entries 23 and 24) [23, 24] methods. From these results, the yields were good and the regioselectivity did not seem to be a big problem.

As for longer helicenes, the yield was relatively lower. Taking [7]helicene as an example, using [1+1+3] or [2+4] strategy, the yields of oxidative photocyclization were not higher than 30 % (Entries 26, 30, 31 and 33) [25, 28, 29]. The [3+3] strategy was investigated: Martin and coworkers synthesized [7]helicenes from stilbene precursors **53** [2] and **56** [28] in 12.5 and 35 % yields (Entry 32), respectively; Laarhoven group utilized an inert atmosphere to promote the yield up to 50 % (Entry 25) [9, 22]. In 1991, Katz and Liu reported a method that using Br atom as a block to improve the regioselectivity assuming the bulky atom would prevent the cyclization path from occurring at its adjacent position [26]. As a result, the yield was greatly increased from 20 to 75 % (Entries 27 and 28) [21]. In the same year, Katz and coworkers proposed an improved methodology for the oxidative photocyclization reactions: adding two equivalent iodine with an excess of propylene oxide under Argon atmosphere [27]. During the reaction, the propylene oxide could scavenge the HI molecules to avoid the reduction of the stilbene precursors that have not been oxidized. In comparison with the condition using catalytic iodine in air, the yields of the helicenes were much higher in the same or even a shorter period of time via their method (Entry 29).

The synthesis of even longer helicenes was all based on similar methodology: (1) annulation of the short fragments, like benzene, naphthalene, phenanthrene, (2) annulation of the short fragments to helicene skeletons. For [8]helicene, [3+4], [2+5], and [1+1+4] methods were utilized with the yields from 30 to 85 % (Entries 34–36); the [4+4], [2+1+4], and [2+1+1+2] strategies were utilized for the synthesis of [9]helicenes (Entries 37–40), the reaction under Katz's methodology provided the highest yield of 67 % (Entry 39); the [1+3+4], [3+1+4], [3+2+3] annulations were developed for [10]helicenes in 20–81 % yields (Entries 41–44); [11]helicene could be prepared by [3+3+3], [2+3+4], [4+1+4] strategies with the yields from 54 to 84 % (Entries 45–47); and the [3+3+4], [3+4+3], [2+6+2] methods were utilized for the preparation of [12]helicene in relatively lower yields (Entries 48–50); for [13]helicene, the [4+8], [4+3+4] annulations were used with moderate yields

(Entries 51 and 52), but the [6+6] method has been reported to be not practical [46]; [4+4+4] and [3+6+3] methods were developed for [14]helicene with yield up to 45 % (Entries 53 and 54). Among these results, the yields of [2+6+2] and [3+6+3] strategies were higher than others for the preparation of [12]helicene and [14]helicene, respectively, which might result from the enhanced π–π interaction when a [6]helicene core presented.

Recently, [2+1+1+2+1+1+2] method was proposed by Mori, Murase, and Fujita to synthesize the longest [16]helicene in 7 % yield via constructing six benzene rings in one step which was demonstrated by X-ray crystallographic study (Entry 55), as well as the [9]helicene (Entry 39) [32]. This method, the photocyclization of an oligomer composed by phenylene and naphthalene units connected by vinylene groups, avoided the tedious synthesis of helicene moieties for constructing the longer one, and avoided the presence of [5]helicene unit during the cyclization to prevent the overannulation as well.

In addition, by photochemical reaction, PAHs, like pyrene, chrysene, and picene, could be annulated to the helical scaffold, giving the molecules with enhanced photophysical properties (Entries 56–60).

Besides the stilbene precursors, helicenes could also be prepared from diarylbut-1-en-3-yne precursors (Entry 61) [43, 42].

For the synthesis of heterohelicenes by photocyclization, nearly all the reported reactions are based on the stilbene precursors with two aryl groups bearing heteroaromatic rings with N and S atoms, while oxahelicenes achieved using this method were seldom reported. In addition to the stilbene precursors, some exceptions were also reported. For example, 2-vinyl-1,1'-biaryl **111** could be transformed into [4]heterohelicenes **112** under radiation in 55 % yield (Entry 1) [47]; di (naphthalen-2-yl)amine **116** could be transformed into aza [5]helicene **117**, but the yield was only 18 % (Entry 3) [49]. By incorporating heteroaromatic rings, helicenes showed different chemical and physical properties. For heterohelicenes, (1) the ones with pyridine rings could be used as chiral organic bases, which find applications in catalysis (Entry 14); and if the N atom is charged, the molecule could be utilized as a kind of water-soluble dye with helicity (Entries 15–16); (2) the ones with pyrrole rings could be applicable for the opto-electric materials (Entries 5–9); (3) the ones with thiophene rings could be good candidates for chirality-responsive materials (Entries 19–37).

As for the synthesis, the presence of heteroaromatic rings affected the reactivity of precursors. Different from carbohelicenes, the positions of nitrogen atoms greatly affected the overannulation of [5]helicene: in some reported reactions (Entries 3–4, 6, and 10–11), the overannulation was not observed, while precursor **134** smoothly underwent double photocyclization to give **135** even in 98 % yield (Entry 12).

For carbohelicenes, one problem is the regioselectivity for the precursors that have two six-membered rings connected to the ethylene unit, like Entries 2 and 14. A solution is to introduce a functional group to improve the selectivity, such as Entries 4, 5, and 8. If two five-membered rings are connected to ethylene unit, the regioselectivity is not a problem.
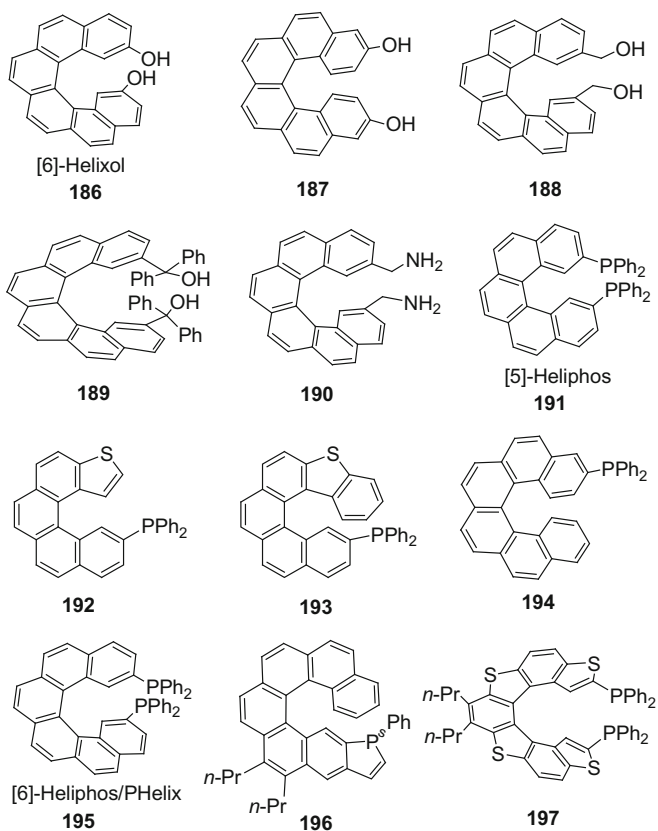
Fig. 3.1 Some functionalized helicenes prepared by photocyclization

Based on this methodology, optically active helicene could be obtained after resolution, which makes these molecules applicable in chiroptical materials, asymmetric synthesis, and chiral sensors [4, 69–72]. Some interesting helicenes are listed in Fig. 3.1, including diols **186** [73], **187** [74], **188** [75], **189** [75], diamine **190** [75], and phosphines **191** [76], **192** [77], **193** [78], **194** [79], **195** [80], **196** [81], **197** [82]. Brunner [76], Reetz [80], and coworkers independently synthesized the first helical phosphine ligands **191** and **195**, which have been used in asymmetric hydrogenation. Marenneti and coworkers developed the first phosphaindole incorporated helicenes, like **196**, which have been utilized in asymmetric cyclization [70].

Although this methodology has been widely utilized, there are some limitations [4]. First, it is difficult to be used for large-scale preparation, because the photocyclization needs highly diluted solution (usually ca. 10^{-3} M) to prevent the [2+2] intermolecular cycloaddition. If large quantity of solvent is used, safety issues should be seriously concerned, since the solvents are all extremely flammable and

Fig. 3.2 A setup for continuous flow synthesis. Reprinted with the permission from [83]. Copyright 2013 Beilstein-Institut

volatile. Second, the reaction lacks the tolerance to amino- and nitro-groups, which would accelerate the process of intersystem crossing. Third, if the difference between the polarity of the target helicene and by-products (for example, the regioisomers) is small, it is difficult to be purified.

Recently, chemists found a solution—the continuous flow strategy—to solve the problem of large-scale preparation. The experiment needs a small setup (Fig. 3.2) [83], including (1) FEP tubing (fluorinated ethylene polymer tubing, which is highly transmittable, flexible, and anticorrosive) with suitable inner/outer diameters, (2) a suitable lamp, and (3) a pump. To improve the efficiency, the reaction is usually covered by aluminum foil. The amount of additives, the concentration of stilbene precursors, and the flow rate are the key factors to be carefully screened to obtain the optimal reaction conditions. Collins and coworkers [84] reported the first example of the preparation of [5]helicene by continuous flow strategy (Scheme 3.1). In comparison with the traditional method via batch reaction, this new method not only shortened the reaction time from 5 days to 10 h under visible light with a higher yield in the presence of Cu complex formed in situ, but also prevented the overannulation and achieved large-scale preparation. Recently, similar method was utilized by the same group for the synthesis of pyrene–helicene hybrid compounds [85]. Rueping and coworkers used an UV lamp as the light
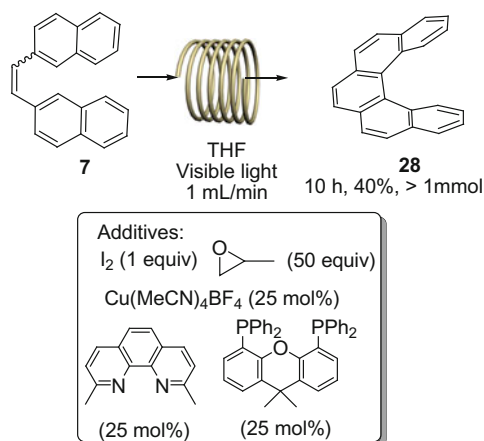
Scheme 3.1 Synthesis of [5]helicene using visible light
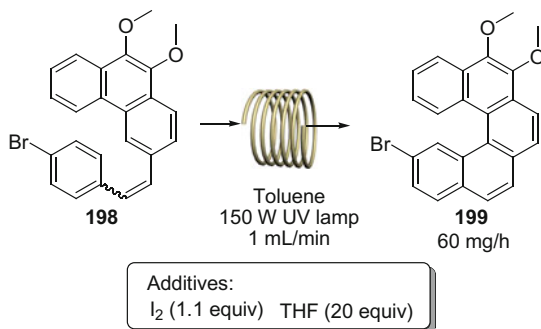
Scheme 3.2 Synthesis of bromo [5]helicene using UV light

source to prepare phenanthrene, [4]- and [5]helicenes (Scheme 3.2) [83]. In the reaction, 1.1 equivalent iodine was added, and THF was used as HI scavenger. Under the optimal condition, the helicene could be prepared at the rate of 60 mg/h.

References

1. Mallory FB, Mallory CW, Halpern EJ (1966) Paper presented at the first middle atlantic regional meeting of the American chemical society, Philadelphia
2. Flammang-Barbieux M, Nasielski J, Martin RH (1967) Synthesis of heptahelicene (1) benzo [c]phenanthro [4, 3-g]phenanthrene. Tetrahedron Lett 8(8):743–744
3. Scholz M, Mühlstädt M, Dietz F (1967) Chemie angeregter zustände. I. Mitt. Die richtung der photocyclisierung naphthalinsubstituierter äthylene. Tetrahedron Lett 8(7):665–668

4. Shen Y, Chen C-F (2012) Helicenes: synthesis and applications. Chem Rev 112(3):1463–1535

5. Gingras M (2013) One hundred years of helicene chemistry. part 1: non-stereoselective syntheses of carbohelicenes. Chem Soc Rev 42(3):968–1006

6. Hoffmann N (2014) Photochemical reactions applied to the synthesis of helicenes and helicene-like compounds. J Photochem Photobio C: Photochem Rev 19:1–19

7. Upadhyay GM, Talele HR, Sahoo S, Bedekar AV (2014) Synthesis of carbazole derived aza [7]helicenes. Tetrahedron Lett 55(39):5394–5399

8. Mallory FB, Regan CK, Bohen JM, Mallory CW, Bohen AA, Carroll PJ (2015) Discovery of deep-seated skeletal rearrangements in the photocyclizations of some tert-butyl-substituted 1,2-diarylethylenes. J Org Chem 80(1):8–17

9. Laarhoven WH, Boumans PGF (1975) Photodehydrocyclizations of stilbene-like compounds XIV photosynthesis and photoreactions of 1,2- and 1,14-diphenylpentahelicene derivatives. Recl Trav Chim Pays-Bas 94(5):114–118

10. Morgan DD, Horgan SW, Orchin M (1972) Photocyclization of stilbene analogs II. the photochemistry of 1-benzylidene-1,2,3,4-tetrahydrophenanthrene and 1-(1-naphthylmethylidene)-1,2,3,4-tetrahydrophenanthrene. Tetrahedron Lett 13(18):1789–1792

11. Laarhoven WH, Cuppen TJHM, Nivard RJF (1970) Photodehydrocyclizations in stilbene-like compounds—II. Tetrahedron 26(4):1069–1083

12. Dietz F, Scholz M (1968) Chemie angeregter zustände-IV: die photocyclisierung der drei isomeren distyrylbenzole. Tetrahedron 24(24):6845–6849

13. Mallory FB, Mallory CW (1983) An unusual fluorine atom rearrangement in the photocyclization of 1-fluoro[5]helicenes. J Org Chem 48(4):526–532

14. Ito N, Hirose T, Matsuda K (2014) Facile photochemical synthesis of 5,10-disubstituted [5]helicenes by removing molecular orbital degeneracy. Org Lett 16(9):2502–2505

15. Bedekar AV, Chaudhary AR, Shyam Sundar M, Rajappa M (2013) Expeditious synthesis of fluorinated styrylbenzenes and polyaromatic hydrocarbons. Tetrahedron Lett 54(5):392–396

16. Frimer AA, Kinder JD, Youngs WJ, Meador MAB (1995) Reinvestigation of the photocyclization of 1,4-Phenylene Bis(Phenylmaleic Anhydride)—preparation and structure of [5]Helicene 5,6-9,10-Dianhydride. J Org Chem 60(6):1658–1664

17. Thulin B, Wennerström O (1976) Propellicene or Bi-2,13-pentahelicenylene. Acta Chem Scand 30B:688–690

18. Moradpou A, Nicoud JF, Balavoin G, Kagan H, Tsoucari G (1971) Photochemistry with circularly polarized light—synthesis of optically active Hexahelicene. J Am Chem Soc 93(9):2353–2354

19. Moradpour A, Kagan H, Baes M, Morren G, Martin RH (1975) Photochemistry with circularly polarized light—III: synthesis of helicenes using bis(arylvinyl) arenes as precursors. Tetrahedron 31(17):2139–2143

20. Biet T, Fihey A, Cauchy T, Vanthuyne N, Roussel C, Crassous J, Avarvari N (2013) Ethylenedithio-Tetrathiafulvalene-Helicenes: electroactive helical precursors with switchable chiroptical properties. Chem Eur J 19(39):13160–13167

21. Laarhove Wh, Brus GJM (1971) Polarographic data and deviations from coplanarity of helicene molecules. J Chem Soc B-Phys Org 7:1433–1434

22. Martin RH, Marchant M-J, Baes M (1971) Rapid syntheses of hexa and heptahelicene. Helv Chim Acta 54(1):358–360

23. Borkent JH, Laarhoven WH (1978) Thermal racemization of methyl-substituted hexahelicenes. Tetrahedron 34(16):2565–2567

24. Schwertel M, Hillmann S, Meier H (2013) Synthesis of highly substituted hexahelicenes. Helv Chim Acta 96(11):2020–2032

25. Martin RH, Flammang M, Cosyn JP, Gelbcke M (1968) 1. × .2. New syntheses of hexa- and heptahelicences. 3. Optical rotation and ord of heptahelicene. Tetrahedron Lett (31):3507–3510

26. Joly M, Defay N, Martin RH, Declerq JP, Germain G, Soubrierpayen B, Vanmeerssche M (1977) Bridged helicenes—3,15-ethano-[7]helicene and 3,15-(2-oxapropano)-[7]helicene—synthesis, h-1-nmr spectrography and x-ray-diffraction study. Helv Chim Acta 60(2):537–560

27. Martin RH, Eyndels C, Defay N (1974) Double helicenes: diphenanthro[4,3-a; 3′,4′-[o]picene and benzo[s]diphenanthro[4,3-a; 3′,4′-[o]picene. Tetrahedron 30(18):3339–3342

28. Liu LB, Katz TJ (1991) Bromine auxiliaries in photosyntheses of [5]helicenes. Tetrahedron Lett 32(47):6831–6834

29. Liu LB, Yang BW, Katz TJ, Poindexter MK (1991) Improved methodology for photocyclization reactions. J Org Chem 56(12):3769–3775

30. Tinnemans AHA, Laarhoven WH (1974) Photodehydrocyclizations in stilbene-like compounds. IX. 1,2-Phenyl shifts in the cyclization of 1-phenylpentahelicenes. J Am Chem Soc 96(14):4611–4616

31. Mallory FB, Mallory CW, Ricker WM (1975) Nuclear spin-spin coupling via nonbonded interactions. III. Effects of molecular structure on through-space fluorine-fluorine and hydrogen-fluorine coupling. J Am Chem Soc 97(16):4770–4771

32. Roose J, Achermann S, Dumele O, Diederich F (2013) Electronically connected [n]Helicenes: synthesis and chiroptical properties of enantiomerically pure (E)-1,2-Di([6]helicen-2-yl) ethenes. Eur J Org Chem 2013 (16):3223–3231

33. Mori K, Murase T, Fujita M (2015) One-step synthesis of [16]helicene. Angew Chem Int Ed 54(23):6847–6851

34. Tinnemans AHA, Laarhoven WH (1976) Photocyclisations of 1,4-diarylbut-1-en-3-ynes. Part III. Scope and limitations of the reaction. J Chem Soc, Perkin Trans 2 (10):1115–1120

35. Tinnemans AHA, Laarhoven WH (1973) A novel photocyclization, starting from 1,4-diarylbutenynes. Tetrahedron Lett 14(11):817–820

36. Veeramani K, Paramasivam K, Ramakrishnasubramanian S, Shanmugam P (1978) Photolysis of 4-Phenyl-3-vinylquinolines; a facile new route to the Benzo[k]phenanthridine System. Synthesis 1978 (11):855–857

37. Schultz AG, Hagmann WK (1978) Synthesis of indole-2-carboxylic esters. J Org Chem 43 (17):3391–3393

38. Gingras M (2013) One hundred years of helicene chemistry. part 3: applications and properties of carbohelicenes. Chem Soc Rev 42(3):1051–1095

39. Aillard P, Voituriez A, Marinetti A (2014) Helicene-like chiral auxiliaries in asymmetric catalysis. Dalton Trans 43(41):15263–15278

40. Saleh N, Shen C, Crassous J (2014) Helicene-based transition metal complexes: synthesis. Properties and Applications. Chem Sci 5(10):3680–3694

41. Virieux D, Sevrain N, Ayad T, Pirat J-L (2015) Chapter two—helical phosphorus derivatives: synthesis and applications. In: Eric FVS, Christopher AR (eds) Advances in heterocyclic chemistry, vol Volume 116. Academic Press, pp 37–83. doi:http://dx.doi.org/10.1016/bs.aihch.2015.06.001

42. Reetz MT, Sostmann S (2001) 2,15-dihydroxy-hexahelicene (HELIXOL): synthesis and use as an enantioselective fluorescent sensor. Tetrahedron 57(13):2515–2520

43. Aloui F, El Abed R, Marinetti A, Ben Hassine B (2009) A new approach to 3,14-dihydroxyhexahelicene: resolution and attribution of the absolute configuration. C R Chim 12(1–2):284–290

44. Wachsmann C, Weber E, Czugler M, Seichter W (2003) New functional hexahelicenes–synthesis, chiroptical properties, X-ray crystal structures, and comparative data bank analysis of hexahelicenes. Eur J Org Chem 15:2863–2876

45. Terfort A, Gorls H, Brunner H (1997) The first helical-chiral phosphane ligands: rac-[5]- and rac-[6]-heliphos. Synthesis-Stuttgart 1:79–86

46. Moussa S, Aloui F, Hassine BB (2013) Synthesis and characterization of a new chiral pentacyclic phosphine. Synth Commun 43(2):268–276

47. Aloui F, Moussa S, Hassine BB (2011) Synthesis and characterisation of a new helically chiral ruthenium complex. Tetrahedron Lett 52(5):572–575

48. Aloui F, Hassine BB (2009) An alternative approach to 3-(diphenylphosphino)hexahelicene. Tetrahedron Lett 50(30):4321–4323
49. Reetz MT, Beuttenmuller EW, Goddard R (1997) First enantioselective catalysis using a helical diphosphane. Tetrahedron Lett 38(18):3211–3214
50. Yavari K, Moussa S, Ben Hassine B, Retailleau P, Voituriez A, Marinetti A (2012) 1H-phosphindoles as structural units in the synthesis of chiral helicenes. Angew Chem Int Ed 51 (27):6748–6752
51. Monteforte M, Cauteruccio S, Maiorana S, Benincori T, Forni A, Raimondi L, Graiff C, Tiripicchio A, Stephenson GR, Licandro E (2011) Tetrathiaheterohelicene phosphanes as helical-shaped chiral ligands for catalysis. Eur J Org Chem 2011 (28):5649–5658
52. Lefebvre Q, Jentsch M, Rueping M (2013) Continuous flow photocyclization of stilbenes–scalable synthesis of functionalized phenanthrenes and helicenes. Beilstein J Org Chem 9:1883–1890
53. Hernandez-Perez AC, Vlassova A, Collins SK (2012) Toward a visible light mediated photocyclization: Cu-based sensitizers for the synthesis of [5]helicene. Org Lett 14(12):2988–2991
54. Bédard A-C, Vlassova A, Hernandez-Perez AC, Bessette A, Hanan GS, Heuft MA, Collins SK (2013) Synthesis, crystal structure and photophysical properties of pyrene-helicene hybrids. Chem Eur J 19(48):16295–16302
55. Kagan H, Moradpou.A, Nicoud JF, Balavoin.G, Martin RH, Cosyn JP (1971) Photochemistry with circularly polarised light .2. Asymmetric synthesis of octa and nonahelicene. Tetrahedron Lett (27):2479–2482
56. Martin RH, Cosyn JP (1971) New synthesis of octahelicene involving non-interconvertible Dl—intermediates. Synth Commun 1(4):257–265
57. Cochez Y, Martin RH, Jespers J (1976) Helicenes: chemically induced asymmetric photosyntheses of helicenes skeletons. Isr J Chem 15(1–2):29–32
58. Laarhove Wh, Cuppen HJM (1973) Photodehydrocyclizations of stilbene-like compounds. 7. Synthesis and properties of double helicene, diphenanthro[3,4-C;3',4'-L]chrysene. Recueil Des Travaux Chimiques Des Pays-Bas 92 (4):553–562
59. Laarhove Wh, Cuppen JHM (1971) Photodehydrocyclizations of stilbene-like compounds. 4. Synthesis of a double helicene rac and meso diphenanthro 3,4-C-3'4-1 chrysene. Tetrahedron Lett 2:163–164
60. Martin RH, Defay N, Eyndels C (1972) Studies in helicene series—determination of structure and of Dl configuration of a double helicene by indor and noe experiments. 18. Tetrahedron Lett 27:2731–2732
61. Martin RH, Baes M (1975) Helicenes–photosyntheses of [11]helicene, [12]helicene and [14]helicene. Tetrahedron 31(17):2135–2137
62. Martin RH, Morren G, Schurter JJ (1969) [13]helicene and [13]helicene-10,21-D2. Tetrahedron Lett 42:3683–3684
63. Hu J-Y, Feng X, Paudel A, Tomiyasu H, Rayhan U, Thuéry P, Elsegood MRJ, Redshaw C, Yamato T (2013) Synthesis, structural, and photophysical properties of the first member of the class of pyrene-based [4]helicenes. Eur J Org Chem 2013 (26):5829–5837
64. Hu J-Y, Paudel A, Seto N, Feng X, Era M, Matsumoto T, Tanaka J, Elsegood MRJ, Redshaw C, Yamato T (2013) Pyrene-cored blue-light emitting [4]helicenes: synthesis, crystal structures, and photophysical properties. Org Biomol Chem 11(13):2186–2197
65. Bock H, Subervie D, Mathey P, Pradhan A, Sarkar P, Dechambenoit P, Hillard EA, Durola F (2014) Helicenes from diarylmaleimides. Org Lett 16(6):1546–1549
66. De Silva O, Snieckus V (1971) Photochemical synthesis of Benzo[c]carbazole and Pyridocarbazoles. Synthesis 1971 (05):254–255
67. Waghray D, Zhang J, Jacobs J, Nulens W, Basarić N, Meervelt LV, Dehaen W (2012) Synthesis and structural elucidation of diversely functionalized 5,10-Diaza[5]Helicenes. J Org Chem 77(22):10176–10183

68. Waghray D, Cloet A, Van Hecke K, Mertens SFL, De Feyter S, Van Meervelt L, Van der Auweraer M, Dehaen W (2013) Diazadithia[7]Helicenes: synthetic exploration, solid-state structure, and properties. Chem Eur J 19 (36):12077-12085
69. Ben Braiek M, Aloui F, Moussa S, Tounsi M, Marrot J, Ben Hassine B (2013) Synthesis, X-ray analysis and photophysical properties of a new N-containing pentacyclic helicene. Tetrahedron Lett 54(40):5421–5425
70. Bucinskas A, Waghray D, Bagdziunas G, Thomas J, Grazulevicius JV, Dehaen W (2015) Synthesis, functionalization, and optical properties of Chiral Carbazole-based Diaza [6] Helicenes. J Org Chem 80(5):2521–2528
71. Upadhyay GM, Bedekar AV (2015) Synthesis and photophysical properties of bi-aza[5] Helicene and bi-aza[6]Helicene. Tetrahedron 71(34):5644–5649
72. Abbate S, Bazzini C, Caronna T, Fontana F, Gambarotti C, Gangemi F, Longhi G, Mele A, Sora IN, Panzeri W (2006) Monoaza[5]Helicenes. Part 2: synthesis, characterisation and theoretical calculations. Tetrahedron 62(1):139–148
73. Bazzini C, Brovelli S, Caronna T, Gambarotti C, Giannone M, Macchi P, Meinardi F, Mele A, Panzeri W, Recupero F, Sironi A, Tubino R (2005) Synthesis and characterization of some Aza[5]Helicenes. Eur J Org Chem 7:1247–1257
74. Martin RH, Deblecker M (1969) Synthesis of 4-Azahexahelicene (benzo[c]Phénanthro[1,2-f] Quinoline). Tetrahedron Lett 10(41):3597–3598
75. Aloui F, El Abed R, Ben Hassine B (2008) Synthesis of a new N-containing Hexahelicene. Tetrahedron Lett 49(9):1455–1457
76. Sato K, Yamagishi T, Arai S (2000) Synthesis of novel Azonia[5]Helicenes containing terminal thiophene rings. J Heterocycl Chem 37(4):1009–1014
77. Arai S, Ishikura M, Yamagishi T (1998) Synthesis of polycyclic azonia-aromatic compounds by photo-induced intramolecular quaternization: azonia derivatives of benzo[c]Phenanthrene, [5]Helicene and [6]Helicene. J Chem Soc Perkin Trans 1(9):1561–1567
78. Luo JK, Federspiel RF, Castle RN (1997) The synthesis of novel polycyclic heterocyclic ring systems via photocyclization. 19. Thieno[3',2':4,5]thieno[2,3-c]-naphtho[1,2-f]quinoline, thieno[3',2':4,5]thieno[2,3-c]naphtho[1,2-f][1,2,4]triazolo[4,3-a]quinoline and thieno [3',2':4,5]-thieno[2,3-c]naphtho[1,2-f]tetrazolo[1,5-a]quinoline. J Heterocycl Chem 34 (5):1597–1601
79. Groen MB, Schadenb H, Wynberg H (1971) Synthesis and resolution of some heterohelicenes. J Org Chem 36 (19):2797-2809
80. Tedjamulia ML, Tominaga Y, Castle RN, Lee ML (1983) The synthesis of benzo[b] phenanthro[d]thiophenes and anthra[b]benzo[d]thiophenes. J Heterocycl Chem 20(4):861–866
81. Dopper JH, Oudman D, Wynberg H (1973) Use of thieno[2,3-b]thiophene in synthesis of heterohelicenes by double photocyclizations. J Am Chem Soc 95(11):3692–3698
82. Lehman P, Wynberg H (1974) The synthesis of a series of regularly annelated 2-methylheterohelicenes. Aust J Chem 27(2):315–322
83. Li C, Zhang Y, Zhang S, Shi J, Kan Y, Wang H (2014) From N, N-diphenyl-N-naphtho [2,1-b]thieno[2,3-b:3',2'-d]dithiophene-5-yl-amine to propeller-shaped N, N, N-tri(naphtho [2,1-b]thieno[2,3-b:3',2'-d]dithiophene-5-yl)-amine: syntheses and structures. Tetrahedron 70 (25):3909–3914
84. Liu X, Yu P, Xu L, Yang J, Shi J, Wang Z, Cheng Y, Wang H (2013) Synthesis for the mesomer and racemate of thiophene-based double helicene under irradiation. J Org Chem 78 (12):6316–6321
85. Waghray D, Dehaen W (2013) A fragment based approach toward thia[n]helicenes. Org Lett 15(12):2910–2913

Chapter 4
Diels–Alder and Friedel–Crafts-Type Reactions
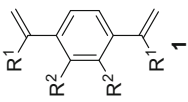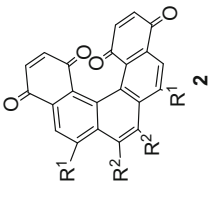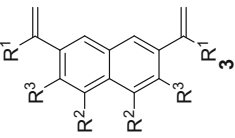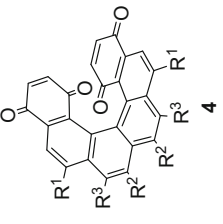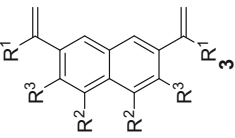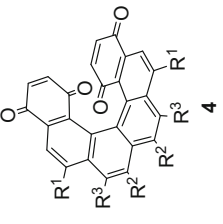
Abstract In this chapter, the synthesis of helicenes via Diels–Alder reactions and Friedel–Crafts-type reactions is described. In the first section, the Diels–Alder reactions are discussed, which not only are practical methods for the preparation of symmetric helicenes, but also can be utilized for the large-scale synthesis of helicene derivatives, especially helicene quinones. The major limitation of the methodology is the limited types of dienes and dienophiles. In the second section, Friedel–Crafts-type reaction is introduced, which is one of the first reported and also a useful strategy for the synthesis of helicenes. The synthesis usually needs less than five steps with moderate-to-good yields. Similarly, heterohelicenes including azahelicenes and phosphahelicene can be synthesized by double Friedel–Crafts acylation or phospha-Friedel–Crafts reaction. Two points should be taken into account in Friedel–Crafts-type reaction: (1) polar unsaturated bonds should be well designed and incorporated into the substrates; (2) it is better to introduce the directing or blocking groups to promote the regioselectivity.

Keywords Diels–alder reaction · Dienes and dienophiles · Friedel–Crafts-type reaction · Helicene quinone · Phosphahelicene · Regioselectivity

4.1 Diels–Alder Reactions
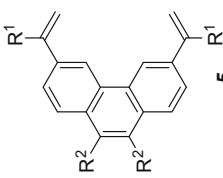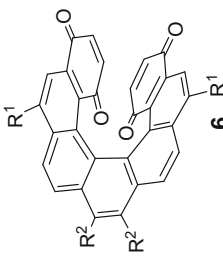
The Diels–Alder reaction was first utilized in 1990 by Katz and Liu [1], which for the first time achieved the large-scale synthesis of helicene bisquinones (Table 4.1, Entry 1). By the reaction between excess *p*-benzoquinone (12–14 equivalents) and the divinylbenzene **1a**, [5]helicene **2** could be obtained in grams by one step. Herein, the quinone performed not only as the dienophile, but also the oxidant that aromatized the Diels–Alder adduct. Similarly, [6]- and [7]helicenes could be prepared via the same methodology (Table 4.1, Entries 2–16). By comparison of them, it was suggested that incorporating the electron-donating functional groups to the diene precursors would greatly promote the yields, which was also predicted by the FMO calculations [2–4]. For example, the yields of the reactions, in which the

Table 4.1 The synthesis of helicenes by Diels–Alder reactions

Entry	Dienes	Dienophiles[a]	Cond.[b]	Time (h)	Products	Yield (%)	Ref.
	1				**2**		
1	**a** $R^1=R^2=H$	p-BQ (12–14 equiv.)	A	33	**a**	17	[1, 16]
2	**b** $R^1=H$, $R^2=On$-$C_{12}H_{25}$	p-BQ (12–14 equiv.)	A	33	**b**	24	[16]
3	**c** $R^1=On$-$C_{12}H_{25}$, $R^2=H$	p-BQ (12–14 equiv.)	B	62	**c**	50	[16, 17]
4	**d** $R^1=$OTIPS, $R^2=H$	p-BQ (12–14 equiv.)	B	108	**d**	74	[16]
	3				**4**		
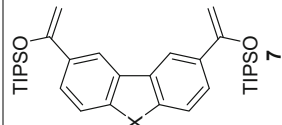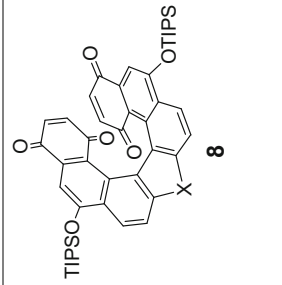
(continued)

Table 4.1 (continued)

Entry	Dienes	Dienophiles[a]	Cond.[b]	Time (h)	Products	Yield (%)	Ref.
5	**a** $R^1=R^2=R^3=H$	p-BQ (12–14 equiv.)	**A**	12	**a**	6	[16, 17]
6	**b** $R^1=R^2=H$, $R^3=On$-$C_{12}H_{25}$	p-BQ (12–14 equiv.)	**A**	21	**b**	11[c]	[16]
7	**c** $R^1=On$-$C_{12}H_{25}$, $R^2=R^3=H$	p-BQ (12–14 equiv.)	**B**	49	**c**	54	[16]
8	**d** $R^1=R^2=OTIPS$, $R^3=H$	p-BQ (15–20 equiv.)	**C**	156	**d**	40	[18]
	5				**6**		
9	**a** $R^1=OTIPS$, $R^2=O(Ph_2C)_{1/2}$	p-BQ (15–20 equiv.)	**C**	63	**a**	22	[19]
10	**b** $R^1=OTIPS$, $R^2=OTBDMS$	p-BQ (15–20 equiv.)	**C**	86	**b**	37	[19]
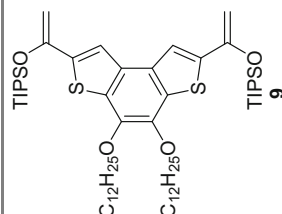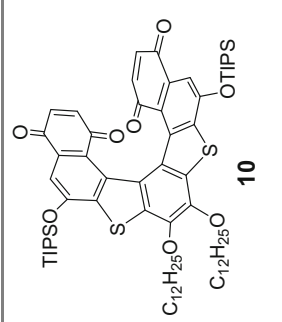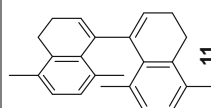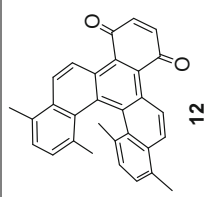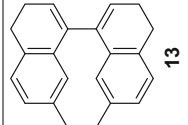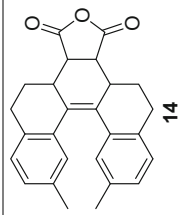
(continued)

Table 4.1 (continued)

Entry	Dienes	Dienophiles[a]	Cond.[b]	Time (h)	Products	Yield (%)	Ref.
11	**c** R^1=OTIPS, R^2=On-C$_{12}$H$_{25}$	p-BQ (15–20 equiv.)	C	96	**c**	20	[20]
12	**a** X=O	p-BQ (30 equiv.)	D	48	**a**	39	[21]
13	**b** X=S	p-BQ (30 equiv.)	E	24	**b**	33	[21]
14	**c** X=NMe	p-BQ (30 equiv.)	F	11	**c**	53	[21]
15	**d** X=Nn-C$_{12}$H$_{25}$	p-BQ (30 equiv.)	G	14	**d**	50	[21]

Dienes structure **7** (TIPSO ... X ... TIPSO); Product structure **8** (TIPSO ... X ... OTIPS)
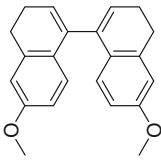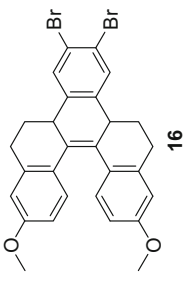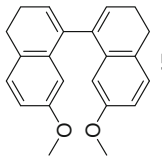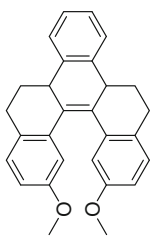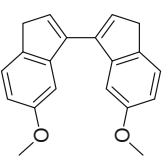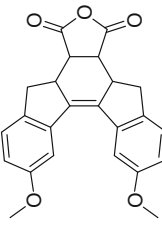
Table 4.1 (continued)

Entry	Dienes	Dienophiles[a]	Cond.[b]	Time (h)	Products	Yield (%)	Ref.
16	**9**	p-BQ (15 equiv.)	**H**	30	**10**	95	[22]
17	**11**	p-BQ (10 equiv.)	**I**	98	**12**	62	[23]
18	**13**	Maleic anhydride	**J**	3	**14**	73	[24]

(continued)

Table 4.1 (continued)

Entry	Dienes	Dienophiles[a]	Cond.[b]	Time (h)	Products	Yield (%)	Ref.
19	**15**	**BZ-1**	**K**	6	**16**	26	[25]
20	**17**	**BZ-2** (2 equiv.)	**L**	6	**18**	71	[26]
21	**19**	Maleic anhydride (10 equiv.)	**M**	4	**20**	81	[27]

(continued)

Table 4.1 (continued)

Entry	Dienes	Dienophiles[a]	Cond.[b]	Time (h)	Products	Yield (%)	Ref.
	21				**22**		
22	**a** R^1=Br, R^2=Me	**BZ-2** (2 equiv.)	**N**	2	**a**	76	[15]
23	**b** R^1=Me, R^2=Br	**BZ-2** (2 equiv.)	**N**	2	**b**	83	[15]
24	**23**	1,4-naphthoquinone (3 equiv.)	**O**	48	**24**	56	[28]

[a]Dienophiles: p-BQ, p-benzoquinone; **BZ-1**, 1.15 equiv. of 1,2,4,5-tetrabromobenzene, 1.59 equiv. of t-BuLi; **BZ-2**, 2 equiv. of 2-carboxylbenzenediazonium chloride; [b]Conditions: **A**, toluene, CCl₃CO₂H (cat.), N₂, reflux; **B**, toluene, basic alumina, reflux; **C**, toluene, Ar or N₂, reflux; **D**, toluene, 100 °C; **E**, toluene, 110 °C; **F**, toluene, N₂, 90 °C; **G**, toluene, N₂, 85 °C; **H**, heptane, reflux; **I**, toluene, reflux; **J**, xylene, reflux; **K**, toluene, −20 °C; **L**, 1,2-dichloroethane (DCE), 2-methyloxirane, reflux; **M**, 150 °C; **N**, DCE, 2-methyloxirane, reflux; **O**, AcOH, reflux. [c]Not fully purified

dienes with alkoxy or silane moieties, were higher than that of parent dienes. According to the results, the basic condition was beneficial to the Diels–Alder reaction and gave helicenes in higher yields than the acidic condition (Table 4.1, Entries 2–16). By introducing one or two benzoquinone moieties, helicenes could be further modified, and several useful applications of the functionalized helicenes have been reported, such as asymmetric catalysis [5], helical metal phthalocyanine derivatives [6], helical conjugated ladder polymers [7, 8], chiral recognition [9, 10], LB film [11, 12], and enhanced nonlinear optical properties [13]. Carreño, Urbano, and colleagues [14] developed the asymmetric synthesis of helicenes via the Diels–Alder reaction between a chiral benzoquinone and different dienes, which will be introduced in asymmetric synthesis afterward.

In addition to the dienes with vinyl part, 3,3′,4,4′-tetrahydro-1,1′-binaphthalene-type derivatives have been widely accepted as the diene precursors for the construction of functionalized [5]helicenes, because (1) the dienes could be easily synthesized from cheap, readily available industrial raw material, such as tetralones, indanones; (2) different dienophiles could be utilized to produce helicenes with various substituents, like benzoquinone (Table 4.1, Entry 16), maleic anhydride (Table 4.1, Entry 21), benzynes formed in situ (Table 4.1, Entries 19, 20, 22, 23), naphthoquinone (Table 4.1, Entry 24); (3) the reactions were usually highly efficient with moderate to good yields, providing the Diels–Alder adducts in gram scale. After aromatization, substituted [5]helicenes could be obtained. This method was limited by the substrates, in which the diene precursors for [6]-, [7]-, and longer helicenes usually need multistep and complicated synthetic procedures. Recently, Chen and co-workers demonstrated that the methyl groups at the C(1) and C(1′) positions would make the [5]helicene **22b** (Table 4.1, Entry 23) optically stable even at 120 °C [15]. For the application of helicity, this is a good choice to construct helicene with good thermal stability in large scale.

The Diels–Alder reaction is a practical method for the preparation of symmetric helicenes, because of the efficiency, the moderate-to-good yields, and the large scale of reactions. Moreover, the substituents on dienes and dienophiles could be further modified and used as functional groups to achieve the optical resolution and change the electronic properties. The major limitation of the methodology is the limited types of dienes and dienophiles.

4.2   Friedel–Crafts-Type Reactions

This method was first utilized by Newman and co-workers in 1950s [29, 30], when they prepared the 1,12-dimethyl [4]helicene and [6]helicene. As shown in Scheme 4.1, **26** was achieved through the condensation of 1-naphthaldehyde **25**. Then by addition of Grignard reagent prepared from 1-bromonaphthalene to **26**, diester **27** could be obtained. After reduction, esterification, substitution by KCN and the alkaline hydrolysis in ethylene glycol, diacid **28** was obtained in high yield. In the presence of HF, monocyclization could be achieved to produce acid **29**. The
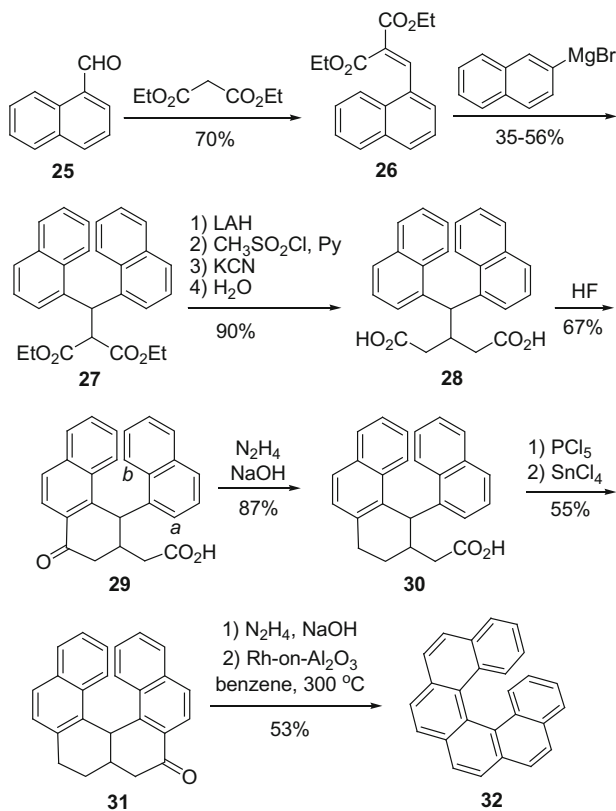
Scheme 4.1 Synthesis of [6]helicene **32**

authors found that the subsequent Friedel–Crafts reaction would happen at position *b* rather than *a*, because of the rigid keto structure. Therefore, after Huang-minlon reduction, the cyclization product **31** could be prepared. The following reduction and aromatization gave [6]helicene **32** in 53 % yield.

Yamaguchi and co-workers utilized the similar route to synthesize [4]helicenes derivatives [31–34], in which the substituents at the most steric hindered positions, namely C(1) and C(12), made the helical structure optically stable (Scheme 4.2). Different from the Newman's method, the R substituents herein on phenylene groups performed as blocking units that directed and facilitated the double acylation, which could be completed in one step. The subsequent addition, aromatization, and hydrolysis afforded the diacids **35a–c** in good yields. These acid groups could be used for the optical resolution by recrystallization in the presence of quinine or chromatography after the preparation of camphorsultam derivatives [31].

Moreover, the heterohelicenes could also be synthesized via double acylation. For example, from triarylamines, it will be convenient to construct azahelicenes via connecting the aromatic rings. Venkataraman and co-workers recently reported a
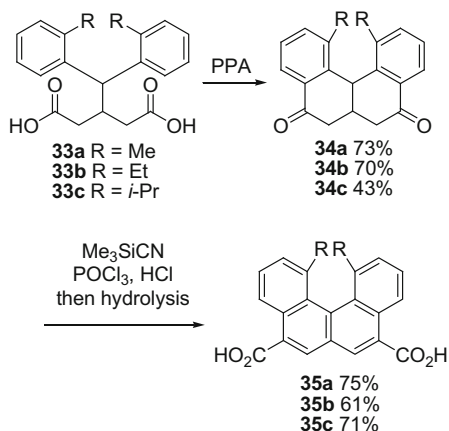
Scheme 4.2 Synthesis of **35a–c**
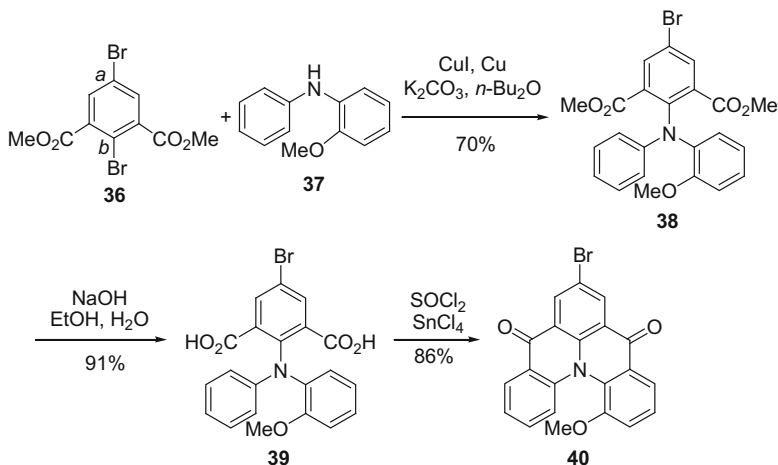
Scheme 4.3 Synthesis of **40**

protocol to prepare multifunctionalized azahelicenes via double Friedel–Crafts acylation (Scheme 4.3) [35]. For the substrate **36**, the C(*a*)-Br bond was sterically unhindered, while the C(*b*)-Br bond was electronically activated due to the two *ortho*-ester functionalities. They achieved the regioselective synthesis, at C(*b*) position, of triarylamine **38** by using Cu/CuI catalyst in 70 % yields, which made the amine a reasonable precursor. By basic hydrolysis and Friedel–Crafts acylation, azahelicene **40** was prepared in 86 % yields. The methoxy group was utilized for optical resolution by forming diastereomers, and the Br and keto groups could be further modified. Also, [5]-, and [6]heterohelicenes could be synthesized by changing
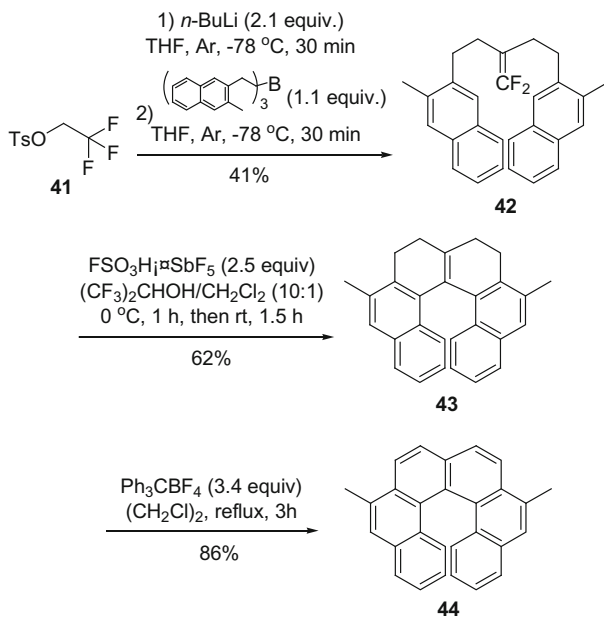
Scheme 4.4 Synthesis of **44**

the diarylamines in moderate-to-good yields [36]. Barnes and co-workers reported that this type of helicenes had strong intrinsic circular dichroism responses [37].

In 2008, Ichikawa and co-workers described another new strategy for the preparation of helicenes [38]. The reaction between 2,2,2-trifluoroethyl-4-methylbenzenesulfonate **41** and borane gave the 1,1′-difluoroethene **42** in 41 % yield. The methyl group at the naphthalene directed the following reaction path and promoted the nucleophilicity of the naphthalene. In the presence of magic acid, the domino cyclization took place giving the tetrahydrohelicene **43** in 62 % yield. After aromatization by Ph_3CBF_4, dimethyl[6]helicene **44** was synthesized in good yield (Scheme 4.4). Based on this method, [4]- to [6]-helicenes were prepared conveniently by varying the aryl groups in boranes [39].

In addition, Gaucher and co-workers reported another Friedel–Crafts-type route from nitrile [40]. As shown in Scheme 4.5, diarylnaphthalene **46** could be easily synthesized from 1,8-dibromonaphthalene **45** via Suzuki–Miyaura cross-coupling reaction in 80 % yield. The subsequent bromination and cyanation afforded dinitrile **47**, which could be transformed into the double cyclization product **48**, bearing two amino groups at C(6) and C(6′) positions, with the help of PPA and acetyl chloride. From the view of reactivity, it is difficult to incorporate functional groups at C(6) or C(6′) position of the parent helicenes.

Scheme 4.5 Synthesis of **48**
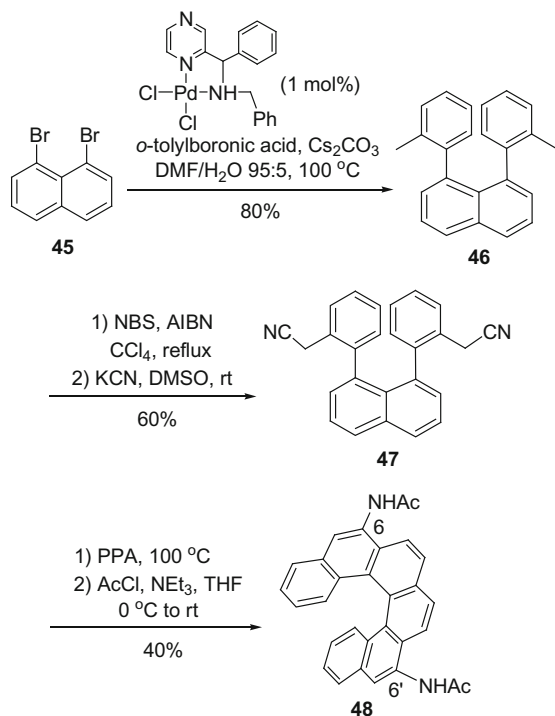
Recently, Nakamura, Hatakeyama, and co-workers reported a double phospha-helicene with a highly distorted benzene ring bearing the bending angle of 23° [41]. Starting from hexabromobenzene **49**, the treatment with the Grignard reagent prepared from 1-bromo-2-methylnaphthalene followed by quenching with iodine gave the tetraaryl benzene **50** in 22 % yield. After lithium–halogen exchange, the 2,3,5,6-tetraaryl-1,4-bisphosphine could be prepared in the presence of bis(*N,N*-diethyl-amino)chlorophosphine. The subsequent sulfurization and double phospha-Friedel–Crafts reaction gave the double-helical structure **51** in 10 % yield for three steps. The X-ray crystal structure with hydrogen atoms omitted was shown as the background: (1) the molecule had C_2-symmetry; (2) the two helical structures had the same helicity; (3) the two S atoms arranged in *cis*-configuration; (4) the distance of *S-S* was 6.403 Å. The desulfurization was achieved by the treatment of triethylphosphine, affording the phosphahelicene **52** in 89 % yield (Scheme 4.6). Since the structure had good thermal stability, it could be resolved and applicable for asymmetric synthesis as a bidentate ligand.

Very recently, Perepichka and co-workers [42] described the synthesis of two types of double [4]helicenes: **54** had the 4-trifluoromethylphenyl groups on the same side, whereas isomer **57** had the groups on the opposite sides. From **53**, after nucleophilic addition of *p*-CF₃PhLi, the subsequent cyclization with the help of TFA gave **54** in 48 % yield and **57** in yield less than 1 %, in which the first
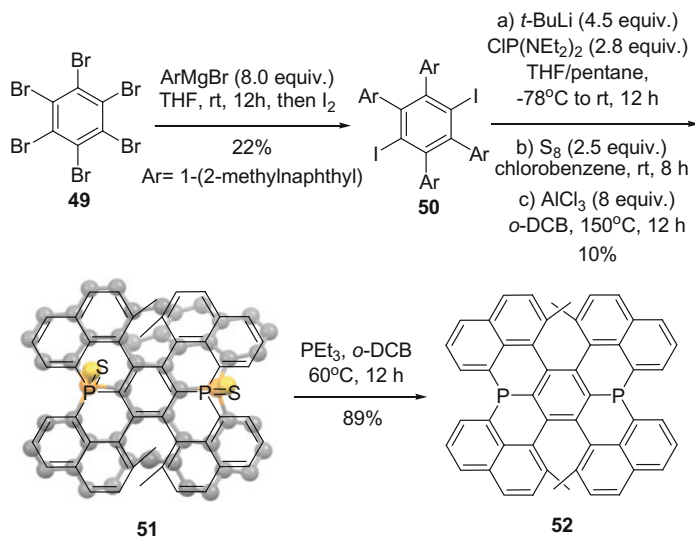
Scheme 4.6 Synthesis of phosphahelicene **52**
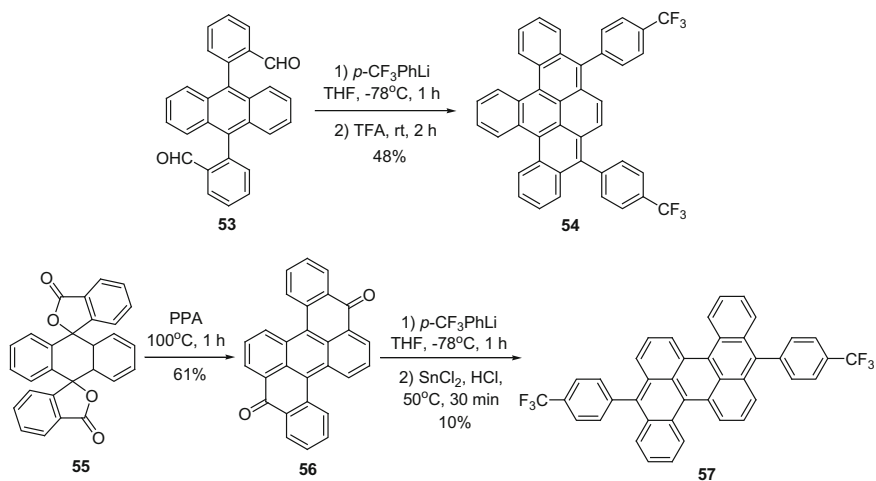
Scheme 4.7 Synthesis of **54** and **57**

cyclization facilitated the second ring closing, resulting from the electron-donating group of −CHAr$_2$ group. Instead, from dilactone **55**, **57** could be easily prepared by intramolecular Friedel–Crafts reaction, nucleophilic addition, and aromatization (Scheme 4.7). The electronic properties showed that **57** could be a good semi-conducting material.

As shown above, Friedel–Crafts-type reaction is a useful strategy that the synthesis usually needs less than five steps with moderate-to-good yields. Two points should be taken into account: (1) polar unsaturated bonds should be well designed and incorporated into the substrates; (2) to promote the regioselectivity, it would be better that the directing or blocking groups were introduced.

References

1. Liu LB, Katz TJ (1990) Simple preparation of a helical quinone. Tetrahedron Lett 31 (28):3983–3986
2. Woodward RB, Katz TJ (1959) The mechanism of the diels-alder reaction. Tetrahedron 5 (1):70–89
3. Sauer J, Wiest H, Mielert A (1964) Eine Studie der DIELS-ALDER-Reaktion, I. Die Reaktivität von Dienophilen gegenüber Cyclopentadien und 9.10-Dimethyl-anthracen. Chem Ber 97(11):3183–3207
4. Sauer J (1967) Diels-alder reactions 2—reaction mechanism. Angew Chem Int Ed 6(1):16–33
5. Dreher SD, Katz TJ, Lam KC, Rheingold AL (2000) Application of the Russig-Laatsch reaction to synthesize a bis[5]helicene chiral pocket for asymmetric catalysis. J Org Chem 65 (3):815–822
6. Fox JM, Katz TJ, Van Elshocht S, Verbiest T, Kauranen M, Persoons A, Thongpanchang T, Krauss T, Brus L (1999) Synthesis, self-assembly, and nonlinear optical properties of conjugated helical metal phthalocyanine derivatives. J Am Chem Soc 121(14):3453–3459
7. Dai YJ, Katz TJ, Nichols DA (1996) Synthesis of a helical conjugated ladder polymer. Angew Chem Int Ed Engl 35(18):2109–2111
8. Dai YJ, Katz TJ (1997) Synthesis of helical conjugated ladder polymers. J Org Chem 62 (5):1274–1285
9. Weix DJ, Dreher SD, Katz TJ (2000) [5]HELOL phosphite: a helically grooved sensor of remote chirality. J Am Chem Soc 122(41):10027–10032
10. Wang DZG, Katz TJ (2005) A [5]HELOL analogue that senses remote chirality in alcohols, phenols, amines, and carboxylic acids. J Org Chem 70(21):8497–8502
11. Lovinger AJ, Nuckolls C, Katz TJ (1998) Structure and morphology of helicene fibers. J Am Chem Soc 120(2):264–268
12. Nuckolls C, Katz TJ, Verbiest T, Van Elshocht S, Kuball HG, Kiesewalter S, Lovinger AJ, Persoons A (1998) Circular dichroism and UV-visible absorption spectra of the Langmuir-Blodgett films of an aggregating helicene. J Am Chem Soc 120(34):8656–8660
13. Verbiest T, Van Elshocht S, Kauranen M, Hellemans L, Snauwaert J, Nuckolls C, Katz TJ, Persoons A (1998) Strong enhancement of nonlinear optical properties through supramolecular chirality. Science 282(5390):913–915
14. Urbano A, Carreno MC (2013) Enantioselective synthesis of helicenequinones and -bisquinones. Org Biomol Chem 11(5):699–708
15. Shen Y, Lu H-Y, Chen C-F (2014) Dioxygen-triggered transannular dearomatization of benzo [5]helicene diols: highly efficient synthesis of chiral π-extended diones. Angew Chem Int Ed 53(18):4648–4651
16. Katz TJ, Liu LB, Willmore ND, Fox JM, Rheingold AL, Shi SH, Nuckolls C, Rickman BH (1997) An efficient synthesis of functionalized helicenes. J Am Chem Soc 119(42):10054–10063
17. Willmore ND, Liu LB, Katz TJ (1992) A diels-alder route to [5]-helicenes and [6]-helicenes. Angew Chem Int Ed Engl 31(8):1093–1095

18. Paruch K, Vyklicky L, Katz TJ, Incarvito CD, Rheingold AL (2000) Expeditious procedure to synthesize ethers and esters of tri- and tetrahydroxy[6]helicenebisquinones from the dye-intermediates disodium 4-hydroxy- and 4,5-dihydroxynaphthalene-2,7-disulfonates. J Org Chem 65(25):8774–8782

19. Fox JM, Goldberg NR, Katz TJ (1998) Efficient synthesis of functionalized [7]helicenes. J Org Chem 63(21):7456–7462

20. Paruch K, Katz TJ, Incarvito C, Lam KC, Rhatigan B, Rheingold AL (2000) First Friedel-Crafts diacylation of a phenanthrene as the basis for an efficient synthesis of nonracemic [7]helicenes. J Org Chem 65(22):7602–7608

21. Dreher SD, Weix DJ, Katz TJ (1999) Easy synthesis of functionalized hetero[7]helicenes. J Org Chem 64(10):3671–3678

22. Phillips KES, Katz TJ, Jockusch S, Lovinger AJ, Turro NJ (2001) Synthesis and properties of an aggregating heterocyclic helicene. J Am Chem Soc 123(48):11899–11907

23. Real MD, Sestelo JP, Sarandeses LA (2002) Inner-outer ring 1,3-bis(trimethylsilyloxy)-1,3-dienes as useful intermediates in the synthesis of helicenes. Tetrahedron Lett 43(50):9111–9114

24. Newman MS (1940) A new synthesis of coronene. J Am Chem Soc 62:1683–1687

25. Sooksimuang T, Mandal BK (2003) [5]helicene-fused phthalocyanine derivatives. New members of the phthalocyanine family. J Org Chem 68(2):652–655

26. Chen JD, Lu HY, Chen CF (2010) Synthesis and structures of multifunctionalized helicenes and dehydrohelicenes: an efficient route to construct cyan fluorescent molecules. Chem Eur J 16(39):11843–11846

27. Li Y-Y, Lu H-Y, Li M, Li X-J, Chen C-F (2014) Dihydroindeno[2,1-c]fluorene-based imide dyes: synthesis, structures, photophysical and electrochemical properties. J Org Chem 79 (5):2139–2147

28. Li X-J, Li M, Lu H-Y, Chen C-F (2015) A dinaphtho[8,1,2-cde:2[prime or minute],1[prime or minute],8[prime or minute]-uva]pentacene derivative and analogues: synthesis, structures, photophysical and electrochemical properties. Org Biomol Chem 13(28):7628–7632

29. Newman MS, Wolf M (1952) A new synthesis of benzo(C)phenanthrene—1,12-dimethylbenzo (C)phenanthrene. J Am Chem Soc 74(13):3225–3228

30. Newman MS, Lednicer D (1956) The synthesis and resolution of hexahelicene. J Am Chem Soc 78(18):4765–4770

31. Yamaguchi M, Okubo H, Hirama M (1996) Synthesis of optically active macrocycles consisting of helical chiral unit 1,12-dimethylbenzo[c]phenanthrene-5,8-dicarboxylate as a novel chiral building block. Chem Commun (Camb) 15:1771–1772

32. Okubo H, Yamaguchi M, Kabuto C (1998) Macrocyclic amides consisting of helical chiral 1,12-dimethylbenzo[c]phenanthrene-5,8-dicarboxylate. J Org Chem 63(25):9500–9509

33. Okubo H, Yamaguchi M (2001) A building block method for the synthesis of higher cycloamides. J Org Chem 66(3):824–830

34. Sugiura H, Sakai D, Otani H, Teranishi K, Takahira Y, Amemiya R, Yamaguchi M (2007) Synthesis and structure of optically active 1,12-diethyl- and 1,12-diisopropylbenzo[c] phenanthrenes: an isopropyl group can be smaller than a methyl group. Chem Lett 36 (1):72–73

35. Surampudi SK, Nagarjuna G, Okamoto D, Chaudhuri PD, Venkataraman D (2012) Apical functionalization of chiral heterohelicenes. J Org Chem 77(4):2074–2079

36. Field JE, Hill TJ, Venkataraman D (2003) Bridged triarylamines: a new class of heterohelicenes. J Org Chem 68(16):6071–6078

37. Hassey R, Swain EJ, Hammer NI, Venkataraman D, Barnes MD (2006) Probing the chiroptical response of a single molecule. Science 314(5804):1437–1439

38. Ichikawa J, Yokota M, Kudo T, Umezaki S (2008) Efficient helicene synthesis: Friedel-Crafts-type cyclization of 1,1-difluoro-1-alkenes. Angew Chem Int Ed 47(26):4870–4873

39. Fuchibe K, Jyono H, Fujiwara M, Kudo T, Yokota M, Ichikawa J (2011) Domino friedel–crafts-type cyclizations of difluoroalkenes promoted by the α-cation-stabilizing effect of fluorine: an efficient method for synthesizing angular PAHs. Chem Eur J 17(43):12175–12185
40. Pieters G, Gaucher A, Prim D, Marrot J (2009) First expeditious synthesis of 6,11-diamino-[6] carbohelicenes. Chem Commun (Camb) 32:4827–4828
41. Hashimoto S, Nakatsuka S, Nakamura M, Hatakeyama T (2014) Construction of a highly distorted benzene ring in a double helicene. Angew Chem Int Ed 53(51):14074–14076
42. Rao MR, Black HT, Perepichka DF (2015) Synthesis and divergent electronic properties of two ring-fused derivatives of 9,10-diphenylanthracene. Org Lett 17(17):4224–4227

Chapter 5
Metal-Mediated Reactions

Abstract With the development of organometallic chemistry, metal-mediated reactions are widely accepted and become one of the most powerful methods for the preparation of helicenes due to their high efficiency (usually constructing more than one ring in one step), moderate to high yields, good functional group tolerance, and the ability to prepare longer helicenes. In this chapter, the [2+2+2] cycloisomerization is first introduced, in which the construction of helical skeleton could be achieved with high efficiency by different routes including platinum-catalyzed dienyne cycloisomerization, palladium-catalyzed intermolecular cyclization of arynes and alkynes, and Ni/Co-mediated intramolecular [2+2+2] cycloisomerization of triynes. By twofold [2+2+2] cycloisomerization of triynes, longer helicenes can be synthesized. Heterohelicenes and different helquats can also be synthesized by the similar [2+2+2] cycloisomerization method. Moreover, other types of metal-mediated reactions are also utilized for the preparation of helicenes, such as Pd-catalyzed twofold Stille cross-coupling reaction, Pd-catalyzed double Suzuki-Miyaura cross-coupling, Ti-mediated McMurry coupling, intramolecular palladium-catalyzed *P*-arylation, Rh-catalyzed ring-closing metathesis, Fe-Mediated Scholl oxidation, Au-catalyzed hydroamination, consecutive hydroarylation reaction, and so on.

Keywords Intramolecular [2+2+2] cycloisomerization · McMurry coupling · Metal-mediated reactions · Ring-closing metathesis · Stille cross-coupling reaction · Suzuki–Miyaura cross-coupling · Scholl oxidation

The development of organometallic chemistry has brought new vitality to the helicene chemistry [1–5]. In this chapter, we will focus on the nonstereoselective metal-mediated strategies. In the first section, the powerful [2+2+2] cycloisomerization will be introduced; in the second section, we will discuss other practical methods.

5.1   [2+2+2] Cycloisomerization

First, we will look at the resonant structures of the phenanthrene moiety of a helicene. As shown in Scheme 5.1, the phenanthrene moiety has three structures, A, B, C [6]. For each one of them, the retrosynthetic analysis displays different precursors or substrates that meet the requirement. In some cases, the usage of similar variants would make the preparation easy and versatile. The construction of helical skeleton could be achieved by building one ring (Routes *a*, *b*), two rings (Routes *a '*), three rings (Routes *c*, *d*), or even more rings (Route *d'*, *d''*) in one step. Therefore, this strategy is highly efficient. The Routes *d*, *d'*, and *d''* will be discussed in the chapter of asymmetric synthesis.
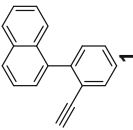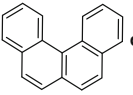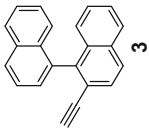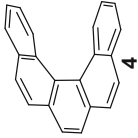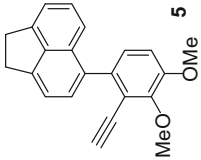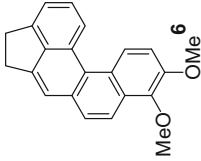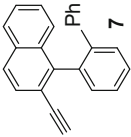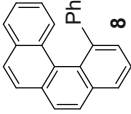
5.1.1   Routes a and a'

In 2004, Fürstner group reported the first two examples of PtCl$_2$-catalyzed synthesis of [4]- and [5]helicenes in moderate yields (Table 5.1, Entries 1 and 2). Since then, platinum-catalyzed dienyne cycloisomerization have been widely used in the synthesis of helicenes. Lakshman and co-workers reported a convenient method to
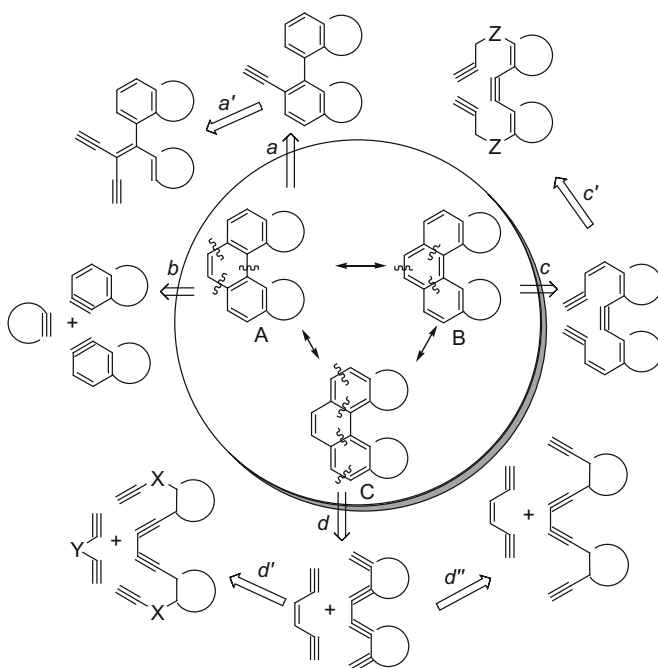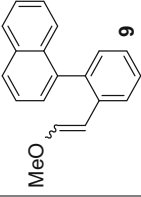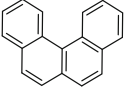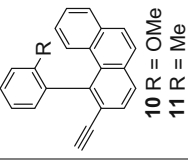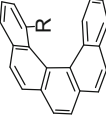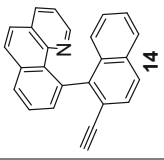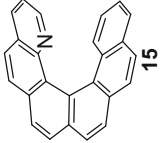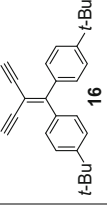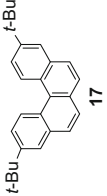
Scheme 5.1 The retrosynthetic analysis of helicenes, X, Y, and Z stands for heteroatoms

Table 5.1 The synthesis of helicenes by routes *a* and *a'*

Entry	Precursor	Catalyst	Condition	Product	Yield (%)	References
1	1	PtCl$_2$ (5 mol%)	Toluene, 80 °C	2	65	[9]
2	3	PtCl$_2$ (5 mol%)	Toluene, 80 °C	4	56	[9]
3	5	PtCl$_2$ (10 mol%)	Toluene, 80 °C	6	72	[10]
4	7	(2 mol%)	AgSbF$_6$ (2 mol%), DCM, rt	8	73	[11]
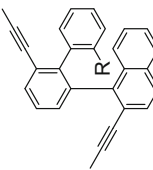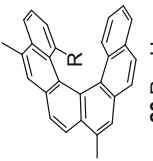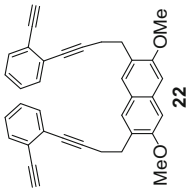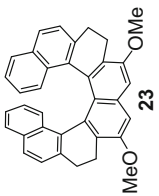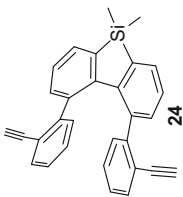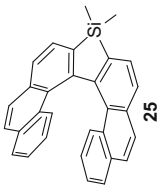
(continued)

Table 5.1 (continued)

Entry	Precursor	Catalyst	Condition	Product	Yield (%)	References
5	MeO, **9**	AuCl$_3$ (5 mol%)	DCE, 25 °C, 2 h	**2**	97	[12]
6	R, **10** R = OMe, **11** R = Me	PtCl$_2$ (10 mol%)	Toluene, 120 °C, 7 h	**12** R = OMe, **13** R = Me	**12** 66, **13** 44	[13]
7	N, **14**	PtCl$_4$ (10 mol%)	DCE, 120 °C, 16 h	N, **15**	65	[14]
8	t-Bu, t-Bu, **16**	RuCl$_2$(PPh$_3$) (20 mol%)	DCE, refluxing	t-Bu, t-Bu, **17**	60	[15]

(continued)

Table 5.1 (continued)

Entry	Precursor	Catalyst	Condition	Product	Yield (%)	References
9	**18** R = H **19** R = OMe	PtCl$_2$ (10 mol%)	Toluene, 90 °C, 20 h	**20** R = H **21** R = OMe	**20** 80 **21** 76	[16]
10	**22**	PtCl$_2$ (20 mol%) PtCl$_4$ (20 mol%)	Toluene, 90 °C, 16 h	**23**	20	[17]
11	**24**	PtCl$_4$ (10 mol%)	DCE, 80 °C	**25**	>42	[18]

prepare the potential biologically active polycyclic compounds from [4]helicene frameworks, which could be obtained in high yield via PtCl$_2$-catalyzed cyclization (Table 5.1, Entry 3). Based on this methodology, Alcarazo group studied the polycationic ligand in gold catalysis, and they found that the cationic groups in phosphine ligand dramatically enhanced the activity of the catalyst for the cyclization, where only 2 mol% loading of catalyst was required (Table 5.1, Entry 4). Murai, Takai, and co-workers utilized another type of precursors, 2-(1-arylphenyl)vinyl ether, to prepare [4]helicene in 97 % yield (Table 5.1, Entry 5). This method could also be utilized to introduce functionalities into the most steric hindered position. Suemune, Usui, and co-workers described the synthesis of C(1)-substituted [5]helicenes via cycloisomerization (Table 5.1, Entry 6), where they also discovered that rearrangement of the helical skeletons might take place in some cases, affording azulene-fused helicenes. In the same year, Fuchter and co-workers reported a scalable and expedient method to synthesize 1-aza[6]helicene in moderate yield (Table 5.1, Entry 7).

In addition to the strategy of monocyclization, cascade cycloisomerization procedures were used as well. In 2004, Scott and Donovan reported a simple method to prepare [4]helicene in the presence of the catalyst (Ph$_3$P)Ru(cymene)Cl$_2$ in moderate yield via double cyclization (Table 5.1, Entry 8). In 2009, Storch group utilized double cyclization in the presence of PtCl$_2$ to synthesize C(1)-substituted [6]helicenes in good yields (Table 5.1, Entry 9). Similar substrate was utilized for the synthesis of 2-aza[6]helicene by the same group [7]. Two years later, Storch group utilized cascade cycloisomerization to prepare tetrahydro [8]helicene via constructing four rings in one step in 20 % yield (Table 5.1, Entry 10), in which the reaction need large loading of catalyst. Recently, Nozaki and co-workers reported that a novel sila[7]helicene was prepared by double PtCl$_2$-catalyzed cycloisomerization, which had a fluorescence quantum yield of 17 % in solid state and a CPL dissymmetric factor (g value) of 3.5×10^{-3} (Table 5.1, Entry 11). Moreover, Waser and Li provided a facile method to prepare the alkyne precursors for this strategy via platinum-catalyzed cyclization and alkylation cascade procedure in combination with ethynylbenziodoxole reagent [8].

5.1.2 Route b

In addition to cycloisomerization of the dienyne precursors, Guitian, Pérez, Peña, and co-workers described a palladium-mediated strategy that achieves the intermolecular cyclization of arynes and alkynes, affording helicenes with one or more helical structures [19–23]. From Fig. 5.1, it is clear that various skeletons could be prepared by changing the combination of different substrates. So far, the alkynes and arynes that have been reported are dimethyl acetylenedicarboxylate (DMAD), 1,2-didehydronaphthalene, 3,4-didehydrophenanthrene, 9,10-didehydrophenanthrene, 1,2-didehydrotriphenylene. All the arynes are generated from the corresponding o-trimethylsilylaryl
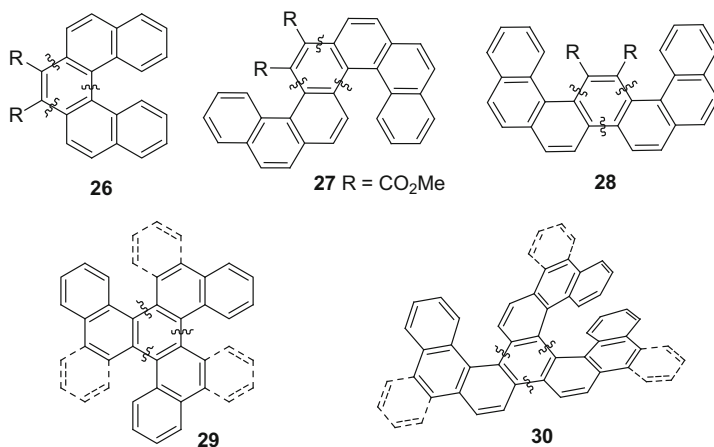
Fig. 5.1 Helicenes synthesized by intermolecular [2+2+2] cyclization

triflates in situ. This method is efficient and expedient for the preparation of polycyclic aromatic compounds, but the scope and synthetic difficulty of the arynes becomes the major limitation.

5.1.3 Routes c and c′

This new strategy, Ni/Co-mediated intramolecular [2+2+2] cycloisomerization of triynes, was developed by Starý, Stará, and co-workers [24, 25]. In 1998, they first reported the synthesis of helicene-like compounds **32–34** in good yield in the presence of CpCo(CO)$_2$ (Scheme 5.2) [26].

One year later, the synthesis of helicene was successfully achieved by the method described above [27]. As shown in Scheme 5.3, under irradiation, the triynes underwent cycloaddition to give tetrahydro[5]-, tetrahydro[6]-, and tetrahydro[7]helicenes **36–38** in good yields, where three six-membered rings were constructed in one step. If Ni(cod)$_2$/PPh$_3$ catalyst was used instead, the reactions did not require the irradiation, and similar yields of the products were observed. These compounds could be easily transformed into helicenes by aromatization in the presence of suitable oxidants.

The direct synthesis of helicenes was realized by the same group employing the dienetriyne precursors (Scheme 5.4) [28]. Enyne **40** was prepared from bromide **39** via Sonogashira coupling, which was converted into iodide **41** by lithium-halogen exchange followed by quenching with iodine. The subsequent Sonogashira coupling between the iodide and acetylene gave the *cis,cis*-dienetriyne **42** in 79 % yield. With the help of Ni(cod)$_2$/PPh$_3$, [5]helicene could be obtained in 76 %, [6]- and [7]helicenes could also be directly prepared in good yields.
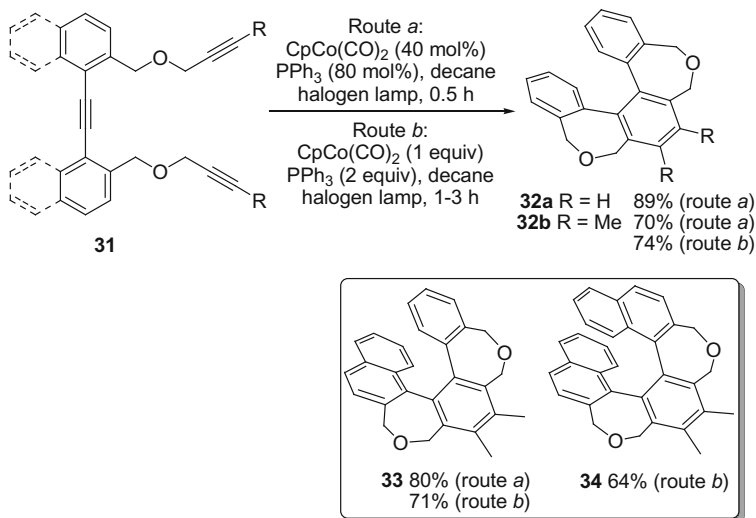
Scheme 5.2 Synthesis of helicene-like compounds **32–34**
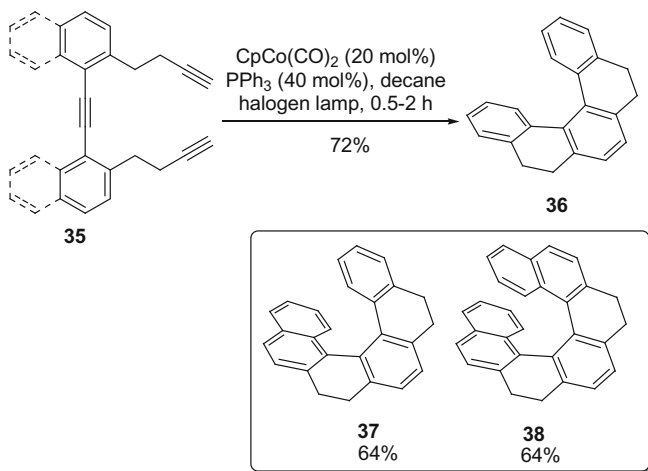
Scheme 5.3 Synthesis of tetrahydro[5]-, tetrahydro[6]-, and tetrahydro[7]helicenes

Using twofold [2+2+2] cycloisomerization, longer helicenes could be synthesized. In 2009, Starý, Stará, and co-workers reported the synthesis of anthra[11] helicene **47** from the precursor hexayne **44** (Scheme 5.5) [29]. In this route, six rings were formed in one step with the total yield up to 40 %. This method was practical and powerful: (1) 100 % atom economy; (2) good to excellent yields; (3) the modular character; (4) the ability for constructing longer helicenes.
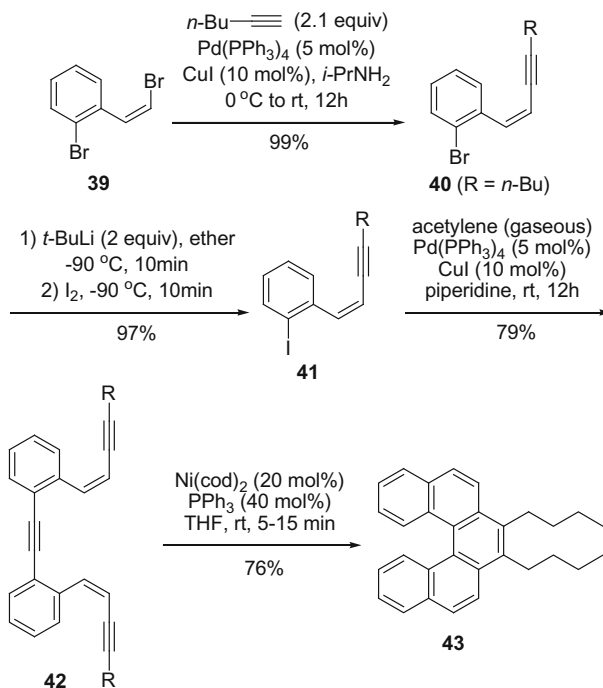
Scheme 5.4 Synthesis of [5]helicene derivative **43**

Base on the similar route, Diedrich and co-workers reported the synthesis of methyl [6]helicene-2-carboxylate (Scheme 5.6) [30]. The acid **48** was transformed into the aldehyde **49** via esterification, bromination, and oxidation. Subsequent Sonogashira reaction with trimethylsilyl acetylene and the desilylation afforded the alkyne **50** in 72 % yield. Then, the second Sonogashira coupling produced the dialdehyde **51**, which underwent nucleophilic addition with Grignard-type reagent generated from 1-bromoprop-2-yne in the presence of Ga and In. After esterification, the triyne precursor **52** was prepared. Helicene **53** was obtained via Co-mediated [2+2+2] cycloaddition and aromatization in 36 % yield. This method was also utilized by the same group to prepare [6]helicene *o*-quinone for chiral recognition [31].

Heterohelicenes could be synthesized by similar method as well. Starý, Stará, and co-workers [32] described the preparation of 1,14-diaza[5]helicene, 1-aza-, and 2-aza[6]helicenes (Scheme 5.7) in moderate yields, which have been applied in asymmetric catalysis [33].

Recently, the same group utilized a new type of substrate, ynedinitriles, to prepare azahelicenes [34], in which the two acetylene moieties were replaced by cyano groups (Scheme 5.8). The Suzuki–Miyaura cross-coupling between the dibromide **61** and boronic acid, unusually, produced diamide **62** in 51 %, which transformed into dinitrile **63** in the presence of trifluoroacetic anhydride and
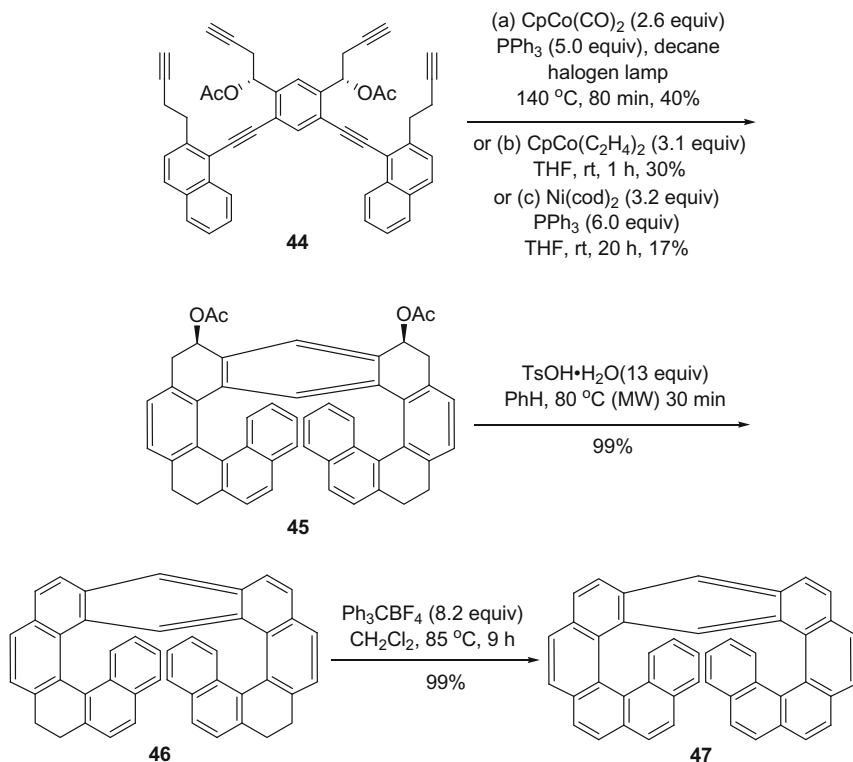
Scheme 5.5   Synthesis of anthra[11]helicene **47**

triethylamine. With the help of CpCo(CO)$_2$, the ynedinitrile was converted into azahelicene **64** in good yield. In addition, [5]- and [6]helicenes could be prepared.

Carbery group designed and synthesized the helicenoidal DMAP Lewis base catalyst **71** via this [2+2+2] cycloisomerization strategy (Scheme 5.9) [35]. The Sonogashira coupling between 1-iodo-2-naphthol **67** and trimethylsilyl acetylene followed by the O-propargylation and the desilylation gave the alkyne **68** in excellent yield. The second Sonogashira coupling with iodopyridine catalyzed by Pd(PPh$_3$)$_4$ produced the diyne **69** in 82 % yield. The final triyne precursor **70** was obtained after N-propargylation, deprotection of Boc group, and N-methylation. At last, the cycloaddition occurred smoothly with the yield of 74 % in the presence of RhCl(PPh$_3$)$_3$.

Teplý group applied this methodology to the preparation of different helquats, which are helicene-like and have two quaternized nitrogen centers [36–40]. Recently, the same group reported the modular synthesis of tricationic helicene-like compound (Scheme 5.10) [41]. Starting from 4,5-diiodoimidazole **72**, the Sonogashira coupling with ethynylpyridine **73** afforded pyridine derivative **74** in 63 % yield. The following alkylation in the presence of K$_2$CO$_3$ and the triple
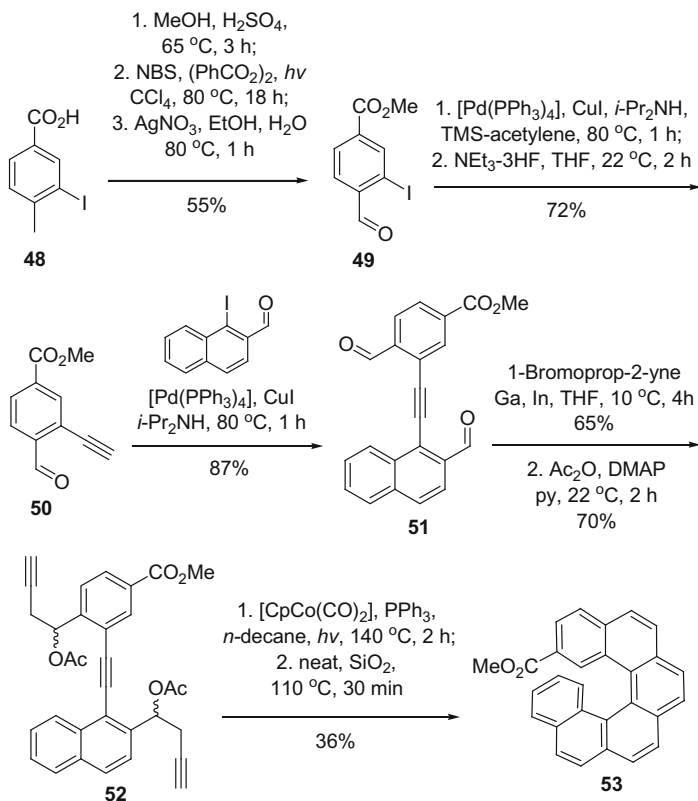
Scheme 5.6 Synthesis of [6]helicene derivative **53**

quaternization with butynyl triflate gave the precursor **76** in 72 and 95 % yields, respectively. With the hexayne precursor in hand, the tricationic helical compound **77** could be obtained efficiently via double Rh-mediated [2+2+2] cycloaddition in 88 % yield for constructing six rings in one step.

5.2 Other Metal-Mediated Reactions

Besides the above methods, other types of metal-mediated reactions were also utilized for the preparation of helicenes. This section will be classified by different metals.
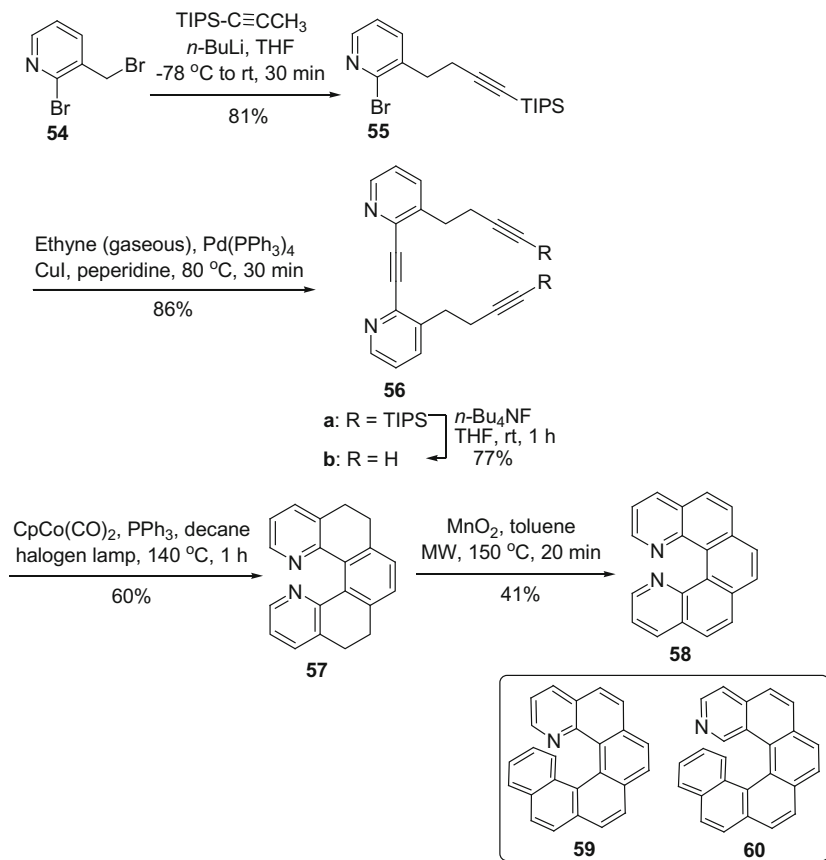
Scheme 5.7 Synthesis of 1,14-diaza[5]helicene **58**, 1-aza-, and 2-aza[6]helicenes **59–60**

5.2.1 Pd-Catalyzed Reactions

Because helicenes were composed by fused aromatics, Pd-catalyzed cross-coupling reactions were widely employed.

In 2007, Kamikawa and co-workers described a method to prepare helicenes with electron-withdrawing functionalities from the substrates of Z,Z-bis(bromostilbene)s **78** via direct C–H arylation (Scheme 5.11) [42]. Using Pd(OAc)$_2$/ PCy$_3$·HBF$_4$ as the optimized catalyst, Ag$_2$CO$_3$ as the additive, K$_2$CO$_3$ as the base, [5]- and [6]helicenes could be obtained in moderate to good yield, especially the ones with F atom at C(3) and C(12) positions. The two methoxy groups were performed as blocks to direct the cyclization. Unfortunately, the preparation of [7] helicene could not be realized by this method. Recently, Tsuji, Nakamura, and co-workers employed similar conditions to prepare double [4]helicenes from tetraaryl alkenes in five steps in good to high yields [43].
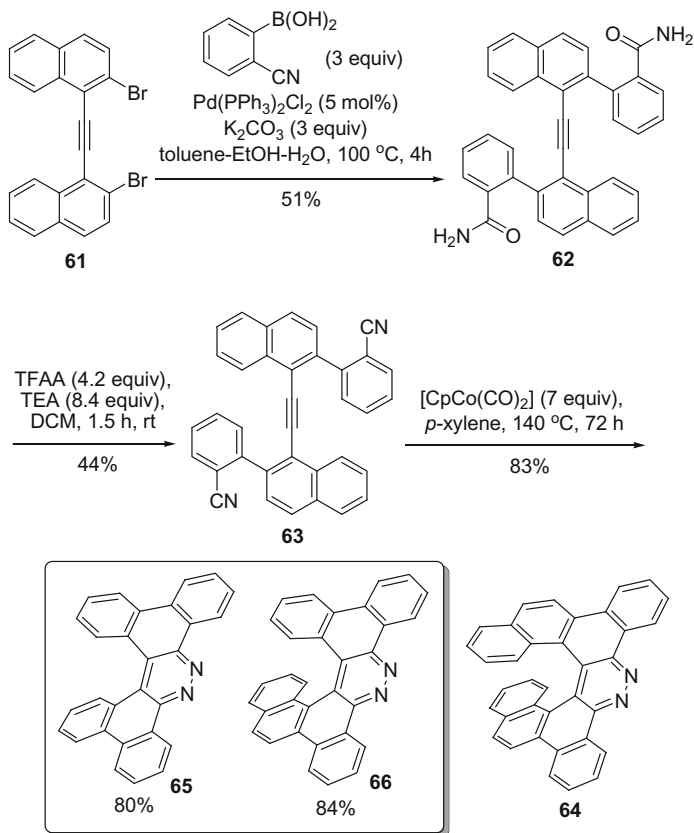
Scheme 5.8 Synthesis of azahelicenes **64–66**

At the same year, Scott and Xue reported the synthesis of benzo[5]helicene **83** from 2,2′-dibromo-1,1′-binaphthyl **81** via twofold Stille cross-coupling reaction in 82 % yield (Scheme 5.12) [44].

In addition, Shimizu and co-workers described the synthesis of diphenyl[5] helicene via double Suzuki–Miyaura cross-coupling between 2,2′-dibromo-1,1′-binaphthyl and *vic*-bis(pinacolatobory)alkene **84** in 32 % yield (Scheme 5.13) [45]. Recently, Kamikawa group employed similar procedure to prepare double [5]helicene **88** in 13 % yield (Scheme 5.13) [46].

Based on *Z*-alkenes, helicenes could be prepared by Stille–Kelly coupling reaction. 1,16-Diaza[6]helicene **90** and 1-aza[6]helicene **16** were synthesized in good yield by Staab group [47] and Takenaka group [48], respectively (Scheme 5.14). The two halogen atoms at the stilbene moiety rendered the Wittig reaction with high *Z*-selectivity during the procedures of olefination.

Dehaen group utilized Buckwald–Hartwig amination (Scheme 5.15) [49] and cross-coupling (Scheme 5.16) [50] reactions to prepare dioxa-aza[7]helicene **94** and

Scheme 5.9 Synthesis of
helicenoidal DMAP Lewis
base catalyst **71**
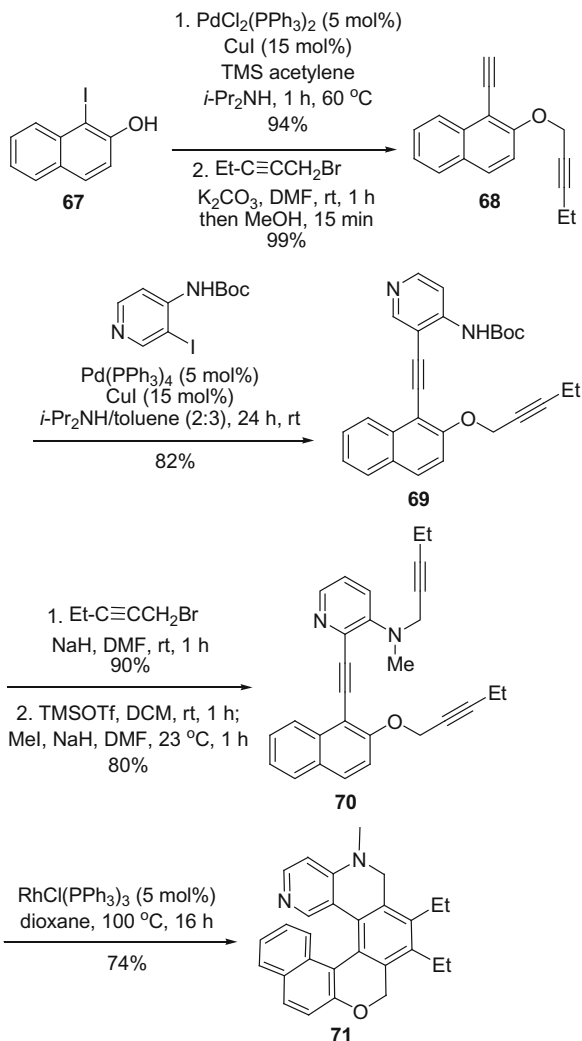
trioxa[7]helicene-like compound **97** in moderate to good yields. By changing the
fragments in the second method, various helical molecules could be obtained.

Palladium-catalyzed *P*-arylation was employed to synthesize the phospha[7]
helicenes by Nozaki group (Scheme 5.17) [51]. The first *P*-arylation between the
sulfonate **98** and ethyl phenylphosphinate gave the phosphorous compound in 46 %
yield. λ^3-Phospha[7]helicene **101** could be obtained via reduction and the second *P*-
arylation. Then, λ^5-phospha[7]helicene **102** was prepared by the oxidation under
ambient condition with an overall yield of 34 %. The authors found that helicene
103 aggregated columnarly with one-way chirality in solid state.
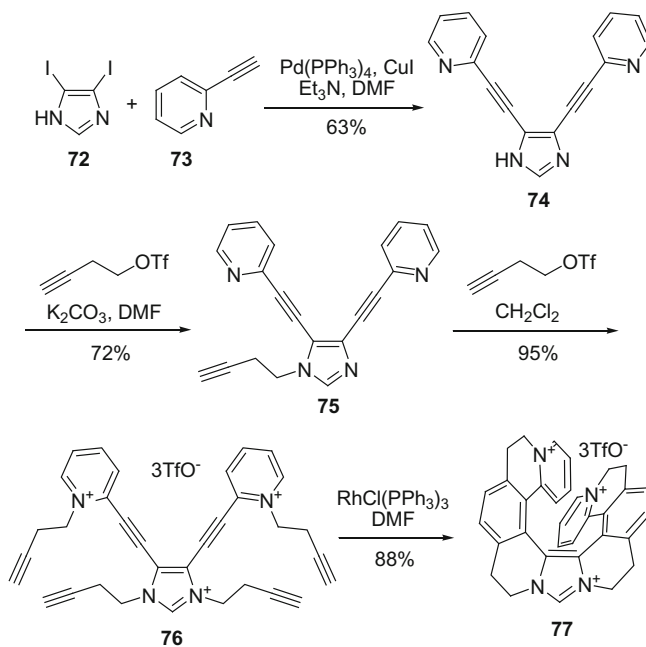
Scheme 5.10 The modular synthesis of tricationic helicene-like compound **77**
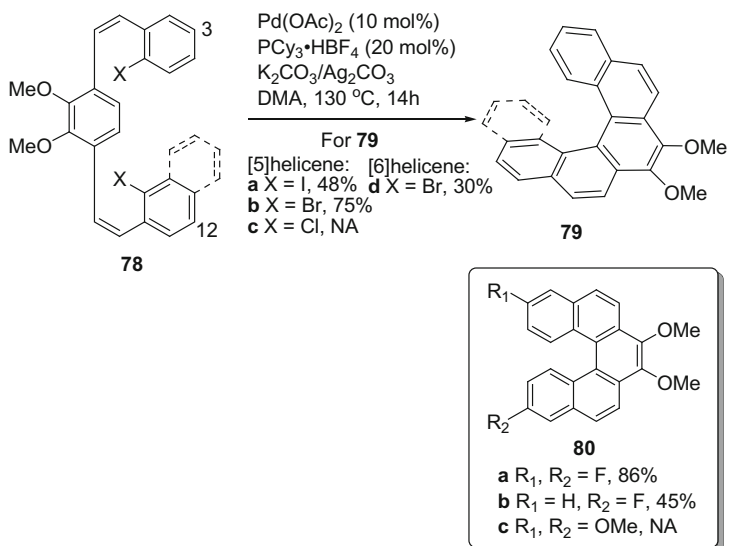
Scheme 5.11 Synthesis of helicene derivatives **79–80**
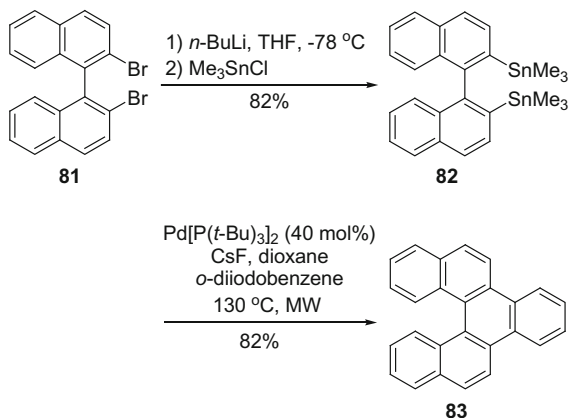
Scheme 5.12 Synthesis of benzo[5]helicene **83**
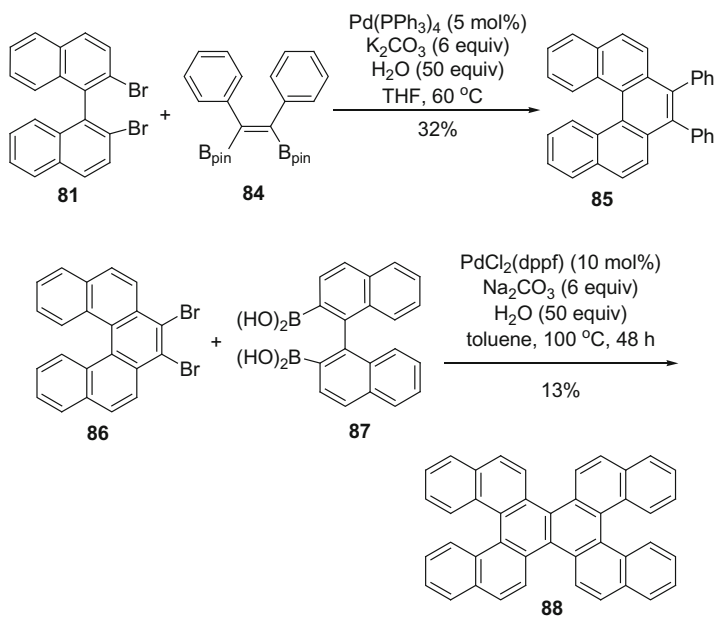
Scheme 5.13 Synthesis of double[5]helicene **88**

Baba, Tobisu, and Chatani reported a novel method to prepare phosphahelicenes, **105** and **106**, from stable triarylphosphines via intramolecular palladium-catalyzed *P*-arylation through the breaking of unactivated *P–C* and *C–H* bonds in the absence of any ligands (Scheme 5.18) [52].
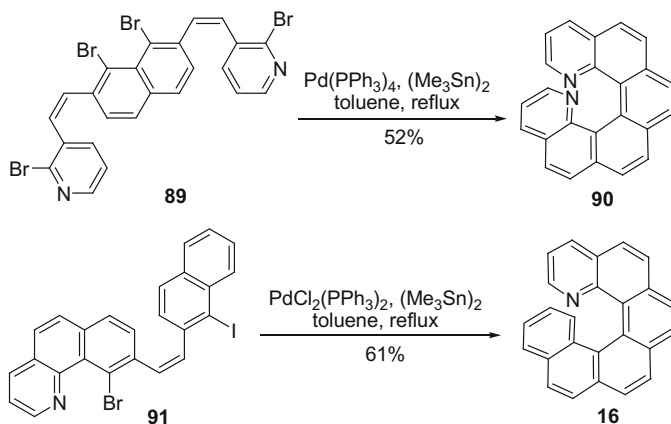
Scheme 5.14 Synthesis of 1,16-diaza[6]helicene **90** and 1-aza[6]helicene **16**
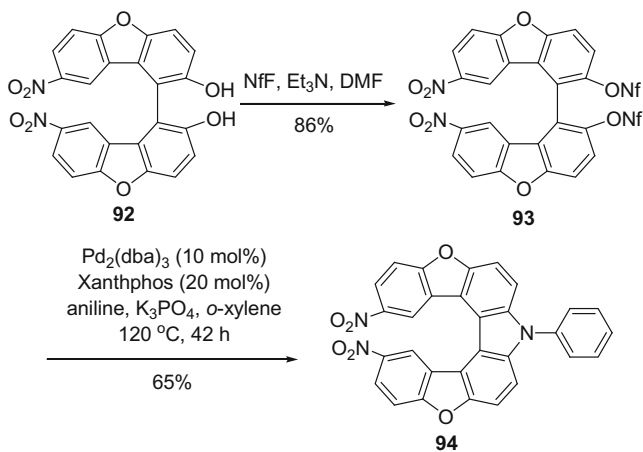
Scheme 5.15 Synthesis of dioxa-aza[7]helicene **94**
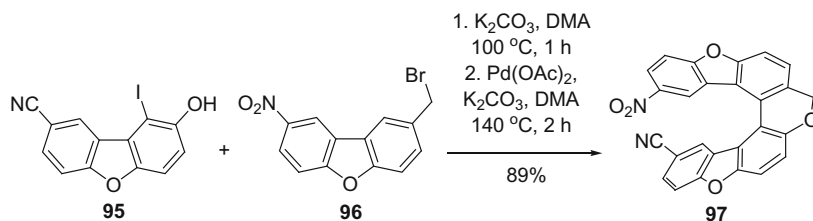
Scheme 5.16 Synthesis of trioxa[7]helicene-like compound **97**
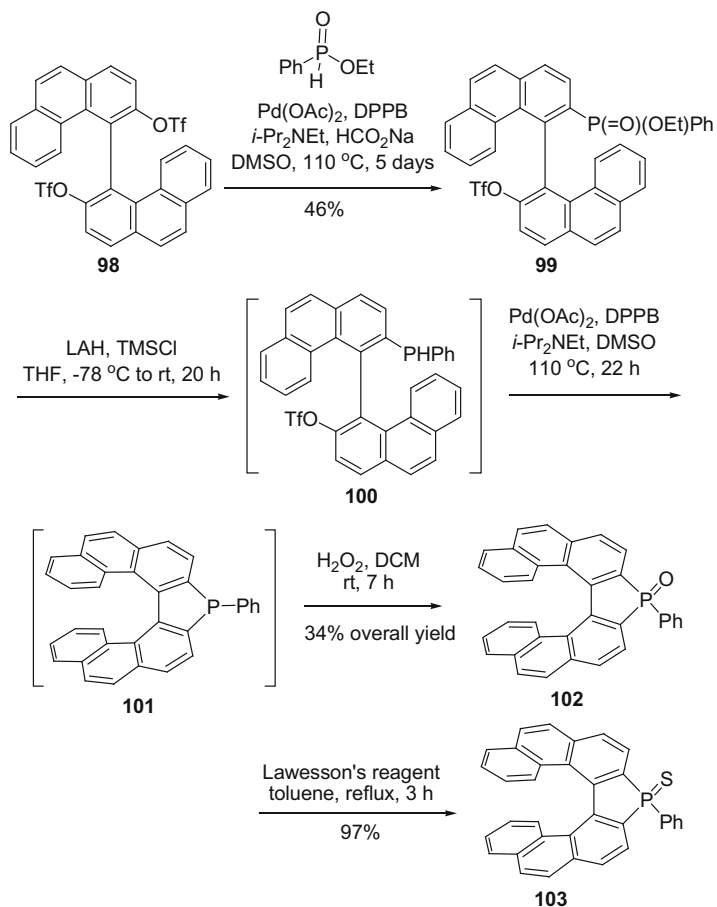
Scheme 5.17 Synthesis of phospha[7]helicene **103**

Scheme 5.18 Synthesis of phosphahelicenes
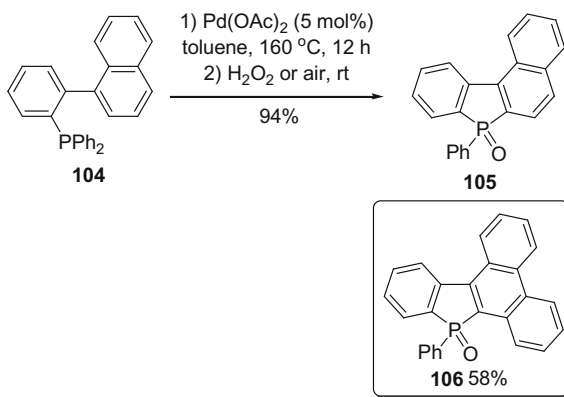
Scheme 5.19 Synthesis of [6]helicene *N*-oxide **108**
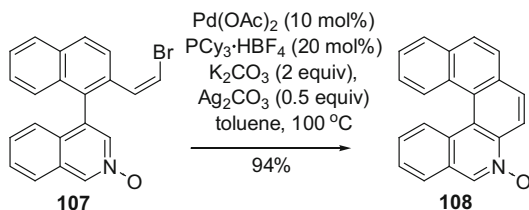
Kamikawa and co-workers employed palladium-catalyzed C–H annulation to construct [5]- and [6]helicenes with *N*-oxide unit in high yields (Scheme 5.19) [53]. If the alkene precursor was optically active, enantioenriched [6]helicene *N*-oxide **108** could be obtained.

In addition, Bogányi and Kámán described the method for preparation of diaza [4]helicenes **112a**-**c** with pyridine and pyrrole rings via Buckwald–Hartwig amination and intramolecular Heck-type annulation under microwave (Scheme 5.20) [54], which were precursors of some indoloquinoline alkaloids.

A new method was reported by Irie and co-workers that *o*-phenylene-linked bis (arenol) underwent tandem Bergman–Masamune cycloaromatization to yield dioxahelicene **114** (Scheme 5.21) [55]. The cyclodehydrogenation took place efficiently in the presence of Pd catalyst, aqueous NaOH, MS 3Å, and oxygen in DMSO. Functionalized [5]- and [6]helicenes were prepared in moderate to high yields.

Liu, Yin, and co-workers reported the synthesis of double [4]helicenes with imides modified picene core (Scheme 5.22) [56]. Imide derivative **116**, prepared from anhydride **115**, was transformed into a dimer **117** via a palladium-catalyzed cross-coupling reaction. The subsequent Suzuki–Miyaura coupling reaction
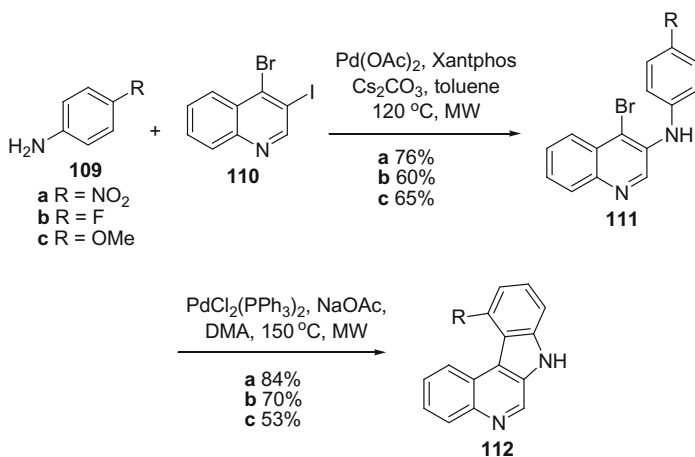
Scheme 5.20 Synthesis of diaza[4]helicenes **112a**-**c**
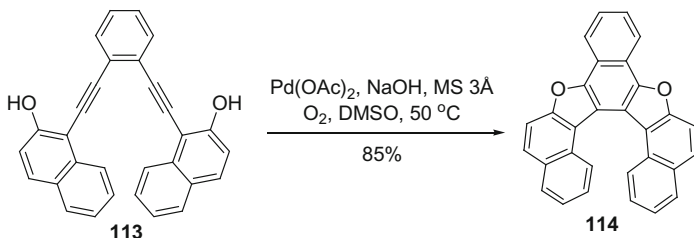
Scheme 5.21 Synthesis of dioxahelicene **114**
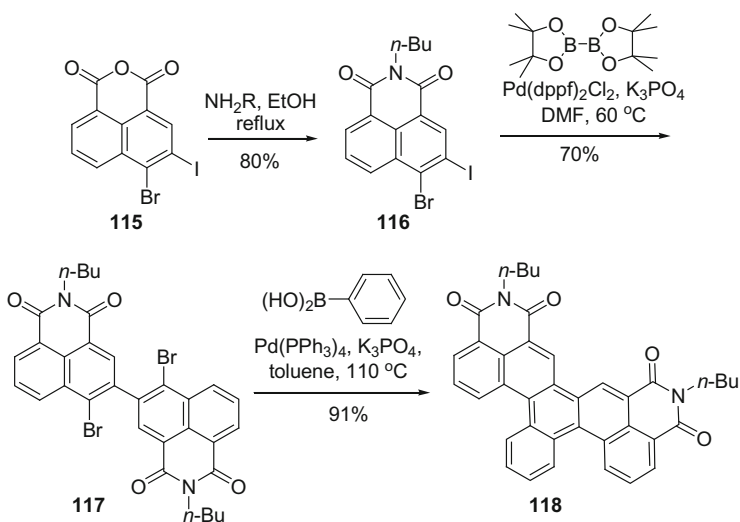
Scheme 5.22 Synthesis of **118**

followed by the C–H arylation gave the diamide **118** in 91 % yield. The authors found that this type of molecules had good optoelectronic properties as well.

Bock, Durola, and co-workers synthesized a series of double [5]helicenes from chrysene via intramolecular Pd-catalyzed annulation (Scheme 5.23) [57]. From the tetraesters, diamides were prepared and found to be good candidates for organoelectronics.

5.2.2 Ru-Mediated Reactions

In 2006, ring-closing metathesis was utilized for the preparation of helicenes by Collins group [58–60]. Diene **121**, in the presence of very small amounts of Grubbs' catalyst, was transformed highly efficiently into [5]helicene with 100 %
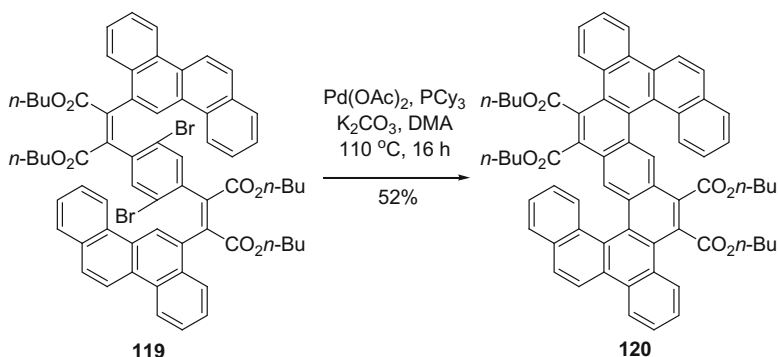
Scheme 5.23 Synthesis of double [5]helicene **120**

Scheme 5.24 Synthesis of [5]helicene **4**
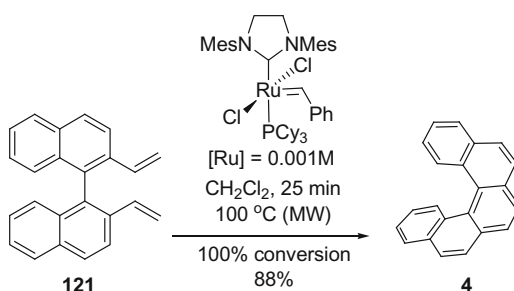
conversion rate and 88 % yield in 25 min (Scheme 5.24). Using this strategy, [6]- and [7]helicenes and their derivatives could be prepared.

5.2.3 Ti-Mediated Reactions

Intramolecular Ti-mediated McMurry coupling was employed by Rajca group (Scheme 5.25) [61] and Wang group (Scheme 5.26) [62] in the preparation of thiahelicenes.

5.2.4 Rh-Mediated Reactions

In 2012, Wang and co-workers reported an improved one-pot Rh-catalyzed method for the synthesis of helicene from dialdehydes (Scheme 5.27) [63]. This reaction was first examined by Gingras and Dubois using the Ti-mediated McMurry
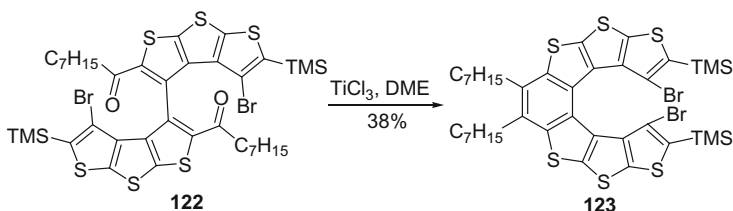
Scheme 5.25 Synthesis of thiahelicene **123**
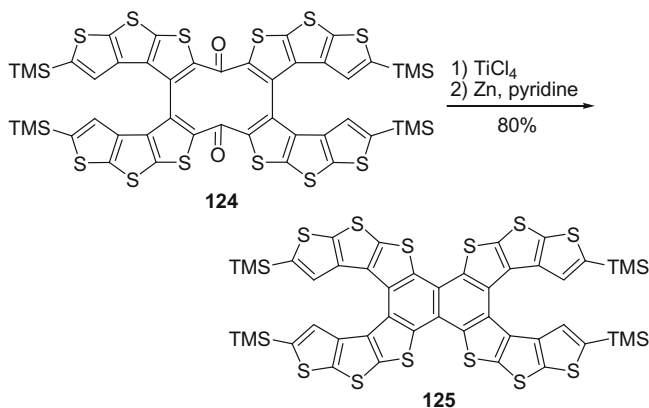
Scheme 5.26 Synthesis of double thiahelicene **125**

Scheme 5.27 Synthesis of [5]helicene **4**
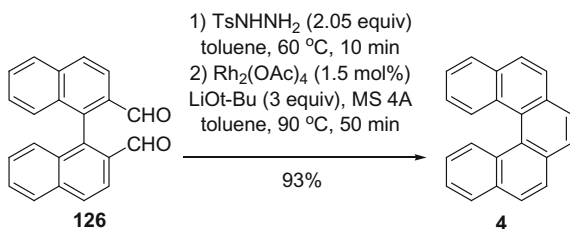
procedure with a yield of 21 % [64]. However, utilizing Wang's approach, the reaction between the dialdehyde **126** and *p*-toluenesulfonyl hydrazine gave the bis (*N*-tosyl-hydrazone) quantitatively and the subsequent Rh-catalyzed cyclization afforded [5]helicene **4** in 93 % yield.

Recently, the first germahelicene was reported by Takai, Murai, and co-workers [65]. The germane **127**, in the presence of [RhCl(cod)]$_2$/PPh$_3$ catalyst with alkene, underwent intramolecular dehydrogenative germylation to give germahelicene **128** in 80 % yield (Scheme 5.28).
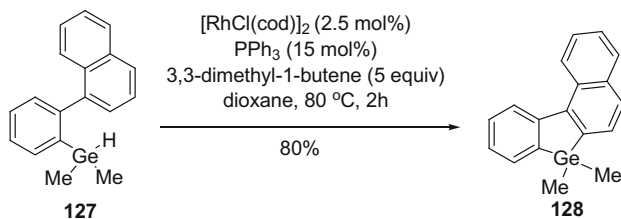
Scheme 5.28 Synthesis of germahelicene **128**

5.2.5 Fe-Mediated Reactions

Recently, Scholl oxidation has been utilized in the synthesis of helicenes, especially for the systems with multiple helicene structures. Chattaraj, Basak, and co-workers described the one-pot method to synthesize helicenes via Garratt–Braverman cyclization followed by Scholl oxidation in moderate to good yields (Scheme 5.29) [66]. Durola group furnished threefold Scholl reactions in the presence of $FeCl_3$ to prepare polycyclic aromatic compounds with helical structures efficiently (Scheme 5.30) [67]. Gao, Hu, and co-workers reported the synthesis of 1,2,3,4,5, 6,7,8-tetra(benzothieno)dibenzothiophene and found that the single crystalline microribbons were good materials for the organic transistor (Scheme 5.31) [68].

Very recently, Plunketti and co-workers described a new method to build contorted aromatics via palladium-catalyzed cyclopentannulation and Scholl cyclodehydrogenation [69] (Scheme 5.32).
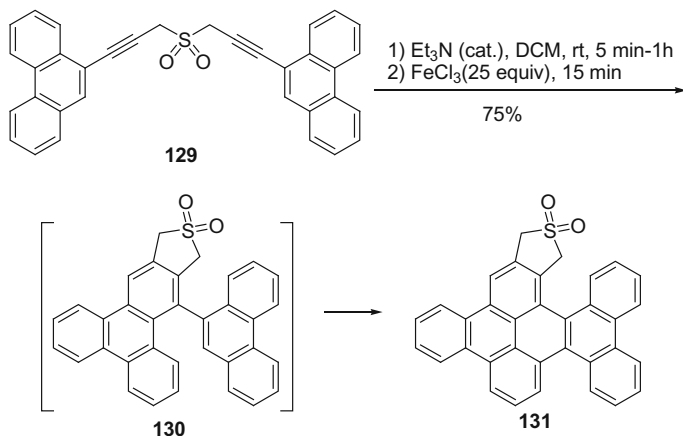
Scheme 5.29 Synthesis of **131**
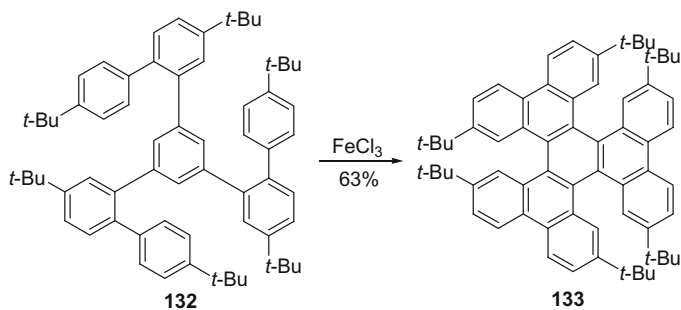
Scheme 5.30 Synthesis of **133**
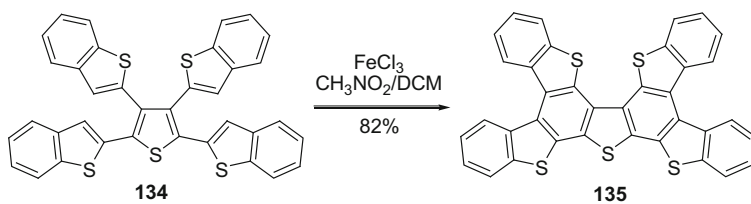
Scheme 5.31 Synthesis of **135**
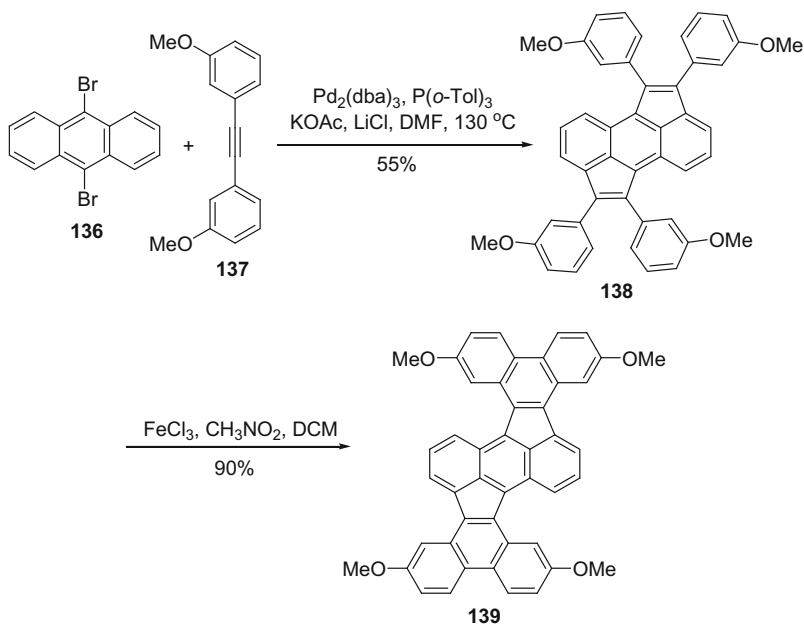
Scheme 5.32 Synthesis of **139**
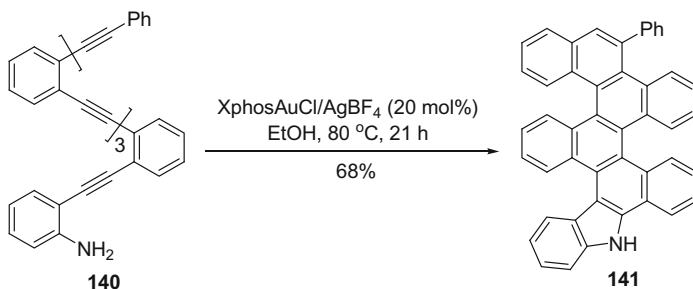
Scheme 5.33 Synthesis of **141**

5.2.6 Au-Mediated Reactions

Moreover, Ohno group reported a new Au-catalyzed hydroamination and consecutive hydroarylation reaction to build helical structures (Scheme 5.33) [70]. Based on this method, molecules with one, two, or three helicene skeletons could be constructed in one step in good yields.

As it was shown above, metal-mediated reactions are widely accepted in the preparation of helicenes, including the [2+2+2] cycloisomerization, ring-closing metathesis, cross-coupling reaction, and Scholl reactions, etc. In comparison, metal-mediated strategy has the advantages of high efficiency (usually constructing more than one ring in one step), moderate to high yields, good functional group tolerance, and the ability to prepare longer helicenes and polycyclic aromatic compounds, although precious metals are involved generally. Another powerful aspect of this strategy is its application in asymmetric synthesis, which will be discussed later.

References

1. Shen Y, Chen C-F (2012) Helicenes: synthesis and applications. Chem Rev 112(3):1463–1535
2. Gingras M (2013) One hundred years of helicene chemistry. Part 1: non-stereoselective syntheses of carbohelicenes. Chem Soc Rev 42(3):968–1006
3. Tanaka K (2013) Synthesis of helically chiral aromatic compounds via [2+2+2] cycloaddition. In: Transition-metal-mediated aromatic ring construction. John Wiley & Sons, Inc., pp 281–298
4. Amatore M, Aubert C (2015) Recent advances in stereoselective [2+2+2] cycloadditions. Eur J Org Chem 2:265–286
5. Tanaka K, Kimura Y, Murayama K (2015) Enantioselective helicene synthesis by rhodium-catalyzed [2+2+2] cycloadditions. Bull Chem Soc Jpn 88(3):375–385
6. Shen Y (2014) Synthesis and reactivity of helicenes. Ph.D. Dissertation, University of Chinese Academy of Sciences, Beijing

7. Storch J, Cermak J, Karban J, Cisarova I, Sykora J (2010) Synthesis of 2-Aza[6]helicene and attempts to synthesize 2,14-Diaza[6]helicene utilizing metal-catalyzed cycloisomerization. J Org Chem 75(9):3137–3140

8. Li Y, Waser J (2015) Platinum-catalyzed domino reaction with benziodoxole reagents for accessing benzene-alkynylated indoles. Angew Chem Int Ed 54(18):5438–5442

9. Mamane V, Hannen P, Fürstner A (2004) Synthesis of phenanthrenes and polycyclic heteroarenes by transition-metal catalyzed cycloisomerization reactions. Chem Eur J 10 (18):4556–4575

10. Thomson PF, Parrish D, Pradhan P, Lakshman MK (2015) Modular, metal-catalyzed cycloisomerization approach to angularly fused polycyclic aromatic hydrocarbons and their oxidized derivatives. J Org Chem 80(15):7435–7446

11. Carreras J, Gopakumar G, Gu L, Gimeno A, Linowski P, Petuškova J, Thiel W, Alcarazo M (2013) Polycationic ligands in gold catalysis: synthesis and applications of extremely π-acidic catalysts. J Am Chem Soc 135(50):18815–18823

12. Murai M, Hosokawa N, Roy D, Takai K (2014) Bismuth-catalyzed synthesis of polycyclic aromatic hydrocarbons (PAHs) with a phenanthrene backbone via cyclization and aromatization of 2-(2-Arylphenyl)vinyl ethers. Org Lett 16(16):4134–4137

13. Yamamoto K, Okazumi M, Suemune H, Usui K (2013) Synthesis of [5]Helicenes with a substituent exclusively on the interior side of the helix by metal-catalyzed cycloisomerization. Org Lett 15(8):1806–1809

14. Weimar M, Correa da Costa R, Lee F-H, Fuchter MJ (2013) A scalable and expedient route to 1-Aza[6]helicene derivatives and its subsequent application to a chiral-relay asymmetric strategy. Org Lett 15(7):1706–1709

15. Donovan PM, Scott LT (2004) Elaboration of diaryl ketones into naphthalenes fused on two or four sides: a naphthoannulation procedure. J Am Chem Soc 126(10):3108–3112

16. Storch J, Sykora J, Cermak J, Karban J, Cisarova I, Ruzicka A (2009) Synthesis of hexahelicene and 1-methoxyhexahelicene via cycloisomerization of biphenylyl-naphthalene derivatives. J Org Chem 74(8):3090–3093

17. Storch J, Bernard M, Sýkora J, Karban J, Čermák J (2013) Intramolecular cascade hydroarylation/cycloisomerization strategy for the synthesis of polycyclic aromatic and heteroaromatic systems. Eur J Org Chem 2:260–263

18. Oyama H, Nakano K, Harada T, Kuroda R, Naito M, Nobusawa K, Nozaki K (2013) Facile synthetic route to highly luminescent sila[7]helicene. Org Lett 15(9):2104–2107

19. Pena D, Perez D, Guitian E, Castedo L (1999) Synthesis of hexabenzotriphenylene and other strained polycyclic aromatic hydrocarbons by palladium-catalyzed cyclotrimerization of arynes. Org Lett 1(10):1555–1557

20. Pena D, Cobas A, Perez D, Guitian E, Castedo L (2000) Kinetic control in the palladium-catalyzed synthesis of C-2-symmetric hexabenzotriphenylene. A conformational study. Org Lett 2(11):1629–1632

21. Pena D, Cobas A, Perez D, Guitian E, Castedo L (2003) Dibenzo[a, o]phenanthro[3,4-s] pycene, a configurationally stable double helicene: synthesis and determination of its conformation by NMR and GIAO calculations. Org Lett 5(11):1863–1866

22. Caeiro J, Pena D, Cobas A, Perez D, Guitian E (2006) Asymmetric catalysis in the [2+2+2] cycloaddition of arynes and alkynes: enantioselective synthesis of a pentahelicene. Adv Synth Catal 348(16–17):2466–2474

23. Romero C, Pena D, Perez D, Guitian E (2008) Palladium-catalyzed [2+2+2] cycloadditions of 3,4-didehydrophenanthrene and 1,2-didehydrotriphenylene. J Org Chem 73(20):7996–8000

24. Stary I, Stara IG (2009) Helicenes. In: Dodziuk H (ed) Strained hydrocarbons: beyond the van't Hoff and Le Bel hypothesis. Wiley-VCH, Weinheim

25. Stara IG, Stary I (2010) Phenanthrenes, Helicenes, and Other Angular Acenes. In: Siegel JS, Tobe Y (eds) Aromatic ring assemblies, polycyclic aromatic hydrocarbons, and conjugated polyenes, vol 45b. Thieme, Stuttgart

26. Stara IG, Stary I, Kollarovic A, Teply F, Saman D, Tichy M (1998) A novel strategy for the synthesis of molecules with helical chirality. Intramolecular [2+2+2] cycloisomerization of triynes under cobalt catalysis. J Org Chem 63(12):4046–4050

27. Stara IG, Stary I, Kollarovic A, Teply F, Vyskocil S, Saman D (1999) Transition metal catalysed synthesis of tetrahydro derivatives of [5]-, [6]- and [7]helicene. Tetrahedron Lett 40 (10):1993–1996

28. Teply F, Stara IG, Stary I, Kollarovic A, Saman D, Rulisek L, Fiedler P (2002) Synthesis of [5]-, [6]-, and [7]helicene via Ni(0)- or Co(I)-catalyzed isomerization of aromatic cis, cis-dienetriynes. J Am Chem Soc 124(31):9175–9180

29. Sehnal P, Stara IG, Saman D, Tichy M, Misek J, Cvacka J, Rulisek L, Chocholousova J, Vacek J, Goryl G, Szymonski M, Cisarova I, Stary I (2009) An organometallic route to long helicenes. Proc Natl Acad Sci U S A 106(32):13169–13174

30. Roose J, Achermann S, Dumele O, Diederich F (2013) Electronically connected [n]Helicenes: synthesis and chiroptical properties of enantiomerically pure (E)-1,2-Di([6]helicen-2-yl) ethenes. Eur J Org Chem 16:3223–3231

31. Schweinfurth D, Zalibera M, Kathan M, Shen C, Mazzolini M, Trapp N, Crassous J, Gescheidt G, Diederich F (2014) Helicene quinones: redox-triggered chiroptical switching and chiral recognition of the semiquinone radical anion lithium salt by electron nuclear double resonance spectroscopy. J Am Chem Soc 136(37):13045–13052

32. Misek J, Teply F, Stara IG, Tichy M, Saman D, Cisarova I, Vojtisek P, Stary I (2008) A straightforward route to helically chiral N-heteroaromatic compounds: Practical synthesis of racemic 1,14-diaza[5]helicene and optically pure 1-and 2-aza[6]helicenes. Angew Chem Int Ed 47(17):3188–3191

33. Narcis MJ, Takenaka N (2014) Helical-chiral small molecules in asymmetric catalysis. Eur J Org Chem 1:21–34

34. Chercheja S, Klívar J, Jančařík A, Rybáček J, Salzl S, Tarábek J, Pospíšil L, Vacek Chocholoušová J, Vacek J, Pohl R, Císařová I, Starý I, Stará IG (2014) The use of cobalt-mediated cycloisomerisation of ynedinitriles in the synthesis of pyridazinohelicenes. Chem Eur J 20 (27):8477–8482

35. Crittall MR, Rzepa HS, Carbery DR (2011) Design, synthesis, and evaluation of a helicenoidal DMAP Lewis base catalyst. Org Lett 13(5):1250–1253

36. Adriaenssens L, Severa L, Salova T, Cisarova I, Pohl R, Saman D, Rocha SV, Finney NS, Pospisil L, Slavicek P, Teply F (2009) Helquats: a facile, modular, scalable route to novel helical dications. Chem Eur J 15(5):1072–1076

37. Pospisil L, Teply F, Gal M, Adriaenssens L, Horacek M, Severa L (2010) Helquats, helical extended diquats, as fast electron transfer systems. Phys Chem Chem Phys 12(7):1550–1556

38. Severa L, Adriaenssens L, Vavra J, Saman D, Cisarova I, Fiedler P, Teply F (2010) Highly modular assembly of cationic helical scaffolds: rapid synthesis of diverse helquats via differential quaternization. Tetrahedron 66(19):3537–3552

39. Severa L, Koval D, Novotna P, Oncak M, Sazelova P, Saman D, Slavicek P, Urbanova M, Kasicka V, Teply F (2010) Resolution of a configurationally stable [5]helquat: enantiocomposition analysis of a helicene congener by capillary electrophoresis. New J Chem 34(6):1063–1067

40. Severa L, Ončák M, Koval D, Pohl R, Šaman D, Císařová I, Reyes-Gutiérrez PE, Sázelová P, Kašička V, Teplý F, Slavíček P (2012) A chiral dicationic [8]Circulenoid: photochemical origin and facile thermal conversion into a helicene congener. Angew Chem Int Ed 51 (48):11972–11976

41. Čížková M, Šaman D, Koval D, Kašička V, Klepetářová B, Císařová I, Teplý F (2014) Modular synthesis of helicene-like compounds based on the imidazolium motif. Eur J Org Chem 26:5681–5685

42. Kamikawa K, Takemoto I, Takemoto S, Matsuzaka H (2007) Synthesis of helicenes utilizing palladium-catalyzed double C-H arylation reaction. J Org Chem 72(19):7406–7408

43. Ueda Y, Tsuji H, Tanaka H, Nakamura E (2014) Synthesis, crystal packing, and ambipolar carrier transport property of twisted Dibenzo[g, p]chrysenes. Chem Asian J 9(6):1623–1628

44. Xue X, Scott LT (2007) Thermal cyclodehydrogenations to form 6-membered rings: cyclizations of [5]helicenes. Org Lett 9(20):3937–3940
45. Shimizu M, Nagao I, Tomioka Y, Hiyama T (2008) Palladium-Catalyzed Annulation of vic-Bis(pinacolatoboryl)alkenes and -phenanthrenes with 2,2′-Dibromobiaryls: Facile Synthesis of Functionalized Phenanthrenes and Dibenzo[g, p]chrysenes. Angew Chem Int Ed 47(42):8096–8099
46. Kashihara H, Asada T, Kamikawa K (2015) Synthesis of a double helicene by a palladium-catalyzed cross-coupling reaction: structure and physical properties. Chem Eur J 21(17):6523–6527
47. Staab HA, Diehm M, Krieger C (1994) Synthesis, structure and basicity of 1,16-Diaza[6] Helicene. Tetrahedron Lett 35(45):8357–8360
48. Takenaka N, Sarangthem RS, Captain B (2008) Helical chiral pyridine N-Oxides: a new family of asymmetric catalysts. Angew Chem Int Ed 47(50):9708–9710
49. Kelgtermans H, Dobrzańska L, Meervelt LV, Dehaen W (2012) Synthesis of functionalized Dioxa-aza[7]helicenes using palladium catalyzed arylations. Org Lett 14(6):1500–1503
50. Kelgtermans H, Dobrzańska L, Van Meervelt L, Dehaen W (2012) A fragment-based approach toward substituted Trioxa[7]helicenes. Org Lett 14(20):5200–5203
51. Nakano K, Oyama H, Nishimura Y, Nakasako S, Nozaki K (2012) λ5-Phospha[7]helicenes: synthesis, properties, and columnar aggregation with one-way chirality. Angew Chem Int Ed 51(3):695–699
52. Baba K, Tobisu M, Chatani N (2013) Palladium-catalyzed direct synthesis of phosphole derivatives from triarylphosphines through cleavage of carbon-hydrogen and carbon-phosphorus bonds. Angew Chem Int Ed 52(45):11892–11895
53. Kaneko E, Matsumoto Y, Kamikawa K (2013) Synthesis of Azahelicene N-Oxide by Palladium-Catalyzed Direct C-H Annulation of a Pendant (Z)-Bromovinyl Side Chain. Chem Eur J 19(36):11837–11841
54. Bogányi B, Kámán J (2013) A concise synthesis of indoloquinoline skeletons applying two consecutive Pd-catalyzed reactions. Tetrahedron 69(45):9512–9519
55. Furusawa M, Imahori T, Igawa K, Tomooka K, Irie R (2013) Palladium-catalyzed Tandem Cyclodehydrogenation of Phenylenediyne-linked Bis(arenol)s to Produce Benzodifuran-containing Condensed Heteroaromatic Ring Systems. Chem Lett 42(10):1134–1136
56. Wu D, Ge H, Chen Z, Liang J, Huang J, Zhang Y, Chen X, Meng X, Liu SH, Yin J (2014) Imides modified benzopicenes: synthesis, solid structure and optoelectronic properties. Org Biomol Chem 12(44):8902–8910
57. Bock H, Huet S, Dechambenoit P, Hillard EA, Durola F (2015) From chrysene to double [5] Helicenes. Eur J Org Chem 5:1033–1039
58. Collins SK, Grandbois A, Vachon MP, Cote J (2006) Preparation of helicenes through olefin metathesis. Angew Chem Int Ed 45(18):2923–2926
59. Grandbois A, Collins SK (2008) Enantioselective synthesis of [7]Helicene: dramatic effects of olefin additives and aromatic solvents in asymmetric olefin metathesis. Chem Eur J 14(30):9323–9329
60. Cote J, Collins SK (2009) Synthesis of higher helicenes via olefin metathesis and C-H activation. Synthesis-Stuttgart 9:1499–1505
61. Miyasaka M, Rajca A, Pink M, Rajca S (2004) Chiral molecular glass: synthesis and characterization of enantiomerically pure thiophene-based [7]helicene. Chem Eur J 10(24):6531–6539
62. Wang ZH, Shi JW, Wang JE, Li CL, Tian XY, Cheng YX, Wang H (2010) Syntheses and crystal structures of Benzohexathia[7]helicene and naphthalene cored double helicene. Org Lett 12(3):456–459
63. Xia Y, Liu Z, Xiao Q, Qu P, Ge R, Zhang Y, Wang J (2012) Rhodium(II)-Catalyzed Cyclization of Bis(N-tosylhydrazone)s: an efficient approach towards polycyclic aromatic compounds. Angew Chem Int Ed 51(23):5714–5717
64. Dubois F, Gingras M (1998) Syntheses of [5]-helicene by McMurry or carbenoid couplings. Tetrahedron Lett 39(28):5039–5040

65. Murai M, Matsumoto K, Okada R, Takai K (2014) Rhodium-catalyzed dehydrogenative germylation of C-H bonds: new entry to unsymmetrically functionalized 9-Germafluorenes. Org Lett 16(24):6492–6495
66. Mitra T, Das J, Maji M, Das R, Das UK, Chattaraj PK, Basak A (2013) A one-pot Garratt-Braverman cyclization and Scholl oxidation route to acene-helicene hybrids. RSC Adv 3(43):19844–19848
67. Pradhan A, Dechambenoit P, Bock H, Durola F (2013) Twisted polycyclic arenes by intramolecular scholl reactions of C3-symmetric precursors. J Org Chem 78(6):2266–2274
68. Liu X, Wang Y, Gao J, Jiang L, Qi X, Hao W, Zou S, Zhang H, Li H, Hu W (2014) Easily solution-processed, high-performance microribbon transistors based on a 2D condensed benzothiophene derivative. Chem Commun (Camb) 50(4):442–444
69. Bheemireddy SR, Ubaldo PC, Finke AD, Wang L, Plunkett KN (2016) Contorted aromatics via a palladium-catalyzed cyclopentannulation strategy. J Mater Chem C 4(18):3963–3969
70. Hirano K, Inaba Y, Takasu K, Oishi S, Takemoto Y, Fujii N, Ohno H (2011) Gold(I)-Catalyzed Polycyclizations of Polyenyne-Type Anilines Based on Hydroamination and Consecutive Hydroarylation Cascade. J Org Chem 76(21):9068–9080

Chapter 6
Other Synthetic Methods

Abstract In this chapter, other methods for the preparation of racemic helicenes are introduced. First, helical skeletons can be constructed by radical cyclizations or cascade radical cyclizations, but the regioselectivity may be a problem for some cases. By oxidative coupling method, BINOL analogues are widely utilized for the preparation of oxahelicenes, while iterative modular synthesis is employed to prepare extended helicene structures and longer helicenes. Some azahelicenes can also be expediently prepared by oxidative homocouplings. Similarly, thiahelicene can be synthesized by DDQ/Lewis acid-mediated Scholl reaction to construct three C–C bonds via a one-pot strategy. Compared with photochemical cyclization, oxidative coupling method has the advantages of short reaction time and simple purification process. Particularly, heterohelicenes including helicenium cations, azahelicenes, thiohelicenes, azabora[6]helicene, and boraoxa[6]helicene can be prepared by microwave reaction of suitable amine or salts, carbenoid coupling, Cu-mediated oxidative coupling, one-pot [4+2]benzannulation strategy, Pictet–Spengler reaction, double electrophilic borylation, and other heteroatom arylation reactions.

Keywords Azabora[6]helicene · Boraoxa[6]helicene · Carbenoid coupling · Heteroatom arylation reaction · Radical cyclization · Oxidative coupling

In this chapter, we will introduce other methods for the preparation of racemic helicenes, including radical cyclization, oxidative coupling, carbenoid coupling, heteroatom arylation reaction, and other gram-scale synthetic methods.

Harrowven and co-workers developed a new approach for the construction of helical skeletons by radical cyclizations [1–3]. As shown in Scheme 6.1, bis(stilbene) precursors **2a–c** were prepared via Wittig reaction quantitatively with moderate diastereoselectivity (*Z,Z/Z,E*). In the presence of stannane and VAZO, the radical cyclization was achieved to give [5]helicenes **3a–c** [3]. The two methoxy groups directed the reaction, otherwise the regioselectivity would be a problem [1].

Wang group described a new strategy to synthesize indeno-fused helicenes via the radical cyclization of polyynes [4–6]. On exposure to *t*-BuOK, tetrayne **4** was
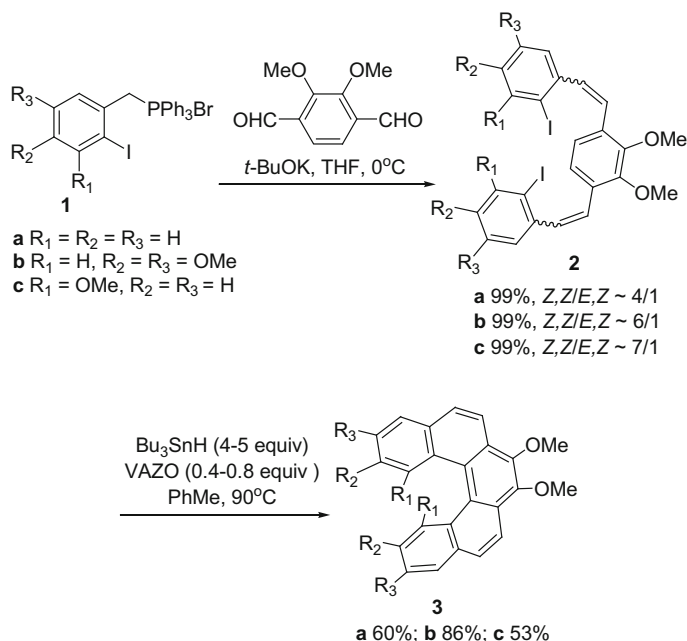
Scheme 6.1 Synthesis of [5]helicenes **3a–c**

transformed into diindeno-fused 1,14-diphenyl[5]helicene **8** in moderate yield via the sequential Schmittel cyclization and biradical coupling (Scheme 6.2). Based on this method, various indeno-fused [4]- and [5]helicenes were prepared in moderate to good yields.

Basak and Roy employed Bergman cyclization to prepare [4]- and [5]helicenes (Scheme 6.3) in dry DMSO with yields of 75–80 % [7]. However, the enediyne precursors need a long route to be obtained.

Recently, another type of cascade radical cyclization was described by Alabugin group [8]. Based on theoretical calculation, the reaction was initiated by the attack of Bu₃Sn radical at the C(sp) adjacent to the C(sp3) of **11** to form vinyl radical, which was directed by the hydroxyl group (Scheme 6.4). Then, the radical was translocated between the skipped alkynes, and finally relocated at the carbon connected to Sn by resonance after constructing four rings. At last, the leaving of hydroxyl radical resulted in the aromatization, which performed as "traceless" directing group. Moreover, the Sn-functionalized product of the first step could be further modified by Stille cross-coupling reaction.

BINOL analogues were widely utilized for the preparation of oxahelicenes. In 1973, Hogberg reported a sealed tube reaction (Scheme 6.5), in which the diol **13** was converted into trioxa[7]helicene **14** on exposure to red phosphorus and HBr [9]. In 1999, Dotz and co-workers directly prepared oxahelicene **16** from ether **15** by adding excess TMSI (Scheme 6.6) [10]. Moreover, the same group described an
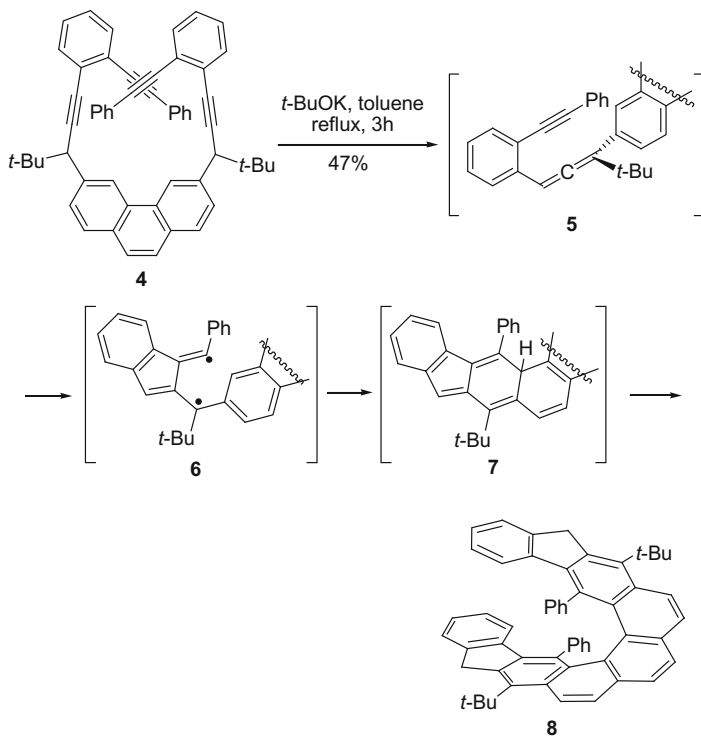
Scheme 6.2 Synthesis of diindeno-fused 1,14-diphenyl[5]helicene **8**
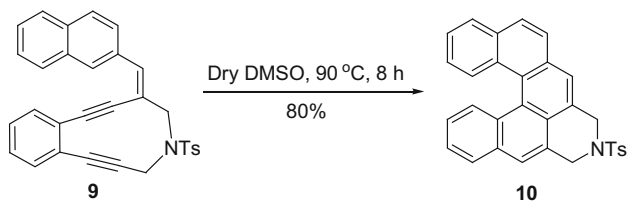
Scheme 6.3 Synthesis of **10**
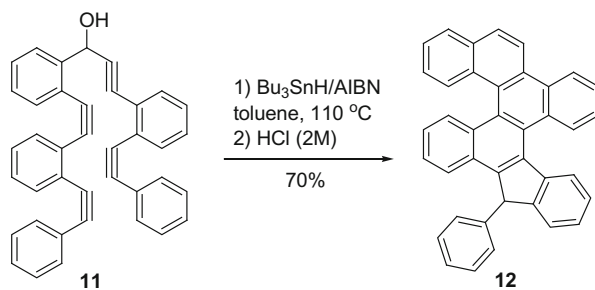
Scheme 6.4 Synthesis of **12**
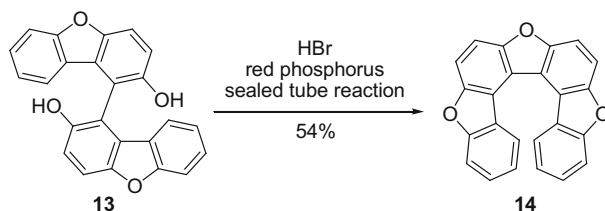
Scheme 6.5 Synthesis of trioxa[7]helicene **14**
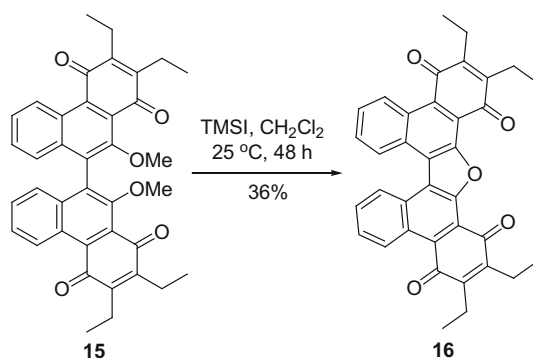
Scheme 6.6 Synthesis of oxahelicene **16**
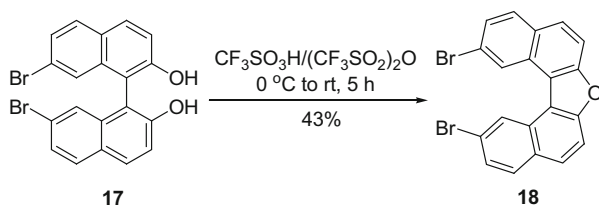
Scheme 6.7 Synthesis of oxahelicene **18**

acid promoted strategy from diol **17** to synthesize oxa[5]helicene **18** (Scheme 6.7) [11]. Thongpanchang and co-workers used similar condition and prepared five different oxahelicenes **22a–e** from the cheap commercially available naphthalene-2,7-diol **19** in good yield (Scheme 6.8) [12].

Based on these strategies, iterative modular synthesis was also employed to prepare extended helicene structures. Tsubaki and co-workers synthesized fan-shaped helicene-fused three-dimensional compound **28** in reasonable yield based on the oxidative coupling of 2-hydroxynaphthalene (Scheme 6.9) [13]. According to DFT calculations, the two adjacent helicene moieties had different
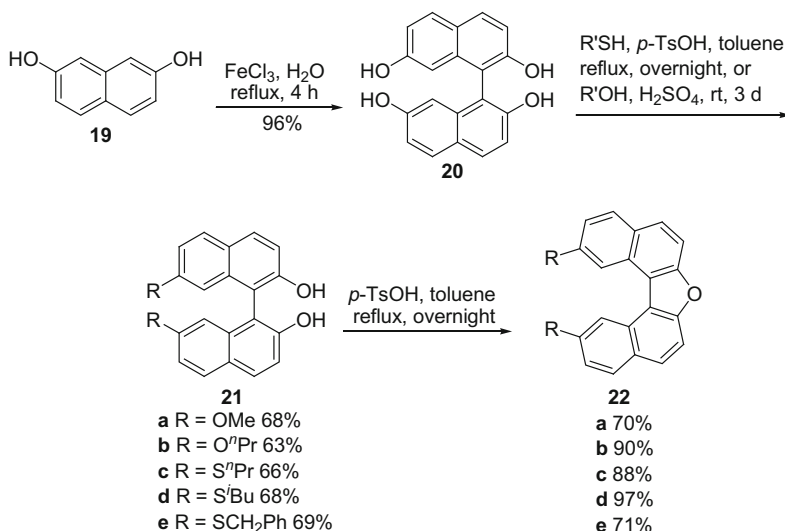
Scheme 6.8 Synthesis of oxahelicenes **22a–e**

helicities, where the naphthalene rings formed an alternate mountain-valley fold conformation. As the π-systems extended, the HOMO–LUMO energy gaps of the compounds decreased. The higher order helicenes, like **28**, would aggregate even at the concentration of 10^{-6} M.

Different from the above method, Bedekar and Sundar employed [1,1′-binaph-thalene]-2,2′,7-triol **29** as the precursor, where one hydroxyl group was incorpo-rated to render the most sterically hindered position as the binding site (Scheme 6.10) [14]. The homocoupling was achieved by Cu-mediated oxidation, and the yellow [11]helicene **32** was obtained via ether formation in the presence of Brönsted acid in 36 % yield.

2-Hydroxyl [4]helicene **33** was utilized for the preparation of longer helicenes by Karikomi group (Scheme 6.11) [15]. Two steps, including the Cu-mediated oxidative coupling and the Lawesson's reagent promoted cyclization, were needed to give the products in moderate to good yields.

Similarly, Hiroto, Shinokubo, and co-workers employed anthracen-2-ol deriva-tives as precursors to prepare π-extended dibenzooxa[5]helicenes [16]. The oxi-dation of anthracen-2-ol **36** on the exposure of MnO_2 gave the ketone **37** in 50 % yield, which could be transformed into diacetal **38** by the treatment of $TsOH \cdot H_2O$ and $HC(OMe)_3$. The two methoxy groups were demonstrated to be positioned at different sides by single crystallographic study, which rendered the molecule a helical skeleton. The final aromatization was easily completed with the help of TfOH (Scheme 6.12).

Some azahelicenes could also be expediently prepared by oxidative homocou-plings. In 2005, Rajca and co-workers reported the synthesis of double helicene via
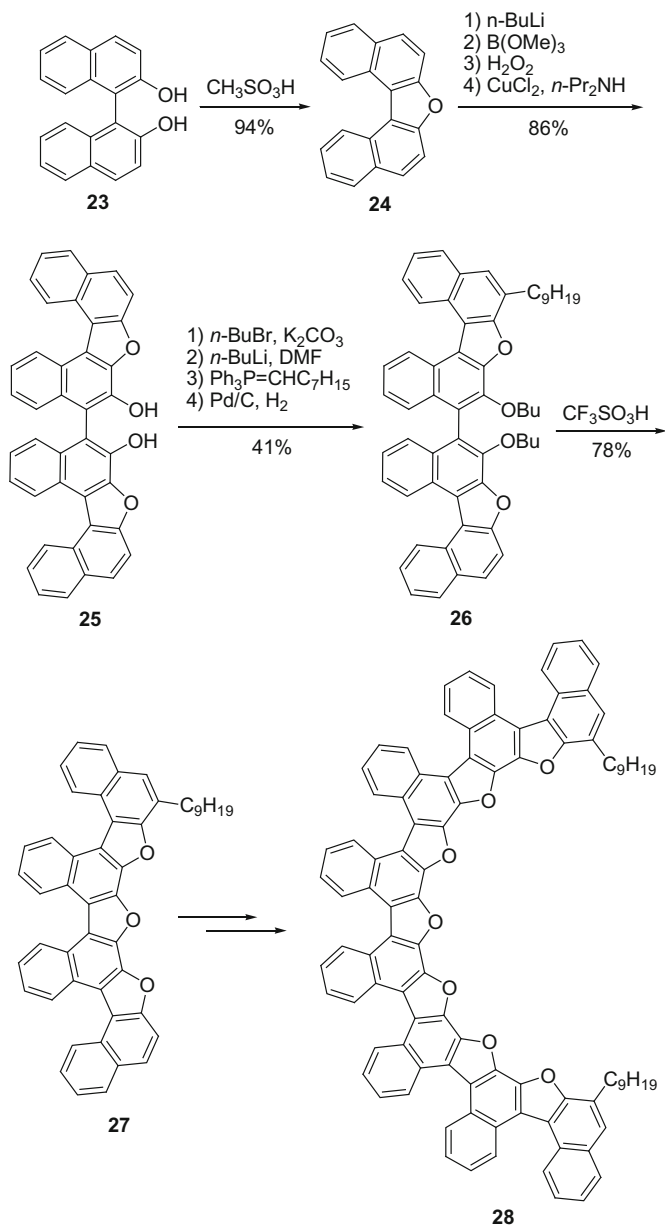
Scheme 6.9 Synthesis of fan-shaped helicene-fused three-dimensional compound **28**

oxidative *C–C* and *N–N* homocouplings [17]. Via the Buckwald–Hartwig *C–N* coupling between 4-*tert*-butylaniline and bromide **40**, diamine **41** was synthesized in 50 % yield. The subsequent alkylation afforded the planarized diamine
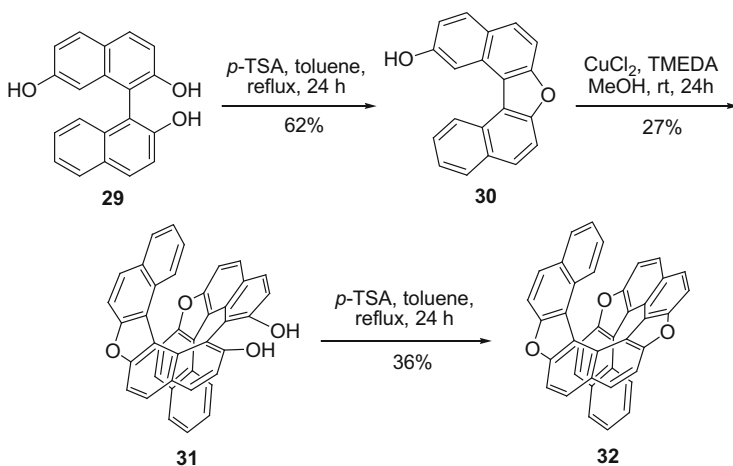
Scheme 6.10 Synthesis of oxa[11]helicene **32**
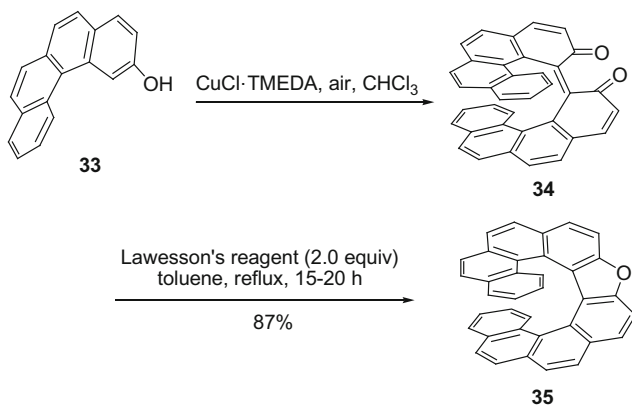
Scheme 6.11 Synthesis of oxahelicene **35**

42, which was transformed into azahelicene **43** with good thermal stability in the presence of benzoyl peroxide (Scheme 6.13).

The homocoupling of anthracen-2-amine derivatives was studied by Hiroto, Shinokubo, and co-workers [18]. They found that the oxidation of amines in the presence of DDQ could produce two products, pyrrole-fused dibenzoaza[5]helicenes and pyrazine-fused bisanthracenes. The major product could be controlled by different additives. For example, if 5 % EtOH was added into the solvent, aza[5] helicene **45** could be obtained in 68 % yield (Scheme 6.14).

Recently, Sakamaki, Seki, and co-workers described the preparation of hetero-helicenes by DDQ oxidation. First, they examined the dimerization of 6,13-dihydrodibenzo[*b,i*]phenazine **46a** and 13*H*-dibenzo[*b,i*]phenoxazine **46b** (Scheme 6.15) [19]. A stepwise route was employed: (1) forming one C–N bond in
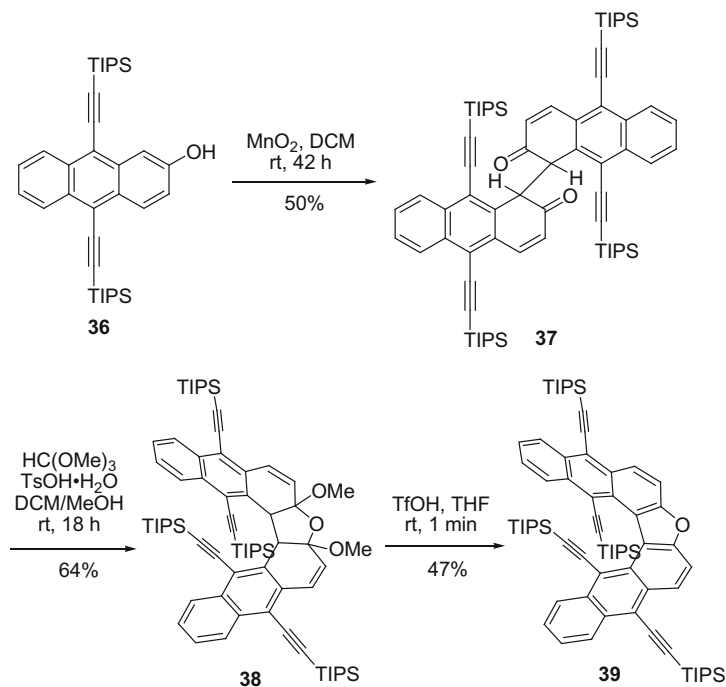
Scheme 6.12 Synthesis of π-extended dibenzooxa[5]helicene **39**

the presence of DDQ, and (2) finishing the following oxidation with the help of combination of DDQ and Sc(OTf)$_3$. In addition, this method could be performed as one-pot reaction by adding DDQ and Lewis acid to the reaction after the first oxidation. Very recently, the same groups synthesized the dimer of phenothiazine **49**, and, fortunately, obtained the crystal structure of the radical cation of helicene **51** (Scheme 6.16). It was found that the helicenium cation structure was less distorted than its parent skeleton [20].

Besides the oxidative coupling of active *N*-heteroaromatic compounds, 2,2′-diamino-1,1′-binaphthyl **52** was also good precursor for the expedient synthesis of azahelicenes. In 2008, Caronna and co-workers described the synthesis of 7,8-diaza [5]helicene **55** in two steps [21]. Diamine **52** was converted into a mixture of *N,N′*-dioxide **53**, *N*-oxide **54**, and a very small amount of helicene **55** in the presence of *m*-CPBA, and the oxides could be reduced by LAH to give the helicene in good yields (Scheme 6.17, route *a*). Moreover, Takeda, Minakata, and co-workers developed a new method for constructing such kind of molecules (Scheme 6.17, route *b*) that the diamine **52** was smoothly oxidized into the helicene **55** in one step with a yield of 97 % [22].

Dehaen group described a DDQ/Lewis acid-mediated Scholl reaction to construct three C–C bonds via a one-pot strategy, affording thia[7]helicene **57** in 70 % yield
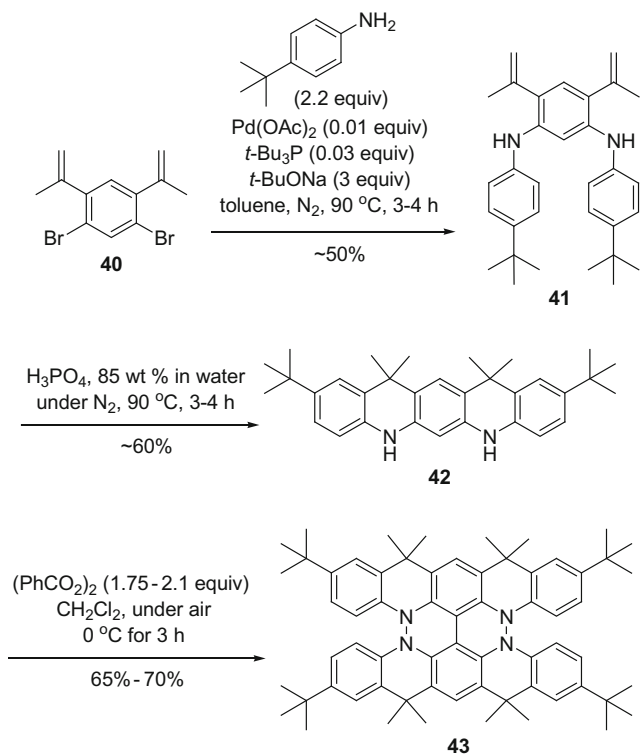
Scheme 6.13 Synthesis of azahelicene **43**
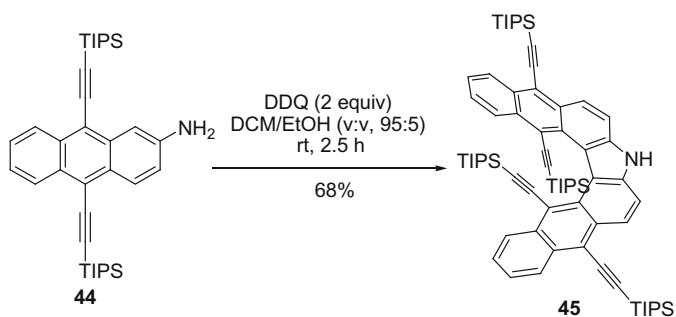
Scheme 6.14 Synthesis of aza[5]helicene **45**
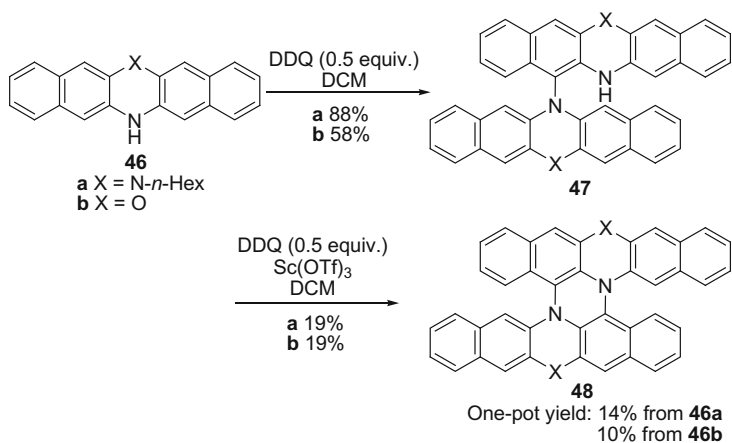
Scheme 6.15 Synthesis of heterohelicenes **48a–b**
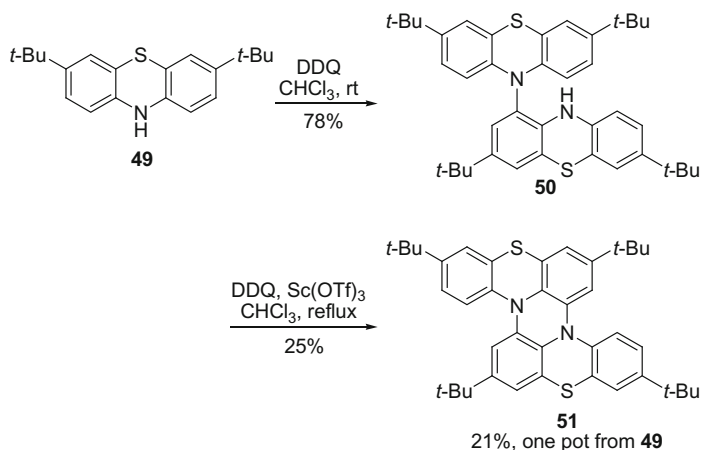
Scheme 6.16 Synthesis of heterohelicene **51**

(Scheme 6.18) [23]. Compared with photochemical cyclization, the FeCl$_3$/CH$_3$NO$_2$ method has advantages of short reaction time and simple purification process.

Hexaaza[5]helicene was prepared by Abarca, Ballesteros, Rius, and co-workers from neocuproine **58** in three steps (Scheme 6.19) [24]. Interestingly, they proposed a dynamic racemization process of helicene in which helicene underwent tautomeric equilibrium between the parent structure **61** and the chain structure (the terminal ring was opened as 2-(diazomethyl)pyridine structure).

Lacour and co-workers prepared a series of helicenium cations, which were highly configurationally stable and had superior chiroptical properties [25]. Recently, they described the synthesis of a series of [6]helicene cations **68–70**
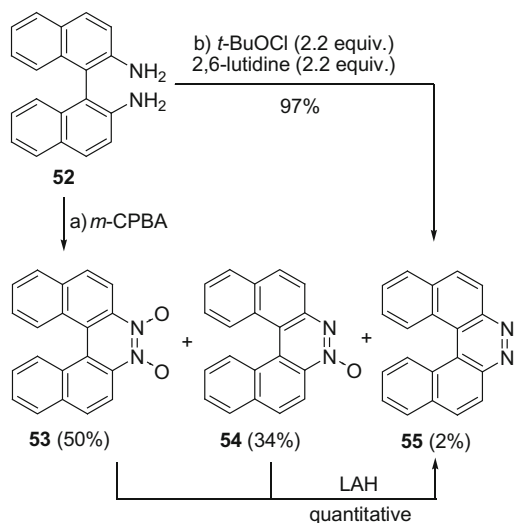
Scheme 6.17 Synthesis of 7,8-diaza[5]helicene **55**, and its *N,N′*-dioxide **53**, *N*-oxide **54**
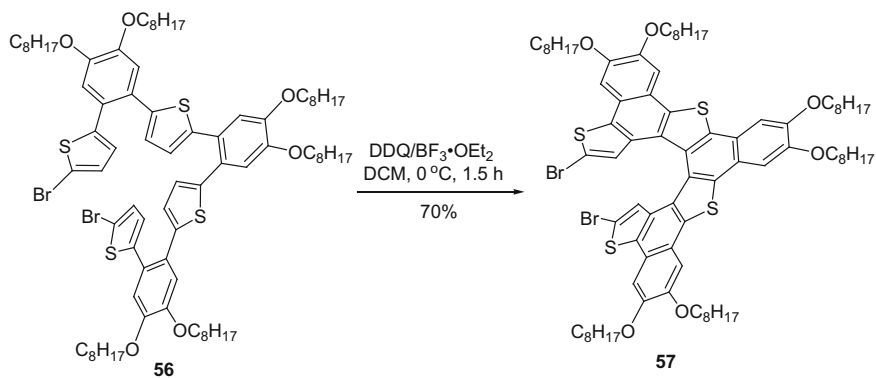
Scheme 6.18 Synthesis of thia[7]helicene **57**
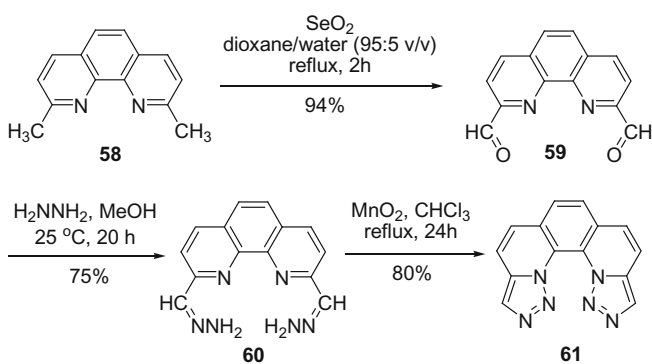
Scheme 6.19 Synthesis of **61**
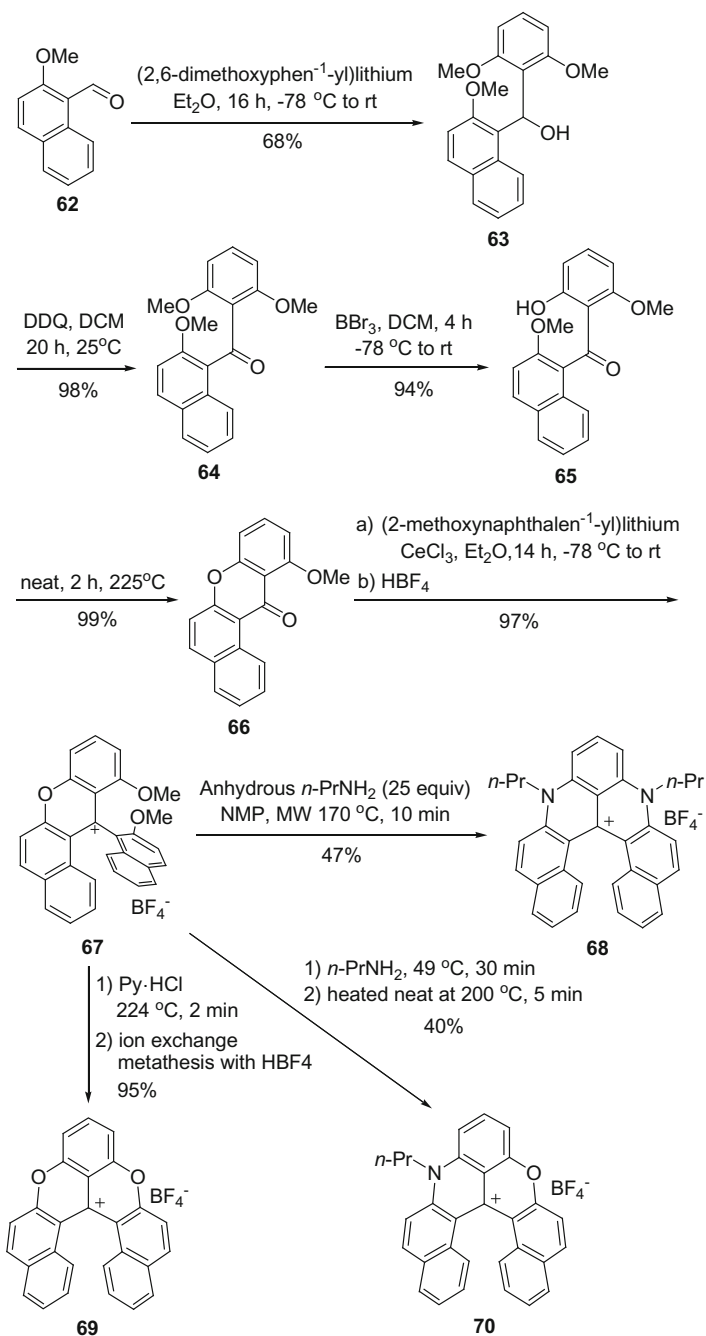
Scheme 6.20 Synthesis of [6]helicene cations **68–70**
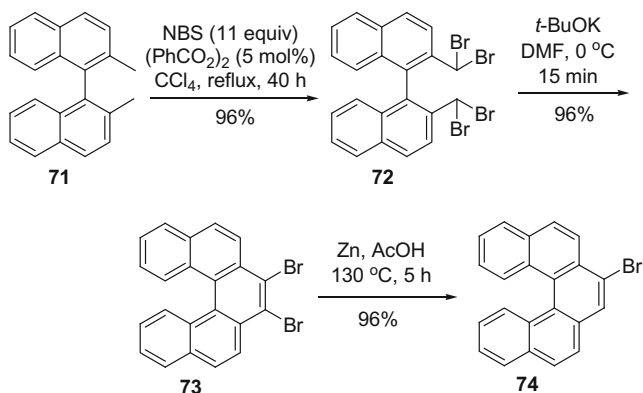
Scheme 6.21 Synthesis of helicene **74**

(Scheme 6.20) [26]. From 2-methoxy-1-naphthaldehyde, cation **67** could be easily synthesized in multigram scale with a total yield of 60 % via addition of aryl lithium reagent, oxidation, demethylation, cyclization, the second addition of aryl lithium reagent, and ion exchange metathesis. The construction of different helicene skeletons were performed under microwave on exposure of suitable amine or salts.

Gingras group developed a strategy for the preparation of [5]helicenes and [7] helicene based on 1,1′-dinaphthyl structure by carbenoid coupling [27, 28]. In addition, this method was improved by the same group via benzylic (dibromo) methine coupling (Scheme 6.21) [29]. The bromination of 2,2′-dimethyl-1,1′-binaphthyl **71** with excess of NBS afforded tetrabromide **72** in 96 % yield. The ring-closing reaction was rapid with the help of *t*-BuOK, giving [5]helicene **73** in high yield, which could be reduced to produce helicene **74**.

As for the synthesis of thiahelicenes, Rajca group developed an iterative approach on the basis of thiophene building blocks [30]. As shown in Scheme 6.22, the dimer **77** could be obtained from the desilylation product of **75** after Li/halogen
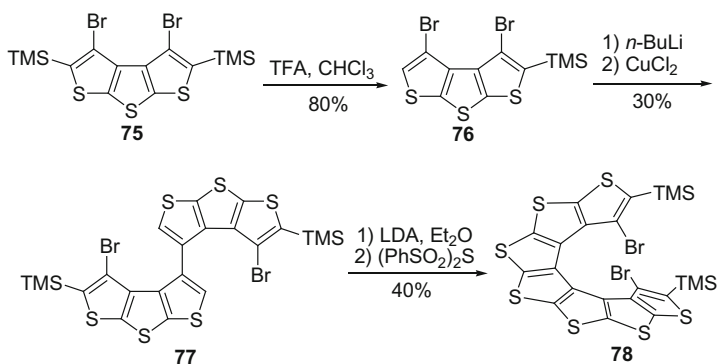
Scheme 6.22 Synthesis of thiahelicene **78**
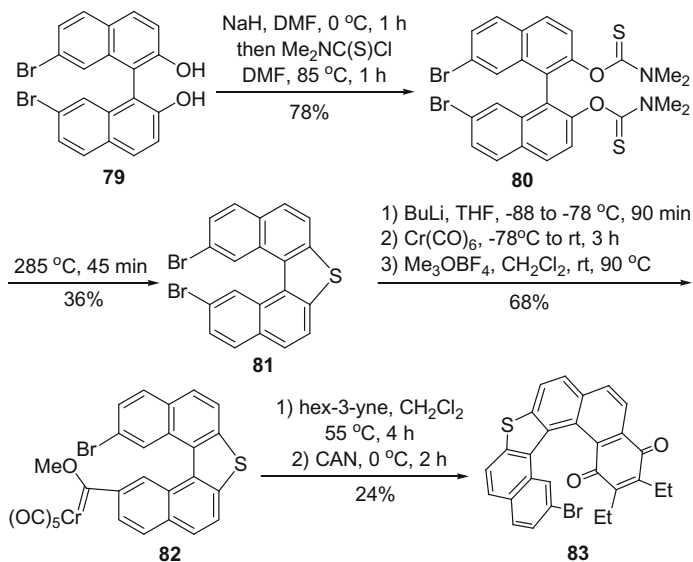
Scheme 6.23 Synthesis of [6]helicene quinone **83**

exchange and the Cu-mediated oxidative coupling. The subsequent annulation was achieved with the help of (PhSO$_2$)$_2$S after the H-abstraction by LDA, affording **78** in 40 % yield.

Another method to construct thiophene ring was reported by Dotz and co-workers via Newman–Kwart rearrangement at high temperature (Scheme 6.23) [11]. In addition, [5]helicene could be extended to [6]helicene quinone by Cr-mediated benzannulation.

Recently, Reddy and co-workers described a one-pot [4+2]benzannulation strategy for the synthesis of helicenes with carbazole moieties [31]. Scheme 6.24 showed the synthesis of aza[5]helicene **87** from indole **84** and 1,5-diphenylpenta-2,4-diyn-1-ol **85** via Lewis acid catalyzed propargylation and cycloisomerization in good yield.

Daugulis and Truong described a new method to construct [4]-, [5]-, and [6] helicenes from phenols and aryl chlorides [32]. As shown in Scheme 6.25, 1-chloronaphthalene **89** was converted into 1,2-didehydronaphthalene in the presence of LiTMP, which underwent [2+2] cycloaddition with dimethyl phenol **88**, affording benzocyclobutene. The following ring-opening of the benzene ring and the second [2+2] cycloaddition and ring-opening gave dinaphthalene-fused ten-membered ring ketone anion. Helicenes **90** and **91** were obtained after intramolecular nucleophilic attack and aromatization.
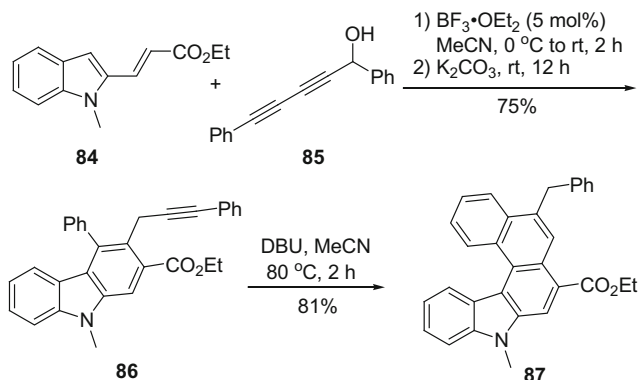
Scheme 6.24 Synthesis of aza[5]helicene **87**

Chen, Lu, and co-workers utilized Pictet–Spengler reaction to prepare functionalized azahelicenes in the presence of TFA at 140 °C (Scheme 6.26) [33]. Some of them were potential bidentate ligands.

Starting from 2,7-dihydroxynaphthalene **19**, Karnic and co-workers prepared 7,8-dioxa[6]helicenes (Scheme 6.27) [34]. The *cis*-7a,14c-dihydro-diol **97** was prepared with glyoxal in the presence of acetic acid in gram scale, which was transformed into helicene diol **100** via protection by esterification, aromatization, and deprotection in good yield.

Hatakeyama, Nakamura, and co-workers reported a novel method to construct azabora[6]helicene via three-step procedure [35]. The bromide **101**, prepared from 1-bromonaphthalen-2-ol, reacted with LiNH$_2$ to give diarylamine **102** with the help of Pd$_2$(dba)$_3$ and Sphos in 74 % yield (Scheme 6.28). After treatment with *n*-BuLi and BCl$_3$, **103** was obtained. The subsequent borylation took place in the present of AlCl$_3$ and HTMP, producing **104** in 68 % yield in three steps. This azabora[6] helicene displayed n-type (racemate) and p-type (enantiomer) semiconductivity.

Recently, Hatakeyama group reported another method to construct bora[4]-, and bora[6]helicene via one-pot procedure with reasonable yield [36]. As shown in Scheme 6.29, after lithiation by *n*-BuLi, a dibromide intermediate was formed from the bromide **105** in the presence of BBr$_3$, which was converted into boraoxa[6] helicene **106** via double electrophilic borylation with the help of Hünig's base in 33 % yield. This type of molecule was utilized in PHOLED for the long lifetime and high efficiency.

From readily available materials, Shi and Dou described a facile and efficient method to build helicene-like molecules in gram-scale diastereoselectively [37]. The [7]helicene-like compound **109** could be prepared from 2-hydroxy-1-naphthaldehyde **107** via condensation, esterification, and reductive coupling,
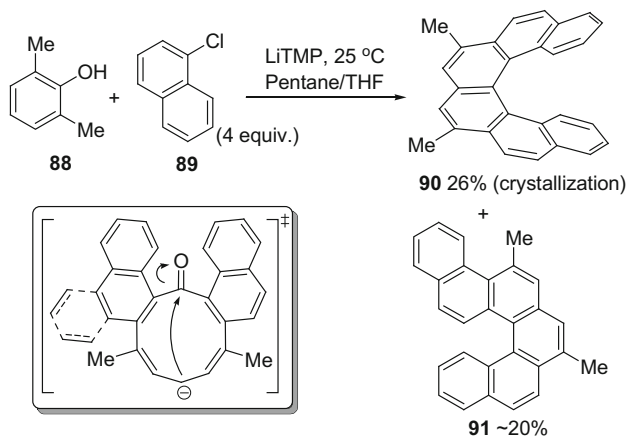
Scheme 6.25 Synthesis of helicenes **90** and **91**
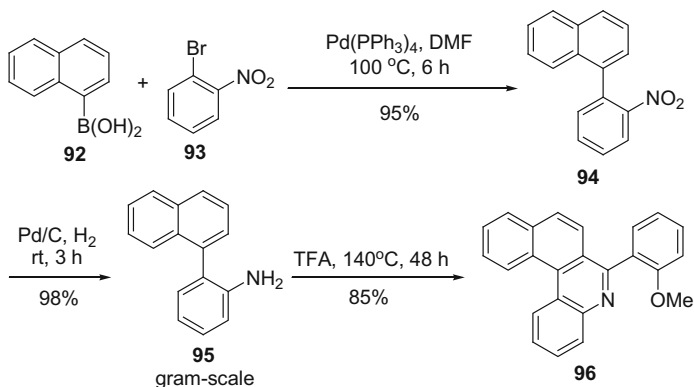
Scheme 6.26 Synthesis of azahelicene **96**

which was easily purified by recrystallization (Scheme 6.30). The central ring of **109** had a chair configuration, which rendered the skeleton helical.

Although different reactions were reported, some common features could be found as follows:

(1) Aryl amines and phenols were utilized: for construction of [4]helicene, Ar group was usually phenyl group; while for [5]-, [6]-, and [7]helicenes, naphthyl, anthracenyl, phenanthyl, or other heteroaryl groups were employed (Fig. 6.1).

(2) The active or the activated reaction sites of the building blocks were generally designed to be a key point, especially for the ring-closing step (Fig. 6.1).
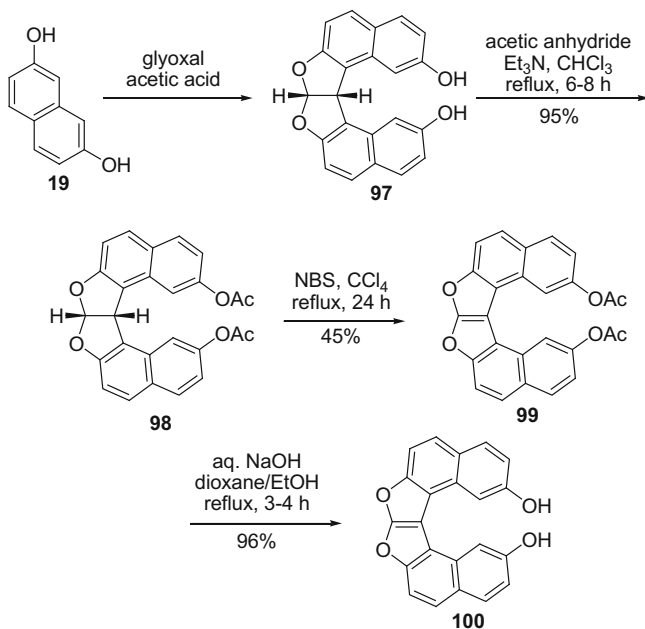
Scheme 6.27 Synthesis of 7,8-dioxa[6]helicene **100**
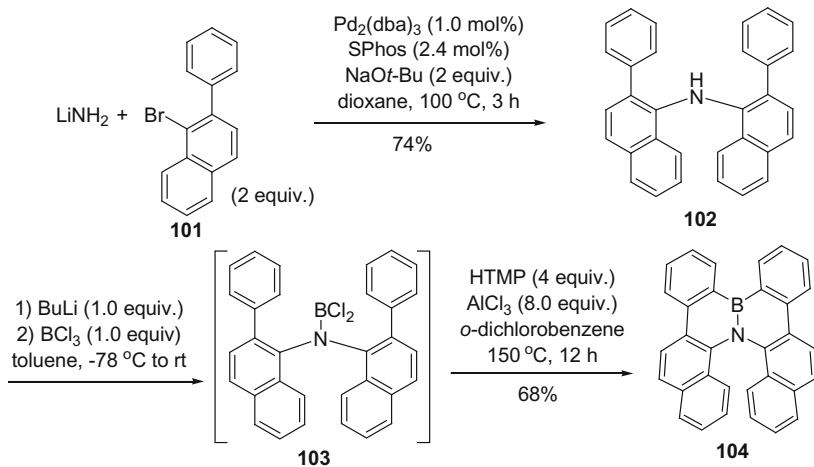
Scheme 6.28 Synthesis of azabora[6]helicene **104**
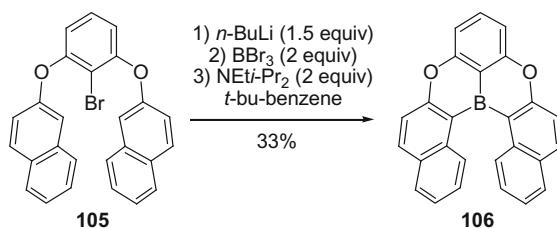
Scheme 6.29 Synthesis of boraoxa[6]helicene **106**
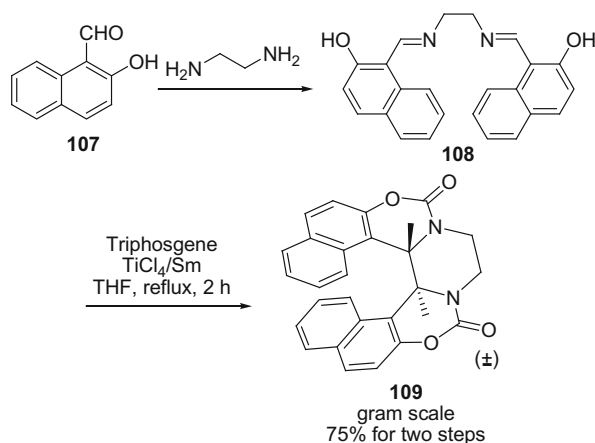
Scheme 6.30 Synthesis of [7]helicene-like compound **109**

R = OH, NH$_2$, OR', NHAr, NAr$_2$
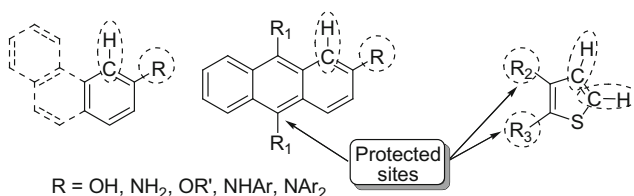
Fig. 6.1 Active reaction sites (*dashed circles*) and activated reaction sites (*dashed ellipses*)

References

1. Harrowven DC, Nunn MIT, Fenwick DR (2002) [5]Helicenes by iterative radical cyclisations to arenes. Tetrahedron Lett 43(17):3189–3191
2. Harrowven DC, Nunn MIT, Fenwick DR (2002) [5]helicenes by tandem radical cyclisation. Tetrahedron Lett 43(41):7345–7347
3. Harrowven DC, Guy IL, Nanson L (2006) Efficient phenanthrene, helicene, and azahelicene syntheses. Angew Chem Int Ed 45(14):2242–2245

4. Yang YH, Dai WX, Zhang YZ, Petersen JL, Wang KK (2006) Ring expansion of 11H-benzo [b]fluorene-11-methanols and related compounds leading to 17,18-diphenyldibenzo[a, o] pentaphene and related polycyclic aromatic hydrocarbons with extended conjugation and novel architectures. Tetrahedron 62(18):4364–4371

5. Zhang YZ, Petersen JL, Wang KK (2007) Synthesis and structures of diindeno-fused 1,12-diphenylbenzo[c]phenanthrene and 1,14-diphenyl[5]helicene bearing severe helical twists. Org Lett 9(6):1025–1028

6. Zhang YZ, Petersen JL, Wang KK (2008) Synthesis and structures of helical polycyclic aromatic hydrocarbons bearing aryl substituents at the most sterically hindered positions. Tetrahedron 64(7):1285–1293

7. Roy S, Basak A (2013) Exploring the scope of Bergman Cyclization mediated cascade reaction of alkenyl enediynes: synthesis of [5]helicene and amino acid appended [4]helicenes. Tetrahedron 69(9):2184–2192

8. Pati K, dos Passos Gomes G, Harris T, Hughes A, Phan H, Banerjee T, Hanson K, Alabugin IV (2015) Traceless directing groups in radical cascades: from oligoalkynes to fused helicenes without tethered initiators. J Am Chem Soc 137(3):1165–1180

9. Hogberg HE (1973) Cyclo-oligomerization of quinones. 6. Synthesis and cyclization of a furohelicene. Acta Chem Scand 27(7):2591–2596

10. Tomuschat P, Kroner L, Steckhan E, Nieger M, Dotz KH (1999) Reactions of complex ligands, Part 86—Benzannulation of axial chiral biscarbene complexes of chromium: An approach to novel C-2-symmetrical redox-active bi(phenanthrenequinones). Chem Eur J 5 (2):700–707

11. Schneider JF, Nieger M, Nattinen K, Dotz KH (2005) A novel approach to functionalized heterohelicenes via chromium-templated benzannulation reactions. Synthesis-Stuttgart 7:1109–1124

12. Areephong J, Ruangsupapichart N, Thongpanchang T (2004) A concise synthesis of functionalized 7-oxa-[5]-helicenes. Tetrahedron Lett 45(15):3067–3070

13. Nakanishi K, Fukatsu D, Takaishi K, Tsuji T, Uenaka K, Kuramochi K, Kawabata T, Tsubaki K (2014) Oligonaphthofurans: fan-shaped and three-dimensional π-compounds. J Am Chem Soc 136(19):7101–7109

14. Shyam Sundar M, Bedekar AV (2015) Synthesis and study of 7,12,17-Trioxa[11]helicene. Org Lett 17(23):5808–5811

15. Salim M, Akutsu A, Kimura T, Minabe M, Karikomi M (2011) Novel synthesis of oxa[9] helicenes by Lawesson's reagent-mediated cyclization of helical quinone derivatives. Tetrahedron Lett 52(35):4518–4520

16. Matsuno T, Koyama Y, Hiroto S, Kumar J, Kawai T, Shinokubo H (2015) Isolation of a 1,4-diketone intermediate in oxidative dimerization of 2-hydroxyanthracene and its conversion to oxahelicene. Chem Commun (Camb) 51(22):4607–4610

17. Shiraishi K, Rajca A, Pink M, Rajca S (2005) pi-conjugated conjoined double helicene via a sequence of three oxidative CC- and NN-homocouplings. J Am Chem Soc 127(26):9312–9313

18. Goto K, Yamaguchi R, Hiroto S, Ueno H, Kawai T, Shinokubo H (2012) Intermolecular oxidative annulation of 2-Aminoanthracenes to diazaacenes and Aza[7]helicenes. Angew Chem Int Ed 51(41):10333–10336

19. Sakamaki D, Kumano D, Yashima E, Seki S (2015) A facile and versatile approach to double N-Heterohelicenes: tandem oxidative C-N couplings of N-Heteroacenes via cruciform dimers. Angew Chem Int Ed 54(18):5404–5407

20. Sakamaki D, Kumano D, Yashima E, Seki S (2015) A double hetero[4]helicene composed of two phenothiazines: synthesis, structural properties, and cationic states. Chem Commun (Camb) 51(97):17237–17240

21. Caronna T, Fontana F, Mele A, Sora IN, Panzeri W, Vigano L (2008) A simple approach for the synthesis of 7,8-diaza[5]helicene. Synthesis-Stuttgart 3:413–416

22. Takeda Y, Okazaki M, Maruoka Y, Minakata S (2015) A facile synthesis of functionalized 7,8-diaza[5]helicenes through an oxidative ring-closure of 1,1′-binaphthalene-2,2′-diamines (BINAMs). Beilstein J Org Chem 11:9–15

23. Waghray D, de Vet C, Karypidou K, Dehaen W (2013) Oxidative transformation to naphthodithiophene and Thia[7]helicenes by intramolecular scholl reaction of substituted 1,2-Bis(2-thienyl)benzene precursors. J Org Chem 78(22):11147–11154

24. Adam R, Ballesteros-Garrido R, Vallcorba O, Abarca B, Ballesteros R, Leroux FR, Colobert F, Amigó JM, Rius J (2013) Synthesis and structural properties of hexaaza[5] helicene containing two [1,2,3]triazolo[1,5-a]pyridine moieties. Tetrahedron Lett 54 (32):4316–4319

25. Bosson J, Gouin J, Lacour J (2014) Cationic triangulenes and helicenes: synthesis, chemical stability, optical properties and extended applications of these unusual dyes. Chem Soc Rev 43 (8):2824–2840

26. Torricelli F, Bosson J, Besnard C, Chekini M, Bürgi T, Lacour J (2013) Modular synthesis, orthogonal post-functionalization, absorption, and chiroptical properties of cationic [6] Helicenes. Angew Chem Int Ed 52(6):1796–1800

27. Dubois F, Gingras M (1998) Syntheses of [5]-helicene by McMurry or carbenoid couplings. Tetrahedron Lett 39(28):5039–5040

28. Gingras M, Dubois F (1999) Synthesis of carbohelicenes and derivatives by "carbenoid couplings". Tetrahedron Lett 40(7):1309–1312

29. Goretta S, Tasciotti C, Mathieu S, Smet M, Maes W, Chabre YM, Dehaen W, Giasson R, Raimundo JM, Henry CR, Barth C, Gingras M (2009) Expeditive syntheses of functionalized pentahelicenes and NC-AFM on Ag(001). Org Lett 11(17):3846–3849

30. Rajca A, Miyasaka M (2007) Synthesis and characterization of novel chiral conjugated materials. In: Miller TJJ, Bunz UHF (eds) Functional organic materials: syntheses, strategies and applications. Wiley-VCH, Weinheim, pp 547–581

31. Raji Reddy C, Rani Valleti R, Dilipkumar U (2016) One-pot sequential propargylation/ cycloisomerization: a facile [4+2]-Benzannulation approach to carbazoles. Chem Eur J 22 (7):2501–2506

32. Truong T, Daugulis O (2013) Divergent reaction pathways for phenol arylation by arynes: synthesis of helicenes and 2-arylphenols. Chem Sci 4(1):531–535

33. Zheng Y-H, Lu H-Y, Li M, Chen C-F (2013) Synthesis, structures, and optical properties of Aza[4]helicenes. Eur J Org Chem 15:3059–3066

34. Hasan M, Pandey AD, Khose VN, Mirgane NA, Karnik AV (2015) Sterically congested chiral 7,8-Dioxa[6]helicene and its dihydro analogues: synthesis, regioselective functionalization, and unexpected domino prins reaction. Eur J Org Chem 17:3702–3712

35. Hatakeyama T, Hashimoto S, Oba T, Nakamura M (2012) Azaboradibenzo[6]helicene: carrier inversion induced by helical homochirality. J Am Chem Soc 134(48):19600–19603

36. Hirai H, Nakajima K, Nakatsuka S, Shiren K, Ni J, Nomura S, Ikuta T, Hatakeyama T (2015) One-step borylation of 1,3-Diaryloxybenzenes towards efficient materials for organic light-emitting diodes. Angew Chem Int Ed 54(46):13581–13585

37. Lin W, Dou G-L, Hu M-H, Cao C-P, Huang Z-B, Shi D-Q (2013) Facile, efficient, and diastereoselective synthesis of heterohelicene-like molecules. Org Lett 15(6):1238–1241

Chapter 7
Asymmetric Synthesis

Abstract Asymmetric synthesis is a practical method for the direct synthesis of optically pure helicenes. This chapter focuses on the recent development of asymmetric synthesis of helicenes from 2012 to early 2016. Enantioselective methods for the asymmetric synthesis of helicenes by the combination of transition metals and chiral ligands to induce the helicity are first introduced. Asymmetric organocatalytic approach for helicenes is also developed. Different from the enantioselective methods, diastereoselective method in which the target helicene has one or two chiral centers besides helicity provides another efficient way for the selective synthesis of helicenes. The combination of biocatalysis and transition metal catalysis is also utilized to achieve the highly stereoselective synthesis of helicenes. Moreover, the strategy for the preparation of helicenes from optically pure substrates with central chirality or axial chirality is accepted as an efficient and practical method to construct helicenes, especially the long ones. In these strategies, transition metal-mediated reactions, especially the [2+2+2] cycloisomerization, Diels-Alder addition, and chiral auxiliary-induced reactions are usually used for the efficient asymmetric synthesis of helicenes and heterohelicenes.

Keywords Asymmetric synthesis · Enantioselectivity · Diastereoselectivity · Transition metal catalysis · Biocatalysis · Chiral ligands · Chiral auxiliary-induced reactions

The asymmetric synthesis of helicenes was reported as early as 1970s, when Kagan [1, 2], Celvin [3–5], and co-workers used circularly polarized light to induce the helicity, where the reaction produced helicenes with a low specific rotation value (Scheme 7.1) [3]. Since then, chemists have been trying to find practical methods for the direct synthesis of optically pure helicenes. The first enantioselective synthesis was reported in 1999 by two papers, respectively. Starý, Stará, and co-workers described a route to asymmetric synthesis of helicene via a Ni-mediated [2+2+2] cycloisomerization of triynes with up to 48 % ee (Scheme 7.2) [6]; while Carreño, Urbano, and co-workers developed a method using asymmetric Diels-Alder reactions
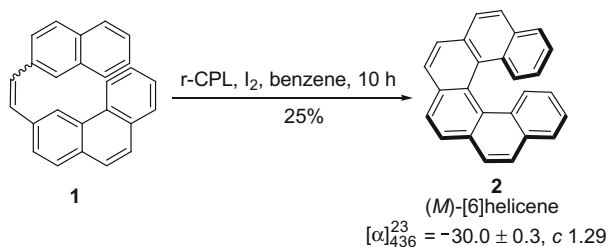
Scheme 7.1 Synthesis of (*M*)-[6]helicene **2**
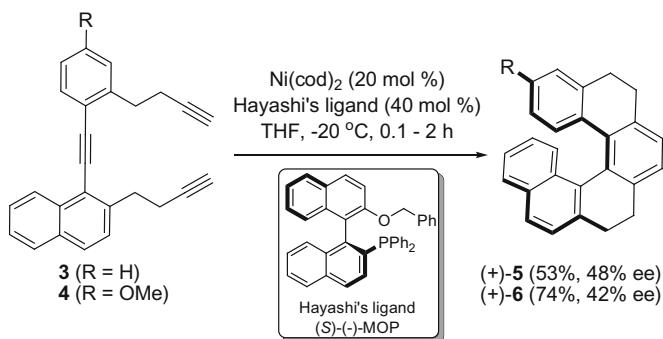
Scheme 7.2 Asymmetric synthesis of helicenes

Scheme 7.3 Asymmetric
Diels-Alder reactions to
helicene quinone in high
enantioselectivity
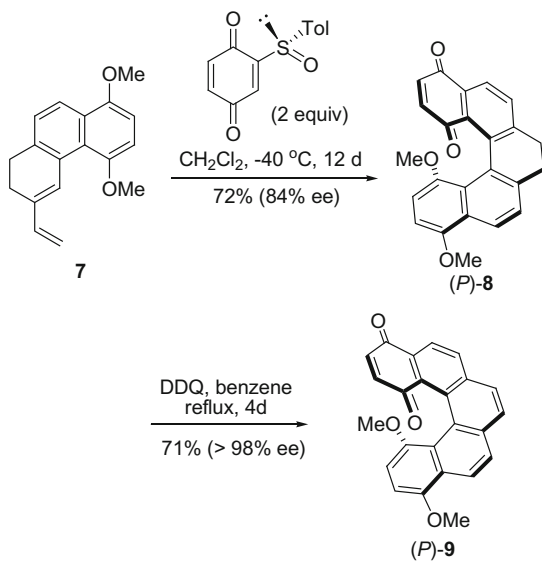
between the dienes and (*SS*)-(+)-2-(*p*-tolylsulfinyl)-1, 4-benzoquinone to achieve the preparation with high enantioselectivity (Scheme 7.3) [7].

In this chapter, we will focus on the recent development, from 2012 to early 2016, of the strategies to obtain enantioenriched helicenes, including (1) enantioselective methods, using the combination of transition metals and chiral ligands to induce the helicity; (2) diastereoselective methods, where the target helicene had one or two chiral centers besides helicity; (3) the approaches that based on enantioenriched substrates, during which the chiral centers disappeared after the control of helicity. Because the optical resolution achieved by introducing chiral auxiliaries and HPLC was nicely summarized by the previous reviews [8, 9], this part will not be discussed here.

7.1 Enantioselective Routes

The routes summarized here were based on transition metal-mediated reactions, especially the [2+2+2] cycloisomerization, where the helicity was induced by the chiral ligands.

Tanaka group developed Rh-catalyzed [2+2+2] cycloisomerization to build helical skeletons via intermolecular cycloaddition [10, 11]. By changing the diyne precursor, carbo-, phospha-, and silahelicenes could be synthesized up to 93 % ee with the help of (*S*)-Segphos ligands in reasonable yields (Scheme 7.4) [12, 13].

The same group utilized this method to construct longer helicenes [14]. From dialdehyde **13**, hexayne **16** could be obtained in six steps in moderate yield, which could be transformed into [11]helicene-like molecule **17** in 91 % ee via double [2+2+2] cycloisomerization (Scheme 7.5).
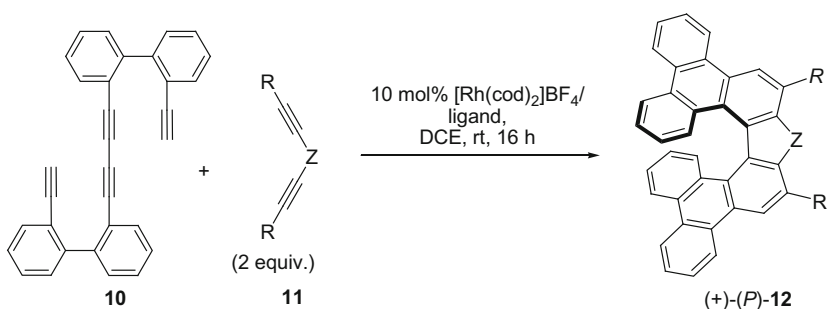
Ligand		
(*S*)-xyl-Segphos	R = *n*-Bu, Z = CO,	59%, 91% ee
(*S*)-Segphos	R = *n*-Bu, Z = P(O)OMe	46%, 68% ee
(*S*)-Segphos	R = CH₂OH, Z = SiMe₂	10%, 91% ee

Scheme 7.4 Rh-catalyzed [2+2+2] cycloisomerization to build helical skeletons via intermolecular cycloaddition
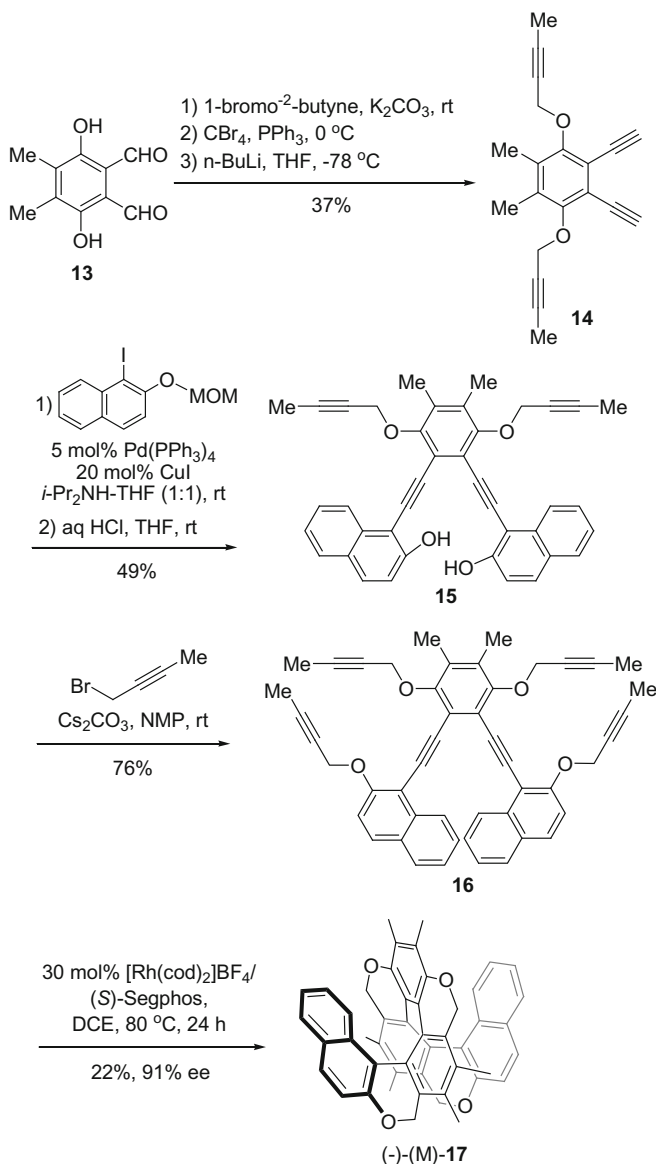
Scheme 7.5 Synthesis of [11]helicene-like molecule **17** via double [2+2+2] cycloisomerization

Shibata and co-workers reported a new method to construct silahelicenes stereoselectively [15]. The reaction was stepwise (Scheme 7.6): (1) the enantiose-lectivity was controlled in the first step, Ir-catalyzed intermolecular [2+2+2] cycloaddition between the tetrayne silane and diyne with carbonyl group, affording the triyne with axial chirality with the help of chiral ferrocene ligand; (2) the
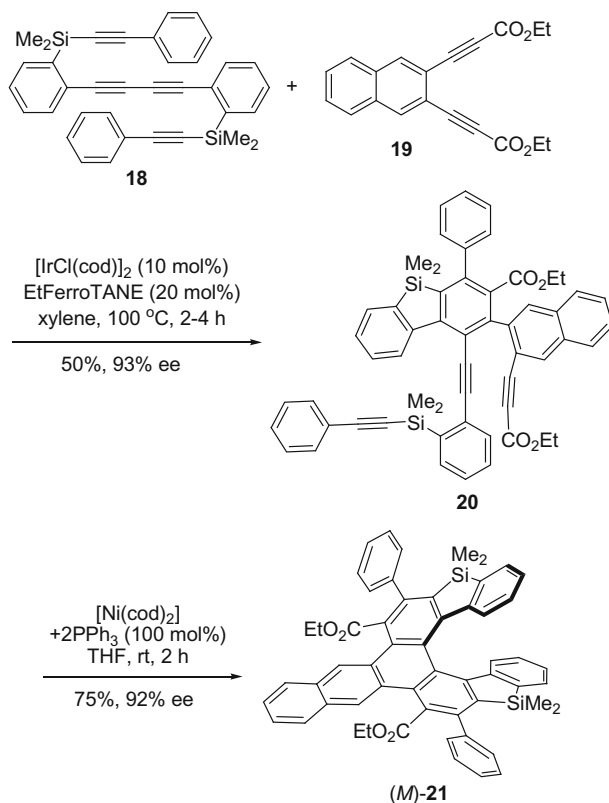
Scheme 7.6 Stereoselective synthesis of silahelicene (*M*)-**21**

subsequent Ni-mediated intramolecular [2+2+2] produced helicene with two Si moieties in a stereospecific manner.

Based on their previous [2+2+2] cycloisomerization of dienetriynes [16], Starý, Stará, and co-workers developed a simple and versatile approach for benzohelicenes, where the "diene" moieties were replaced by "*o*-phenylene" units [17]. The triyne precursor **22** could be easily prepared from readily available reagents via Sonogashira and Suzuki-Miyaura cross-coupling reactions. The helicity was controlled by the QUINAP ligand, giving the helicene **23** in 85 % ee. The optical purity could be promoted up to >99 % ee after crystallization (Scheme 7.7). Moreover, Heller, Stará, and co-workers reexamined the enantioselective [2+2+2] cycloisomerization of triynes by chiral Ni(0)/Co(I) complexes, which produced helicenes with ee values up to 64 % [18].

In addition to this, Au(I)-catalyzed [2+2+2] asymmetric cycloisomerization was explored by Tanaka and co-workers [19]. As shown in Scheme 7.8, from 2-hydroxy-1-naphthaldehyde **24** and 4-hydroxybenzonitrile **27**, tetrayne **30** could be accessed in five steps in moderate yield. The enantioselective cyclization was achieved in the presence of Au(I)-(*S*)-BINAP catalyst, in which excess of silver
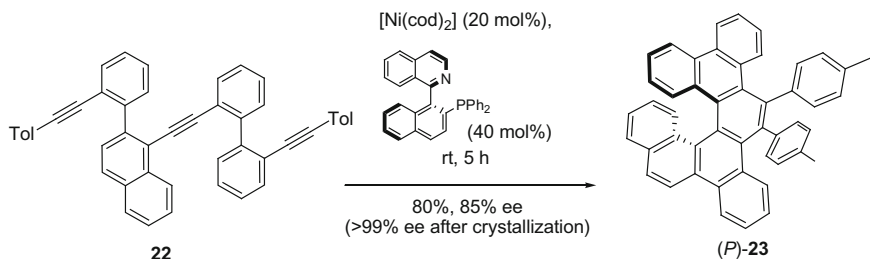
Scheme 7.7 Synthesis of helicene (*P*)-**23** by enantioselective [2+2+2] cycloisomerization of triynes
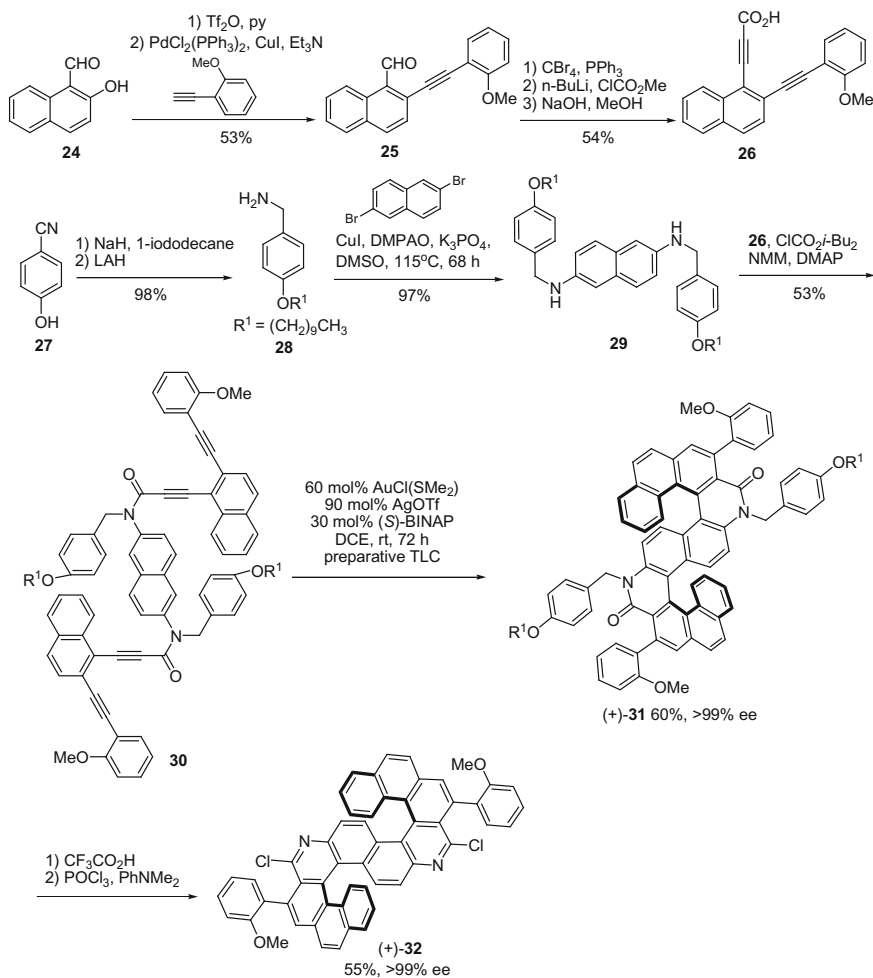
Scheme 7.8 Synthesis of helicene (+)-**32** by the enantioselective cyclization
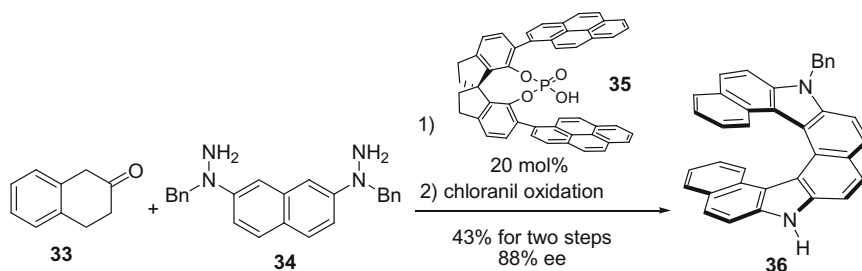
Scheme 7.9 Synthesis of diazahelicene **36** by double enantioselective Fisher indole reactions

triflate was crucial for this transformation. Finally, the *S*-shaped double azahelicene was prepared in 55 % yield with >99 % ee. This type of helicenes showed high CPL activity.

In 2014, List group reported the first example of asymmetric organocatalytic approach for helicenes [20]. In this reaction, the substituents on SPINOL-based Brønsted acid were critical for the high enantioselectivity. For **35**, two 1-pyrenyl groups helped the long-range control via π-π interactions between the substrates and the catalyst in the pocket of *ca.* 1.5 nm width. By double enantioselective Fisher indole reactions, diazahelicene **36** was prepared in 43 % yield and 88 % ee (Scheme 7.9).

As mentioned previously, Kagan and co-workers reported that circularly polarized light could induce the stilbene precursors to give enantioenriched helicenes [1, 2]. Recently, Fuchter and Kuimova reexamined the asymmetric photochemical synthesis of helicenes under the circularly polarized light irradiation [21]. They found that the asymmetric induction exist in both the ring-closing (**37** → **38**) and ring-opening (**38** → **37**) procedures (Scheme 7.10). According to
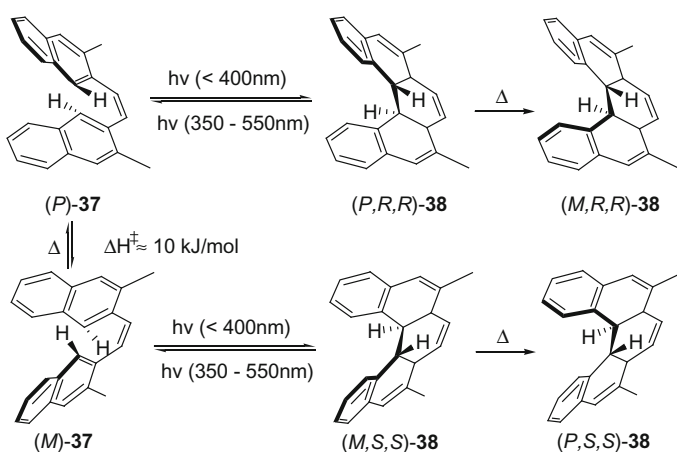
Scheme 7.10 Asymmetric photochemical synthesis of helicenes

their experimental and theoretical studies, utilizing opposite polarized lights could promote the asymmetric induction approximately for two times. For example, the irradiation of the solution with right circularly polarized (RCP) 355 nm and left circularly polarized (LCP) 532 nm, the enantioselectivity was equal to $(g^{355} + g^{532})/2$; while if RCP 355 nm and RCP 532 nm were used, the enantios-electivity was half of the difference of the g-factors of the transitions.

7.2   Diastereoselective Routes

Different from the enantioselective methods, the helicity was not induced by the catalysts or CPL, but by the chiral centers on the helical skeletons.

In 2012, Marinetti and co-workers reported the first example of 1H-phosphindole-embedded helicenes [22]. As shown in Scheme 7.11, the stilbene precursor **42** could be synthesized from bromo[4]helicene **39** and dioxaborolane **40** via stepwise Pd-catalyzed cross-coupling reactions in 43 % yield. Fortunately, the subsequent oxidative photocyclization was proved to be region- and stereoselective,
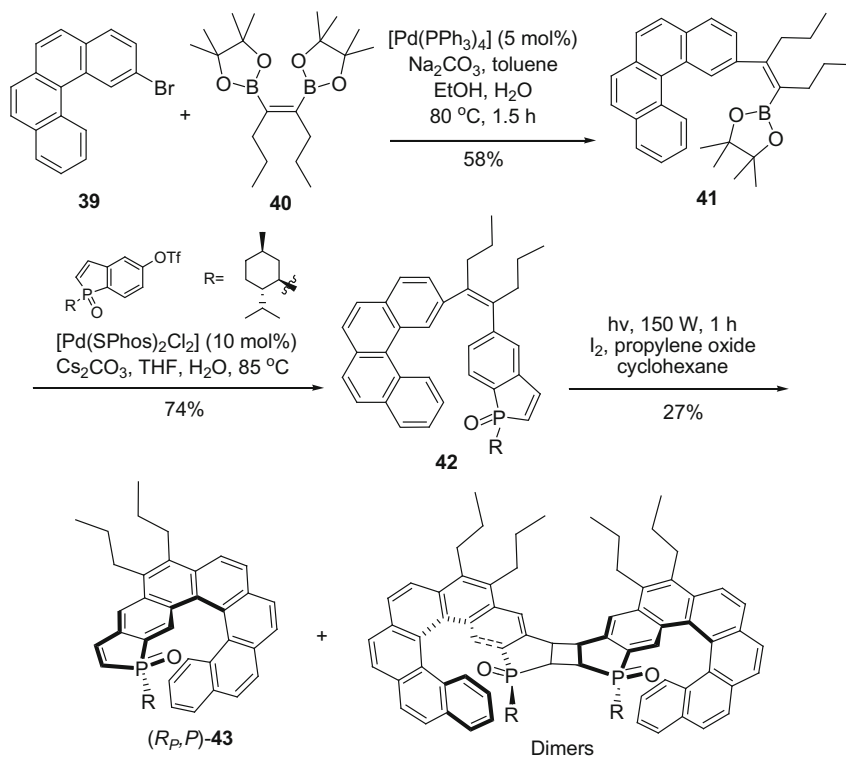
Scheme 7.11 Synthesis of (R_P,P)-**43** and the dimers
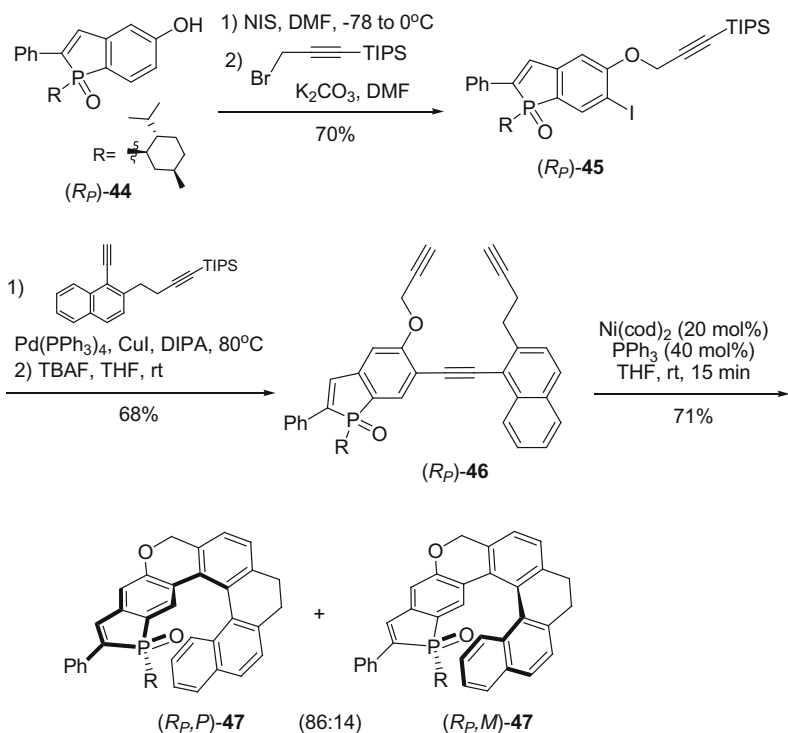
Scheme 7.12 Chemoselective synthesis of phosphorus embedded helicenes

although the product might be composed by six isomers: (R_P,P)-**43** was the major product, and its dimers were the byproducts.

Later, Marinetti, Voituriez, and co-workers utilized Ni(0)-catalyzed [2+2+2] cycloisomerization to construct phosphorus embedded helicenes (Scheme 7.12) [23]. Compared to the above photochemical strategy, this method showed good chemoselectivity (only one helical scaffold could be prepared) and excellent synthetic efficiency. However, the stereoselectivity was moderate. Importantly, although the scaffold was not rigid, the final products had good optical stability, which would not undergo epimerization after heating at 100 °C overnight.

Even if the chiral centers were not so close to the helical scaffold, the helicity could be well controlled. Recently, Dehaen group reported a diastereoselective strategy to construct thia[5]helicenes [24]. The chiral centers, with two tertiary carbons, had a distance of three bonds to the helical skeleton, but the selectivity could be promoted to 100 % de by screening the solvents (Scheme 7.13). In addition, the oxazoline rings at C(1) and C(1′) positions increased the racemization barrier, which was comparable to that of [7]helicenes.
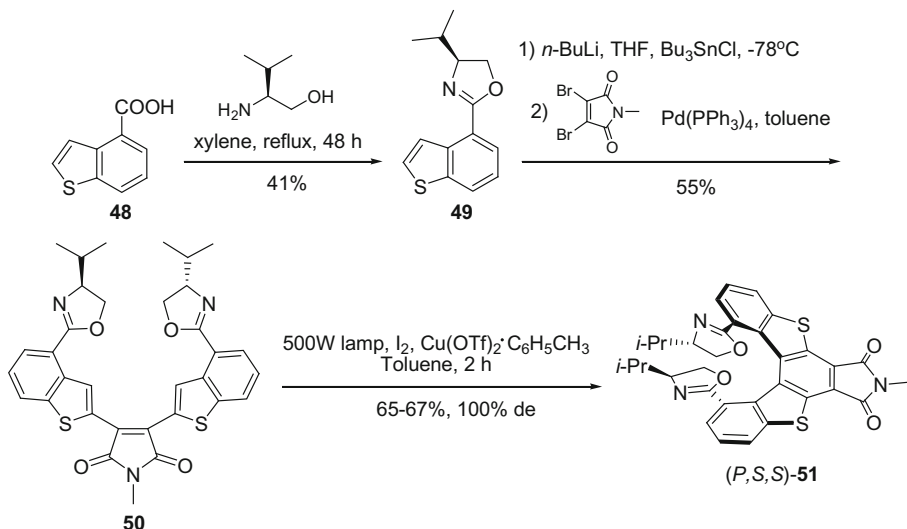
Scheme 7.13 A diastereoselective strategy to construct thia[5]helicene derivative
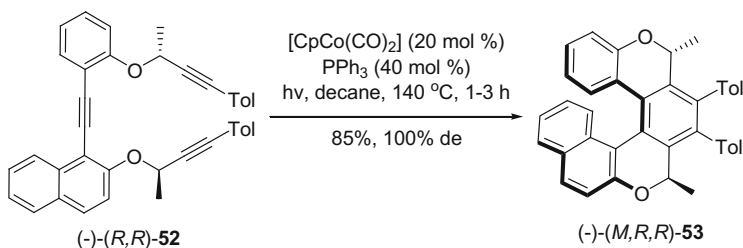
Scheme 7.14 Diastereoselective synthesis of dioxa [7]helicene (−)-(*M*,*R*,*R*)-**53** via co-catalyzed [2+2+2] cycloisomerization

Starý, Stará, and co-workers reported a general method for the synthesis of optically pure [5]-, [6]-, and [7]helicenes via Ni(0)/Co(I)-catalyzed [2+2+2] cycloisomerization. Different from the above methods, the chiral centers were on the helicene skeletons (Scheme 7.14). By the virtue of 1,3-allylic-type strain, the diastereoselectivity was excellent (100 % de), even for [5]helicenes, of which the parent structure racemized very quickly at room temperature.

Recently, the same group utilized the combination of biocatalysis and transition metal catalysis to achieve the highly stereoselective synthesis of helicenes [25]. The route started from the kinetic resolution of racemic secondary alcohol by lipase-catalyzed transesterification (Scheme 7.15). As the precursors could be obtained in high optical purity and yield, the triyne **59**, with one racemic and one optically pure carbon atoms, was prepared via Pd-catalyzed coupling reactions. The subsequent Co-mediated [2+2+2] cycloisomerization under microwave successfully
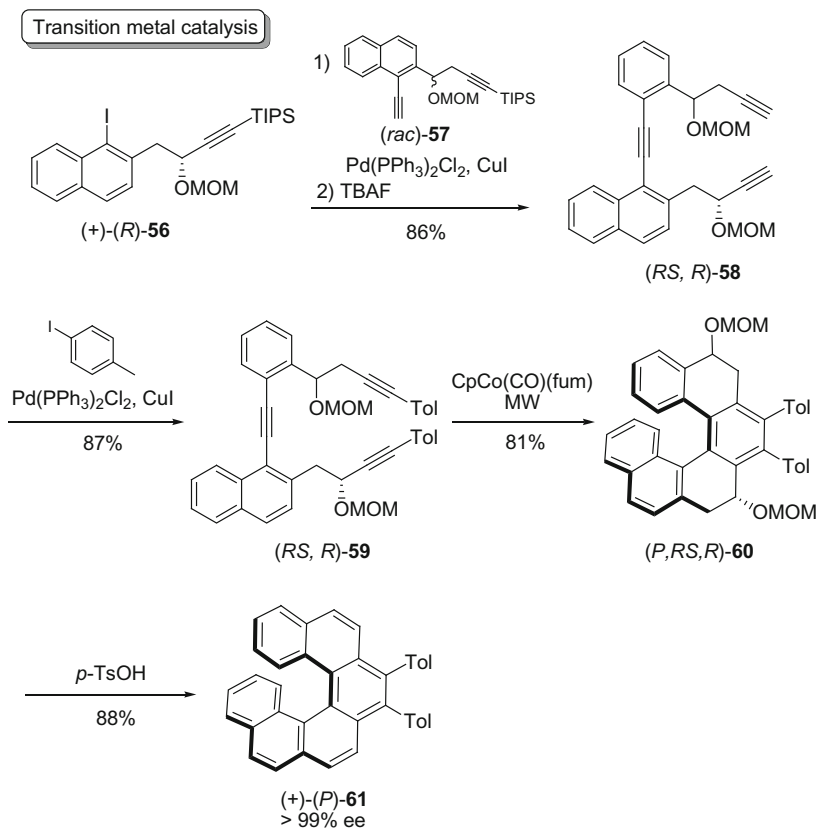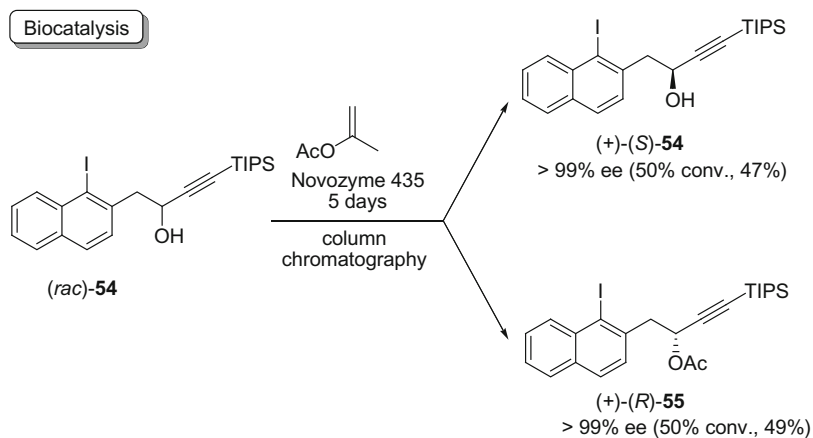
Scheme 7.15 Synthesis of (+)-(*P*)-**61** by combination of biocatalysis and transition metal catalysis

transferred the central chirality to helicity of tetrahydrohelicene **60**, where the 1,3-allylic-type strain between the OMOM group and the adjacent tolyl group played a key role. Finally, the central chirality was removed by elimination of methoxymethoxy group in the presence of *p*-toluenesulphonic acid to give fully aromatized skeleton **61** in >99 % ee. This ultimate method had excellent tolerance of functional groups, and [5]-, [6]-, [7]helicenes could all be prepared with ee value of >99 %.

7.3 Routes Based on Optically Pure Precursors

Although the catalytically asymmetric synthesis has been developed, the strategy, where helicenes are prepared from optically pure substrates with central chirality or axial chirality, is accepted as an efficient and practical method to construct helicenes, especially the long ones. For example, Nozaki group reported Pd-catalyzed arylation to prepare [7]helicenes [26]; Tanaka et al. described the thia[7]helicene by McMurry reaction [27]. Gingras group described the synthesis of bromohelicenes via benzylic coupling reactions (Scheme 7.16) [28]. Starting from similar biaryl precursor **62**, which could be resolved in large scale, tetrabromobiaryl **65** could be obtained and underwent intramolecular coupling in the presence of *t*-BuOK. The helicity could be easily predicted from the axial chirality, since [7]helicene hardly racemized in the reaction conditions.
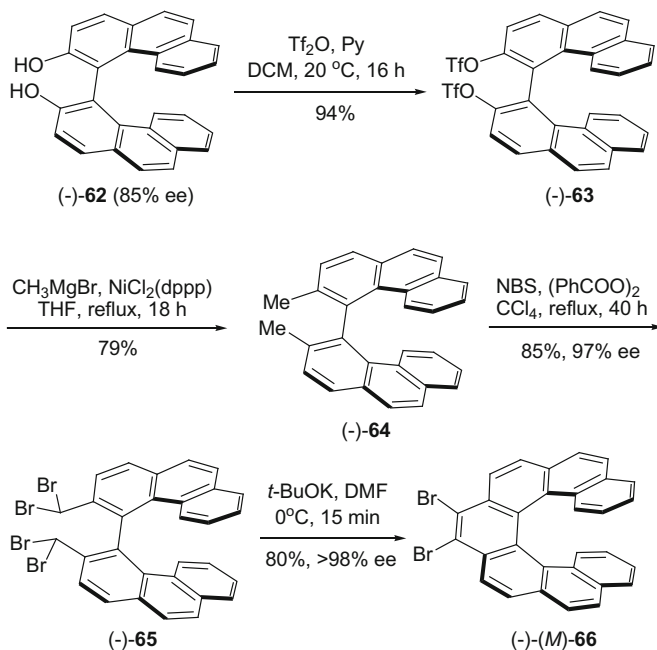
Scheme 7.16 Synthesis of bromohelicene **66** via benzylic coupling reaction
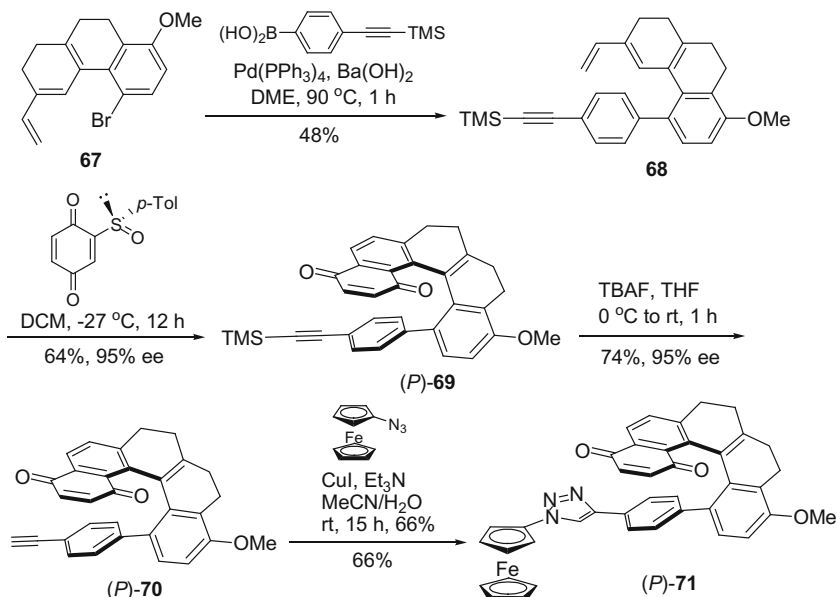
Scheme 7.17 Synthesis of helicene (*P*)-**71** with ferrocene moiety

Recently, Carreño, Urbano, and co-workers utilized their strategy to synthesize ferrocenyl-substituted helicenequinones [29, 30]. As shown in Scheme 7.17, from diene **67**, tetrahydrohelicene quinone **69** could be prepared in 95 % ee by Diels-Alder addition with (S*S*)-2-(*p*-tolylsulfinyl) quinone. Ferrocene moiety could be introduced by CuAAC reaction, which displayed enhanced chiroptical properties [29]. Very recently, the same group realized the synthesis of four stereoisomers (>94 % ee) with central, planar and helical chirality via asymmetric synthesis, chemical resolution, kinetic resolution from the reaction of racemic ferrocenyl-substituted diene **72** and optically pure quinone (*S*$_S$)-**73**. For example, (*P*,*S*$_p$,*S*$_S$)-**74** was produced by asymmetric synthesis in 67 % yield and 94 % ee via cycloaddition, sulfoxide elimination, and aromatization in one step (Scheme 7.18).
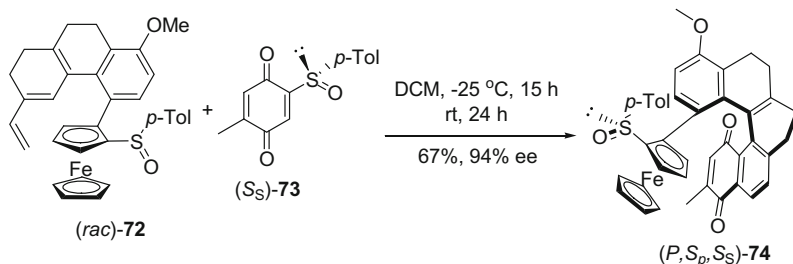
Scheme 7.18 Synthesis of helicene (*P*,*S*$_p$,*S*$_s$)-**74** with ferrocene moiety

In this chapter, we introduced the progress of asymmetric synthesis of helicenes in the past 3 years. The [2+2+2] cycloisomerization, Diels-Alder addition, and chiral auxiliary-induced reactions have been accepted as efficient strategies, and the selectivity is as high as >99 % ee or de. Therefore, the next step is to prepare functionalized helicenes, expand the structural diversity, and develop their applications in chiral recognition, chemical biology, asymmetric catalysis, and organic electronics, which makes it more meaningful.

References

1. Kagan H, Moradpou A, Nicoud JF, Balavoin G, Martin RH, Cosyn JP (1971) Photochemistry with circularly polarised light 2. Asymmetric synthesis of octa and nonahelicene. Tetrahedron Lett (27):2479–2482
2. Moradpou A, Nicoud JF, Balavoin G, Kagan H, Tsoucari G (1971) Photochemistry with circularly polarized light—synthesis of optically active hexahelicene. J Am Chem Soc 93 (9):2353-2354
3. Bernstei WJ, Calvin M, Buchardt O (1972) Absolute asymmetric synthesis. 1. On mechanism of photochemical synthesis of nonracemic helicenes with circularly polarized-light-wavelength dependence of optical yield of octahelicene. J Am Chem Soc 94(2):494–498
4. Bernstei WJ, Calvin M (1972) Absolute asymmetric synthesis. 2. Mechanism of synthesis of nonracemic helicenes with circularly polarized-light-structural effects. Tetrahedron Lett (22):2195–2198
5. Bernstei WJ, Calvin M, Buchardt O (1973) Absolute asymmetric synthesis. 3. Hindered rotation about aryl-ethylene bonds in excited-states of diaryl ethylenes—structural effects on asymmetric synthesis of 2-substituted and 4-substituted hexahelicenes. J Am Chem Soc 95 (2):527–532
6. Stara IG, Stary I, Kollarovic A, Teply F, Vyskocil S, Saman D (1999) Transition metal catalysed synthesis of tetrahydro derivatives of [5]-, [6]- and [7]helicene. Tetrahedron Lett 40 (10):1993–1996
7. Carreno MC, Hernandez-Sanchez R, Mahugo J, Urbano A (1999) Enantioselective approach to both enantiomers of helical bisquinones. J Org Chem 64(4):1387–1390
8. Shen Y, Chen C-F (2012) Helicenes: synthesis and applications. Chem Rev 112(3):1463–1535
9. Gingras M, Felix G, Peresutti R (2013) One hundred years of helicene chemistry. Part 2: stereoselective syntheses and chiral separations of carbohelicenes. Chem Soc Rev 42(3):1007–1050
10. Tanaka K (2013) Synthesis of helically chiral aromatic compounds via [2+2+2] cycloaddition. In: Transition-metal-mediated aromatic ring construction. Wiley, pp 281-298
11. Tanaka K, Kimura Y, Murayama K (2015) Enantioselective helicene synthesis by rhodium-catalyzed [2+2+2] cycloadditions. Bull Chem Soc Jpn 88(3):375–385
12. Sawada Y, Furumi S, Takai A, Takeuchi M, Noguchi K, Tanaka K (2012) Rhodium-catalyzed enantioselective synthesis, crystal structures, and photophysical properties of helically chiral 1,1′-bitriphenylenes. J Am Chem Soc 134(9):4080–4083
13. Murayama K, Oike Y, Furumi S, Takeuchi M, Noguchi K, Tanaka K (2015) Enantioselective synthesis, crystal structure, and photophysical properties of a 1,1′-bitriphenylene-based sila[7]helicene. Eur J Org Chem 2015 (7):1409–1414
14. Kimura Y, Fukawa N, Miyauchi Y, Noguchi K, Tanaka K (2014) Enantioselective synthesis of [9]- and [11]helicene-like molecules: double intramolecular [2+2+2] cycloaddition. Angew Chem Int Ed 53(32):8480–8483

15. Shibata T, Uchiyama T, Yoshinami Y, Takayasu S, Tsuchikama K, Endo K (2012) Highly enantioselective synthesis of silahelicenes using Ir-catalyzed [2+2+2] cycloaddition. Chem Commun (Camb) 48(9):1311–1313
16. Teply F, Stara IG, Stary I, Kollarovic A, Saman D, Rulisek L, Fiedler P (2002) Synthesis of [5]-, [6]-, and [7]helicene via Ni(0)- or Co(I)-catalyzed isomerization of aromatic cis, cis-dienetriynes. J Am Chem Soc 124(31):9175–9180
17. Jančařík A, Rybáček J, Cocq K, Vacek Chocholoušová J, Vacek J, Pohl R, Bednárová L, Fiedler P, Císařová I, Stará IG, Starý I (2013) Rapid access to dibenzohelicenes and their functionalized derivatives. Angew Chem Int Ed 52(38):9970–9975
18. Heller B, Hapke M, Fischer C, Andronova A, Starý I, Stará IG (2013) Chiral cobaltI and nickel- complexes in the synthesis of nonracemic helicenes through the enantioselective [2+2+2] cyclotrimerisation of alkynes. J Organomet Chem 723:98–102
19. Nakamura K, Furumi S, Takeuchi M, Shibuya T, Tanaka K (2014) Enantioselective synthesis and enhanced circularly polarized luminescence of s-shaped double azahelicenes. J Am Chem Soc 136(15):5555–5558
20. Kötzner L, Webber MJ, Martínez A, De Fusco C, List B (2014) Inside cover: asymmetric catalysis on the nanoscale: the organocatalytic approach to helicenes angew. Chem Int Ed 53(20):4980–4980
21. Richardson RD, Baud MGJ, Weston CE, Rzepa HS, Kuimova MK, Fuchter MJ (2015) Dual wavelength asymmetric photochemical synthesis with circularly polarized light. Chem Sci 6(7):3853–3862
22. Yavari K, Moussa S, Ben Hassine B, Retailleau P, Voituriez A, Marinetti A (2012) 1H-Phosphindoles as structural units in the synthesis of chiral helicenes. Angew Chem Int Ed 51(27):6748–6752
23. Aillard P, Retailleau P, Voituriez A, Marinetti A (2014) A [2+2+2] cyclization strategy for the synthesis of phosphorus embedding [6]helicene-like structures. Chem Commun (Camb) 50(17):2199–2201
24. Waghray D, Bagdziunas G, Jacobs J, Van Meervelt L, Grazulevicius JV, Dehaen W (2015) Diastereoselective strategies towards thia[n]helicenes. Chem Eur J 21(51):18791–18798
25. Šámal M, Chercheja S, Rybáček J, Vacek Chocholoušová J, Vacek J, Bednárová L, Šaman D, Stará IG, Starý I (2015) An ultimate stereocontrol in asymmetric synthesis of optically pure fully aromatic helicenes. J Am Chem Soc 137(26):8469–8474
26. Nakano K, Hidehira Y, Takahashi K, Hiyama T, Nozaki K (2005) Stereospecific synthesis of hetero[7]helicenes by Pd-catalyzed double N-arylation and intramolecular O-arylation. Angew Chem Int Ed 44(43):7136–7138
27. Tanaka K, Suzuki H, Osuga H (1997) A novel route to disubstituted [7]thiaheterohelicene via biaryl- and carbonyl-coupling reactions. Tetrahedron Lett 38(3):457–460
28. Terrasson V, Roy M, Moutard S, Lafontaine M-P, Pepe G, Felix G, Gingras M (2014) Benzylic-type couplings provide an important asymmetric entry to functionalized, non-racemic helicenes. RSC Adv 4(61):32412–32414
29. Hoyo AMd, Latorre A, Díaz R, Urbano A, Carreño MC (2015) Enantiopure helical ferrocene–triazole–quinone triads: synthesis and properties. Adv Synth Catal 357(6):1154–1160
30. del Hoyo AM, Urbano A, Carreño MC (2016) Enantioselective synthesis of four stereoisomers of sulfinyl ferrocenyl quinones with central, planar, and helical chirality. Org Lett 18(1):20–23

Chapter 8
Reactivity and Transformations

Abstract This chapter describes the reactions and transformations of helicenes, which are classified into four sections. First, transformation of the helical skeletons is discussed. By intramolecular Diels–Alder reaction, unusual [2+2] cycloaddition of C=C double bonds on the terminal rings, and dioxygen-triggered transannular dearomatization of helicene, some unprecedented reaction products can be obtained. The second section describes the direct C–H functionalization, which provides the most useful method for modification of the helicene structures. Functionalization of helicenes can be easily achieved by electrophilic aromatic substitution including nitration, halogenation, and acylation. For heterohelicenes, some C–H bonds can be activated by themselves, while the functionalizations of helicenium cation and azahelicenes are also shown. In third section, the transformations of bromohelicenes and hydroxyl helicenes are introduced, which can conveniently produce various functionalized helicene derivatives. Finally, recent advances in the preparation of helicene-embedded organometallics are discussed. When two Cp rings are embedded into the termini of the helicene skeleton, helical metallocene or polymeric metallocene can be obtained. With helicenes as monodentate ligands, bidentate ligands, or multitopic ligands, various metal complexes of helicenes and metallahelicenes are produced, and they exhibit the enhanced chiroptical properties of helicene core, redox switching, and acid–base switching phenomena, and even the acid/base-triggered switch of circularly polarized luminescence. Moreover, they are also potential candidates for the application of asymmetric synthesis.

Keywords Bidentate ligands · Direct C–H functionalization · Helical ligands · Helicene-embedded organometallic · Metallahelicene · Monodentate ligands · Multitopic ligands · Transannular dearomatization

In this chapter, we will discuss the reactions of helicenes, which will be classified into four sections as follows: (1) transformation of the helical skeletons, in which the reaction occurs at quaternary carbons; (2) direct C–H functionalization, the most

useful method for modification of the structures; (3) transformation of the functional groups, including some common conversions of the functionalities; (4) recent advances in the preparation of helicene-embedded organometallics.

8.1 Transformation of the Helical Skeletons

When reactive functional group is incorporated at C(1) position, the rearrangement of the skeleton would be observed. For example, 1-hydroxymethyl group was converted into carbocation species in the presence of *p*-toluenesulfonic acid, the subsequent addition and rearrangement afforded the spiro-compound **2** in 63 % yield (Scheme 8.1) [1]. The *N*-tosylhydrazone **3** could be converted into a carbene under NaH, which is inserted into the benzene ring to give compound **4** with a seven-membered ring (Scheme 8.2) [2].

Fuchter group reported an unprecedentedly reaction of [7]helicene during the preparation of helicene-derived metallocene (Scheme 8.3). In the presence of AlCl₃, an oxidative reaction occurred to produce a mixture of **6** and **7** [3]; while the reaction would afford benzo[*cd*]pyrenium cation species **8** on exposure to Au(I) [4], which was proposed to facilitate the Diels–Alder reaction between the terminal rings on two different sides.

In 1975, Martin group reported the first intramolecular Diels–Alder reaction of helicene [5]. As shown in Scheme 8.4, the aldehyde **9** was converted into alkene via Horner-Wadsworth-Emmons reaction, which underwent [4+2] addition spontaneously in the reflux benzene.

Similarly, Katz and co-workers described the synthesis of multifunctionalized helicene **12**, which underwent two types of [4+2] reactions in the presence of

Scheme 8.1 Synthesis of spiro-compound **2**
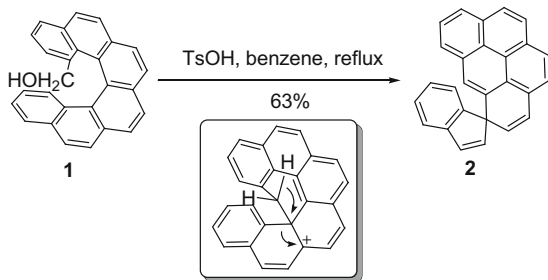
Scheme 8.2 Synthesis of compound **4**
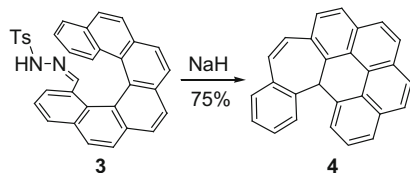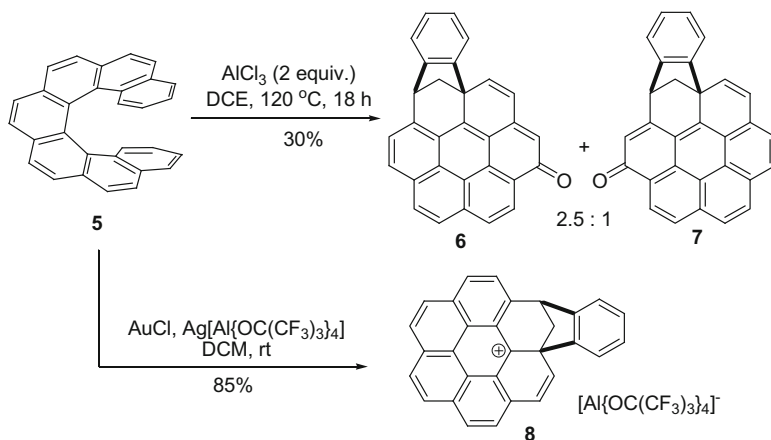
Scheme 8.3 Oxidative reaction and transformation of [7]helicene **5**
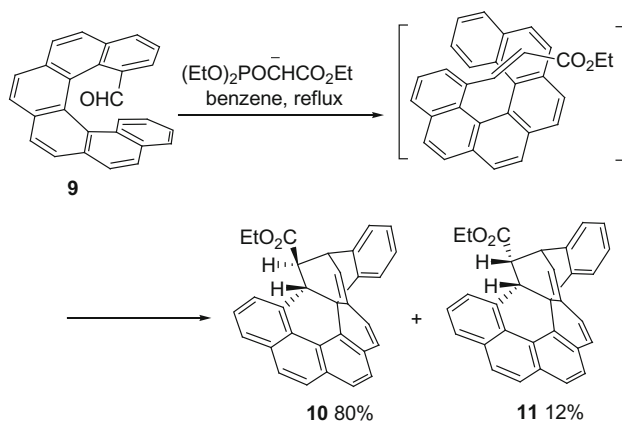
Scheme 8.4 The intramolecular Diels–Alder reaction of helicene

Me$_4$NF, after the benzyne rings were formed in situ [6]. One was between the benzyne ring and the solvent furan, the other was between the benzene ring on helical skeleton (Scheme 8.5). Compared with the reaction in Scheme 8.2, the migration of benzene ring was not observed.

Another unusual reaction was the [2+2] cycloaddition of C=C double bonds on the terminal rings. Garcia and colleagues reported this transformation in a Ru complex [7]. By the loss of one PPh$_3$, the coordination of nitrile group changed from end-on to side-on, resulting into the weak interaction between Ru and the H atom on the other end (Scheme 8.6). The following [2+2] addition took place in a stereospecific manner.
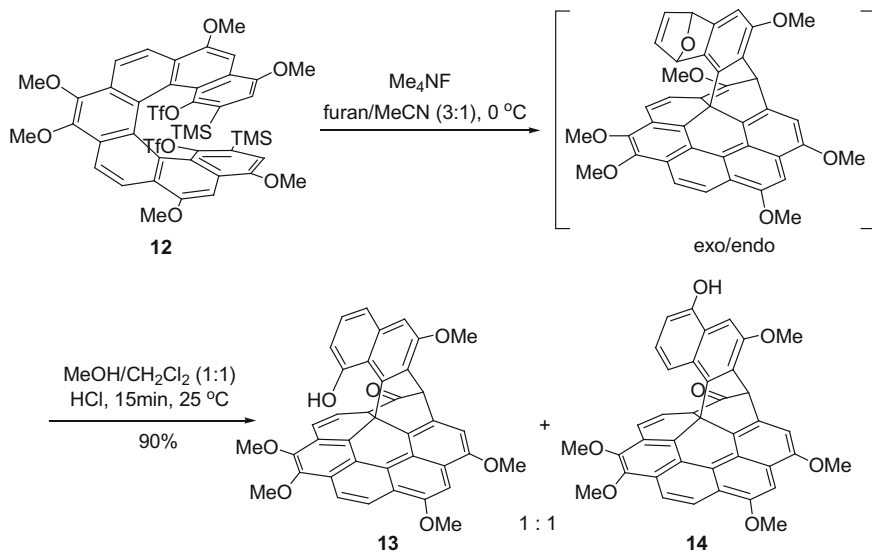
Scheme 8.5 Transformation of multifunctionalized helicene **12**
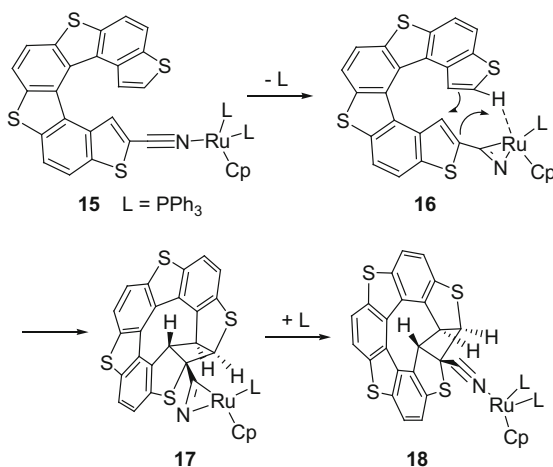
Scheme 8.6 Transformation of thiahelicene derivative **15**

Marinetti and co-workers reported that the C=C double bond adjacent to the P atom of the terminal ring was reactive and underwent dimerization rapidly during the photocyclization (Scheme 8.7) [8].

Recently, Sakai et al. described the synthesis of 1,2-dialkyl-substituted quinoxaline via nucleophilic addition in 35 % yield (Scheme 8.8) [9]. According to their study, **22** had a larger interplanar angle (56°) than that of **21** (44°) without any loss of conjugation, which was applicable for CPL and OLED.
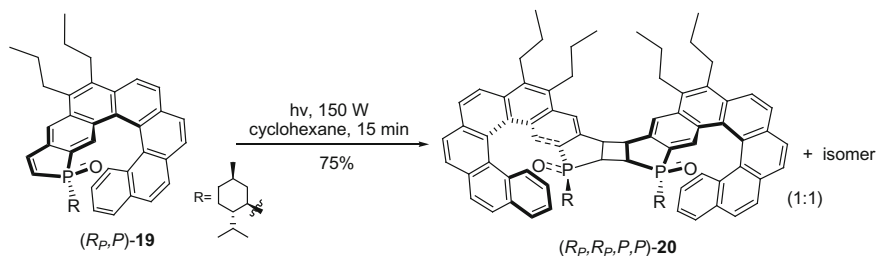
Scheme 8.7 Photocyclization of phosphindole-embedded helicene **19**
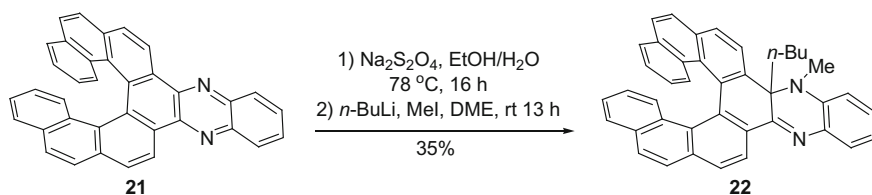
Scheme 8.8 Transformation of helicene derivative **21**
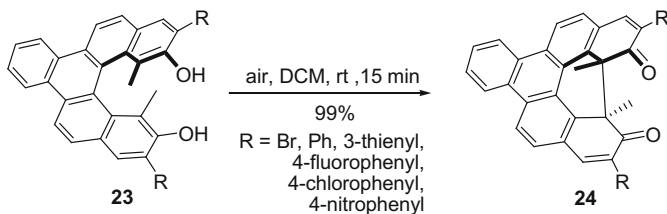
Scheme 8.9 Dioxygen-triggered transannular dearomatization of helicene diol **23**

Chen and co-workers unprecedentedly discovered the first example of dioxygen-triggered transannular dearomatization, where the terminal rings were oxidized with the formation of two quaternary carbon centers (Scheme 8.9) [10]. This reaction was stereospecific and quantitative, and the diol **23** could be easily resolved by column chromatography with the help of chiral auxiliaries.

8.2   Direct C–H Functionalization

Early studies [11] demonstrated that for electrophilic aromatic substitution, including nitration, halogenation, and acylation (Scheme 8.10), the C(5) position is the most reactive site and C(7) position took the second place.
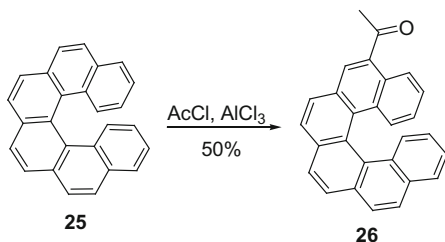
Scheme 8.10 Acylation of [6]helicene **25**
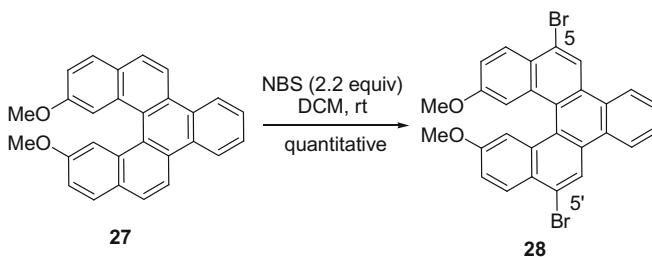
Scheme 8.11 Bromination of benzo [5]helicene **27**
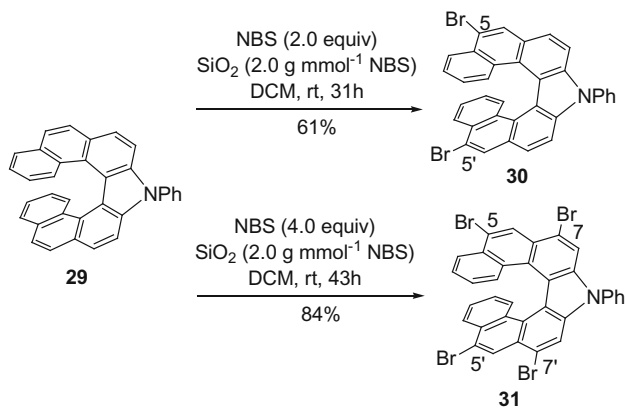
Scheme 8.12 Bromination of aza [7]helicene **29**

This conclusion was also demonstrated by other groups. Chen group [12] and Nozaki group [13] examined the bromination of helicenes. Chen and co-workers prepared benzo[5]helicene **27**, and the subsequent bromination occurred at C(5) and C(5′) positions (Scheme 8.11). As for Nozaki's aza[7]helicene **29**, it was much clearer that C(5) was more reactive than C(7) (Scheme 8.12).
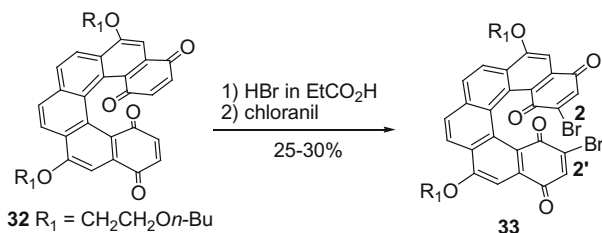
Scheme 8.13 Bromination of helicenebisquinone **32**
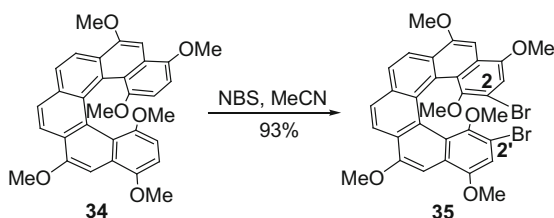
Scheme 8.14 Bromination of methoxy-substituted helicene **34**
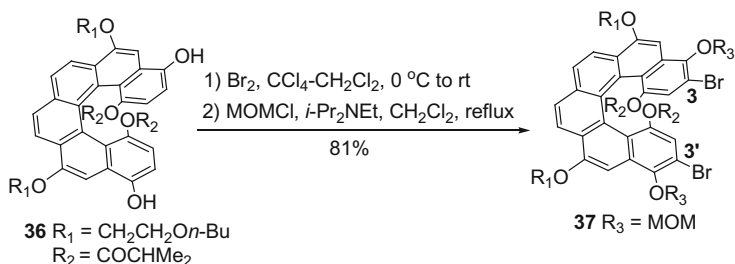
Scheme 8.15 Bromination of phenol-type substrate **36**

The reactivity stated above is applicable for the simple helicenes. If helicene is multifunctionalized, the chemoselectivity will change. For example, Katz group prepared the substrates for bromination, and the products varied as the functionalities changed. Helicenebisquinone gave the bromide at C(2) and C(2′) (Scheme 8.13) [14] as well as tetramethoxy-substituted helicene (Scheme 8.14) [15]. However, the phenol-type substrate **36** gave the product with Br atoms at C(3) and C(3′) (Scheme 8.15) [14].

Moreover, for heterohelicenes, some C–H bonds can be activated by themselves. Maiorana and colleagues examined the direct formylation of thiahelicene **38** via deprotonation followed by quenching with DMF or Vilsmeier–Haack reaction to afford 2-formyl helicene **39** in 66 and 34 % yield, respectively (Scheme 8.16) [16].
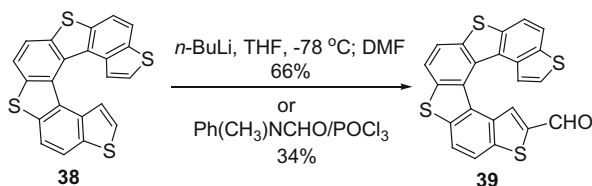
Scheme 8.16 The direct formylation of thiahelicene **38**
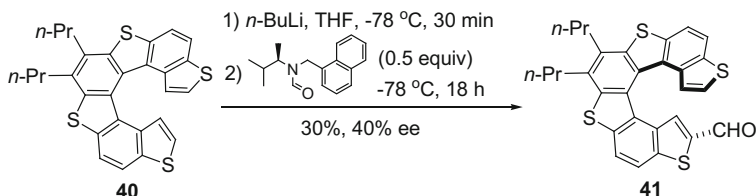
Scheme 8.17 The asymmetric synthesis of formylated helicene **41**

Stephenson and Doulcet described a new approach for the asymmetric synthesis of formylated helicenes via kinetic resolution (Scheme 8.17) [17]. By the weak interaction between the helicene anion and chiral formamide, enantioenriched 2-formyl helicene **41** was prepared in 30 and 40 % ee.

Lacour group reported the functionalization of helicenium cation **42** [18]. By the treatment of NaCN, dinitrile **43** could be obtained in an open flask, in which the nucleophilic substitution took place at C(5) and C(5′) positions (Scheme 8.18). The subsequent [3+2] cycloaddition with trimethylsilyl azide produced bis(tetrazole) analogue **44** in 60 % yield. By the virtue of the cationic feature, amine could be directly incorporated under ambient condition.

Takenaka group described the functionalization of 1-aza[6]helicene, of which the products were organocatalysts for Friedel–Crafts alkylation, Diels–Alder addition, ring opening of epoxides, and propargylation of aldehydes [19, 20]. N-oxide **47** could be easily prepared by oxidation with m-CPBA in 62 % yield [21]. By nucleophilic addition and elimination, 2-aminohelicene **48** was obtained, which could be utilized as a hydrogen-bonding-donor catalyst after protonation and anion exchange (Scheme 8.19). If aryl lithium reagents were used, aryl-substituted helical N-oxides could be prepared, like the bidentate catalyst **50** [22]. In addition, Kamikawa group utilized Pd-catalyzed arylation to prepare similar product **52** (Scheme 8.20) [23].

By utilizing the activity of C(2)–H bonds of the terminal thiophene ring, it was easy to introduce functionalities by deprotonation and subsequent nucleophilic substitution. Cauteruccio, Dreuw, and co-workers prepared helicene borane **53** in a one-pot reaction with a yield of 76 % (Scheme 8.21) [24].
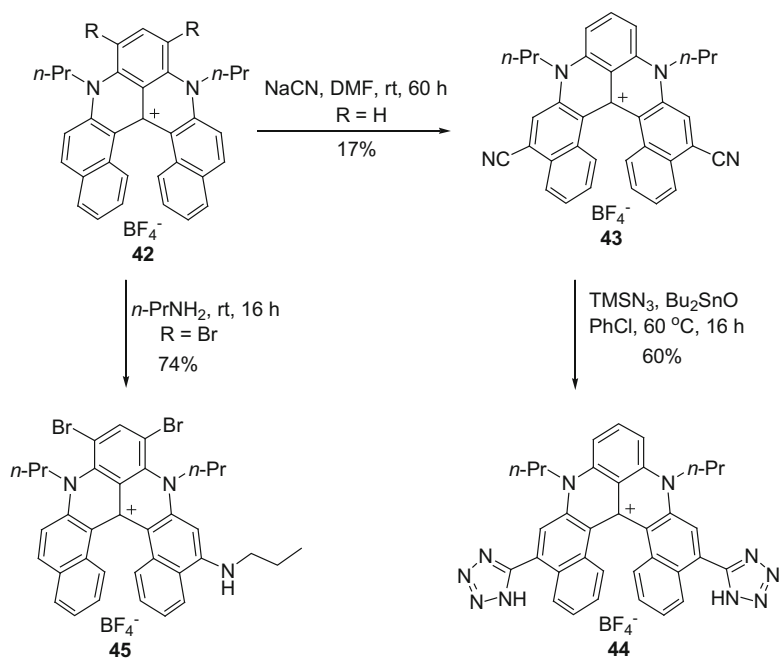
Scheme 8.18 The functionalization of helicenium cation **42**

BArF$_{24}^-$ = tetrakis[3,5-bis(trifluoromethyl)phenyl]borate
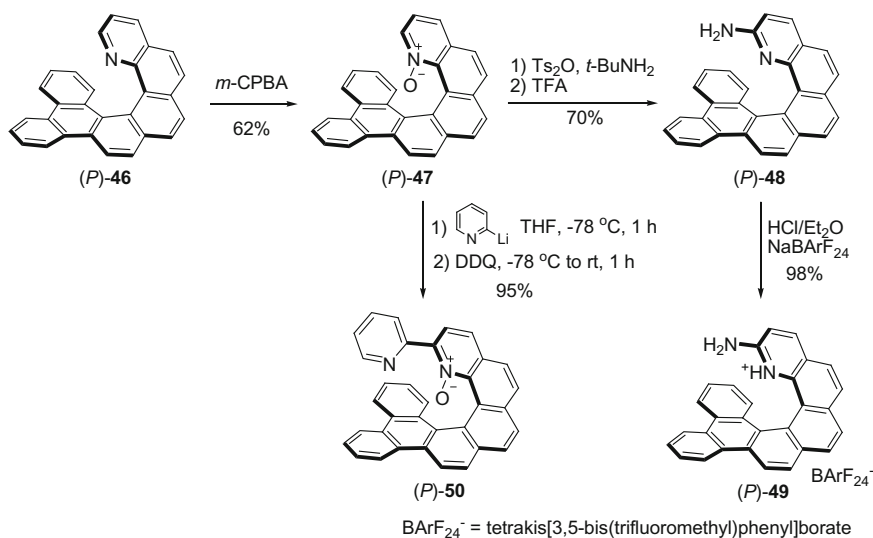
Scheme 8.19 The functionalization of 1-aza [6]helicene (*P*)-**46**
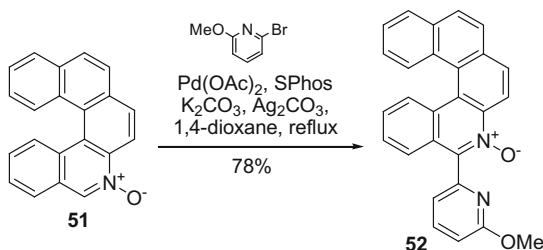
Scheme 8.20 Pd-catalyzed arylation of helical *N*-oxide **51**
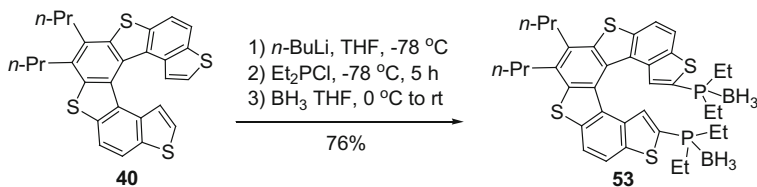
Scheme 8.21 Synthesis of helicene borane **53**

Scheme 8.22 Photochemical
cyclization of [5]helicene **54**
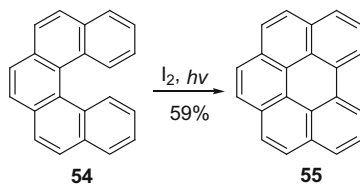
Besides the above conversions, helicenes could undergo Scholl-type reactions in the presence of oxidants. For this reason, photochemical cyclization did not give parent [5]helicene but benzo[*ghi*]pyrelene instead by photochemical cyclization (Scheme 8.22) [25]. The exceptions, for the oxidative photocyclization of [5]helicenes, are listed in Fig. 8.1, which would not be overoxidized under the condition [26–28].

Moreover, Yamamoto group [29] and Scott group [30] performed the thermal intramolecular dehydrogenation under flash vacuum pyrolysis (FVP) conditions. And thiahetero[6]helicenes could undergo Scholl cyclization on the exposure to AlCl$_3$ and NaCl at high temperature as well [26, 31–34]. In addition to the strategies that needed harsh conditions, Chen group reported the synthesis of naphtho[*ghi*] perylene from benzohelicene in the presence of DDQ and trifluoroacetic acid at 0 °C in quantitative yields (Scheme 8.23) [12]. Rajca and co-workers utilized C(1)- and C (1′)-dibromosubstituted thia[7]helicenes to prepare dehydrogen helicenes via radical, Pd-mediated, or acid-promoted reactions in good to moderate yields [35, 36].
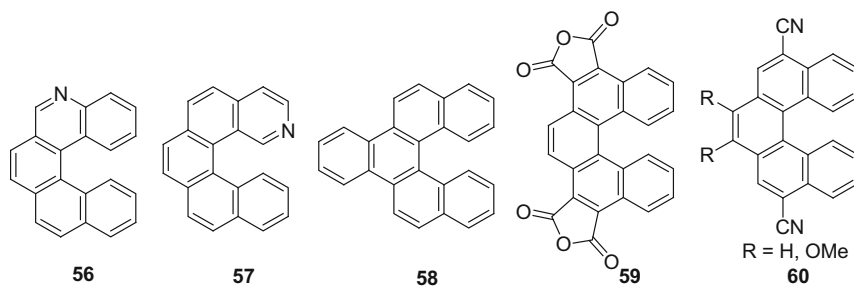
Fig. 8.1 Chemical structures of aza[5]helicene and [5]helicene derivatives **56–60**
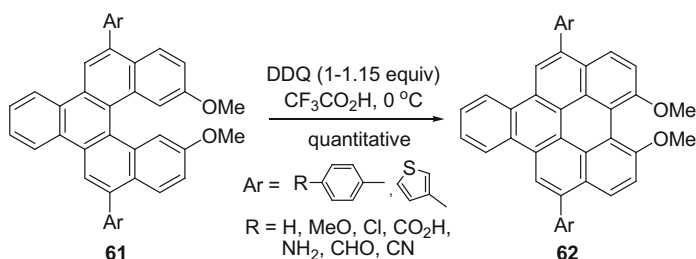
Scheme 8.23 Synthesis of naphtho[*ghi*]perylenes from benzo[5]helicene derivatives

8.3   Transformation of the Functional Groups

In this section, we would like to discuss the transformation of bromohelicenes and hydroxyl helicenes, because most of other functional groups could be embedded based on Br and hydroxyl groups. The Br atom could be incorporated to the substrates or via bromination of helicenes, while the hydroxyl groups should be embedded into the precursors, usually as methoxy group.

Storch group [37] and Gingras group [38] had extensively studied the reactivity of bromohelicene. Herein, we would like to use Storch's results as an example (Scheme 8.24). By Suzuki–Miyaura cross-coupling reaction, phenyl group could be incorporated. This method was also utilized by other groups [10, 12, 39]. In some cases, the substituent on aryl group would reduce the solubility of the helicene greatly [10]. Helicene-embedded phosphine **65** could be prepared by direct Pd-catalyzed *P*-arylation, which could be further oxidized as a stable species **66**. As an alternative strategy, phosphine could also be prepared via Li/Br exchange and quenched by ClPPh$_2$ or ClP(O)Ph$_2$ [40–42]. Helicene nitrile **67** could be obtained via nucleophilic substitution of CuCN, and alkynyl-substituted helicene **68** was synthesized via Sonogashira reaction. In addition, Pd-mediated *N*-arylation afforded helical amine **69** in excellent yield. Also, thioether **70** could be obtained via Pd-catalyzed reaction, which is converted into thiol **71** with the help of *t*-BuSNa at
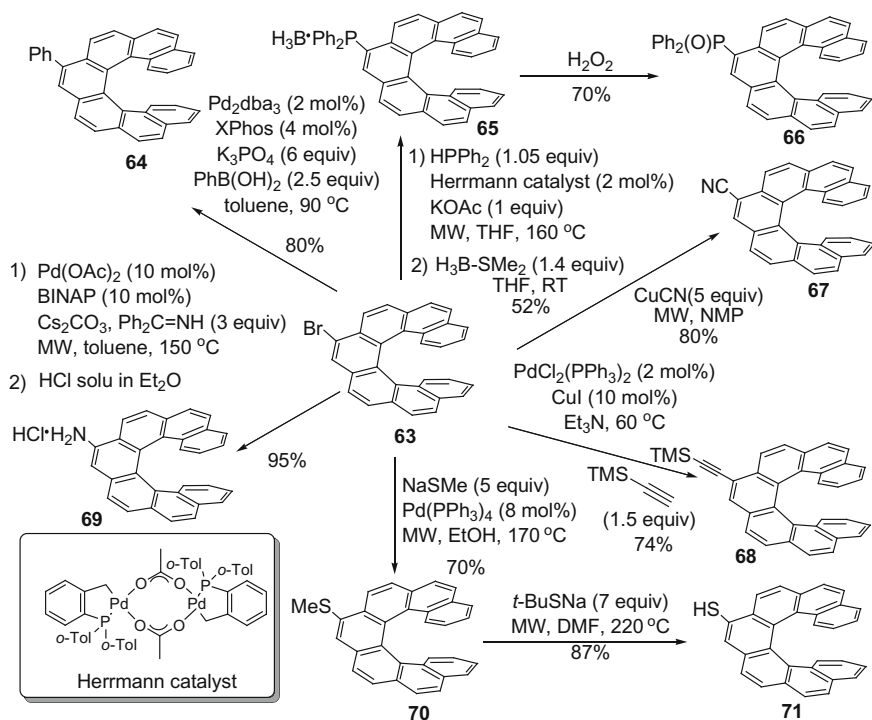
Scheme 8.24 The functionalization of bromohelicene **63**

high temperature. Thioether could be prepared via Pd-catalyzed reaction between bromide and organotin reagent [43]. Besides the reactions mentioned above, after Li/Br exchange, the substrate could be transformed into aldehyde if quenched by DMF or converted into acid in the presence of CO_2 [41].

Starý, Stará, and co-workers explored the reactivity of 3-methoxy[6]helicene [44]. As shown in Scheme 8.25, by demethylation, 3-hydroxyl[6]helicene **73** was obtained in good yield. The subsequent reaction with n-BuLi/Tf_2O or NaH/NfF would give triflate **74** and sulfonate **75** in 50 and 85 %, respectively. From triflate, via Pd-mediated reactions, amines, phosphine, phosphine oxide, ester could be obtained in moderate to good yields. Triflate precursors could also be utilized to construct aryl-substituted helicenes by Suzuki–Miyaura cross-coupling reaction [45].

Another common reaction for hydroxyl helicenes was oxidation. For example, **84** [46], **85** [47], and **86** [48] (Fig. 8.2) could be easily oxidized to o-helicene-quinones. In addition to the intramolecular oxidation, the intermolecular oxidation would afford helicene dimers. Katz group (Scheme 8.26a) [49] and Yamaguchi group (Scheme 8.26b) [50] reported the synthesis of two BINOL analogues based on the oxidative couplings with the help of Ag_2O and Cu-TMEDA complex,
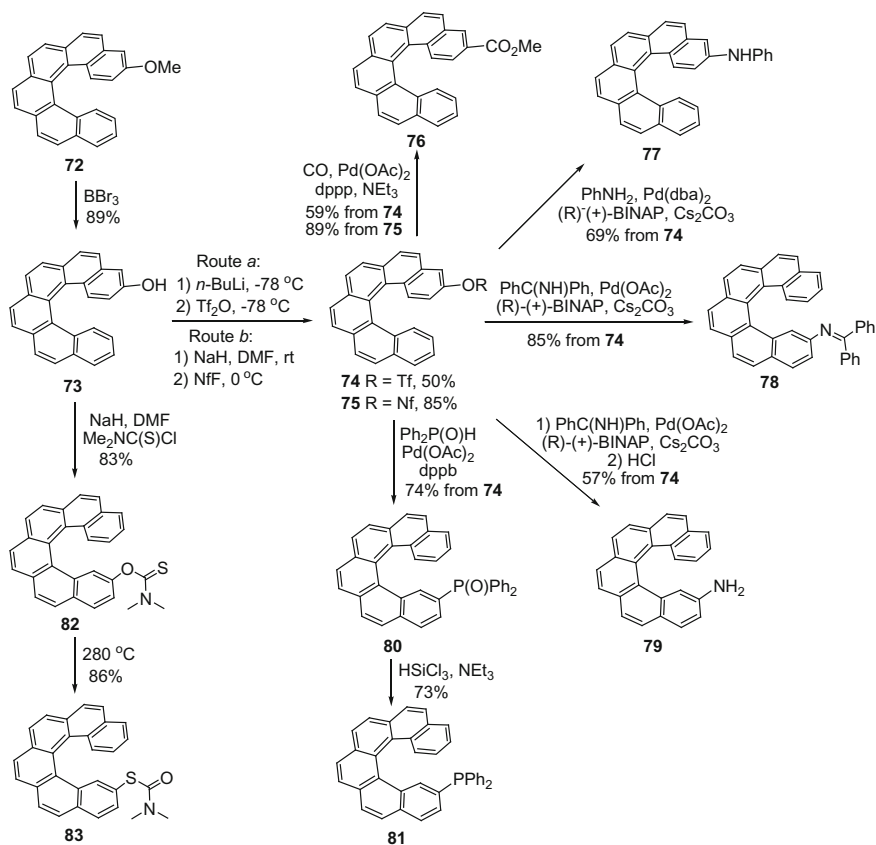
Scheme 8.25 Reactivity and transformations of 3-methoxy [6]helicene **72**
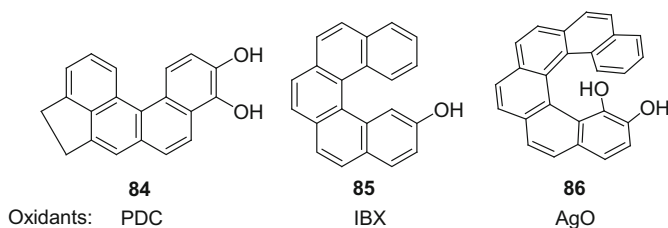
Fig. 8.2 Chemical structures of hydroxyl helicenes **84–86**

respectively. Storch, Vacek, and co-worker reported a new method to prepare helicene-embedded polymers by electropolymerization of the thiophene units, which provided an alternative approach to deposit helicene to solid surfaces (Scheme 8.27) [51].
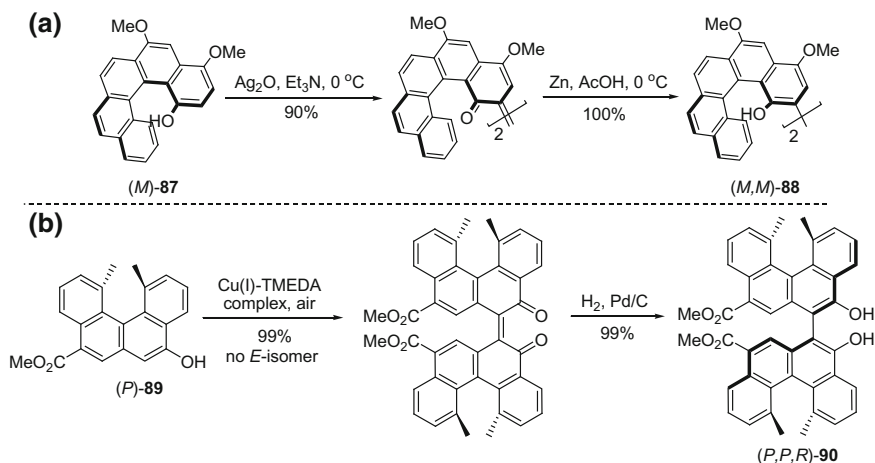
Scheme 8.26   The synthesis of two BINOL analogues based on the oxidative couplings
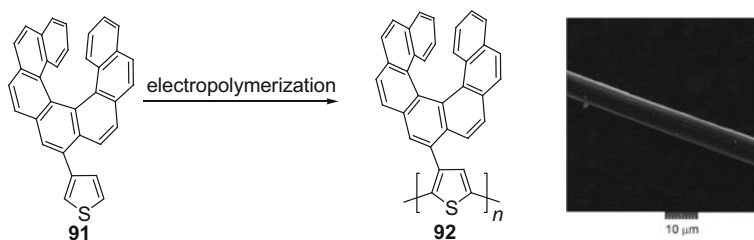
Scheme 8.27   Synthesis of helicene-embedded polymers by electropolymerization of the thiophene units. Reproduced from Ref. [51] with permission from the Royal Society of Chemistry

8.4   Preparation of Helicene-Embedded Organometallics

8.4.1   Metallocenes with Helicenes

In 1979, Katz et al. [52] proposed that if two Cp rings were embedded into the termini of the helicene skeleton, metallocene polymers would be obtained. Unfortunately, for [4]- and [5]helicenes, sandwich structures bearing two metal centers were obtained (Fig. 8.3) [52]; while the metal atom would be captured by the terminal Cp rings to give helical metallocenes [53]. In 1986, Katz and Sudhakar prepared the first optically pure helical metallocene (Scheme 8.28) [54]. To obtain metallocene polymers, longer helicene is needed to be synthesized to meet the structural requirement. Finally, the oligomers **100** (Fig. 8.4) were successfully prepared from optically active [9]helicene dianion [55–57].
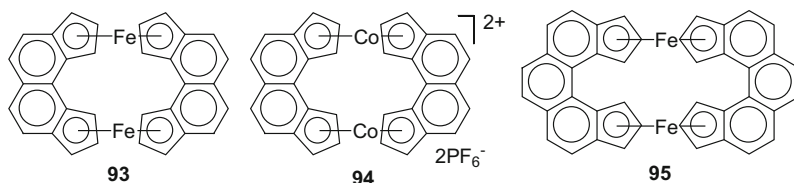
Fig. 8.3 Helicenes **93–95** with sandwich structures bearing two metal centers
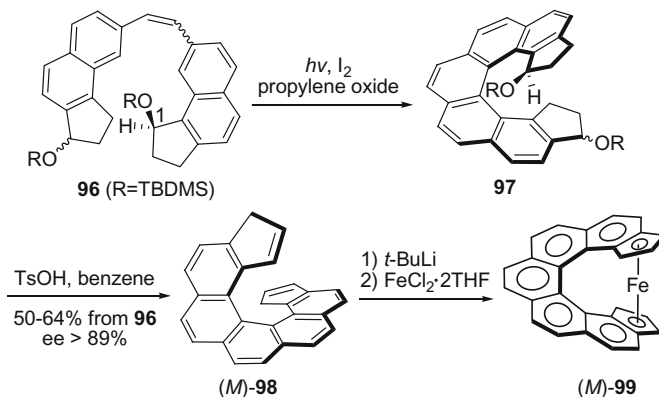
Scheme 8.28 Synthesis of optically pure helical metallocene

Fig. 8.4 Structure of polymeric metallocene

100 R $=$ H, TMS
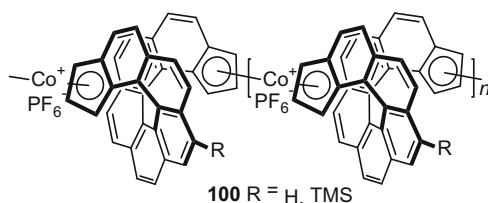
Tessier, Youngs, and co-workers prepared dimeric organolithium sandwich structure **105** from tribenzocyclotriyne (Scheme 8.29) [58]. Helicene dianion **103** was easily synthesized in high yield, which reacted with TMSCl to give silane **104**. In the presence of *n*-BuLi, **105** could be obtained, and the structure was demonstrated by X-ray analysis, where Li atoms bound with the Cp ring in a η^5-coordination manner.

Thiel and colleagues prepared ferrocene analogues [Fe(DBF)$_2$] **106** and [(DBF)Fe (^{4}Cp)] **107** (DBF = dibenzo[*c,g*]fluorenide, ^{4}Cp = 1,2,3,4-tetraisopropylcyclopentadienyl) by the reaction between Li(DBF) and FeBr$_2$/[(^{4}Cp)Fe(μ^2-Br)]$_2$ (Fig. 8.5) [59]. These compounds showed good electrochemical properties and were potential candidates for the application of asymmetric synthesis.
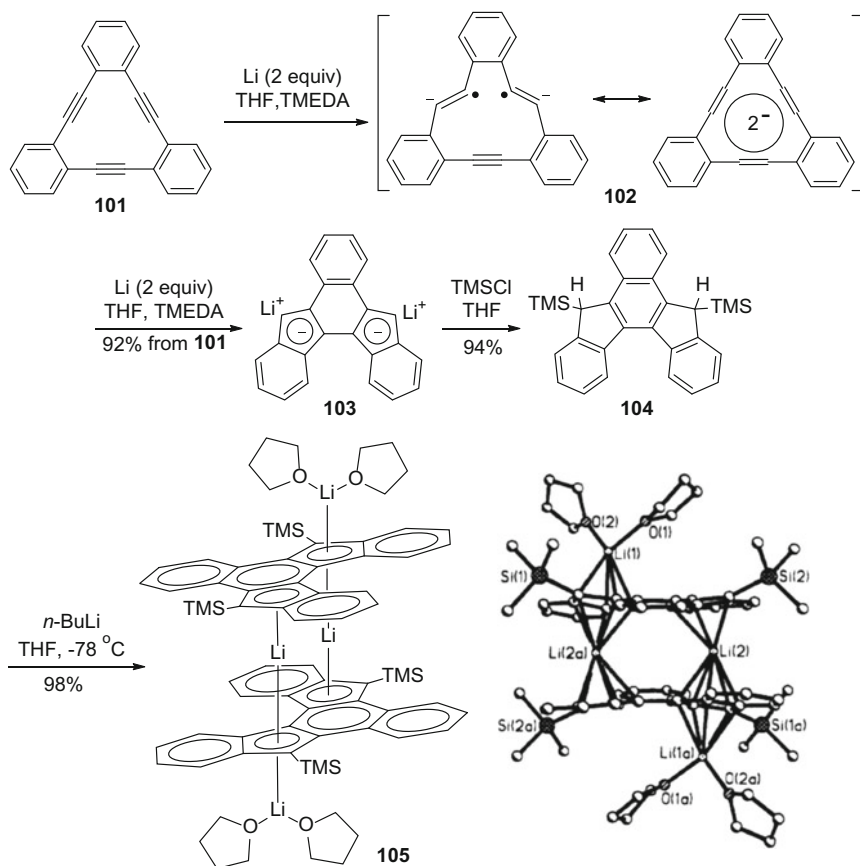
Scheme 8.29 Synthesis of dimeric organolithium sandwich structure **105** from tribenzocyclotriyne. Reprinted with the permission from Ref. [58]. Copyright 1993 American Chemical Society

Fig. 8.5 Chemical structures of **106–107**
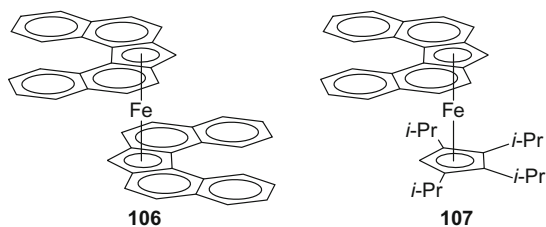
Álvarez and co-workers described the first synthesis of η^6-complexes of iridium and ruthenium with [6]helicene [60]. As Scheme 8.30 shows, adequate Ir reagent was added to the reaction, bimetallic complex **109** was formed, where two terminal
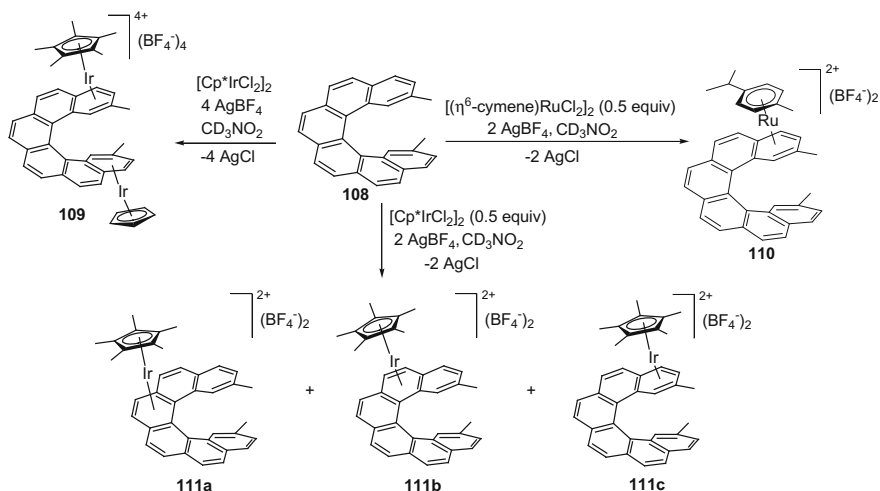
Scheme 8.30 Synthesis of η^6-complexes of iridium and ruthenium with [6]helicene **108**

rings bound with Ir atoms based on η^6-coordination, while 0.5 equivalent of [(η^6-cymene)RuCl$_2$]$_2$ was added to the reaction, Ru preferentially bound with the terminal ring of helicene. However, if 0.5 equivalent of [(Cp*)IrCl$_2$]$_2$ (Cp* = 1,2,3,4,5-pentamethylcyclopentadienyl) was added, three complexes were produced, **111a-c**, in which **111a** and **111b** would gradually disappear and transform into **111c** that the [Cp*Ir] moiety ran along the helical surface from the middle benzene ring to the terminal benzene ring of [6]helicene.

Rose-Munch, Licandro, and co-workers described the synthesis of helicene derivatives with ferrocenyl and (η^5-cyclohexadienyl)Mn(CO)$_3$ groups by double Sonogashira coupling from helicenyl iodide **112** (Scheme 8.31) [61]. The electrochemical investigation showed that the ferrocenyl (Fc), triple bonds, and helical π-skeleton were all conjugated, and the HOMO–LUMO gap decreased.
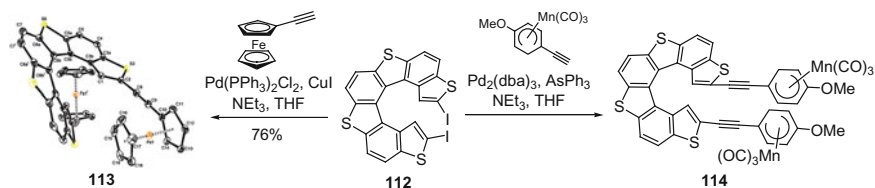
Scheme 8.31 Synthesis of helicene derivatives with ferrocenyl and (η^5-cyclohexadienyl)Mn (CO)$_3$ groups. Reprinted with the permission from Ref. [61]. Copyright 2012 American Chemical Society

8.4.2   Complexes with Helicenic Ligands

8.4.2.1   Monodentate Ligands

Hassine, Marinetti, and co-workers utilized helicene phosphines to prepare Pd- and Ru complex [62, 63]. For example, heptahelicene **116** could be resolved by forming diastereomers **117** with Pd-complex **115**, which could be easily resolved by column chromatography [62] (Scheme 8.32). 3-(Diphenylphophino)[6]helicene **118** reacted with 0.5 equivalent of [(η^6-cymene)RuCl$_2$]$_2$ in CH$_2$Cl$_2$ to afford Ru complex in 63 % yield [63] (Scheme 8.33).

Marinetti, Voituriez, and co-workers prepared phosphahelicene–Au complexes from optically pure helicene **120** [64]. After reduction with (Et$_2$O)$_2$MeSiH, the phosphine was generated in situ, and the subsequent coordination with NaAuCl$_4$ in the presence of 2,2′-thiodiethanol produced diastereomeric compounds, in which, *P*–Au bond was either oriented to the other terminal ring of the backbone (the *endo*-configuration) or away from the helicene moiety (the *exo*-configuration) (Scheme 8.34). (R_P,P)-**121**-*endo* showed good catalytic activity for the cyclization of *N*-tethered dienynes.

Garcia et al. reported the synthesis of Ru(II) and Fe(II) complexes with thia[7] helicenes utilizing the coordination between the *N* atom and Fe/Ru atom (Scheme 8.35) [7]. Crassous, Lescop, and co-workers utilized similar reaction and prepared bimetallic complexes such as **124** (Fig. 8.6) [65]. In solid state, the molecule was found to be head-to-tail infinite π-stacked columns.
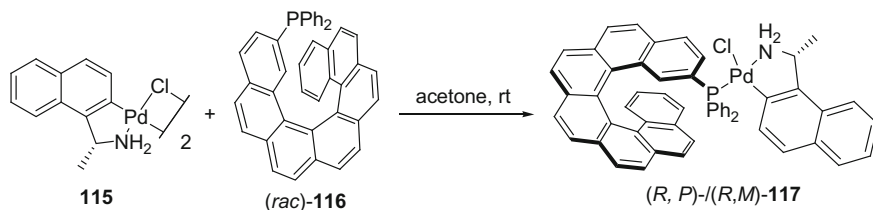
Scheme 8.32   Heptahelicene **116** resolved by forming diastereomers **117** with Pd-complex **115**
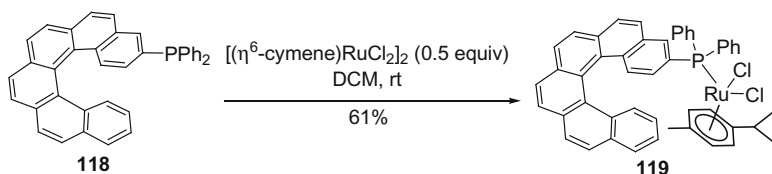
Scheme 8.33   Synthesis of Ru complex of 3-(diphenylphophino)[6]helicene **118**
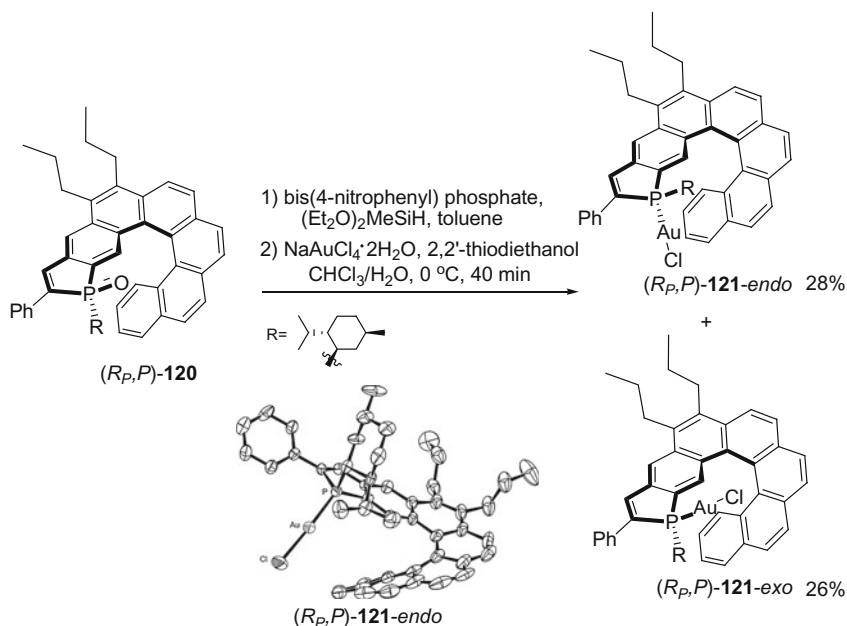
Scheme 8.34 Synthesis of phosphahelicene–Au complexes from optically pure helicene **120**. Reprinted with the permission from Ref. [64]. Copyright 2014 John Wiley and Sons
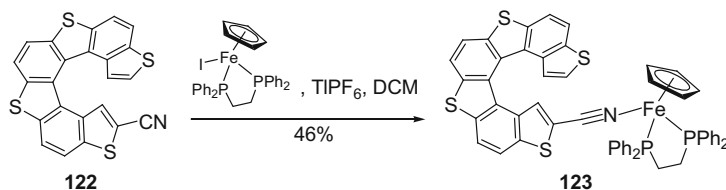
Scheme 8.35 Synthesis of Fe(II) complex of thia [7]helicene **122**

In 2008, Starý and Stará reported the first example that 2-aza[6]helicene could form Ag-complex [Ag{(*P*)-2-aza[6]helicene}₂]OSO₂CF₃ in T-shape structure [66]. Later, Crassous group investigated the coordination of 4-aza[6]helicene with Pt and found that the isomerism of *cis* and *trans* structures of [Pt(4-aza[6]helicene)PPh₃] Cl₂ could be controlled by the forms of helicene: if the helicene was enantiopure, the complex bore the *trans* structure; if helicene was racemic, the complex was in *cis* configuration (Scheme 8.36) [67].

Autschbach, Crassous, and co-workers prepared a series of metal-grafted vinylhelicenes (Scheme 8.37) [68–70]. Due to the electronic interaction of ligand and metal center, the complexes displayed enhanced chiroptical properties and redox [68, 70] and acid–base switching [69] phenomena.
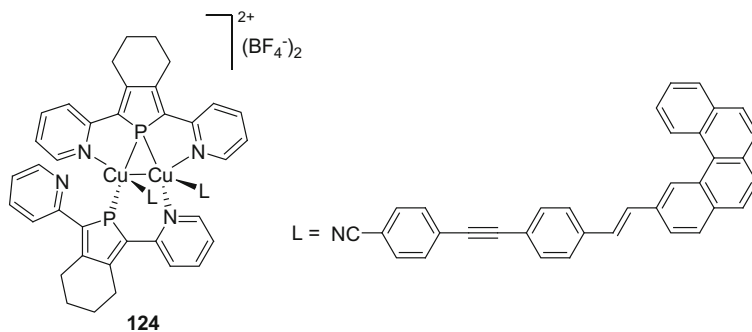
Fig. 8.6 Chemical structure of bimetallic complex **124**
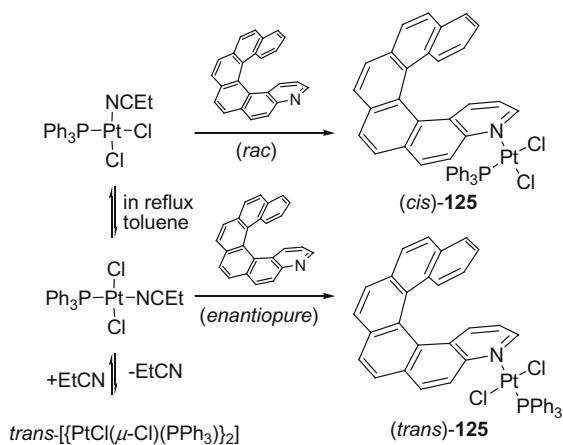
Scheme 8.36 Controlled formation of the *cis* and *trans* isomers of [Pt(4-aza [6]helicene)PPh$_3$]Cl$_2$
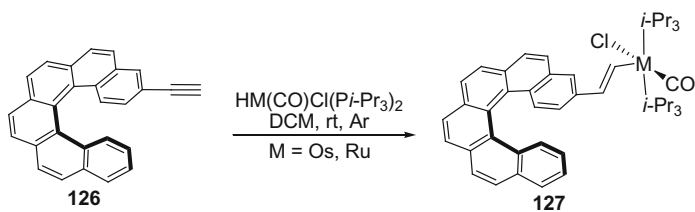
Scheme 8.37 Synthesis of metal-grafted vinylhelicene **127**
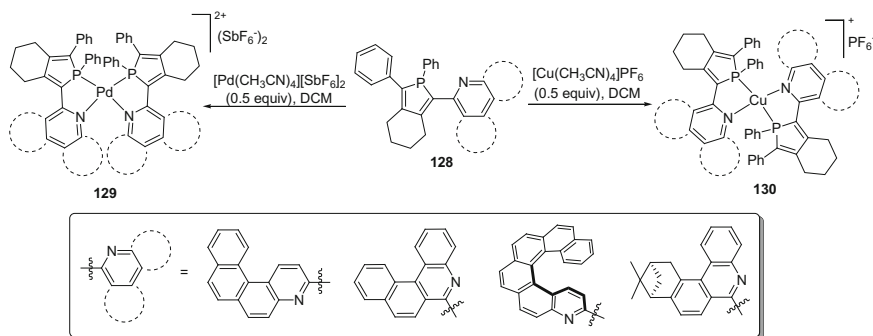
Scheme 8.38 The coordination behaviors of *N,P*-bidentate ligands with Pd(II) and Cu(I)

8.4.2.2   Bidentate Ligands

Autschbach, Crassous, Réau, and co-workers investigated the coordination behaviors of *N,P*-bidentate ligands with Pd(II) and Cu(I) [71–73]. It was found that Pd center displayed a highly distorted square planar geometry, where the ligands were in *cis* configuration while the Cu center was in distorted tetrahedron configuration (Scheme 8.38).

Based on direct C–H activation, the preparation of Pt complexes was reported by Autschbach, Crassous, Réau, and co-workers [74–78]. By the reaction between the 1-(2-pyridine)-[4]helicene with K₂PtCl₂, Pt(II)-metallahelicene formed as **132** and **134**, and Pt(IV)- and Pt(III)-Pt(III)-complexes could be obtained after oxidation. Interestingly, (*rac*)-**135** could be spontaneously converted into homochiral bis(Pt (III)-[6]helicene) (Scheme 8.39) [74, 75]. The σ-π conjugation between the Pt–Pt structure and the π-surface enhanced the chiroptical properties [75].

Autschbach, Crassous, and co-workers developed a diastereo- and enantioselective strategy to prepare enantioenriched dimers [76]. Starting from (*M*)-**136**, cation (*M*)-**137** could be obtained, which transferred the chirality of the ligand to the second ligand via the metal center during the C–H activation and the isomerization between the (*P,M*)- and (*M,M*)-, *cis*- and *trans*-configurations (Scheme 8.40). Similar metalla[8]helicenes were also prepared via the same strategy. By the comparison of the circularly polarized phosphorescence, **132** displayed the highest |g_{lum}| value of 0.013 [77]. If the terminal benzene ring was replaced by pyridine, the acid/base-triggered switch of circularly polarized luminescence could be observed (Scheme 8.41) [78]. If Re(CO)₅Cl reacted with (*M*)-**139**, bipyridinyl-Re complexes (*M*, A_{Re})-**142** and (*M*, A_{Re})-**142** could be obtained in 28 and 52 % yields, respectively [79]. This pair of diastereomers could be resolved by chromatography, and the relative isocyanide-Re complex **143** was prepared in good yields. These were the first examples of Re complexes that exhibited circularly polarized luminescence.
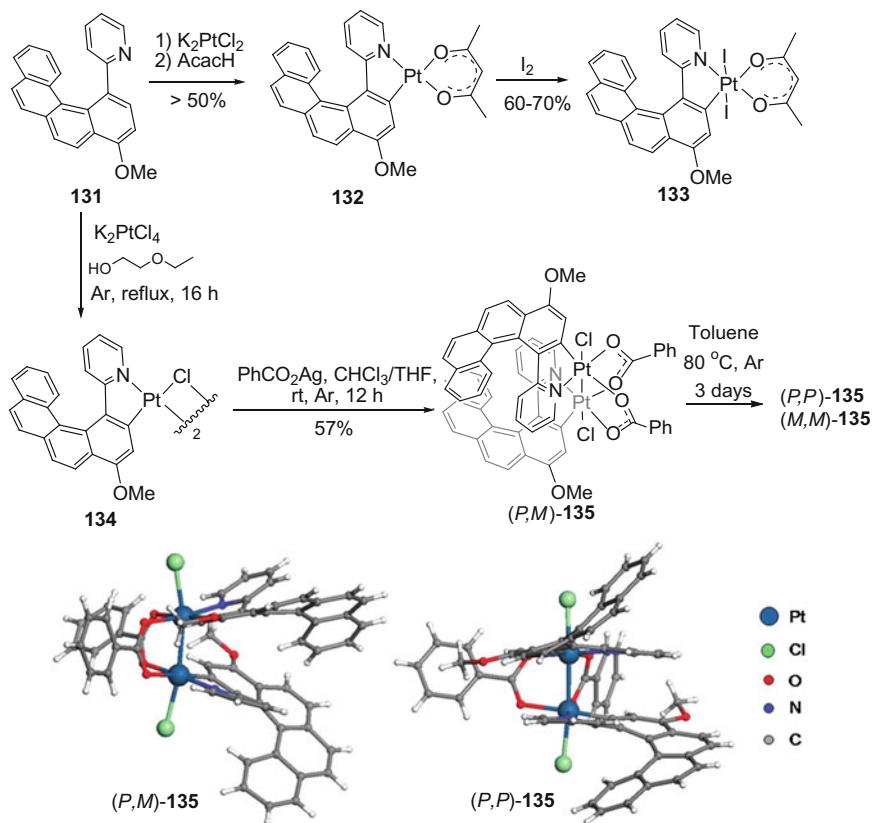
Scheme 8.39 Synthesis and crystal structures of **135**. Reprinted with the permission from Ref. [75]. Copyright 2011 American Chemical Society

Esteruelas, Sierra, and co-workers described the synthesis d^4-metallahelicene by the reaction between the hydride **144** and pyridyl[4]helicene/pyrazinyl[4]helicene in moderate yield (Scheme 8.42) [80]. Azaosma[6]helicenes, **146a** and **146b**, showed different photophysical properties by the virtue of interaction between d orbitals with the π-backbone. Compared with **145a-b**, the absorption was red-shifted from 250 and 380 nm to 500 and 520 nm for **146a** and **146b**, respectively.

A new diphosphine-Au(I) complex was conveniently prepared quantitatively by Licandro and Hashmi (Scheme 8.43) [81]. The structure of **148** was unambiguously determined by X-ray analysis, in which the Au–Au interaction with a distance of 3.18 Å was observed. In addition, the complex was efficient catalyst for the intramolecular hydroarylation of allenes and hydrocarboxylation of allene caboxylates.
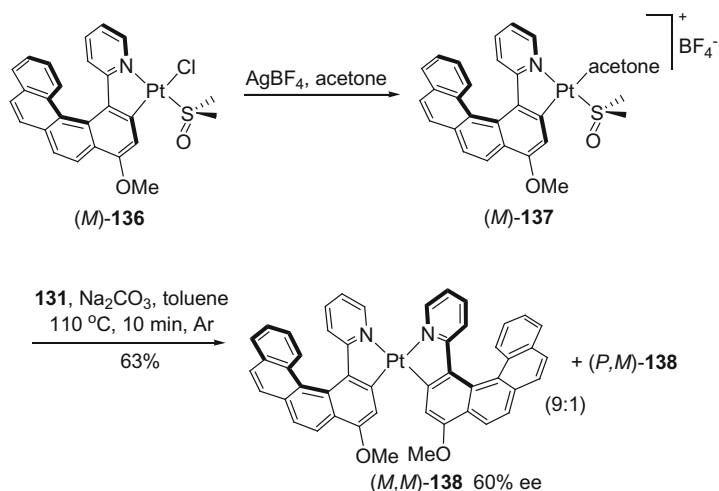
Scheme 8.40 A diastereo- and enantioselective strategy to form enantioenriched metallahelicene dimers
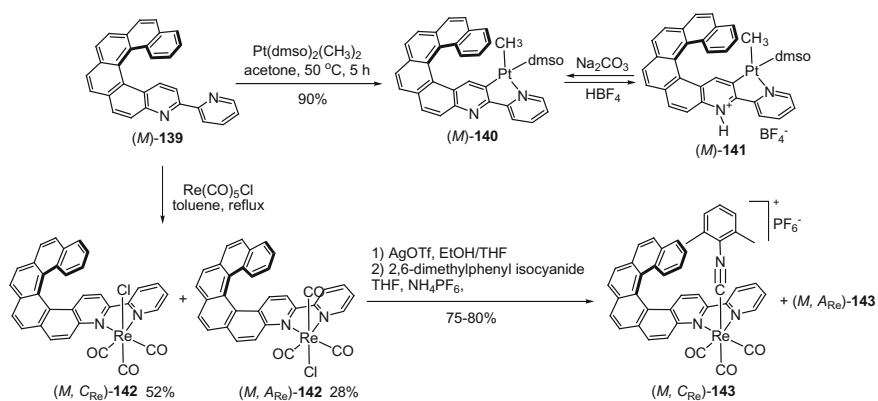
Scheme 8.41 Transformations of (*M*)-**139** to form metal complexes
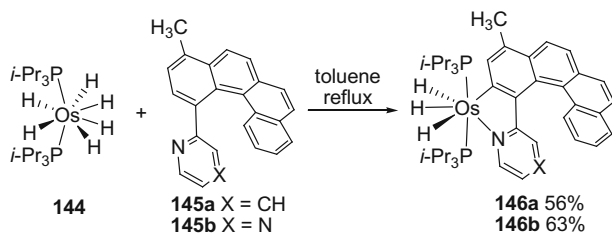
Scheme 8.42 Synthesis d^4-metallahelicenes **146a** and **146b**
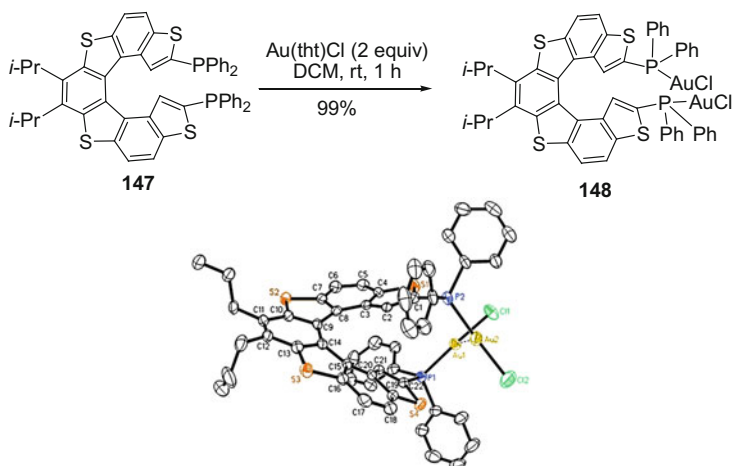
Scheme 8.43 Synthesis and crystal structure of diphosphine–Au(I) complex **148**. Reprinted with the permission from Ref. [81]. Copyright 2013 American Chemical Society
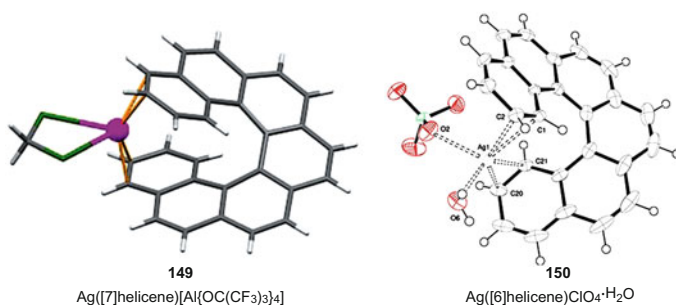
Fig. 8.7 Ag-helicene complexes. Reprinted with the permission from Ref. [82]. Copyright 2012 Royal Society of Chemistry and Ref. [83]. Copyright 2015 Elsevier

Above we discussed the coordination of functional groups incorporated to the helical backbone, the helicene structure itself could act like a tweezer for metal cations. Fuchter group first reported the structure of Ag([7]helicene)[Al{OC(CF$_3$)$_3$}$_4$] **149** (Fig. 8.7, left), in which Ag(I) bound to the bonds of C(3) = C(4) and C(3$'$) = C(4$'$) (the hapticity was between η^1 and η^2) and one dichloromethane solvent molecule [82]. The binding constant was determined in the order of 10^2 M^{-1}. Recently, Makrlík group obtained the crystal structure of Ag([6]helicene)ClO$_4$·H$_2$O **150** (Fig. 8.7, right) [83]. Interestingly, in this example, Ag(I) was coordination to the inner bonds of C(1)=C(2) and C(1$'$)=C(2$'$) (the hapticity was η^2).
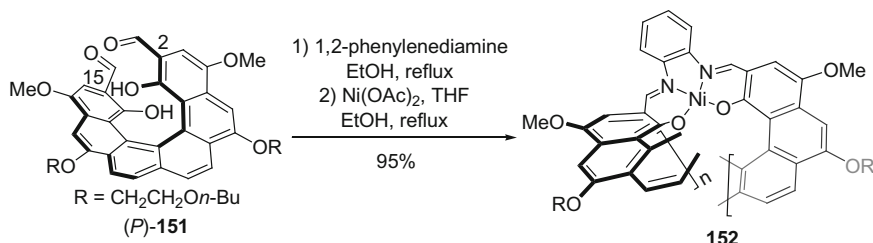
Scheme 8.44 Synthesis of ladder polymer **152** of [7]helicene moieties linked by nickel–salophen units
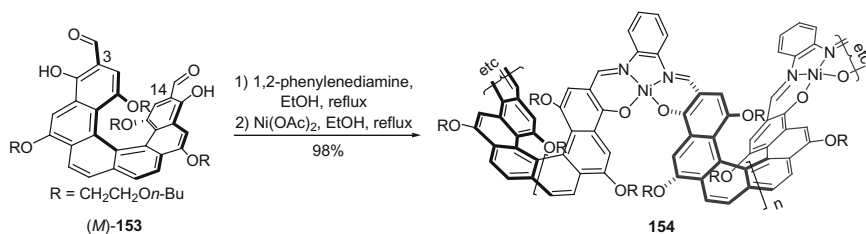
Scheme 8.45 Synthesis of ladder polymer **154** of [7]helicene moieties linked by nickel–salophen units

8.4.2.3   Multitopic Ligands

If two suitable functionalities were embedded into the termini of a helicene, it was possible to build linear polymers. Katz and co-workers introduced two formyl groups to [6]helicene diols to realize this idea [14, 84]. By changing the positions of the functionalities, they prepared two new types of ladder polymers, where [7] helicene moieties were linked by nickel–salophen units (Schemes 8.44 and 8.45). For (P)-**151**, the hydroxyl groups were at C(1) and C(16) positions, and the formyl groups were at C(2) and C(15) positions; while (M)-**151** had the hydroxyl groups at C(4) and C(13) positions, and the formyl groups at C(3) and C(14) positions. By the dynamic forming of polysalophen and coordination with Ni(II), ladder polymers could be prepared in 95–98 % yields. Polymer **152** is winded in a single helical sense; while polymer **154** was composed by (P)-Ni–salophen units and (M)-helicene cores. Both of them had good solubility in organic solvents, and polymer **152** displayed enhance chiroptical properties.

In 1999, Katz group prepared the first optically pure [7]helicene-fused octaazaphthalocyanine from dicyanopyrazine **155** with Cu(OAc)₂ and Ni(OAc)₂ at high temperature in reasonable yields [85] (Scheme 8.46). It was found that **156a-b** would form a bimolecular aggregate with a distance of *ca.* 3.4 Å and rotation of 35°. The aggregates were observed perpendicular to the surface of mica substrate due to AFM analysis.

For **156a**

Cu(OAc)$_2$, 150 °C for 1.5 h
then 140 °C for 3.5 h

For **156b**

Ni(OAc)$_2$, 140 °C for 3 h

R = OC$_{12}$H$_{25}$
155

(*M*)-[7]helicene-fused octaazaphthalocyanine
156a M = Cu 30%
156b M = Ni 20%
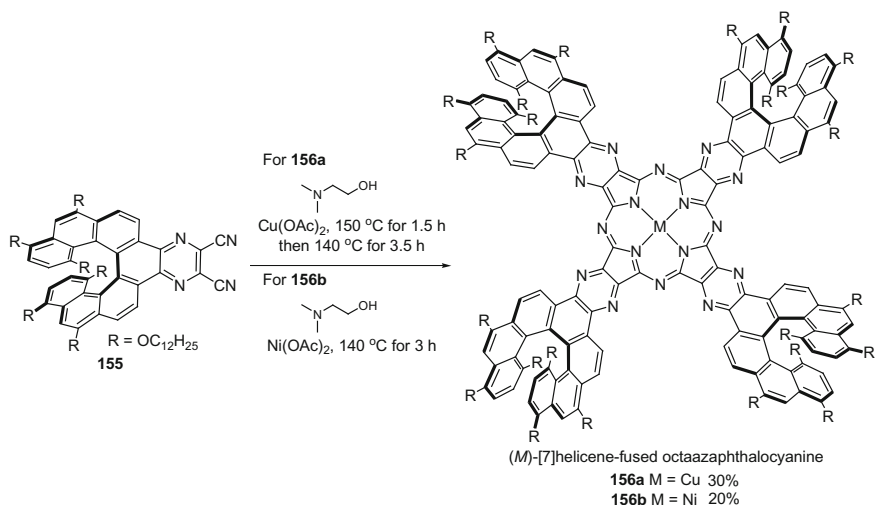
Scheme 8.46 Synthesis of optically pure [7]helicene-fused octaazaphthalocyanines

For **158a**
ZnCl$_2$, DBU, 2-pentanol, reflux

For **158b**
PbCl$_2$, DBU, 2-pentanol, reflux

R = OC$_{12}$H$_{25}$
157

[5]helicene-fused phthalocyanine
158a M = Zn 37%
158b M = Pb 23%
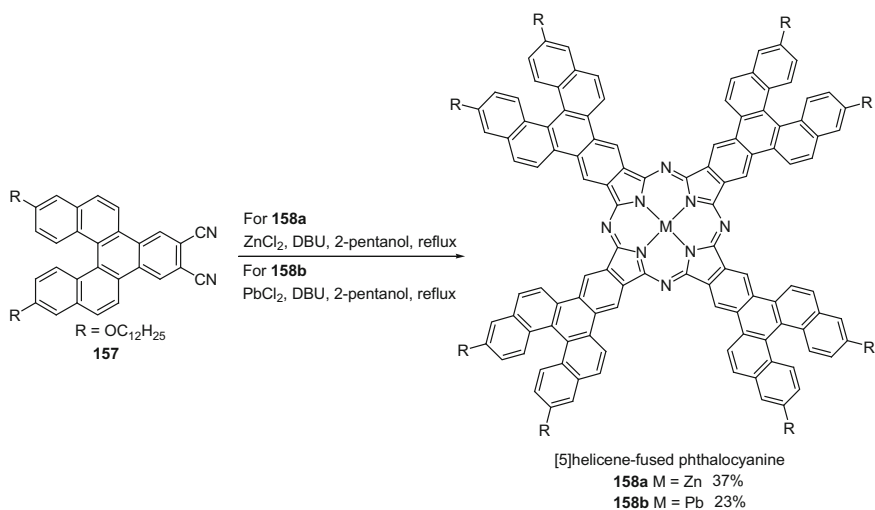
Scheme 8.47 Synthesis of [5]helicene-fused phthalocyanines **158a–b**

Moreover, Mandal and Sooksimuang prepared [5]helicene-fused phthalocyanines **158a-b** from dicyanobenzo[5]helicene **157** [86] (Scheme 8.47). Similarly, **158a** preferentially formed dimers in a wide range of concentrations (10^{-3}–10^{-6} M) with the absorption spectrum covering almost entire visible region and near UV region [87].
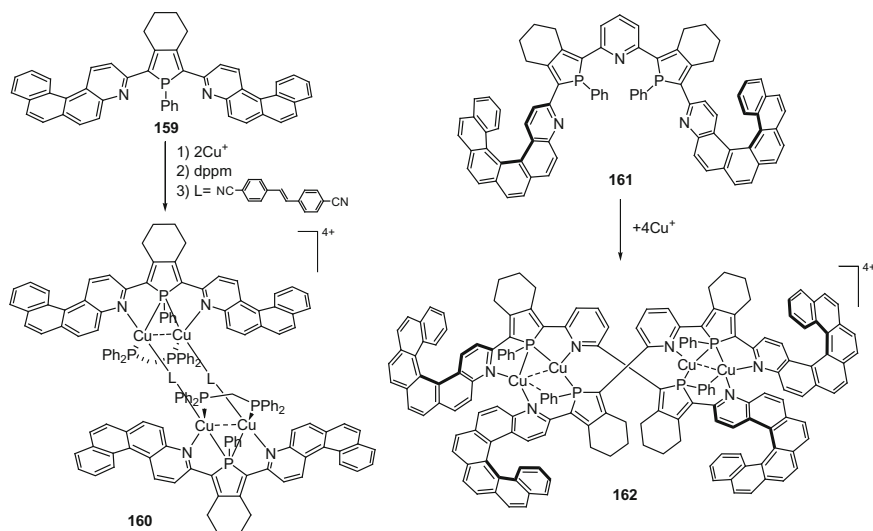
Scheme 8.48 Synthesis of *N,P,N*-pincer ligand **159** and *N,P,N,P,N*-ligand **161** and their coordination to Cu(I)

In addition, Crassous, Réau, and co-workers prepared *N,P,N*-pincer ligand **159**, which self-assembled into a supramolecular assembly **160**, that was supported by a rectangular core bearing four Cu(I) atoms and two linear dicyanostilbene ligands (Scheme 8.48) [88]. Two dppm ligands and two **159** molecules chelated to metal centers, where two types of π-π interactions were disclosed in the solid state—one was between helicenes and the other was between the dicyanostilbene and helicene. Later, Crassous et al. described the synthesis of *N,P,N,P,N*-ligand **161** and its coordination to Cu(I) [89]. As shown in Scheme 8.48, an optically pure supramolecular double-strand assembly **162** was obtained, where two Cu(I) interact with *N,P*-sites in one ligand and *N,P,N*-sites in the other one. The chiroptical properties of **162** were significantly impacted by ligand–ligand charge transfer.

References

1. Martin RH, Jespers J, Defay N (1975) 1-Hydroxymethyl[6]Helicene—Acid-Catalyzed intramolecular rearrangement involving Helicene Skeleton. Tetrahedron Lett 13:1093–1096
2. Jespers J, Defay N, Martin RH (1977) Helicenes—Intramolecular insertion reaction involving Helicene Skeleton. Tetrahedron 33(16):2141–2142
3. Fuchter MJ, Weimar M, Yang X, Judge DK, White AJP (2012) An unusual oxidative rearrangement of [7]-helicene. Tetrahedron Lett 53(9):1108–1111
4. Berger RJF, Fuchter MJ, Krossing I, Rzepa HS, Schaefer J, Scherer H (2014) Gold(I) mediated rearrangement of [7]-helicene to give a benzo[cd]pyrenium cation embedded in a chiral framework. Chem Commun (Camb) 50(40):5251–5253

5. Martin RH, Jespers J, Defay N (1975) Helicenes—Thermally induced intramolecular 4+2 Cycloadditions involving [6]Helicene Skeleton. Helv Chim Acta 58(3):776–779

6. Wang DZ, Katz TJ, Golen J, Rheingold AL (2004) Diels-Alder additions of benzynes within helicene skeletons. J Org Chem 69(22):7769–7771

7. Garcia MH, Florindo P, Piedade MDM, Maiorana S, Licandro E (2009) New organometallic Ru(II) and Fe(II) complexes with tetrathia-[7]-helicene derivative ligands. Polyhedron 28 (3):621–629

8. Yavari K, Moussa S, Ben Hassine B, Retailleau P, Voituriez A, Marinetti A (2012) 1H-Phosphindoles as structural units in the synthesis of Chiral Helicenes. Angew Chem Int Ed 51(27):6748–6752

9. Sakai H, Shinto S, Kumar J, Araki Y, Sakanoue T, Takenobu T, Wada T, Kawai T, Hasobe T (2015) Highly Fluorescent [7]Carbohelicene Fused by Asymmetric 1,2-Dialkyl-Substituted Quinoxaline for Circularly Polarized Luminescence and Electroluminescence. J Phys Chem C 119(24):13937–13947

10. Shen Y, Lu H-Y, Chen C-F (2014) Dioxygen-Triggered Transannular Dearomatization of Benzo[5]helicene Diols: highly efficient synthesis of Chiral π-Extended Diones. Angew Chem Int Ed 53(18):4648–4651

11. Laarhoven WH, Prinsen WJC (1984) Carbohelicenes and Heterohelicenes. Top Curr Chem 125:63–130

12. Chen JD, Lu HY, Chen CF (2010) Synthesis and structures of Multifunctionalized Helicenes and Dehydrohelicenes: an efficient route to construct cyan fluorescent molecules. Chem Eur J 16(39):11843–11846

13. Nakano K, Hidehira Y, Takahashi K, Hiyama T, Nozaki K (2005) Stereospecific synthesis of hetero[7]helicenes by Pd-catalyzed double N-arylation and intramolecular O-arylation. Angew Chem Int Ed 44(43):7136–7138

14. Dai YJ, Katz TJ (1997) Synthesis of helical conjugated ladder polymers. J Org Chem 62 (5):1274–1285

15. Shi SH, Katz TJ, Yang BWV, Liu LB (1995) Use of Thiazyl Chlorides, Alkyl Carbamates, and Thionyl Chloride to Fuse 1,2,5-Thiadiazoles to Quinones and to Oxidize, Chlorinate, and Aminate Them. J Org Chem 60(5):1285–1297

16. Maiorana S, Papagni A, Licandro E, Annunziata R, Paravidino P, Perdicchia D, Giannini C, Bencini M, Clays K, Persoons A (2003) A convenient procedure for the synthesis of tetrathia-[7]-helicene and the selective alpha-functionalisation of terminal thiophene ring. Tetrahedron 59(34):6481–6488

17. Doulcet J, Stephenson GR (2015) Novel asymmetric formylation of aromatic compounds: enantioselective synthesis of formyl 7,8-Dipropyltetrathia[7]helicenes. Chem Eur J 21 (38):13431–13436

18. Torricelli F, Bosson J, Besnard C, Chekini M, Bürgi T, Lacour J (2013) Modular synthesis, orthogonal post-functionalization, absorption, and Chiroptical properties of cationic [6] Helicenes. Angew Chem Int Ed 52(6):1796–1800

19. Peng Z, Takenaka N (2013) Applications of helical-chiral pyridines as Organocatalysts in Asymmetric Synthesis. Chem Rec 13(1):28–42

20. Narcis MJ, Takenaka N (2014) Helical-Chiral small molecules in asymmetric catalysis. Eur J Org Chem 1:21–34

21. Takenaka N, Chen JS, Captain B, Sarangthem RS, Chandrakumar A (2010) Helical Chiral 2-Aminopyridinium Ions: a new class of hydrogen bond donor catalysts. J Am Chem Soc 132 (13):4536–4537

22. Chen J, Captain B, Takenaka N (2011) Helical Chiral 2,2′-Bipyridine N-Monoxides as Catalysts in the Enantioselective Propargylation of Aldehydes with Allenyltrichlorosilane. Org Lett 13(7):1654–1657

23. Kaneko E, Matsumoto Y, Kamikawa K (2013) Synthesis of Azahelicene N-Oxide by Palladium-Catalyzed Direct C–H Annulation of a Pendant (Z)-Bromovinyl Side Chain. Chem Eur J 19(36):11837–11841

24. Dova D, Cauteruccio S, Prager S, Dreuw A, Graiff C, Licandro E (2015) Chiral Thiahelicene-Based Alkyl Phosphine-Borane Complexes: Synthesis, X-ray Characterization, and Theoretical and Experimental Investigations of Optical Properties. J Org Chem 80(8):3921–3928

25. Liu LB, Katz TJ (1991) Bromine Auxiliaries in Photosyntheses of [5]Helicenes. Tetrahedron Lett 32(47):6831–6834

26. Tinnemans AHA, Laarhoven WH, Sharafiozeri S, Muszkat KA (1975) Photodehydrocyclizations of stilbene-like compounds. 15. Electronic overlap population as a reactivity measure in Photocyclizations of Pentahelicenes. Recueil Des Travaux Chimiques Des Pays-Bas 94(11):239–243

27. Frimer AA, Kinder JD, Youngs WJ, Meador MAB (1995) Reinvestigation of the Photocyclization of 1,4-Phenylene Bis(Phenylmaleic Anhydride)—Preparation and Structure of [5]Helicene 5,6-9,10-Dianhydride. J Org Chem 60(6):1658–1664

28. Ito N, Hirose T, Matsuda K (2014) Facile photochemical synthesis of 5,10-Disubstituted [5] Helicenes by removing molecular orbital degeneracy. Org Lett 16(9):2502–2505

29. Yamamoto K, Sonobe H, Matsubara H, Sato M, Okamoto S, Kitaura K (1996) Convenient new synthesis of [7]circulene. Angew Chem Int Ed Engl 35(1):69–70

30. Shimizu M, Nagao I, Tomioka Y, Hiyama T (2008) Palladium-Catalyzed Annulation of vic-Bis(pinacolatoboryl)alkenes and -phenanthrenes with 2,2′-Dibromobiaryls: facile synthesis of functionalized Phenanthrenes and Dibenzo[g, p]chrysenes. Angew Chem Int Ed 47 (42):8096–8099

31. Groen MB, Schadenb H, Wynberg H (1971) Synthesis and resolution of some heterohelicenes. J Org Chem 36(19):2797–2809

32. Dopper JH, Oudman D, Wynberg H (1973) Use of Thieno[2,3-B]Thiophene in Synthesis of Heterohelicenes by Double Photocyclizations. J Am Chem Soc 95(11):3692–3698

33. Dopper JH, Oudman D, Wynberg H (1975) Dehydrogenation of Heterohelicenes by a scholl type reaction—Dehydrohelicenes. J Org Chem 40(23):3398–3401

34. Tinnemans AHA, Laarhoven WH (1974) Photodehydrocyclizations in stilbene-like compounds. IX. 1,2-Phenyl shifts in the cyclization of 1-phenylpentahelicenes. J Am Chem Soc 96(14):4611–4616

35. Rajca A, Miyasaka M, Xiao SZ, Boratynski PJ, Pink M, Rajca S (2009) Intramolecular cyclization of thiophene-based [7]Helicenes to Quasi-[8]Circulenes. J Org Chem 74 (23):9105–9111

36. Rajca A, Pink M, Xiao SZ, Miyasaka M, Rajca S, Das K, Plessel K (2009) Functionalized thiophene-based [7]Helicene: Chirooptical properties versus electron delocalization. J Org Chem 74(19):7504–7513

37. Žádný J, Velíšek P, Jakubec M, Sýkora J, Církva V, Storch J (2013) Exploration of 9-bromo [7]helicene reactivity. Tetrahedron 69(30):6213–6218

38. Goretta S, Tasciotti C, Mathieu S, Smet M, Maes W, Chabre YM, Dehaen W, Giasson R, Raimundo JM, Henry CR, Barth C, Gingras M (2009) Expeditive syntheses of functionalized Pentahelicenes and NC-AFM on Ag(001). Org Lett 11(17):3846–3849

39. Songis O, Misek J, Schmid MB, Kollarovie A, Stara IG, Saman D, Cisarova I, Stary I (2010) A versatile synthesis of functionalized pentahelicenes. J Org Chem 75(20):6889–6899

40. Moussa S, Aloui F, Hassine BB (2013) Synthesis and characterization of a new chiral pentacyclic phosphine. Synth Commun 43(2):268–276

41. Yamamoto K, Ikeda T, Kitsuki T, Okamoto Y, Chikamatsu H, Nakazaki M (1990) Synthesis and chiral recognition of optically-active crown ethers incorporating a Helicene moiety as the chiral center. J Chem Soc Perkin Trans 1(2):271–276

42. Paruch K, Vyklicky L, Wang DZ, Katz TJ, Incarvito C, Zakharov L, Rheingold AL (2003) Functionalizations of [6]- and [7]Helicenes at their most sterically hindered positions. J Org Chem 68(22):8539–8544

43. Biet T, Fihey A, Cauchy T, Vanthuyne N, Roussel C, Crassous J, Avarvari N (2013) Ethylenedithio-Tetrathiafulvalene-Helicenes: Electroactive Helical Precursors with Switchable Chiroptical Properties. Chem Eur J 19(39):13160–13167

44. Teply F, Stara IG, Stary I, Kollarovic A, Saman D, Vyskocil S, Fiedler P (2003) Synthesis of 3-hexahelicenol and its transformation to 3-hexahelicenylamines, diphenylphosphine, methyl carboxylate, and dimethylthiocarbamate. J Org Chem 68(13):5193–5197

45. Weimar M, Correa da Costa R, Lee F-H, Fuchter MJ (2013) A scalable and expedient route to 1-Aza[6]Helicene derivatives and its subsequent application to a chiral-relay asymmetric strategy. Org Lett 15(7):1706–1709

46. Thomson PF, Parrish D, Pradhan P, Lakshman MK (2015) Modular, Metal-Catalyzed Cycloisomerization approach to angularly fused Polycyclic Aromatic Hydrocarbons and Their Oxidized Derivatives. J Org Chem 80(15):7435–7446

47. Usui K, Yamamoto K, Shimizu T, Okazumi M, Mei B, Demizu Y, Kurihara M, Suemune H (2015) Synthesis and resolution of substituted [5]Carbohelicenes. J Org Chem 80(12):6502–6508

48. Schweinfurth D, Zalibera M, Kathan M, Shen C, Mazzolini M, Trapp N, Crassous J, Gescheidt G, Diederich F (2014) Helicene Quinones: Redox-Triggered Chiroptical switching and chiral recognition of the semiquinone radical anion lithium salt by electron nuclear double resonance spectroscopy. J Am Chem Soc 136(37):13045–13052

49. Dreher SD, Katz TJ, Lam KC, Rheingold AL (2000) Application of the Russig-Laatsch reaction to synthesize a bis[5]Helicene chiral pocket for asymmetric catalysis. J Org Chem 65 (3):815–822

50. Nakano D, Hirano R, Yamaguchi M, Kabuto C (2003) Synthesis of optically active bihelicenols. Tetrahedron Lett 44(18):3683–3686

51. Hrbac J, Storch J, Halouzka V, Cirkva V, Matejka P, Vacek J (2014) Immobilization of Helicene onto carbon substrates through electropolymerization of [7]helicenyl-thiophene. RSC Advances 4(86):46102–46105

52. Katz TJ, Slusarek W (1979) Helical Hydrocarbons Capped by 5-Membered Rings as Precursors of Polymeric Metallocenes. J Am Chem Soc 101(15):4259–4267

53. Katz TJ, Pesti J (1982) Synthesis of a helical ferrocene. J Am Chem Soc 104(1):346–347

54. Sudhakar A, Katz TJ (1986) Asymmetric-Synthesis of helical metallocenes. J Am Chem Soc 108(1):179–181

55. Sudhakar A, Katz TJ, Yang BW (1986) Synthesis of a helical Metallocene oligomer. J Am Chem Soc 108(10):2790–2791

56. Gilbert AM, Katz TJ, Geiger WE, Robben MP, Rheingold AL (1993) Synthesis and properties of an optically-active helical bis-cobaltocenium ion. J Am Chem Soc 115(8):3199–3211

57. Katz TJ, Sudhakar A, Teasley MF, Gilbert AM, Geiger WE, Robben MP, Wuensch M, Ward MD (1993) Synthesis and properties of optically-active helical Metallocene Oligomers. J Am Chem Soc 115(8):3182–3198

58. Malaba D, Djebli A, Chen L, Zarate EA, Tessier CA, Youngs WJ (1993) Lithium-Induced Cyclization of Tribenzocyclyne—synthesis and structural characterization of a novel Helicene Dianion, Its protonated form, Silylated Isomers of a substituted Fulvalene ligand, and a novel dimeric lithium complex. Organometallics 12(4):1266–1276

59. Pammer F, Sun Y, Pagels M, Weismann D, Sitzmann H, Thiel WR (2008) Dibenzo[c, g] fluorenyliron: an organometallic relative of pentahelicene. Angew Chem Int Ed 47(17):3271–3274

60. Álvarez CM, Barbero H, García-Escudero LA, Martín-Alvarez JM, Martínez-Pérez C, Miguel D (2012) η6-Hexahelicene Complexes of Iridium and Ruthenium: running along the Helix. Inorg Chem 51(15):8103–8111

61. Rose-Munch F, Li M, Rose E, Daran JC, Bossi A, Licandro E, Mussini PR (2012) Tetrathia [7]helicene-Based complexes of ferrocene and (η5-Cyclohexadienyl)tricarbonylmanganese: synthesis and electrochemical studies. Organometallics 31(1):92–104

62. El Abed R, Aloui F, Genet JP, Ben Hassine B, Marinetti A (2007) Synthesis and resolution of 2-(diphenylphosphino)heptahelicene. J Organomet Chem 692(5):1156–1160

63. Aloui F, Hassine BB (2009) An alternative approach to 3-(diphenylphosphino)hexahelicene. Tetrahedron Lett 50(30):4321–4323

64. Yavari K, Aillard P, Zhang Y, Nuter F, Retailleau P, Voituriez A, Marinetti A (2014) Helicenes with embedded Phosphole units in enantioselective gold catalysis. Angew Chem Int Ed 53(3):861–865

65. El Sayed Moussa M, Guillois K, Shen W, Réau R, Crassous J, Lescop C (2014) Dissymmetrical U-Shaped π-Stacked supramolecular assemblies by using a Dinuclear CuI Clip with Organophosphorus ligands and Monotopic Fully π-Conjugated Ligands. Chem Eur J 20(45):14853–14867

66. Misek J, Teply F, Stara IG, Tichy M, Saman D, Cisarova I, Vojtisek P, Stary I (2008) A straightforward route to helically chiral N-heteroaromatic compounds: Practical synthesis of racemic 1,14-diaza[5]helicene and optically pure 1-and 2-aza[6]helicenes. Angew Chem Int Ed 47(17):3188–3191

67. Mendola D, Saleh N, Vanthuyne N, Roussel C, Toupet L, Castiglione F, Caronna T, Mele A, Crassous J (2014) Aza[6]helicene platinum complexes: chirality control of cis–trans Isomerism. Angew Chem Int Ed 53(23):5786–5790

68. Anger E, Srebro M, Vanthuyne N, Toupet L, Rigaut S, Roussel C, Autschbach J, Crassous J, Réau R (2012) Ruthenium-vinylhelicenes: remote metal-based enhancement and redox switching of the Chiroptical properties of a Helicene Core. J Am Chem Soc 134(38):15628–15631

69. Anger E, Srebro M, Vanthuyne N, Roussel C, Toupet L, Autschbach J, Reau R, Crassous J (2014) Helicene-grafted vinyl- and Carbene-osmium complexes: an example of acid-base Chiroptical switching. Chem Commun (Camb) 50(22):2854–2856

70. Srebro M, Anger E, Moore Ii B, Vanthuyne N, Roussel C, Réau R, Autschbach J, Crassous J (2015) Ruthenium-Grafted Vinylhelicenes: Chiroptical Properties and redox switching. Chem Eur J 21(47):17100–17115

71. Shen WT, Graule S, Crassous J, Lescop C, Gornitzka H, Reau R (2008) Stereoselective coordination of ditopic phospholyl-azahelicenes: a novel approach towards structural diversity in chiral pi-conjugated assemblies. Chem Commun (Camb) 7:850–852

72. Graule S, Rudolph M, Vanthuyne N, Autschbach J, Roussel C, Crassous J, Reau R (2009) Metal-Bis(helicene) assemblies incorporating pi-Conjugated Phosphole-Azahelicene ligands: impacting Chiroptical properties by metal variation. J Am Chem Soc 131(9):3183

73. Graule S, Rudolph M, Shen WT, Williams JAG, Lescop C, Autschbach J, Crassous J, Reau R (2010) Assembly of pi-Conjugated Phosphole Azahelicene derivatives into chiral coordination complexes: an experimental and theoretical study. Chem Eur J 16(20):5976–6005

74. Norel L, Rudolph M, Vanthuyne N, Williams JAG, Lescop C, Roussel C, Autschbach J, Crassous J, Reau R (2010) Metallahelicenes: easily accessible Helicene derivatives with large and tunable Chiroptical properties. Angew Chem Int Ed 49(1):99–102

75. Anger E, Rudolph M, Shen C, Vanthuyne N, Toupet L, Roussel C, Autschbach J, Crassous J, Réau R (2011) From Hetero- to Homochiral Bis(metallahelicene)s Based on a PtIII−PtIII bonded scaffold: isomerization, structure, and Chiroptical Properties. J Am Chem Soc 133(11):3800–3803

76. Shen C, Anger E, Srebro M, Vanthuyne N, Toupet L, Roussel C, Autschbach J, Réau R, Crassous J (2013) Diastereo- and enantioselective synthesis of organometallic Bis(helicene)s by a combination of C–H activation and dynamic isomerization. Chem Eur J 19(49):16722–16728

77. Shen C, Anger E, Srebro M, Vanthuyne N, Deol KK, Jefferson TD, Muller G, Williams JAG, Toupet L, Roussel C, Autschbach J, Reau R, Crassous J (2014) Straightforward access to mono- and bis-cycloplatinated Helicenes displaying circularly polarized phosphorescence by using crystallization resolution methods. Chem Sci 5(5):1915–1927

78. Saleh N, Moore B, Srebro M, Vanthuyne N, Toupet L, Williams JAG, Roussel C, Deol KK, Muller G, Autschbach J, Crassous J (2015) Acid/Base-Triggered switching of circularly polarized luminescence and electronic circular dichroism in organic and organometallic Helicenes. Chem Eur J 21(4):1673–1681

79. Saleh N, Srebro M, Reynaldo T, Vanthuyne N, Toupet L, Chang VY, Muller G, Williams JAG, Roussel C, Autschbach J, Crassous J (2015) Enantio-Enriched CPL-active helicene-bipyridine-rhenium complexes. Chem Commun (Camb) 51(18):3754–3757
80. Crespo O, Eguillor B, Esteruelas MA, Fernandez I, Garcia-Raboso J, Gomez-Gallego M, Martin-Ortiz M, Olivan M, Sierra MA (2012) Synthesis and characterisation of [6]-azaosmahelicenes: the first d4-heterometallahelicenes. Chem Commun (Camb) 48(43):5328–5330
81. Cauteruccio S, Loos A, Bossi A, Blanco Jaimes MC, Dova D, Rominger F, Prager S, Dreuw A, Licandro E, Hashmi ASK (2013) Gold(I) complexes of Tetrathiaheterohelicene Phosphanes. Inorg Chem 52(14):7995–8004
82. Fuchter MJ, Schaefer J, Judge DK, Wardzinski B, Weimar M, Krossing I (2012) [7]-Helicene: a chiral molecular tweezer for silver(i) salts. Dalton Trans 41(27):8238–8241
83. Klepetářová B, Makrlík E, Dytrtová JJ, Böhm S, Vaňura P, Storch J (2015) [6]Helicene as a novel molecular tweezer for the univalent silver cation: Experimental and theoretical study. J Mol Struct 1097:124–128
84. Dai YJ, Katz TJ, Nichols DA (1996) Synthesis of a helical conjugated ladder polymer. Angew Chem Int Ed Engl 35(18):2109–2111
85. Fox JM, Katz TJ, Van Elshocht S, Verbiest T, Kauranen M, Persoons A, Thongpanchang T, Krauss T, Brus L (1999) Synthesis, self-assembly, and nonlinear optical properties of conjugated helical metal phthalocyanine derivatives. J Am Chem Soc 121(14):3453–3459
86. Sooksimuang T, Mandal BK (2003) [5]Helicene-fused phthalocyanine derivatives. New members of the phthalocyanine family. J Org Chem 68(2):652–655
87. Chen LX, Shaw GB, Tiede DM, Zuo XB, Zapol P, Redfern PC, Curtiss LA, Sooksimuang T, Mandal BK (2005) Excited state dynamics and structures of functionalized phthalocyanines. 1. Self-regulated assembly of zinc helicenocyanine. J Phys Chem B 109(35):16598–16609
88. Aranda Perez AI, Biet T, Graule S, Agou T, Lescop C, Branda NR, Crassous J, Réau R (2011) Chiral and Extended π-Conjugated Bis(2-pyridyl)phospholes as Assembling N,P,N Pincers for Coordination-Driven synthesis of supramolecular [2,2]Paracyclophane analogues. Chem Eur J 17(4):1337–1351
89. Vreshch V, El Sayed Moussa M, Nohra B, Srebro M, Vanthuyne N, Roussel C, Autschbach J, Crassous J, Lescop C, Réau R (2013) Assembly of Helicene-Capped N,P,N,P,N-Helicands within CuI Helicates: Impacting Chiroptical Properties by Ligand–Ligand Charge Transfer. Angew Chem Int Ed 52(7):1968–1972

Part III
What Are the Applications of Helicenes?

In this part, we will review the applications of helicenes in catalysis, sensors and recognition, biochemistry, assembly, and organic electronics, with a focus on the recent development in the past 4 years.
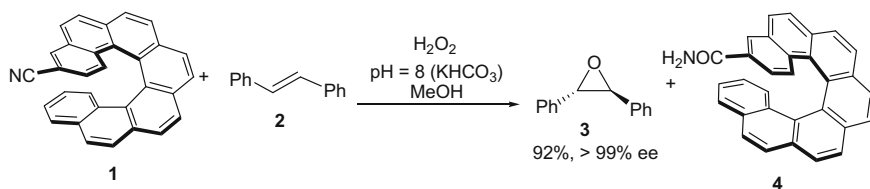
Chapter 9
Helicenes in Catalysis

Abstract With the development of synthetic protocols, the application of helicenes in asymmetric catalysis has attracted more attentions. So far, dozens of helicene-based catalysts have been reported, and they are summarized in this chapter in terms of functionalities of helicenes. First, the non-functionalized helicenes can be utilized as an asymmetric trigger for the autocatalytic addition reactions. Both the macro-cyclic amide based on [4]helicene and bihelicenyls can catalyze the addition of diethylzinc to aldehyde in moderate to good enantioselectivity. Optically pure (*P*)-1-aza[6]helicene and (*M*)-2-aza[6]helicene can be used as the catalyst in the kinetic resolution of alcohol. *N*-oxides of 1-aza[6]helicene are good catalysts for the asymmetric ring-opening of epoxides, and also show high efficiency for the asymmetric propargylation of aldehyde. The protonated 2-amino-1-aza[1]helicenes are excellent dual hydrogen bonding donor catalysts for the asymmetric addition reaction between dihydroindole and nitroalkene, and also for the asymmetric Diels-Alder reaction of nitroalkene with dienes. Helicenes with phosphorus functionality can be used for the asymmetric hydrogenation of itaconate, the kinetic resolution of vinyl alcohol ester, Rh-catalyzed asymmetric hydroformylation and Ir-catalyzed asymmetric allylic amination. Moreover, a series of phosphole-embedded helicene ligands were also developed, which can be used as gold catalysis and HelPhos organocatalysts for the cyclization of *N*-tethered enynes, asymmetric [2+2] cycloaddition of allenenes and [2+4] cycloaddition of allene-dienes in good enantioselectivity. Phosphahelicenes can also be utilized as organocatalyst for the [3+2] cycloaddition between the allene and electron-poor alkenes with excellent diastereoselectivity and enantioselectivity.

Keywords Asymmetric catalysis · Asymmetric trigger · Autocatalytic addition · Azahelicene · Enantioselectivity · Kinetic resolution · Organocatalysis · Organocatalyst · Phosphole-embedded helicene ligand · Phosphahelicene

Although the problems of synthesis and optical resolution of helicenes had been overcome, unexpectedly, the first helicene-based ligand was reported by Reetz group in 1997 [1]. This might be because the photochemical strategy could not be

Scheme 9.1 Epoxidation of stilbene **2** with helicene **1** as chiral reagent

scaled up. During 1985–1987, Martin and co-workers carried out preliminary study on the reactions that helicenes performed as chiral auxiliaries or chiral reagents (stoichiometry), such as epoxidation (Scheme 9.1) [2], reduction of ketones [3], hydroxyamination [4], the ene reaction [5], and the preparation of atrolactic ester [6]. With the development of synthetic protocols, the application in asymmetric catalysis has attracted more attention, and dozens of helicene-based catalysts have been reported [7, 8]. In this chapter, we would like to review this topic in terms of functionalities of helicenes.

9.1   Helicenes as Inducers

The non-functionalized helicenes were utilized by Soai and colleagues as an asymmetric trigger for the autocatalytic addition reactions [9, 10]. As shown in Scheme 9.2, both the (P)-[6]helicene **7** [9] and (P)-tetrathia[7]helicene **8** [10] could
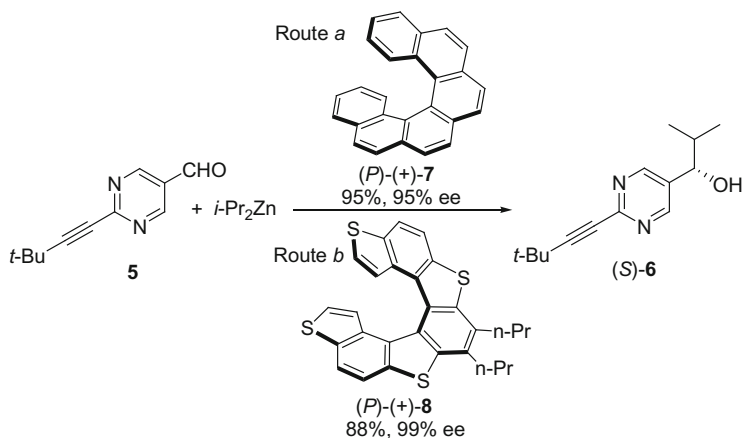
Scheme 9.2 Autocatalytic addition reactions with non-functionalized helicenes as asymmetric triggers

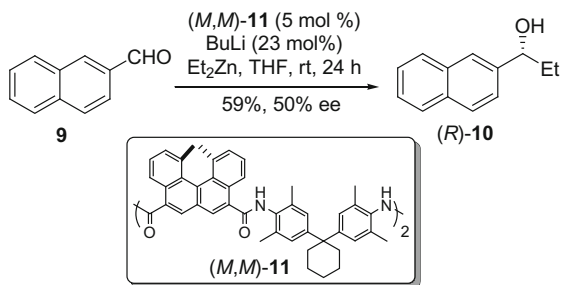**Scheme 9.3** The addition of diethylzinc to aldehyde catalyzed by macrocyclic amide (*M,M*)-**11**

induce the transformation to yield secondary alcohol (*S*)-**6** with excellent enantioselectivity. If the inducer **7** had the ee value as low as 0.13 %, the final product would be obtained in 56 % ee [9].

9.2   Helicene Amide

Yamaguchi and co-workers synthesized the macrocyclic amide (*M,M*)-**11** and found that the lithiated cycle by BuLi would catalyze the addition of diethylzinc to aldehyde in moderate enantioselectivity (Scheme 9.3) [11]. This might result from the interaction between the cyclic anion and zinc atom. If (*P,P*)-**11** was added, (*S*)-**10** would be the major product.

9.3   Helicenes with Oxygen Functionalities

A BINOL analogy, bihelicenyls (*P,P,S*)-[5]HELOL **14**, was prepared by Katz and co-workers, in which two [5]helicene subunits established a chiral groove and had two hydroxyl groups in it [12]. The addition reaction between the aldehyde and diethylzinc was reexamined and afforded alcohol in 93 % yield and 81 % ee (Scheme 9.4). The intermediate structure was proposed that one zinc atom bound to [5]HELOL and the O atom on the substrate, and the chiral groove rendered the attack of the ethyl unit from the *Si*-face.

9.4   Helicenes with Nitrogen Functionalities

Because azahelicenes were Lewis bases, Starý, Stará, and co-workers examined the catalytic activities of optically pure (*P*)-1-aza[6]helicene and (*M*)-2-aza[6]helicene **17** in the kinetic resolution of alcohol [13]. The 1-aza[6]helicene was proved to be
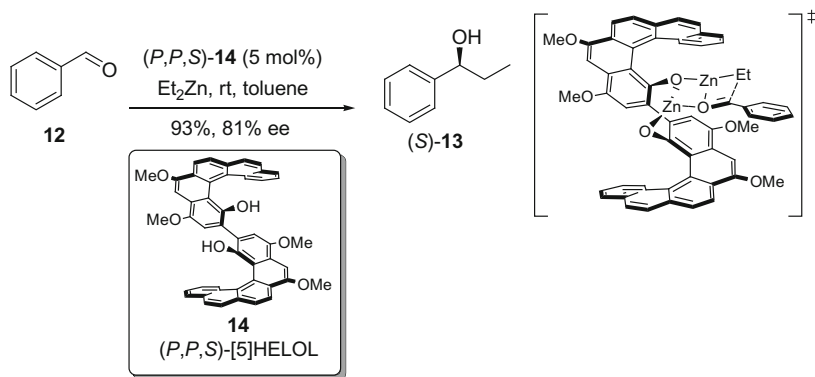
Scheme 9.4 The addition reaction between the aldehyde and diethylzinc catalyzed by **14**
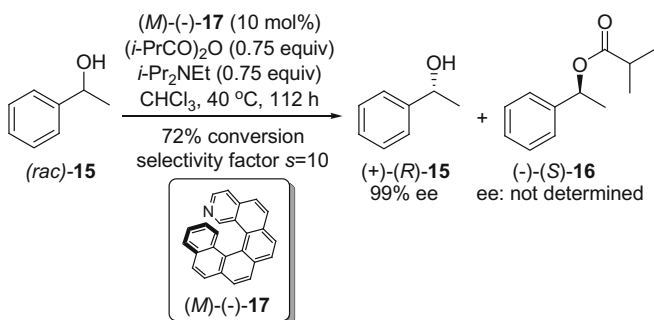
Scheme 9.5 The kinetic resolution of alcohol catalyzed by (M)-2-aza[6]helicene **17**

inactive, resulting from the steric hindrance of *N* atom; while (*M*)-**17** showed good activity with a conversion rate of 72 % and a stereoselectivity of 99 % ee for (*R*)-**15** (Scheme 9.5).

Carbery and co-workers described the synthesis of a helicenoidal DMAP analogue **20** by [2+2+2] cycloaddition and reexamined its catalytic activity for the same reaction [14]. This organocatalyst showed higher selectivity (*s* = 116) in 51 % conversion rate and gave (*R*)-**18** and (*S*)-**19** in 98 and 92 % ee, respectively (Scheme 9.6). It is worth mentioning that the loading of catalyst was as low as 0.5 mol%.

Based on 1-aza[6]helicene, Takenaka group developed a series of catalysts [8]. By the oxidation with *m*-CPBA, *N*-oxides **23**–**25**, were easily prepared in high yields. It was found that the products were good catalysts for the asymmetric ring-opening of epoxides via a cationic intermediate (Scheme 9.7). After screening, they discovered that (*P*)-**25** showed the best catalytic efficiency, giving (*R,R*)-**22** in
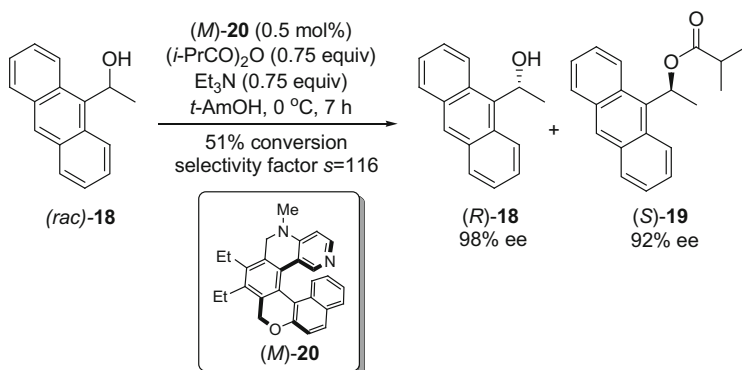
Scheme 9.6 The kinetic resolution of alcohol catalyzed by helicenoidal DMAP analogue **20**
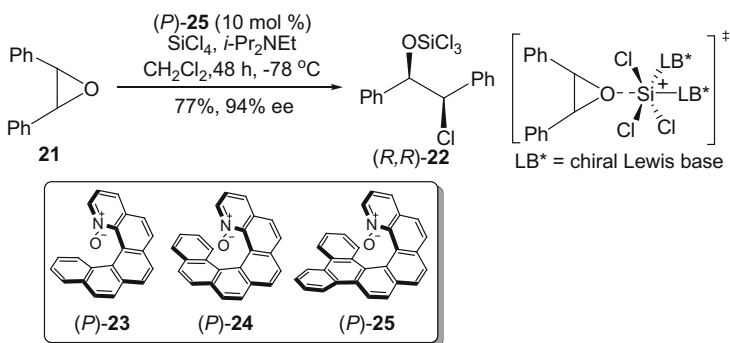
Scheme 9.7 The asymmetric ring-opening of epoxides catalyzed by 1-aza[6]helicene *N*-oxides **23–25**

77 % yield and 94 % ee from (*meso*)-**21**. Afterwards, bidentate ligands were synthesized by the same group. By the reaction of (*P*)-**25** with 2-pyridinyl lithium, followed by the oxidation by DDQ, (*P*)-**29** could be prepared in 95 % yield [15]. Compared with (*P*)-**23**–**25**, (*P*)-**29** showed higher efficiency for the asymmetric propargylation of aldehyde with up to 96 % ee (Scheme 9.8). The protonated 2-amino-1-aza[1]helicenes were proved to be excellent dual hydrogen bonding donor catalysts. For example, in the presence of (*M*)-**33**, the stereoselectivity could be promoted up to 96 % ee for the addition reaction between dihydroindole **30** and nitroalkene **31** (Scheme 9.9) [16]. However, for the Diels–Alder reaction of nitroalkene with dienes, the catalysts showed unsatisfied enantioselectivity up to 40 % ee [17, 18] (Scheme 9.10).
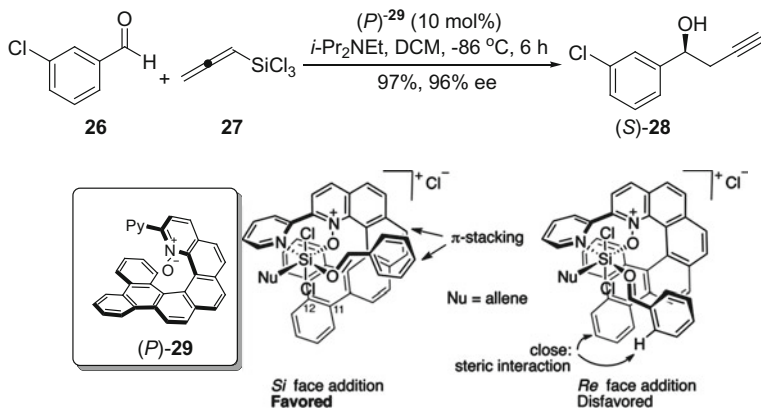
Scheme 9.8 The asymmetric propargylation of aldehyde catalyzed by (*P*)-**29**. Reprinted with the permission from Ref. [15]. Copyright 2011 American Chemical Society
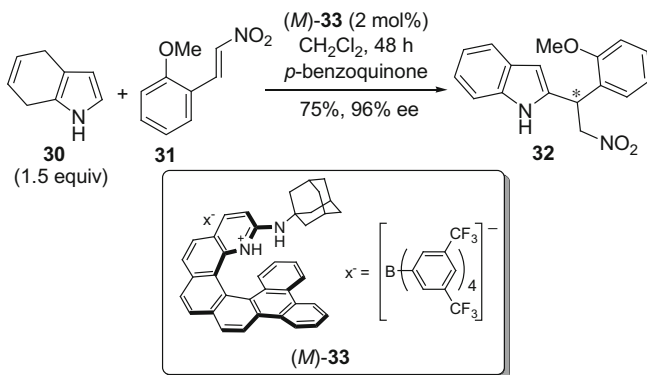
Scheme 9.9 The asymmetric addition reaction between dihydroindole **30** and nitroalkene **31** catalyzed by (*M*)-**33**

9.5   Helicenes with Phosphorus Functionalities

Reetz group reported the first example of helicene ligand (*M*)-**40**, which was used for the asymmetric hydrogenation of itaconate with [Rh(cod)$_2$]BF$_4$ [1]. The product (*S*)-**39** could be obtained in 54 % yield and 39 % ee (Scheme 9.11, Route *a*). Later, Yamaguchi group reexamined this reaction by changing the chiral ligand [19]. Under high pressure of hydrogen, the transformation showed excellent efficiency with a quantitative yield and 96 % ee in the presence of (*M*,*M*,*S*,*l*)-**41**-Rh complex (Scheme 9.11, Route *b*).

In addition, the kinetic resolution of **42** by Pd-mediated substitution with the help of the ligand (*P*)-(+)-**40** was explored by Reetz and Sostmann [20]
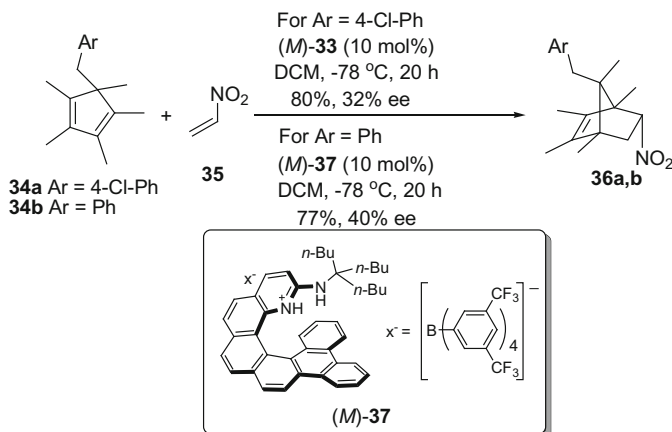
Scheme 9.10 The Diels-Alder reaction of nitroalkene with dienes catalyzed by (*M*)-**37**
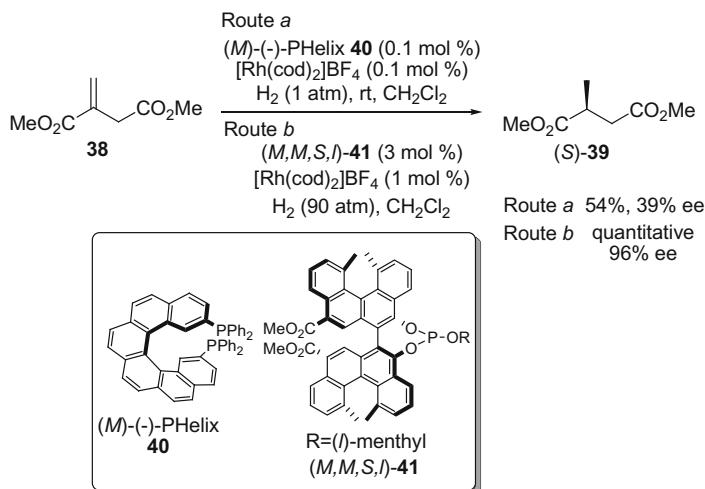
Scheme 9.11 The asymmetric hydrogenation of dimethyl itaconate catalyzed by [Rh(cod)$_2$]BF$_4$ with helicenes as the chiral ligands

(Scheme 9.12). According to their study, PHelix **40** performed as a monodentate ligand, because the distance between the two P atoms was 6.481 Å, which was determined by single crystal X-ray analysis. The optimized condition was obtained utilizing PHelix/Pd (4:1) as the catalyst system, affording (*R*)-**42** in >99 % ee with a conversion rate of 81 %.

Starý, Stará, and co-workers described the synthesis of helicene-like phosphates and their applications in Rh-catalyzed hydroformylation and Ir-catalyzed allylic amination [21]. For the asymmetric hydroformylation, (*P,S*)-**45** had the best
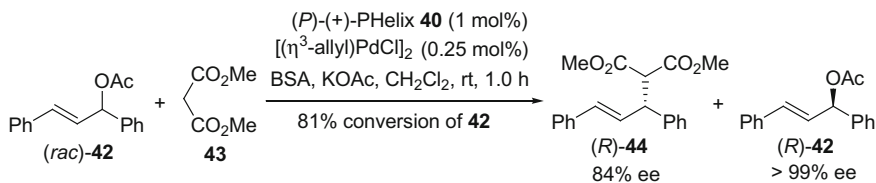
Scheme 9.12 The kinetic resolution of **42** by Pd-mediated substitution with the help of the ligand (*P*)-(+)-**40**
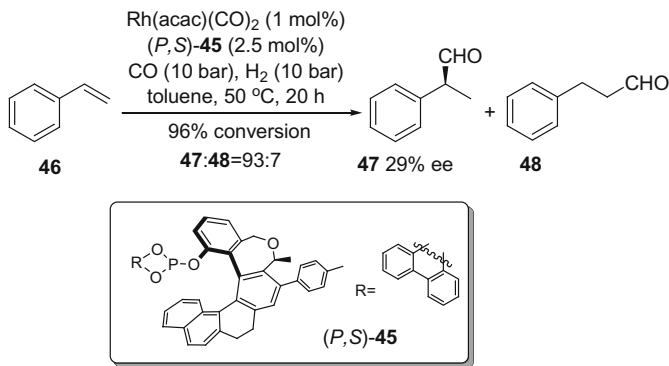
Scheme 9.13 The Rh-catalyzed asymmetric hydroformylation with (*P,S*)-**45** as the chiral ligand

catalytic efficiency, which showed good conversion rate (96 %) and regioselectivity (93:7) but low enantioselectivity (29 % ee) (Scheme 9.13). With the help of (*P,S*)-**51**, asymmetric allylic amination could be achieved with up to 94 % ee and excellent regioselectivity (Scheme 9.14).

Marinetti, Voituriez, and co-workers developed a series of phosphole-embedded helicene ligands, namely HelPHos, for gold catalysis and HelPhos organocatalysts (Fig. 9.1) [7]. Herein, S_P or R_P stood for the central chirality of *P* atoms, and *endo-* or *exo-*configuration indicated the orientation of the AuCl moiety, in which AuCl facing towards the other terminal ring of helicene was in *endo-*configuration and the other direction was in *exo-*configuration. The helical skeleton could be prepared by oxidative photochemical cyclization under irradiation or metal-mediated [2+2+2] cycloisomerization of triynes. The diastereomers could be conveniently separated by column chromatography. Interestingly, during the preparation of **57**, only one diastereomer was obtained [22].

The cyclization of *N*-tethered enynes was first studied. For **61**, catalyst (*S_P,P*)-**53**-*endo* displayed better enantioselectivity than (*S_P,P*)-**57**, which afforded (*1R,6S*)-**62** in 74 % ee under the same condition (Scheme 9.15) [22, 23]. When the phenyl group was replaced by cyclohex-1-en-1-yl group, (*S_P,P*)-**57** showed higher activity (96 % ee) than the carbohelicene-Au catalysts (up to 86 % ee) for the same transformation [22, 23]. If phenyl group was incorporated to the terminal vinyl
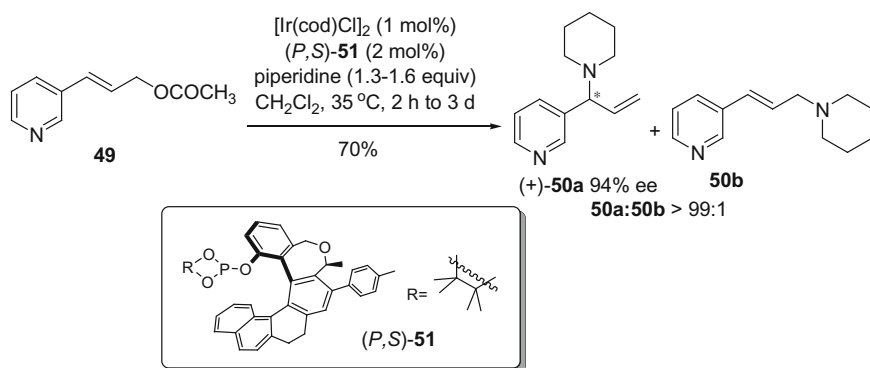
Scheme 9.14 The Ir-catalyzed asymmetric allylic amination with (*P*,*S*)-**51** as the chiral ligand
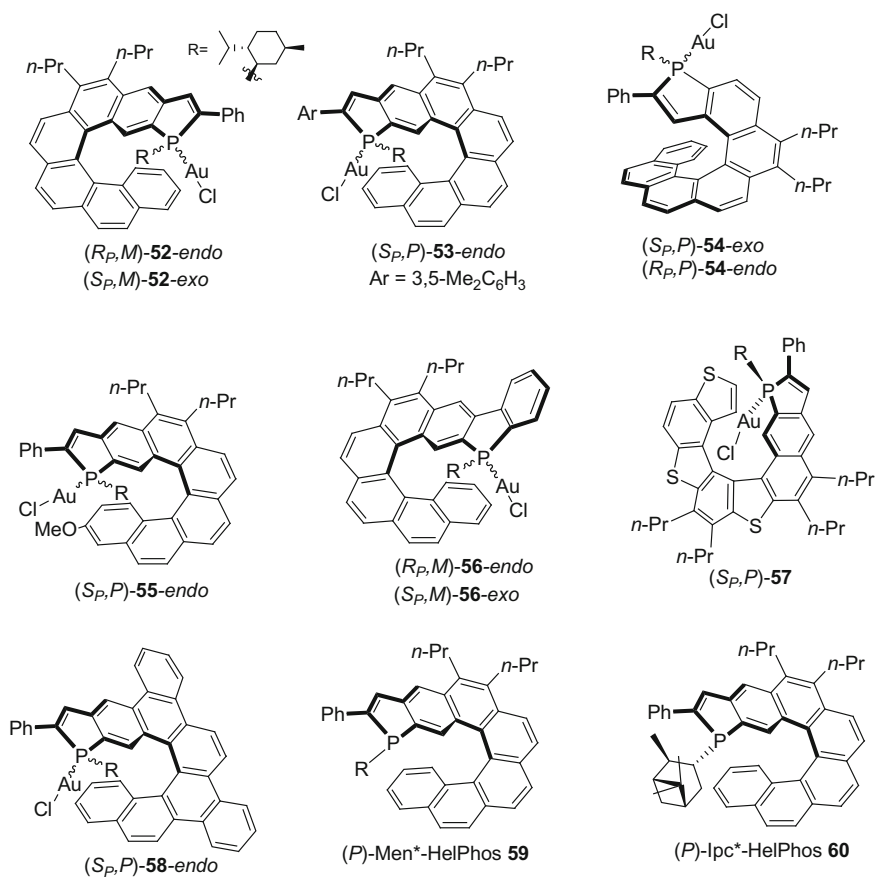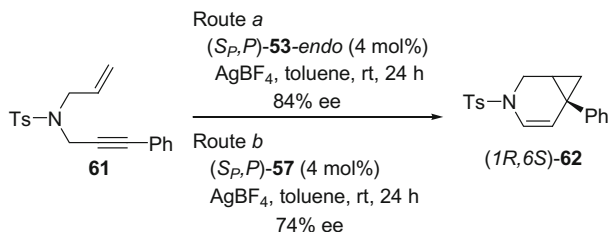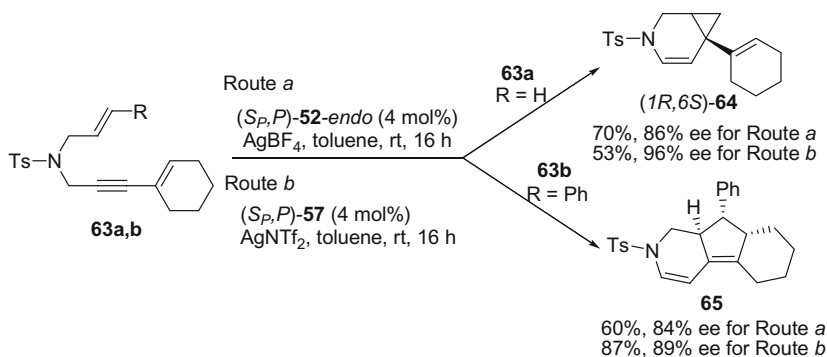

Fig. 9.1 Phosphole-embedded HelPhos-Au complexes and HelPhos organocatalysts

Scheme 9.15 The asymmetric cyclization of *N*-tethered enynes catalyzed by HelPhos-Au complexes

Scheme 9.16 The asymmetric intramolecular [2+3] cyclization catalyzed by HelPhos-Au complexes

group, like **63b**, intramolecular [2+3] cyclization was observed, and (S_P,P)-**57** showed the best result for such conversions [22] (Scheme 9.16).

Later, the applications of the complexes in [2+2] cycloaddition of allenenes and [2+4] cycloaddition of allene-dienes were explored by Marinetti, Voituriez, and co-workers [24]. By activation with AgSbF$_6$, (S_P,P)-**58**-*endo* showed better activity and enantioselectivity than (S_P,P)-**57** and (S_P,P)-**52**-*endo*, giving the [2+2] product **67** in 85 % yield and 92 % ee and the [4+2] product **68** in 83 % yield and 84 % ee, respectively (Scheme 9.17). Interestingly, the cationic intermediate in such step-wise transformations could be trapped by nucleophiles, like **69**.

Recently, they reported the utilization of phosphahelicenes as organocatalyst for the [3+2] cycloaddition between the allene and electron-poor alkenes [25]. The catalyst (*P*)-**60** showed high catalytic activity with excellent diastereoselectivity (>95:5 d.r.) and enantioselectivity (up to 97 % ee) (Scheme 9.18).

Cauterucio, Benaglia, and co-workers described the asymmetric aldol-type reaction using bis(phosphine oxide) **75** as Lewis base organocatalyst (Scheme 9.19) [26]. The reaction showed good diastereoselectivity, but the enantioselectivity was unsatisfied.
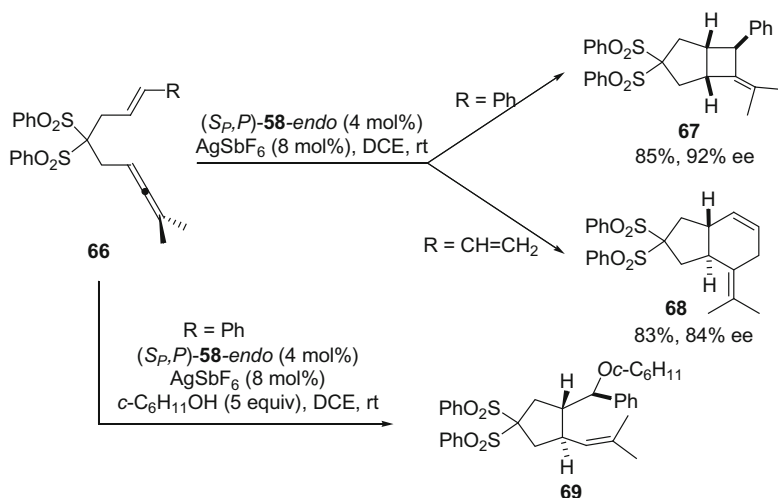
Scheme 9.17 The asymmetric [2+2] cycloaddition of allenenes and [2+4] cycloaddition of allene-dienes catalyzed by (S_P,P)-**58**-*endo*
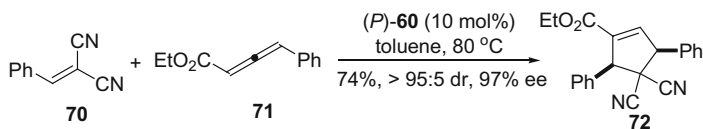
Scheme 9.18 The [3+2] cycloaddition between the allene and electron-poor alkenes catalyzed by phosphahelicene (*P*)-**60**

In addition, the preliminary study of racemic Au(I)-thiahelicene phosphine complexes in hydroarylation of allene and hydrocarboxylation of allene-carboxylates has been carried out by Licandro and Hashmi groups, which showed good conversion rates during the transformation [27].

All the reported helicene-based catalysts developed before 2016 were summarized above, and the features are concluded as follows:

(1) Azahelicenes are good precursors for construction of organocatalysts, because they could be both hydrogen bonding donors and acceptors in protonated states; also they could be easily modified on the pyridine ring, usually adjacent to the nitrogen atom.

(2) Helicenols and phosphorus-embedded helicenes are proved to be good ligands for the transition metal catalysis, in which the configuration of the complexes significantly impacts the enantioselectivity, like the *endo*- and *exo*-configurations. It means that the substrates would have interactions with helicenes after binding to the metal center to transfer the helicity successfully.
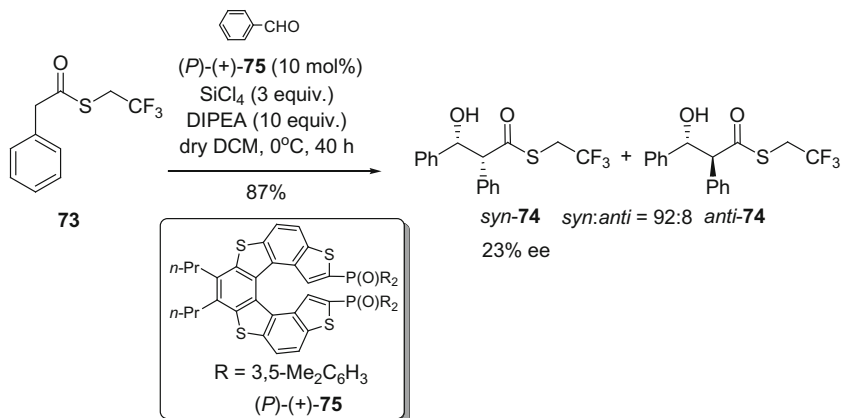
Scheme 9.19 The asymmetric aldol-type reaction using bis(phosphine oxide) **75** as Lewis base organocatalyst

(3) The position of catalytic or binding site on the helical skeleton (usually at C(1) or C(2) positions) and the functional groups nearby should be carefully designed that there should be enough space for it to bind to metal or substrate but the space should not be too large in order to transfer the chirality.

References

1. Reetz MT, Beuttenmuller EW, Goddard R (1997) First enantioselective catalysis using a helical diphosphane. Tetrahedron Lett 38(18):3211–3214
2. Hassine BB, Gorsane M, Pecher J, Martin RH (1986) Synthèses et Synthèses Enantiosélectives D'Epoxydes Derivant du (E)-Stilbène et de L'α-Méthylstyrène Par la Méthode de Payne. Bull Soc Chim Belg 95(7):557–566
3. Hassine BB, Gorsane M, Pecher J, Martin RH (1985) Diastereoselective NaBH$_4$ Reductions of (dl) α-Keto Esters. Bull Soc Chim Belg 94(8):597–603
4. Hassine BB, Gorsane M, Pecher J, Martin RH (1985) Synthèses Asymétriques et Synthèses Asymétriques Potentielles D'α-Amino Alcools: Hydroxyamination D'Oléfines par la Méthode de Sharpless. Bull Soc Chim Belg 94(11–12):759–769
5. Hassine BB, Gorsane M, Pecher J, Martin RH (1987) Synthèses Asymétriques Potentielles Impliquant la Réaction "Ene". Bull Soc Chim Belg 96(10):801–808
6. Hassine BB, Gorsane M, Geerts-Evrard F, Pecher J, Martin RH, Castelet D (1986) Utilisation de la Synthèse Atrolactique Pour L'Évaluation de L'Efficacité D'Inducteurs de Synthèse Asymétrique. Bull Soc Chim Belg 95(7):547–556
7. Aillard P, Voituriez A, Marinetti A (2014) Helicene-like chiral auxiliaries in asymmetric catalysis. Dalton Trans 43(41):15263–15278
8. Narcis MJ, Takenaka N (2014) Helical-chiral small molecules in asymmetric catalysis. Eur J Org Chem 1:21–34
9. Sato I, Yamashima R, Kadowaki K, Yamamoto J, Shibata T, Soai K (2001) Asymmetric induction by helical hydrocarbons: [6]- and [5]helicenes. Angew Chem Int Ed 40(6):1096

10. Kawasaki T, Suzuki K, Licandro E, Bossi A, Maiorana S, Soai K (2006) Enantioselective synthesis induced by tetrathia-[7]-helicenes in conjunction with asymmetric autocatalysis. Tetrahedron-Asymmetry 17(14):2050–2053

11. Okubo H, Yamaguchi M, Kabuto C (1998) Macrocyclic amides consisting of helical chiral 1,12-dimethylbenzo[c]phenanthrene-5,8-dicarboxylate. J Org Chem 63(25):9500–9509

12. Dreher SD, Katz TJ, Lam KC, Rheingold AL (2000) Application of the Russig-Laatsch reaction to synthesize a bis[5]helicene chiral pocket for asymmetric catalysis. J Org Chem 65 (3):815–822

13. Samal M, Misek J, Stara IG, Stary I (2009) Organocatalysis with azahelicenes: the first use of helically chiral pyridine-based catalysts in the asymmetric acyl transfer reaction. Collect Czech Chem Commun 74(7–8):1151–1159

14. Carbery DR, Crittall MR, Rzepa HS (2011) Design, synthesis, and evaluation of a helicenoidal DMAP lewis base catalyst. Org Lett 13(5):1250–1253

15. Chen J, Captain B, Takenaka N (2011) Helical Chiral 2,2′-Bipyridine *N*-Monoxides as Catalysts in the Enantioselective Propargylation of Aldehydes with Allenyltrichlorosilane. Org Lett 13(7):1654–1657

16. Takenaka N, Chen JS, Captain B, Sarangthem RS, Chandrakumar A (2010) Helical chiral 2-Aminopyridinium ions: a new class of hydrogen bond donor catalysts. J Am Chem Soc 132 (13):4536–4537

17. Narcis MJ, Sprague DJ, Captain B, Takenaka N (2012) Enantio- and periselective nitroalkene Diels-Alder reaction. Org Biomol Chem 10(46):9134–9136

18. Peng Z, Narcis M, Takenaka N (2013) Enantio- and Periselective Nitroalkene Diels-Alder reactions catalyzed by helical-chiral hydrogen bond donor catalysts. Molecules 18(8):9982

19. Nakano D, Yamaguchi M (2003) Enantioselective hydrogenation of itaconate using rhodium bihelicenol phosphite complex. Matched/mismatched phenomena between helical and axial chirality. Tetrahedron Lett 44(27):4969–4971

20. Reetz MT, Sostmann S (2000) Kinetic resolution in Pd-catalyzed allylic substitution using the helical PHelix ligand. J Organomet Chem 603(1):105–109

21. Krausová Z, Sehnal P, Bondzic BP, Chercheja S, Eilbracht P, Stará IG, Šaman D, Starý I (2011) Helicene-Based Phosphite Ligands in Asymmetric Transition-Metal Catalysis: Exploring Rh-Catalyzed Hydroformylation and Ir-Catalyzed Allylic Amination. Eur J Org Chem 3849–3857

22. Aillard P, Voituriez A, Dova D, Cauteruccio S, Licandro E, Marinetti A (2014) Phosphathiahelicenes: synthesis and uses in enantioselective gold catalysis. Chem Eur J 20 (39):12373–12376

23. Yavari K, Aillard P, Zhang Y, Nuter F, Retailleau P, Voituriez A, Marinetti A (2014) Helicenes with embedded Phosphole units in enantioselective gold catalysis. Angew Chem Int Ed 53(3):861–865

24. Aillard P, Retailleau P, Voituriez A, Marinetti A (2015) Synthesis of New Phosphahelicene scaffolds and development of Gold(I)-Catalyzed enantioselective Allenene Cyclizations. Chem Eur J 21(34):11989–11993

25. Gicquel M, Zhang Y, Aillard P, Retailleau P, Voituriez A, Marinetti A (2015) Phosphahelicenes in Asymmetric Organocatalysis: [3+2] Cyclizations of γ-Substituted Allenes and Electron-Poor Olefins. Angew Chem Int Ed 54(18):5470–5473

26. Cauteruccio S, Dova D, Benaglia M, Genoni A, Orlandi M, Licandro E (2014) Synthesis, characterisation, and Organocatalytic activity of chiral Tetrathiahelicene Diphosphine Oxides. Eur J Org Chem 13:2694–2702

27. Cauteruccio S, Loos A, Bossi A, Blanco Jaimes MC, Dova D, Rominger F, Prager S, Dreuw A, Licandro E, Hashmi ASK (2013) Gold(I) complexes of tetrathiaheterohelicene phosphanes. Inorg Chem 52(14):7995–8004

Chapter 10
Recognition, Sensors, and Responsive Switches

Abstract Both the helicity and the π–conjugated structure of helicenes endow them with a wide range of potential applications in molecular recognition and fluorescent sensing, and the environmentally responsive switches, especially in the chiral recognition and chiroptical switches. Thus, chiral recognition of helicene crown ethers toward racemic amine salts, recognition of diacids by helicopodand, chiral recognition between the BINOL-modified Au nanoparticles and Helquat via donor–acceptor interactions, and chiral recognition between the helicene quinone radical anion and BINAPO were sequentially found. It was also found that stereoregular helical acetylenes with [6]helicene units as the pendants generated by Rh-catalyzed polymerization display the ability to adsorb one enantiomer preferentially in a racemic mixture solution. Moreover, 2,15-dihydroxyl[6]helicene as fluorescence sensor for chiral amines and aminoalcohols, diaza[4]helicenes with pyridine and amino moieties for pH-sensitive sensing, tetrahydro[5]helicene thioimide-based chemodosimeter for Hg^{2+}, and a humidity sensor based on [6] helicene-derived imidazolium salt were also developed. Recently, a series of fast-responsive explosive sensors based on the polymerization of [5]helicenes were reported as well. Furthermore, helicenes and their derivatives can be applied in the design and development of various acid-base responsive switches, redox-responsive switches, photo-responsive switches, and chiroptical switches.

Keywords Acid-base responsive switches · Chiroptical switches · Fluorescent chemosensor · Molecular recognition · Nanoparticle · Photo-responsive switches · Redox-responsive switches

In this chapter, we would like to examine the interactions between the helicenes and small molecules, including the molecular recognition and helicene-derived sensors, and the environmentally responsive switches. It was proved that both of the helicity and π–conjugated helical structure were essential for these applications [1], especially for the chiral recognition and chiroptical properties.

10.1　Helicenes for Molecular Recognition

As early as 1983, Nakazaki group described the synthesis of helicene crown ethers
1–2, and examined their chiral recognition toward racemic amine salts **3–5** [2, 3].
The hosts were prepared by photochemical cyclization of stilbene-type precursors
to build helicene moiety, followed by the construction of crown ether rings. As
depicted in Fig. 10.1, the host was resolved in the organic layer (CHCl₃), and the
amine salt was resolved in outer part of the aqueous phase, which was separated by
the tube. With stirring, the host transports the amine salt to the aqueous phase in the
tube. And the selectivity could be calculated by analysis of inner aqueous solution.
It was found that (1) the selectivity of the (R)-/(S)-enantiomer was totally reversed
for the crown ethers with the same helicity; (2) the enantioselectivity of **1** was much
better than that of **2**, which meant that the complementarity between the hosts and
the guests was important.

In 1993, Diederich and co-workers reported a new helicopodand and investi-
gated its recognition of diacids (Fig. 10.2) [4]. The helicopodand had two pyridyl
amino groups on the terminal rings, which could bind with the substrates bearing
hydrogen bond functionalities. They observed 1:1 host–guest complexes. Diacid **7**
showed the strongest binding with the helicopodand **6** among four diacids, of which
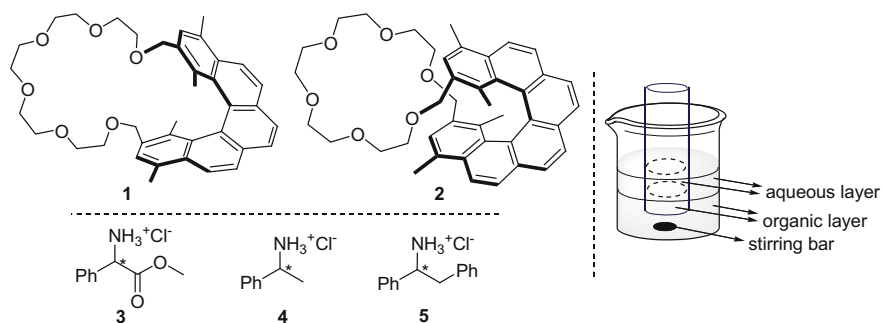the binding constant was determined to be $5500 \pm 810 \text{ M}^{-1}$ by ¹H NMR titration.

Fig. 10.1 Helicene-derived chiral crown ethers, guest molecules and the experimental apparatus
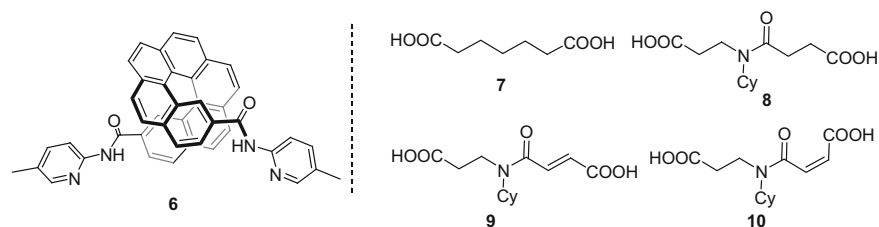

Fig. 10.2 The helicopodand and diacid guests

By theoretical calculation, the distance between two N/NH functionalities was determined to be 7.98, and 7.77 Å was the distance between the two acid functional groups of **7** in fully staggered configuration. The comparison of **9** and **10** suggested that (*E*)-diacid **9** was more complementary to the host.

In addition, the chiral recognition between 1,12-dimethyl[4]helicene-5,8-dicarboxylic acid **11** and linear dextrins [5] and cyclodextrins [6, 7] via hydrogen bonding interaction was investigated by Kano and co-workers. [4]Helicene dicarboxylic acid could be resolved by capillary zone electrophoresis with the help of linear dextrins as chiral selector [5]. For the cyclodextrins, the diacid **11** did not interact with α-CD because of the small cavity; while β-CD had binding constants (K_a) of $18,700 \pm 1700$ M^{-1} for (*M*)-**11** and 2200 ± 100 M^{-1} for (*P*)-**11**. If the cavity was enlarged further, like γ-CD, the diacid **11** was included loosely ($K_a = 3100 \pm 100$ M^{-1} for (*M*)-**11** and 690 ± 20 M^{-1} for (*P*)-**11**) [6, 7].

Willner, Teplý, and co-workers reported the chiral recognition between the BINOL-modified Au NPs **12** and Helquat **13** via donor–acceptor interactions [8]. The results showed that (*S*)-**12** ((*S*)-BINOL modified Au NPs) bond more strongly with (*M*)-**13**, while (*R*)-**12** ((*R*)-BINOL modified Au NPs) bond more strongly with (*P*)-**13** and the binding constants were determined as $(4.0 \pm 0.5) \times 10^5$ M^{-1} for (*S*)/(*M*), $(4.0 \pm 0.5) \times 10^5$ M^{-1} for (*S*)/(*P*), $(7.0 \pm 0.5) \times 10^5$ M^{-1} for (*R*)/(*P*), and $(2.5 \pm 0.3) \times 10^5$ M^{-1} for (*R*)/(*M*). This could also be clearly observed from STEM images (Fig. 10.3).

Similarly, Yamaguchi et al. described the chiral recognition between the helicene/amino-modified Si NPs and secondary alcohols. Based on the recognition that (*P*)-helicene had stronger interaction with (*S*)-alcohol (Fig. 10.4), the dispersed silicon nanoparticles were aggregated in the presence of racemic alcohol, where (*S*)-enantiomer was dominated. After 12 h, precipitation of Si NPs was separated by centrifugation, which could include enantioenriched alcohol molecules. After the subsequent elution, (*S*)-secondary alcohol could be obtained up to 61 % ee.

Diederich, Gescheidt, and co-workers discovered the chiral recognition between the helicene quinone radical anion and BINAPO [9]. Li$^+${(±)-**14**$^{\bullet-}$} was prepared by the reduction of 1,2-[6]helicene-quinone **14** in the presence of Li. According to the DFT theoretical study, the lithium hyperfine coupling was very sensitive to the structural changes. By adding (*R*)-BINAPO to Li$^+${(*P*)-(+)-**14**$^{\bullet-}$} and Li$^+${(*M*)-(−)-**14**$^{\bullet-}$}, the diastereomers formed in situ could be discriminated from their ENDOR spectra at 210 K (Fig. 10.5). The [{(*R*)-(+)-BINAPO}Li$^+${(*P*)-(+)-**14**$^{\bullet-}$}] complex showed a A(^{7}Li) value of −1.76 MHz, and [{(*R*)-(+)-BINAPO}Li$^+${(*M*)-(−)-**14**$^{\bullet-}$}] was determined to be −1.62 MHz, while [{(*R*)-(+)-BINAPO} Li$^+${(±)-**14**$^{\bullet-}$}] displayed an average value of −1.69 MHz.

Yashima, Crassous, and co-workers synthesized the first examples of stereoregular helical acetylenes with [6]helicene units as the pendants by Rh-catalyzed polymerization (Fig. 10.6) [10]. The optically pure polymers **16** displayed the ability to adsorb one enantiomer preferentially of the racemic analytes in solution. As listed in Table 10.1, (*P*)-**16** had selectivity for (*P*)-**15**, (*S*)-**17**, and (*S*)-**18** (up to 37 % ee), while (*M*)-**16** had selectivity for the other enantiomers (up to 26 % ee). The better degree of recognition for the racemic 1,1′-binaphthyl derivatives mainly
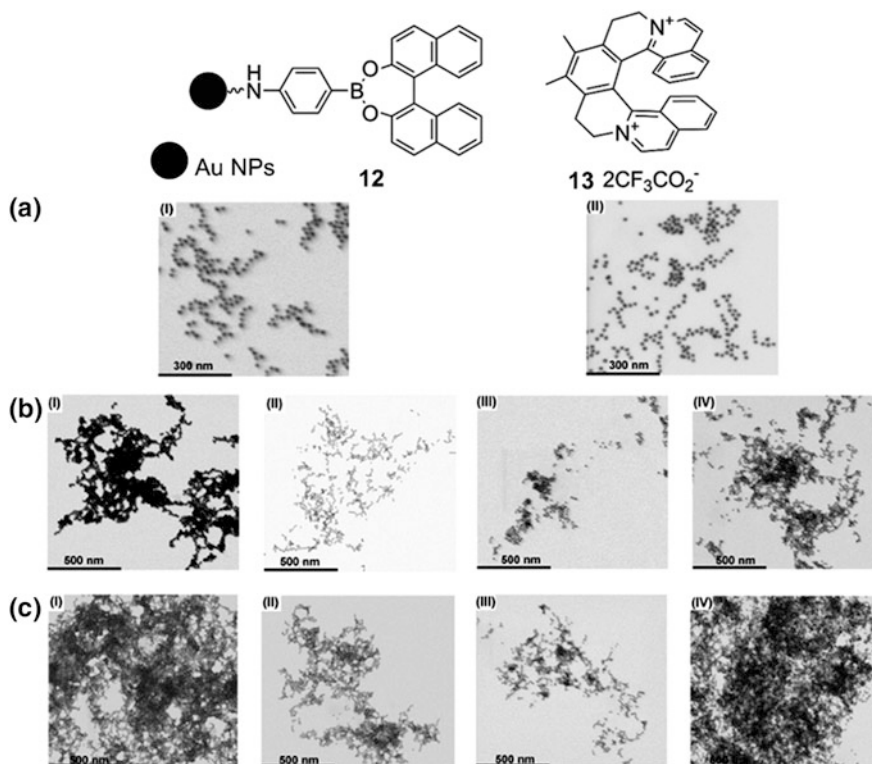
Fig. 10.3 Structures of BINOL-modified Au NPs **12** and Helquat **13**, and the STEM images corresponding to **a** (I) the (S)-**12** and (II) the (R)-**12**. **b** (I) The (S)-**12** treated with (M)-**13** after 10 min of interaction; (II) the (S)-**12** treated with (P)-**13** after 10 min of interaction; (III) the (R)-**12** treated with (M)-**13** after 10 min of interaction; and (IV) the (R)-**12** treated with (P)-**13** after 10 min of interaction. **c** (I) The (S)-**12** treated with (M)-**13** after 100 min of interaction; (II) the (S)-**12** treated with (P)-**13** after 100 min of interaction; (III) the (R)-**12** treated with (M)-**13** after 100 min of interaction; and (IV) the (R)-**12** treated with (P)-**13** after 100 min of interaction. In all systems, the Au NPs **13** ((4.5 $\pm$ 0.5) $\times$ 10^{-9} M) were interacted in triple distilled water with the respective helquats **12** (2 $\times$ 10^{-4} M). Reprinted with the permission from Ref. [8]. Copyright 2012 American Chemical Society

resulted from the helical array formed by the helicene pendants. Moreover, the selectivity factor of **16** for **17** and **18** was high enough for the separation of the enantiomers by using optically pure **16** as chiral stationary phase for HPLC.

Recently, Yamaguchi and co-workers utilized (P)-[4]helicene-modified Si NPs to induce the equilibrium shift of Rh-catalyzed disulfite exchange reaction [11]. In the reaction between (R,R)-**19**, **20**, and (R)-**21**, the chiral recognition between the diol (R,R)-**19** and Si NPs and their precipitation changed the ratio of the components in solution phase (Fig. 10.7a), resulting in the equilibrium shift to produce more **20**, and the (R,R)-**19** was enriched in the precipitate (Fig. 10.7b).
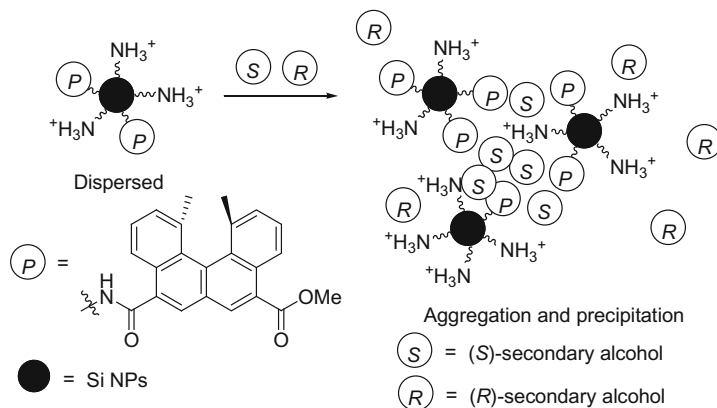
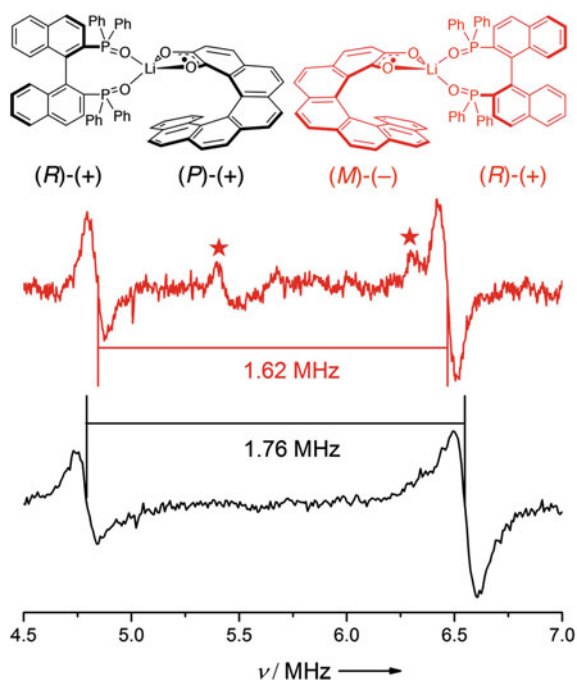**Fig. 10.4** Chiral recognition between Si NPs and secondary alcohols

Fig. 10.5 ENDOR spectra of [{(R)-(+)-BINAPO}Li$^+${(P)-(+)-**14**$^{\bullet-}$}] (*black*) and [{(R)-(+)-BINAPO}Li$^+${(M)-(−)-**14**$^{\bullet-}$}] (*red*) in THF at 210 K. Asterisks showed artifacts arising from strong RF irradiation. Reprinted with the permission from Ref. [9]. Copyright 2014 American Chemical Society
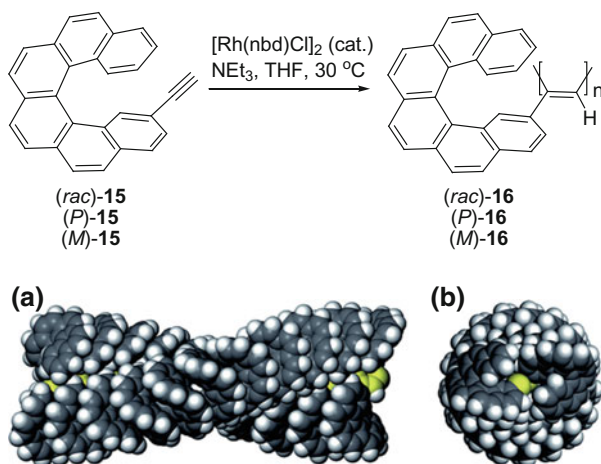
Fig. 10.6 The synthesis of polyacetylenes (*upper*); **a** *side view* and **b** *top view* of a possible structure of **16**. The main-chain atoms were shown in *yellow* for clarity. Reproduced from Ref. [10] with permission from the Royal Society of Chemistry

Table 10.1 Enantioselective adsorption of racemates

Entry	Analyte	Polymer	Yield of adsorption analyte (%)	ee of adsorption analyte (%)
1	**15**	(*P*)-**16**	5.0	3.6 (*P*)
2		(*M*)-**16**	5.0	3.7 (*M*)
3	**17**	(*P*)-**16**	0.64	37 (*S*)
4		(*M*)-**16**	0.66	35 (*R*)
5	**18**	(*P*)-**16**	2.1	26 (*S*)
6		(*M*)-**16**	2.3	29 (*R*)

10.2   Helicenes as Sensors

Katz and colleagues utilized [5]HELOL to sense the remote central chirality [12, 13]. After the diols, **22** and **23**, reacted with PCl$_3$, chlorophosphite was obtained (Scheme 10.1). The following reactions with reagents with a chiral center, like alcohols (Y=O), amines (Y=NH), and carboxylic acids (Y=CO$_2$) would give the relative diastereomeric structures, **24** and **25**. By the interactions between the chiral
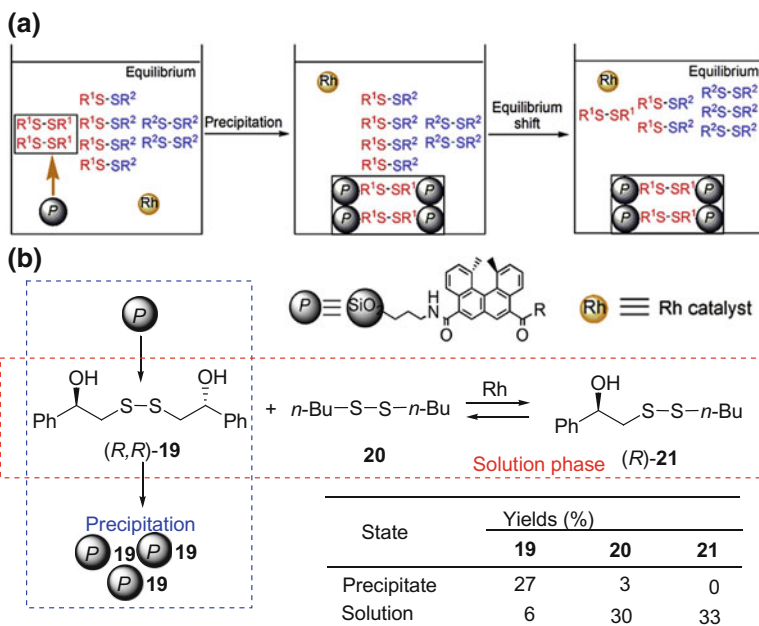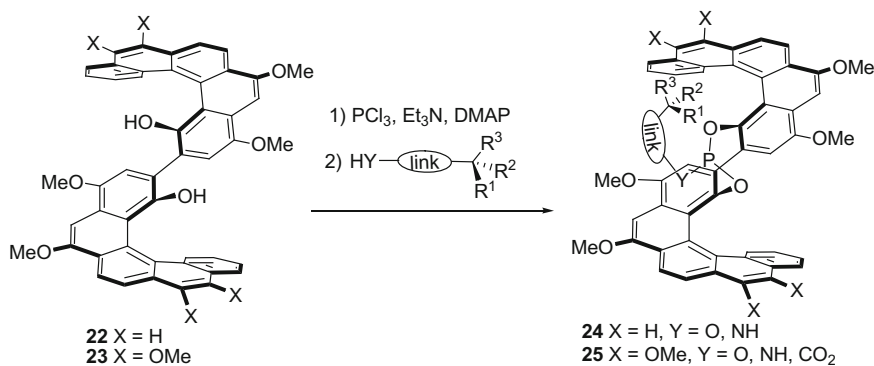
Fig. 10.7 a Schematic presentation of equilibrium shift; **b** equilibrium shift in Rh-catalyzed disulfide exchange reaction. Reprinted with the permission from Ref. [11]. Copyright 2015 Elsevier

Scheme 10.1 Synthesis of chlorophosphites **24–25**

centers and the chiral groove, it generated different ^{31}P NMR spectroscopic signals; the ratio of the integration of respective peaks represented the *ee* values of the reagent added previously. Herein, the helicene-based chlorophosphites performed as excellent chiral derivatizing agents, and even the enantiomeric purity of 8-phenylnonan-1-ol could be analyzed.
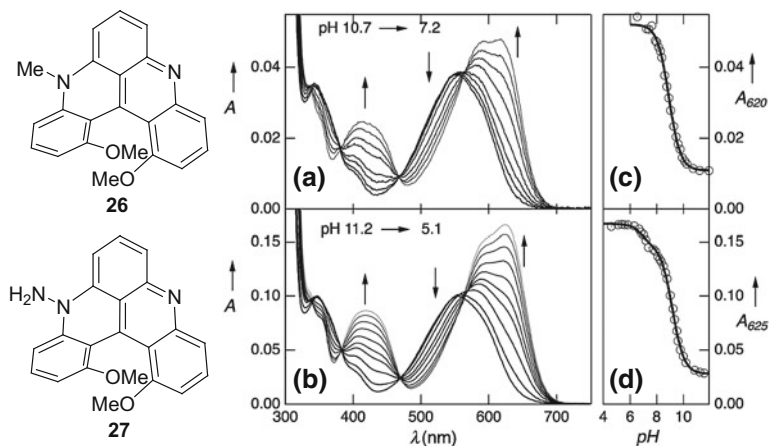
Fig. 10.8 Structures of diaza[4]helicenes (*left*) and electronic absorption spectra and titration curves for **26** (**a** and **c**) and **27** (**b** and **d**) (*right*). Reprinted with the permission from Ref. [15]. Copyright 2014 John Wiley and Sons

Reetz and Sostmann utilized 2,15-dihydroxyl[6]helicene, HELIXOL, as fluorescence sensor for chiral amines and aminoalcohols [14]. By monitoring the quenching of (*M*)-HELIXOL via adding the amine/aminoalcohol in different concentrations, the Stern–Volmer plots could be obtained for each enantiomer. The ratio of slopes, $k_{SV}(R)/k_{SV}(S)$, could be calculated. Since the enantiomeric excess could be linearly correlated with the ratio of slopes, optically pure HELIXOL could be a useful fluorescence sensor for its high degree of recognition.

Lacour, Vauthey, and co-workers prepared a series of diaza[4]helicenes with pyridine and amino moieties, which was proved to pH-sensitive [15]. As the pH change of environment from basic to neutral and acidic, the absorption for **26** at 620 nm and **27** at 625 nm decreased (Fig. 10.8). The titration experiment showed the sensor **27** had a broader window for pH-sensing from 11.2 to 5.1.

A tetrahydro[5]helicene thioimide-based chemodosimeter **28** was developed by Chen, Lu, and co-worker [16]. The fluorescence spectra of **28** with different metal ions were investigated, and significant increase of emission intense was observed with the addition of Hg^{2+} to the solution of **28** in CH_3CN/water (Fig. 10.9). The enhancement was estimated to be 200-fold, and the detection limit of **28** for Hg^{2+} was about 5.0×10^{-7} M.

Storch, Vacek, and co-workers reported a humidity sensor based on [6] helicene-derived imidazolium salt [17]. The crystalline sample was prepared by annealing of the spin-coated film of **29** at 190 °C, which was composed by crystals with a size of hundred microns, and they overlapped and connected with each other with enhanced conductivity than the amorphous sample (annealing spin-coated film at 100 °C). During the study of its I–V curves, the authors discovered that the conductivity was significantly impacted by the air humidity, which renders the crystalline sample a humidity sensor. As Fig. 10.10 states, the film was exposed to
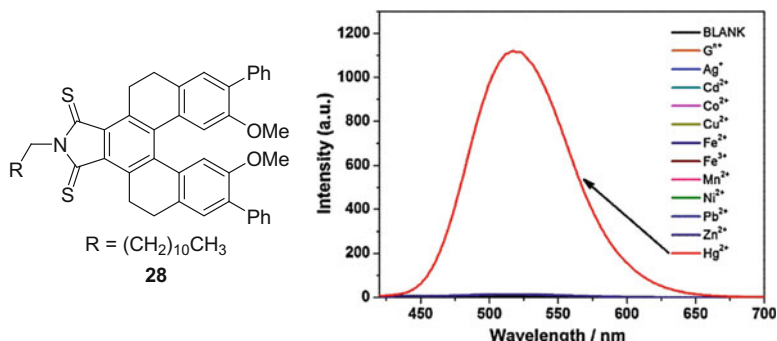
Fig. 10.9 Structure of chemodosimeter (*left*) and fluorescence spectra (*right*) of **28** $(1.0 \times 10^{-5}$ M, CH_3CN/water 19:1, v/v, pH 5.0) with the addition of 20 equiv. of metal ions (G^{n+} = Na^+, K^+, Mg^{2+}, Ca^{2+}). λ_{ex} = 385 nm. Reprinted with the permission from Ref. [16]. Copyright 2014 Elsevier
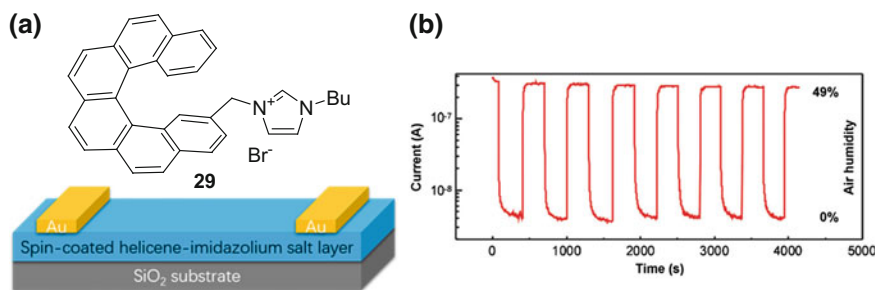

Fig. 10.10   a Structure of helicene-derived imidazolium salt and the configuration of the device; and **b** reversible current dependence on air humidity at the voltage of 28 V and the temperature of 24 °C measured on the thin film prepared by spin-coating. Reprinted with the permission from Ref. [17]. Copyright 2014 John Wiley and Sons

the air humidity of 0 and 49 % under N_2 atmosphere for 300 s for each step, and the current was promoted nearly two orders of magnitude from 0 to 49 % humidity.

A series of fast-responsive explosive sensors was prepared by Chen, Lu, and co-workers, via the polymerization of [5]helicenes with the help of Pd(0)/Ni(0)-mediated cross-coupling reactions [18]. Four nitroaromatics (DNT, TNT, PA, NT) were examined and benzophone (BP) was used as a control (Fig. 10.11). According to the fluorescence spectra of the interaction between the polymer film and analytes, the intense of fluorescence was reduced by 87 and 70 % on the exposure of DNT and TNT in 10 s, respectively (Fig. 10.11a). Moreover, the film showed good reversibility after washing with methanol (Fig. 10.11b).
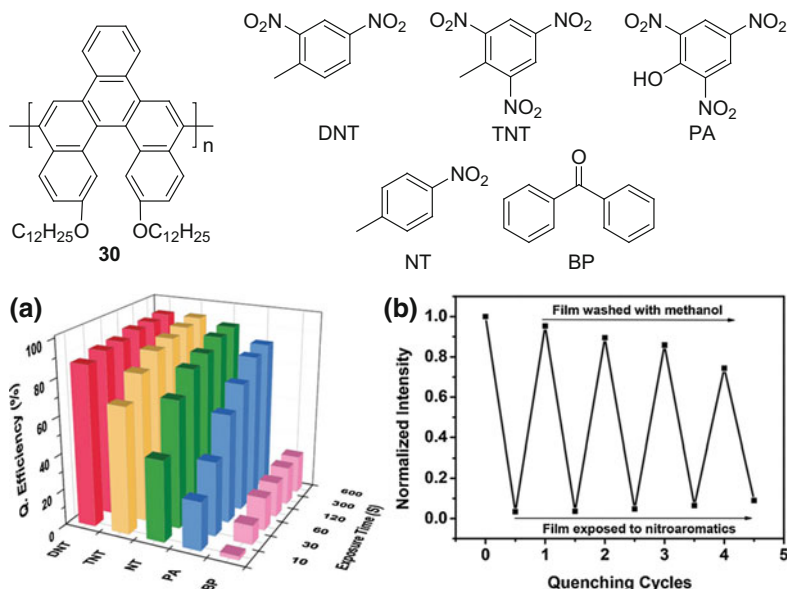
Fig. 10.11 Structure of helicene-based sensor for explosives and analytes (*top*). **a** Fluorescence quenching efficiency of the film prepared by spin casting on exposure towards saturated vapor of different explosives for different times. **b** The reversibility of the film of **30** to DNT. Reprinted with the permission from Ref. [18]. Copyright 2015 Royal Society of Chemistry

10.3   Responsive Switches

10.3.1   pH-Responsive Switches

The first helicene-based Os complex bearing acid-base switching properties was reported by Crassous, Autschbach, and co-workers [19]. By addition of HCl molecule to vinyl-Os complex **31** (red), carbene-Os complex **32** could be obtained as yellow solid. The reversible transformation could be achieved upon exposure to bases, which was demonstrated by ECD and UV-vis spectra. As shown in Fig. 10.12, this system performed as an acid/base-responsive switch that in the presence of HCl, the stretching band of CO, v_{CO}, shifted from 1895 to 1932 cm^{-1}, while Et_3N would reverse the conversion.

The same groups reported another two switches that had OR, CD, and CPL activity [20]. As depicted in Fig. 10.13, for example, the addition of excess of HBF_4 to (*P*)-**33** afforded [(*P*)-**33**·2H +][$2BF_4^-$], with the generation of a new peak near 420 nm and the significant decrease of $\Delta\varepsilon$ around 330 nm. The subsequent deprotonation by Na_2CO_3 reproduced the spectra.

Helicene-like molecules, helquats, incorporated with phenol units was described as pH-responsive chiroptical switch by Teplý group [21]. As shown in Fig. 10.14, the bathochromic shift was observed for both of them, and the maximum of $\Delta(\Delta\varepsilon)$
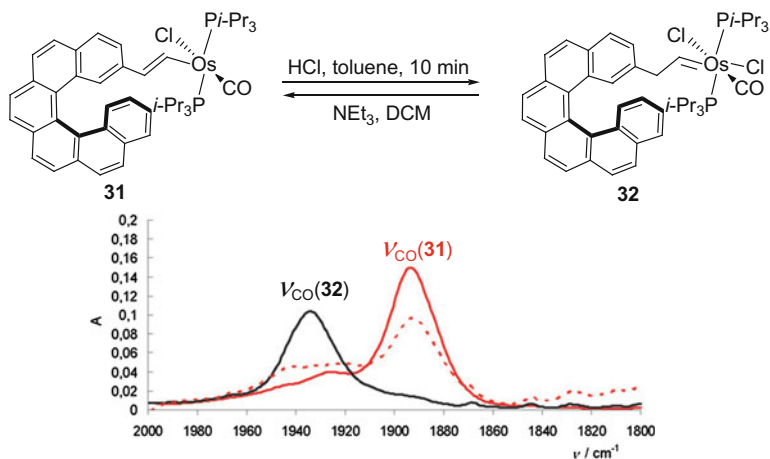
Fig. 10.12 Reversible transformation between vinyl-Os complex **31** and carbene-Os complex **32** (*top*); IR spectra of the transformation (**31**→**32**→**31**) in DCM solution (*bottom*). Reprinted with the permission from Ref. [19]. Copyright 2013 Royal Society of Chemistry
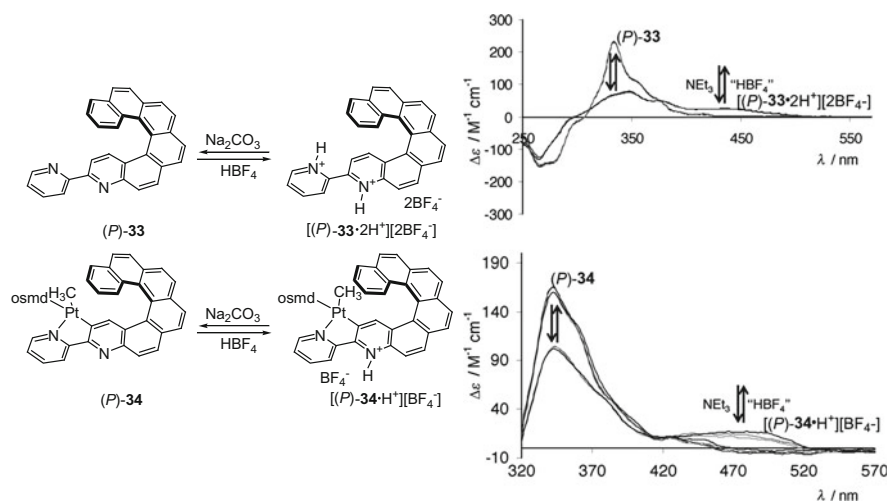

Fig. 10.13 Reversible protonation/deprotonation transformations of pyridyl azahelicene and helicene-Pt complex (*left*) and ECD spectra of the reversible transformation for several runs. Reprinted with the permission from Ref. [20]. Copyright 2014 John Wiley and Sons

for (+)-(*P*)-**35** was calculated to be 100 M^{-1} cm^{-1} at 650 nm. If the reversible transformation was monitored at *ca.* 500 nm, the shift between the positive and negative $\Delta\varepsilon$ values would be observed.
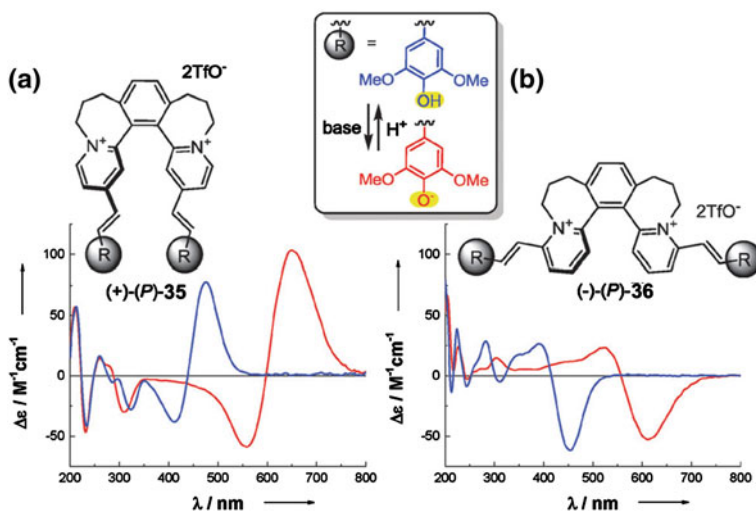
Fig. 10.14 The switching properties of optically pure helquats via protonation (*blue*) and deprotonation (*red*). Reproduced from Ref. [14] with permission from the Royal Society of Chemistry
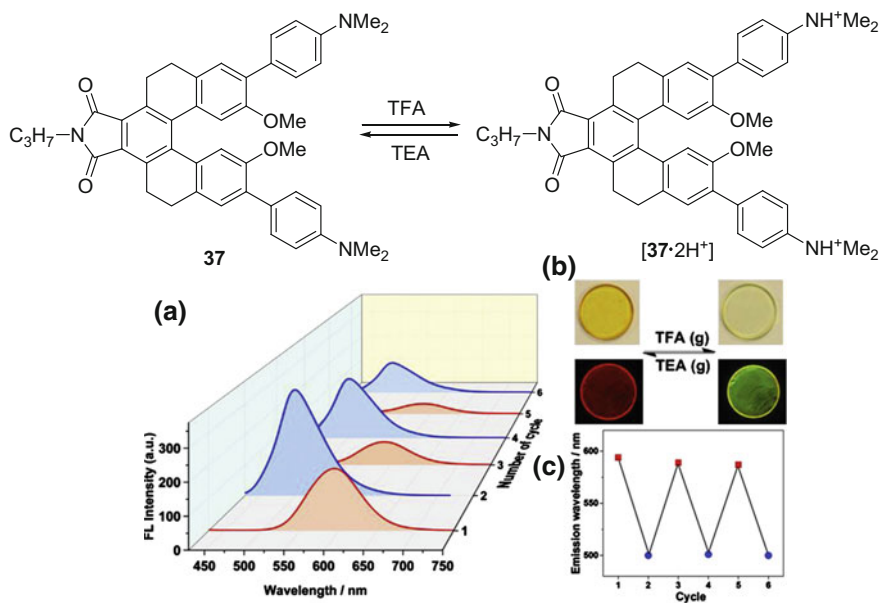
Fig. 10.15 The transformation of protonation and deprotonation (*top*); **a** fluorescence spectra of "ON" (**37**) and "OFF" ([**37**·2H$^+$]) states in different cycles; **b** photos of the film under different states; **c** the max emission wavelength of **37** in different cycles. Reprinted with the permission from Ref. [22]. Copyright 2015 Elsevier

Scheme 10.2   The reversible conversion between helicity (*P*)-**38** and axial chirality (*S*)-**39**

(*P*)-**38**   (*S*)-**39**
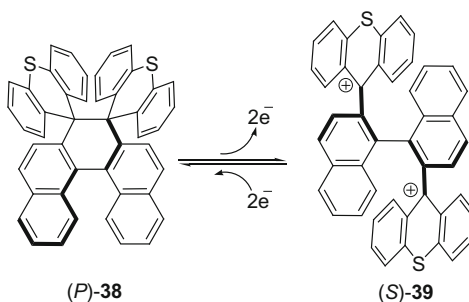
An acid-base-triggered fluorescence switch was described by Chen, Lu, and co-workers [22]. Upon exposure to the vapors of TFA and TEA, tetrahydrohelicene **37** was protonated and deprotonated, respectively. Because the π-conjugated skeleton and the pull-push effect of the functional groups, this reversible reaction could be represented by the change of fluorescence spectra (Fig. 10.15). In "ON" state, λ_{max} was at 594 nm with Φ_f of 7.4 %; while in "OFF" state, λ_{max} was at 500 nm with Φ_f of 16.3 %. The theoretical study suggested that the gap of HOMO-LUMO increased after protonated, because the intramolecular charge transfer was restrained.

10.3.2   Redox-Responsive Switches

Similarly, if electro-active functional groups were connected with helicene core, the oxidized species and the reduced species could be obtained either by chemical reagents or electric field.

The first example of redox switch which showed a dramatic chiroptical response was described by Suzuki and colleagues, utilizing dihydro[5]helicene structure as a core [23]. By electron transfer, the reversible conversion between helicity (*P*)-**38** and axial chirality (*S*)-**39** (Scheme 10.2) with a significant change of structures was reported, the change of which was also observed in CD spectra. By monitoring the modulation at $\lambda = 290$ nm, a switch could be obtained with a $\Delta(\Delta\varepsilon)$ of 140 M^{-1} cm^{-1}.

The first redox-responsive metal-helicene complex switch **40** was reported by Crassous, Réau, Autschbach, and co-workers [24], of which the chiroptical properties were enhanced by the interaction between the vinyl helicene moiety and the metal center [25]. The reversible process was monitored in a transparent thin-layer cell under different voltage in a solution of dichloroethane. As depicted in Fig. 10.16, the switching properties could be monitored at 340 nm, 500 nm, and even 900 nm, at which the redox process displayed a $\Delta(\Delta\varepsilon)$ of −45 M^{-1} cm^{-1} for 340 nm, +17 M^{-1} cm^{-1} for 500 nm, and +8.7 M^{-1} cm^{-1} for 900 nm. Switch **41**, likewise, showed a $\Delta(\Delta\varepsilon)$ of 20 M^{-1} cm^{-1} for 500 nm [25].

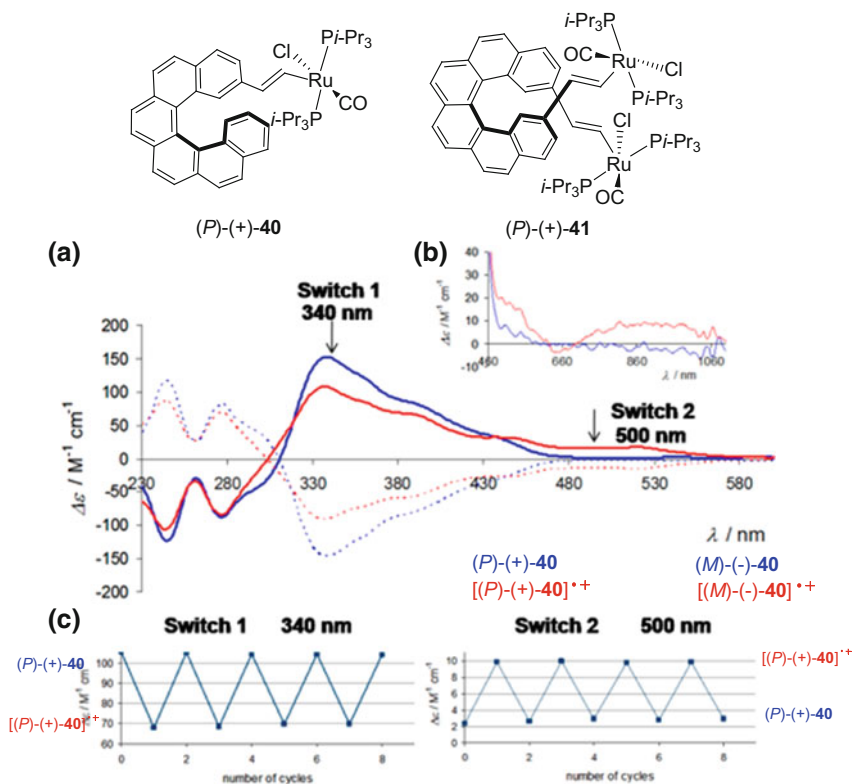**Fig. 10.16** Structures of ruthenium-grafted vinylhelicenes; **a** CD spectra of (*P*)-(+)-**40**, [(*P*)-(+)-**40**]$^{•+}$, (*M*)-(−)-**40**, and [(*M*)-(−)-**40**]$^{•+}$; **b** NIR-CD region of (*P*)-(+)-**40**, [(*P*)-(+)-**40**]$^{•+}$; **c** switching between (*P*)-(+)-**40** and [(*P*)-(+)-**40**]$^{•+}$ monitored by CD spectroscopy at 340 and 500 nm. Reprinted with the permission from Ref. [24]. Copyright 2012 American Chemical Society

Avarvari, Crassous, and co-workers prepared electro-active dithio-tetrathiaful valene-fused [4]- and [6]helicenes, and discovered [6]helicene **42** displayed excellent chiroptical properties [26]. After one-electron-oxidation, [(*P*)-**42**]$^{•+}$ and [(*M*)-**42**]$^{•+}$ showed absorption in the NIR region; and if the modulation between (*M*)-**42** and [(*M*)-**42**]$^{•+}$ was monitored at 306 nm by CD spectroscopy, a switch with a $\Delta(\Delta\varepsilon)$ of 20 mdeg could be obtained (Fig. 10.17).

A dicationic helicene-like helquat displaying intense chiroptical switching properties was reported by Pospíšil, Teplý, and co-workers [27]. The viologen-type electro-active [(*P*)-**43**]$^{2+}$ could be reduced to [(*P*)-**43**]$^{•+}$ by one-electron-reduction and to (*P*)-**43** further with another electron (Fig. 10.18). This transformation was fully reversible via stepwise oxidation. Monitoring by CD and UV-vis spectroscopy, the researchers found that the switch gave intense chiroptical response with the $\Delta(\Delta\varepsilon)$ of 135 M^{-1} cm^{-1}.
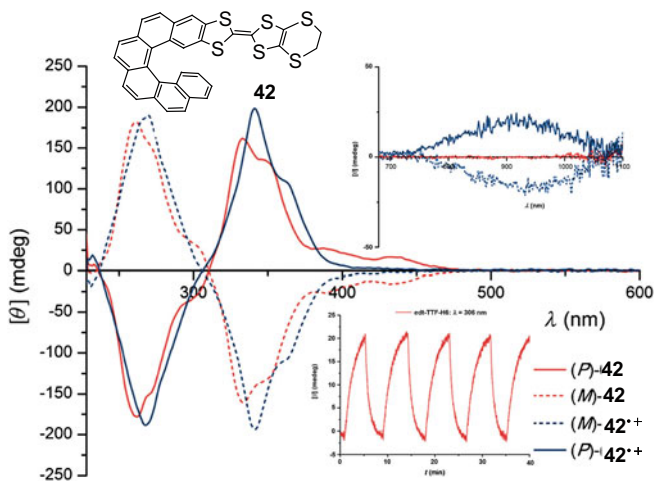
Fig. 10.17 CD spectra of enantiomers of **42** and **42**[•+]. Insects: *top* NIR-CD spectra and *bottom* redox chiroptical switching at 306 nm between (*M*)-**42** and [(*M*)-**42**][•+]. Reprinted with the permission from Ref. [26]. Copyright 2013 John Wiley and Sons
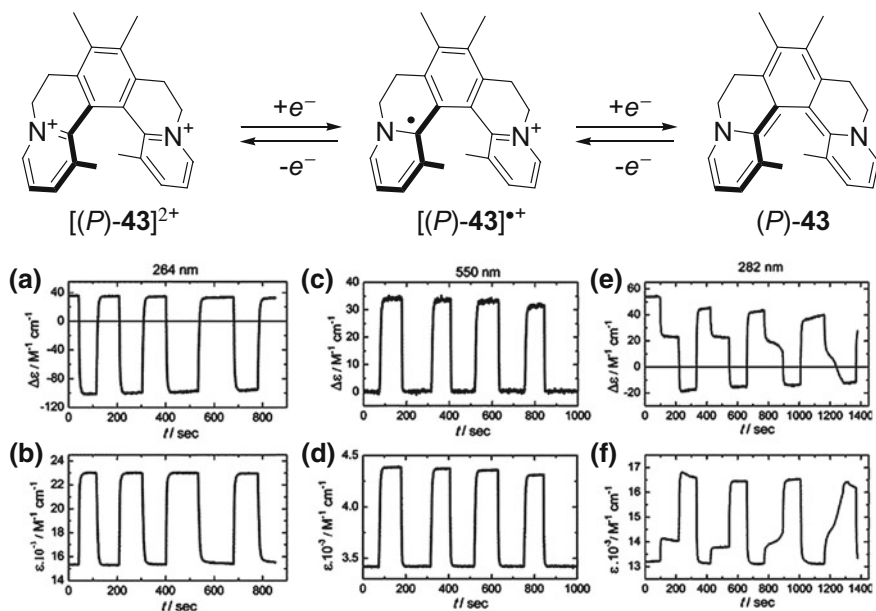

Fig. 10.18 A stepwise oxidation and reduction of **43**; redox switching of CD response: **a**, **c** showed the change for the modulation between [(*P*)-**43**]$^{2+}$↔(*P*)-**43**, and **b**, **d** represented the corresponding changes in UV-vis absorption for [(*P*)-**43**]$^{2+}$↔(*P*)-**43**; **e** showed the CD response for a stepwise process for [(*P*)-**43**]$^{2+}$↔[(*P*)-**43**]$^{•+}$↔(*P*)-**43**, and **f** showed the corresponding changes in UV-vis absorption for [(*P*)-**43**]$^{2+}$↔[(*P*)-**43**]$^{•+}$↔(*P*)-**43**. The selected wavelengths were listed under the structure. Reprinted with the permission from Ref. [27]. Copyright 2014 American Chemical Society
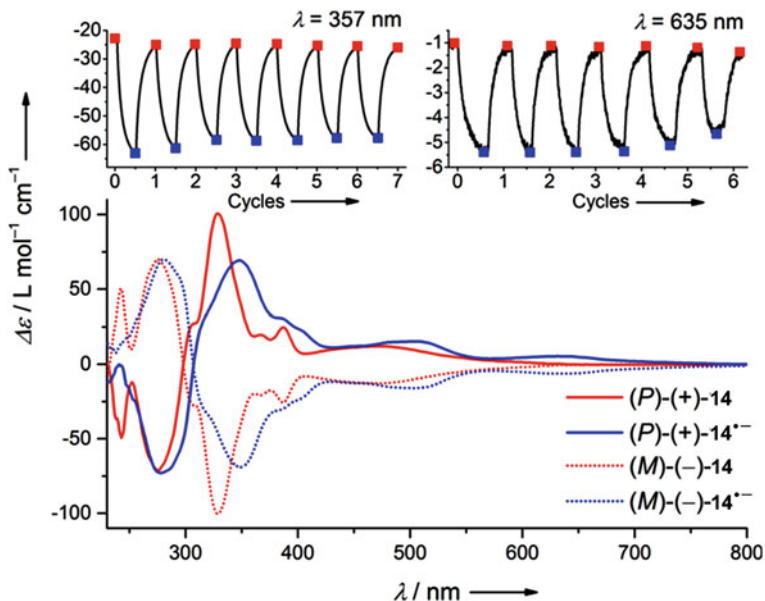
Fig. 10.19 *Top* The chiroptical switching at λ = 357 and 635 nm between the (*M*)-**14** and [(*M*)-**14**]·−; *bottom* CD spectra of enantiomers of **14** and its radical anion. Reprinted with the permission from Ref. [9]. Copyright 2014 American Chemical Society

Fig. 10.20 UV-vis spectra of **44** *red* and **44**·+·SbF₆⁻ *purple*. Reproduced from Ref. [28] with permission from the Royal Society of Chemistry
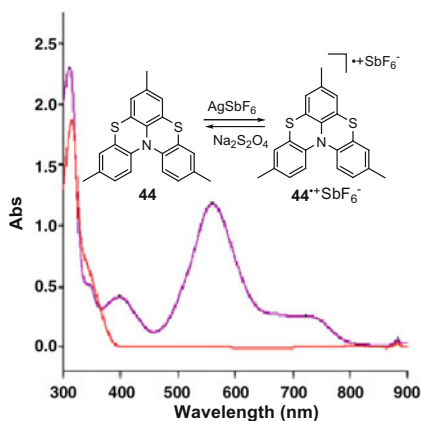

Diederich, Gescheidt, and co-workers reported that the reduction and oxidation of helicene quinone **14** could also be utilized as a chiroptical switch [9] (Fig. 10.19). When the modulation was monitored at 357 nm, $\Delta(\Delta\varepsilon)$ was estimated to be 40 M^{-1} cm^{-1}, while, at visible region, the change of $\Delta\varepsilon$ was found to be *ca.* 4 M^{-1} cm^{-1}.
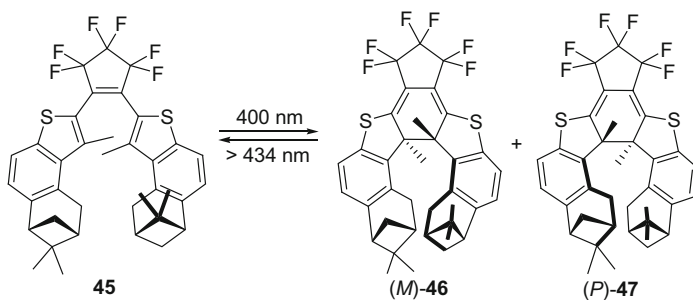
Scheme 10.3 Diastereoselective [2+2+2] electrocyclization of triene **45**

Scheme 10.4 The asymmetric electrocyclization
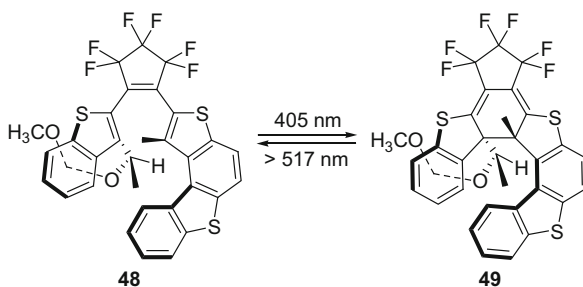
Menichetti, Viglianisi, and co-workers found that azathiahelicenes could be easily oxidized by $AgSbF_6$ quantitatively and recovered by $Na_2S_2O_4$ [28]. Interestingly, $44^{\bullet+} \cdot SbF_6^-$ was exceptionally stable either at room temperature or upon exposure to air for two years. And X-ray analysis of $44^{\bullet+} \cdot SbF_6^-$ showed a decrease for the interplanar angel of terminal rings (from 61.4° to 52.2°), which suggested better accommodating of delocalized spin density. This could also be read from the UV-vis spectra (Fig. 10.20), and by monitoring the modulation, for example, at $\lambda = 560$ nm, a fluorescence-responsive could be obtained.

10.3.3 Photo-Responsive Switches

Based on the [2+2+2] electrocyclization of trienes, Branda group prepared a series of [7]helicene-like compounds, which performed as photo-responsive switches [29–31]. For example, upon exposure to light ($\lambda = 400$ nm), **45** underwent cyclization in a diastereoselective manner, giving (*M*)-**46** as the major product (Scheme 10.3). The chiral groups in the terminal rings induced the selectivity. Such a system could be used as an OR switch, during which the difference of the optical rotation [α] was as large as 8698° [31].

Fig. 10.21 The
photochromic transformation
of **50** (*top*); the absorption
spectra of **50** before (*black*)
and after (*red*) irradiation
(*bottom*). Reprinted with the
permission from Ref. [34].
Copyright 2013 American
Chemical Society
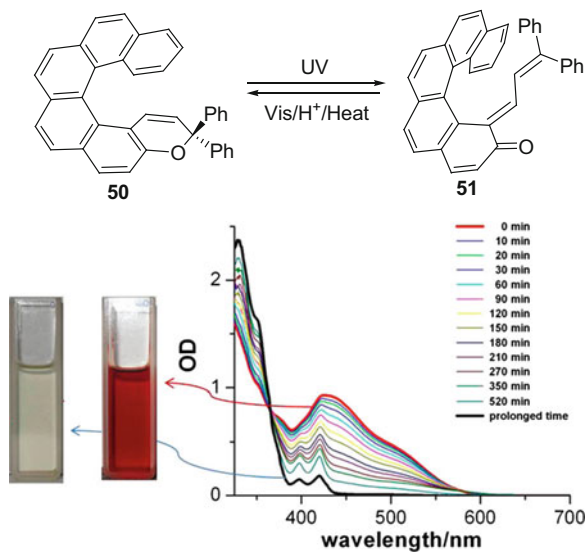
Differently, Yokoyama group utilized an inner central carbon atom to induce the asymmetric electrocyclization [32, 33]. As shown in Scheme 10.4, the reaction gave the (*M*)-**49** with a de of 47 % by irradiation with the light ($\lambda = 405$ nm) in the photostationary state (*PSS*) of 36:64 (**48**:**49**). The retro-electrocyclization was performed under the light of $\lambda > 517$ nm. This molecule was another candidate for OR switcher, because the difference of the optical rotation for the *PSS* and precursor was 1300° [32].

Moorthy group utilized helicity as a steric force and constructed helical chromenes with a half-life of 46 years at room temperature [34]. Take chromene **50** as an example, under irradiation of UV light, the pyran ring was opened to give 1,2-quinone-type [5]helicene **51** via bonds rotation and configuration change (Fig. 10.21). This state could be easily reversed by irradiation of visible light, adding protons, or heat. The whole process of similar *P*-type photochromism was reexamined experimentally and theoretically by Frigoli et al. [35].

References

1. Isla H, Crassous J (2016) Helicene-based chiroptical switches. C R Chim 19(1–2):39–49
2. Nakazaki M, Yamamoto K, Ikeda T, Kitsuki T, Okamoto Y (1983) Synthesis and chiral recognition of novel crown ethers incorporating helicene chiral centres. J Chem Soc, Chem Commun 14:787–788
3. Yamamoto K, Ikeda T, Kitsuki T, Okamoto Y, Chikamatsu H, Nakazaki M (1990) Synthesis and chiral recognition of optically-active crown ethers incorporating a Helicene moiety as the chiral center. J Chem Soc, Perkin Trans 1(2):271–276

4. Owens L, Thilgen C, Diederich F, Knobler CB (1993) A new helicopodand—molecular recognition of dicarboxylic-acids with high diastereoselectivity. Helv Chim Acta 76(8):2757–2774

5. Kano K, Negi S, Takaoka R, Kamo H, Kitae T, Yamaguchi M, Okubo H, Hirama M (1997) Chiral recognition of tetrahelicene dicarboxylic acid by linear dextrins. Chem Lett 8:715–716

6. Kano K, Negi S, Kamo H, Kitae T, Yamaguchi M, Okubo H, Hirama M (1998) Recognition of helicity by native cyclodextrins. Highly enantioselective complexation of tetrahelicene dicarboxylic acid with beta-cyclodextrin. Chem Lett 2:151–152

7. Kano K, Kamo H, Negi S, Kitae T, Takaoka R, Yamaguchi M, Okubo H, Hirama M (1999) Chiral recognition of an anionic tetrahelicene by native cyclodextrins. Enantioselectivity dominated by location of a hydrophilic group of the guest in a cyclodextrin cavity. J Chem Soc, Perkin Trans 2(1):15–21

8. Balogh D, Zhang Z, Cecconello A, Vavra J, Severa L, Teply F, Willner I (2012) Helquat-Induced Chiroselective aggregation of Au NPs. Nano Lett 12(11):5835–5839

9. Schweinfurth D, Zalibera M, Kathan M, Shen C, Mazzolini M, Trapp N, Crassous J, Gescheidt G, Diederich F (2014) Helicene quinones: Redox-Triggered chiroptical switching and chiral recognition of the semiquinone radical anion lithium salt by electron nuclear double resonance spectroscopy. J Am Chem Soc 136(37):13045–13052

10. Anger E, Iida H, Yamaguchi T, Hayashi K, Kumano D, Crassous J, Vanthuyne N, Roussel C, Yashima E (2014) Synthesis and chiral recognition ability of helical polyacetylenes bearing helicene pendants. Polym. Chem 5(17):4909–4914

11. Miyagawa M, Arisawa M, Yamaguchi M (2015) Equilibrium shift induced by chiral nanoparticle precipitation in rhodium-catalyzed disulfide exchange reaction. Tetrahedron 71 (30):4920–4926

12. Weix DJ, Dreher SD, Katz TJ (2000) [5]HELOL phosphite: A helically grooved sensor of remote chirality. J Am Chem Soc 122(41):10027–10032

13. Wang DZG, Katz TJ (2005) A [5]HELOL analogue that senses remote chirality in alcohols, phenols, amines, and carboxylic acids. J Org Chem 70(21):8497–8502

14. Reetz MT, Sostmann S (2001) 2,15-dihydroxy-hexahelicene (HELIXOL): synthesis and use as an enantioselective fluorescent sensor. Tetrahedron 57(13):2515–2520

15. Wallabregue A, Sherin P, Guin J, Besnard C, Vauthey E, Lacour J (2014) Modular synthesis of pH-Sensitive fluorescent Diaza[4]helicenes. Eur J Org Chem 29:6431–6438

16. Li M, Li X-J, Lu H-Y, Chen C-F (2014) Tetrahydro[5]helicene thioimide-based fluorescent and chromogenic chemodosimeter for highly selective and sensitive detection of Hg^{2+}. Sensors and Actuators B: Chem 202:583–587

17. Storch J, Zadny J, Strasak T, Kubala M, Sykora J, Dusek M, Cirkva V, Matejka P, Krbal M, Vacek J (2015) Synthesis and characterization of a Helicene-Based Imidazolium salt and its application in organic molecular electronics. Chem Eur J 21(6):2343–2347

18. Zhou L-L, Li M, Lu H-Y, Chen C-F (2016) Benzo[5]helicene-based conjugated polymers: synthesis, photophysical properties, and application for the detection of nitroaromatic explosives. Polym Chem 7(2):310–318

19. Anger E, Srebro M, Vanthuyne N, Roussel C, Toupet L, Autschbach J, Reau R, Crassous J (2014) Helicene-grafted vinyl- and carbene-osmium complexes: an example of acid-base chiroptical switching. Chem Commun 50(22):2854–2856

20. Saleh N, Moore B, Srebro M, Vanthuyne N, Toupet L, Williams JAG, Roussel C, Deol KK, Muller G, Autschbach J, Crassous J (2015) Acid/Base-triggered switching of circularly polarized luminescence and electronic circular dichroism in organic and organometallic helicenes. Chem Eur J 21(4):1673–1681

21. Reyes-Gutiérrez PE, Jirásek M, Severa L, Novotná P, Koval D, Sázelová P, Vávra J, Meyer A, Císařová I, Šaman D, Pohl R, Štěpánek P, Slavíček P, Coe BJ, Hájek M, Kašička V, Urbanová M, Teplý F (2015) Functional helquats: helical cationic dyes with marked, switchable chiroptical properties in the visible region. Chem Commun 51(9):1583–1586

22. Li M, Niu Y, Lu H-Y, Chen C-F (2015) Tetrahydro[5]helicene-based dye with remarkable and reversible acid/base stimulated fluorescence switching properties in solution and solid state. Dyes Pigm 120:184–189
23. Nishida J, Suzuki T, Ohkita M, Tsuji T (2001) A redox switch based on dihydro[5]helicene: Drastic chiroptical response induced by reversible C-C bond making/breaking upon electron transfer. Angew Chem Int Ed 40(17):3251–3354
24. Anger E, Srebro M, Vanthuyne N, Toupet L, Rigaut S, Roussel C, Autschbach J, Crassous J, Réau R (2012) Ruthenium-Vinylhelicenes: remote metal-based enhancement and redox switching of the chiroptical properties of a helicene core. J Am Chem Soc 134(38):15628–15631
25. Srebro M, Anger E, Moore Ii B, Vanthuyne N, Roussel C, Réau R, Autschbach J, Crassous J (2015) Ruthenium-Grafted Vinylhelicenes: Chiroptical properties and redox switching. Chem Eur J 21(47):17100–17115
26. Biet T, Fihey A, Cauchy T, Vanthuyne N, Roussel C, Crassous J, Avarvari N (2013) Ethylenedithio-Tetrathiafulvalene-Helicenes: electroactive helical precursors with switchable chiroptical properties. Chem Eur J 19(39):13160–13167
27. Pospíšil L, Bednárová L, Štěpánek P, Slavíček P, Vávra J, Hromadová M, Dlouhá H, Tarábek J, Teplý F (2014) Intense chiroptical switching in a dicationic helicene-like derivative: exploration of a viologen-type redox manifold of a non-racemic helquat. J Am Chem Soc 136 (31):10826–10829
28. Menichetti S, Cecchi S, Procacci P, Innocenti M, Becucci L, Franco L, Viglianisi C (2015) Thia-bridged triarylamine heterohelicene radical cations as redox-driven molecular switches. Chem Commun (Camb) 51(57):11452–11454
29. Murguly E, McDonald R, Branda NR (2000) Chiral discrimination in hydrogen-bonded [7] helicenes. Org Lett 2(20):3169–3172
30. Norsten TB, Peters A, McDonald R, Wang MT, Branda NR (2001) Reversible [7]-thiahelicene formation using a 1,2-dithienylcyclopentene photochrome. J Am Chem Soc 123(30):7447–7448
31. Wigglesworth TJ, Sud D, Norsten TB, Lekhi VS, Branda NR (2005) Chiral discrimination in photochromic helicenes. J Am Chem Soc 127(20):7272–7273
32. Okuyama T, Tani Y, Miyake K, Yokoyama Y (2007) Chiral helicenoid diarylethene with large change in specific optical rotation by photochromism. J Org Chem 72(5):1634–1638
33. Tani Y, Ubukata T, Yokoyama Y, Yokoyama Y (2007) Chiral helicenoid diarylethene with highly diastereoselective photocyclization. J Org Chem 72(5):1639–1644
34. Moorthy JN, Mandal S, Mukhopadhyay A, Samanta S (2013) Helicity as a steric force: stabilization and helicity-dependent reversion of colored *o*-Quinonoid intermediates of helical chromenes. J Am Chem Soc 135(18):6872–6884
35. Frigoli M, Marrot J, Gentili PL, Jacquemin D, Vagnini M, Pannacci D, Ortica F (2015) *P*-Type photochromism of new helical naphthopyrans: synthesis and photochemical, photophysical and theoretical study. Chem Phys Chem 16(11):2447–2458

Chapter 11
Helicenes in Biochemistry

Abstract In this chapter, the applications of helicenes in biochemistry including their interactions with biomolecules and cell imaging are summarized. It was found that the helicene amine shows the chiral recognition toward DNA/nucleosides. Studies on the selective binding of helicenes to Z-DNA and B-DNA suggested that the amino groups on helicene skeletons are essential for the interaction with Z-DNA. The interactions between *N*-methyl-5-aza[5]helicenium salts and DNA show marked counterion effects. Effective inhibition of telomerase by small molecules bridged helicenes indicates that appropriate interplanar angle and helicity are of great importance. Moreover, the investigation on the interactions between spermine-functionalized optically pure [5]helicene and B-, and Z-DNA indicates that (*P*)-isomer shows a strong affinity to B-DNA, while (*M*)-isomer displays preference to Z-DNA. Because of the π-conjugated helical structures, helicenes can also be applied to cell imaging. Thus, a series of tetrahydrohelicene nanoparticles for fluorescence cell imaging show interesting structure-dependent distribution, which provides a new perspective for the design of fluorescence probes. In addition, thiahelicene labeled by rhodamine probe can also visualize the loaded nanoparticles in cell.

Keywords Biochemistry · Cell imaging · Chiral recognition · Counterion effect · Helicenes · Nanoparticle · Telomerase · Structure-dependent distribution · Z-DNA and B-DNA

In last chapter, we discussed the interactions between the small molecules and the responses under the environmental stimulus. Herein, the applications in biochemistry would be summarized, including the interaction with biomolecules and cell imaging.

In 2001, Yamada group discovered that the incorporation of 2-hydroxymethyl-3, 6,9-trithia-[5]helicene to the chiral bilayered phosphatidylcholine (PC) vesicle renders helicene as a probe [1], which displayed corresponding Cotton effects and intensity in the CD spectra [2].

One year later, the chiral recognition between the helicene amine **1** and DNA/nucleosides was first disclosed by Yamaguchi and co-workers [3]. By the study of isothermal titration calorimetry, fluorescence titration, ^{1}H NMR titration experiment, it was demonstrated that (*P*)-**1** had bigger associate constants with calf thymus DNA, deoxyribonucleosides, and ribonucleosides than that of (*M*)-**1** (Fig. 11.1).

The effect of functionalities on the helicene skeletons was examined by Sugiyama group [4]. When they were added to solution of Z-DNA or B-DNA, helicene **2** was found to have the selectivity binding with Z-DNA and convert B-DNA into Z-DNA (Fig. 11.2). The associate constant for (*P*)-**2** was five times larger than that for (*M*)-**2**. In comparison, helicene **3** did not exhibit any selectivity, which suggested that the amino groups were essential for the interaction with Z-DNA.

In addition, Latterini and co-workers investigated the counterion effects on the interactions between *N*-methyl-5-aza[5]helicenium salts and DNA [5]. According to their analysis, **4a** and **4c** was found to preferentially form intercalation complexes with DNA, with the constant K_a of 1.9×10^5 M^{-1} and 2.4×10^5 M^{-1}, respectively. While **4b**, with an occupation number of 2.5, interacted with DNA to form intercalation and grove binding complex with a constant of 0.9×10^5 M^{-1}. The AFM images of plasmid DNA and plasmid DNA-**4b** complex were shown in Fig. 11.3.

In 2010, Sugiyama group reported the first example of telomerase inhibition by small molecules—bridged helicenes [6]. Three thiahelicenophanes were examined, in which the terminal rings were connected by thioether linkers (Fig. 11.4). The different lengths of linkers afforded chiral wedges with different interplanar angles, 22° for **5a**, 53° for **5b**, and 58° for **5c**. Two G-quadruplex dimers, ODN1 [AGGG-(TTAGGG)$_3$-TTAGGG-(TTAGGG)$_3$] and ODN2 [AGGG-(TTAGGG)$_3$-(TTA) 6GGG-(TTAGGG)$_3$], were used as substrates. The former was separated by one TTA unit, while for the later, as a control, the linker was composed by six TTA
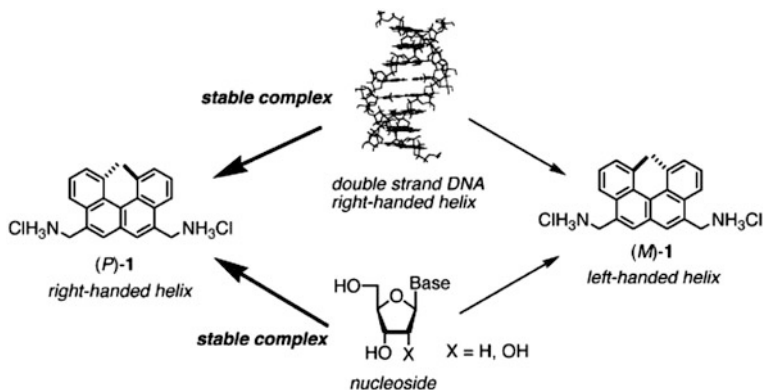
Fig. 11.1 Interaction of helicene amine with DNA and nucleosides. Reprinted with the permission from Ref. [3]. Copyright 2002 Elsevier
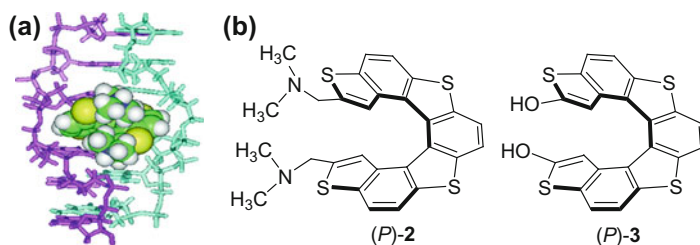
Fig. 11.2 a Schematic representation of Z-DNA with (*P*)-**2**; **b** structures of different functionalized thiahelicenes. Reprinted with the permission from Ref. [4]. Copyright 2004 American Chemical Society
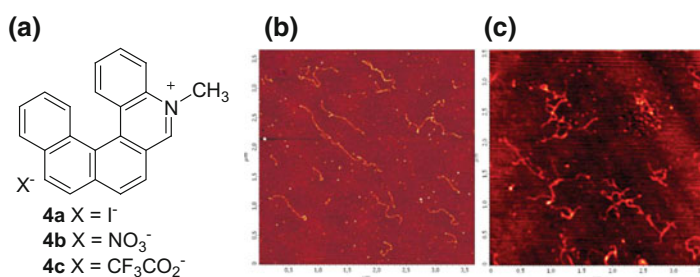
Fig. 11.3 a The structure of helicenium cation with different anions; AFM images for **b** plasmid DNA, and **c** plasmid DNA with **4b**. Reprinted with the permission from Ref. [5]. Copyright 2009 Royal Society of Chemistry
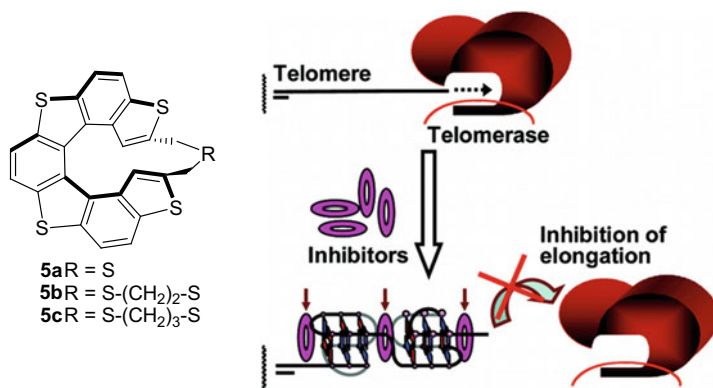
Fig. 11.4 Telomerase inhibition by bridged helicenes. Reprinted with the permission from Ref. [6]. Copyright 2010 American Chemical Society

units. The results proved that only (*M*)-**5a** was found to be an effective inhibitor for telomerase, which indicated that appropriate interplanar angle and helicity were of great importance for this.

Sasaki and co-workers utilized spermine-functionalized optically pure [5]helicene to investigate the interactions between helicene and B-, and Z-DNA [7]. (*P*)-**6** showed a strong affinity to B-DNA, while (*M*)-**6** displayed preference to Z-DNA. By isothermal calorimeter measurements, the binding constants, K_a, were determined to be $6.7 \times 10^6 \, M^{-1}$ [(*P*)-**6**/Z-DNA], $1.7 \times 10^6 \, M^{-1}$ [(*M*)-**6**/Z-DNA], $3.67 \times 10^8 \, M^{-1}$ [(*P*)-**6**/B-DNA], and $8.3 \times 10^5 \, M^{-1}$ [(*M*)-**6**/B-DNA], respectively. The proposed interaction mode was depicted in Fig. 11.5: the spermine moiety bound with the phosphate backbone of the minor groove via electrostatic interactions, while the helicene skeletons interacted with DNA by end-stacking.

Because of the π-conjugated helical structures, helicenes could also be applicable in cell imaging. Latterini group used their helicenium salts to label the cell interior by a green color [8]. As Fig. 11.6 showed, **4b** gradually came into the cell and finally enriched at the nuclear region in 1 h. The distribution did not change with prolonged uptake. The molecule in the green region was in monomeric form, whereas the emission of aggregates in longer wavelength could be observed in cytoplasm.

Lu, Wang, Chen, and co-workers reported a series of tetrahydrohelicene nanoparticles for fluorescence cell imaging [9]. As listed in Fig. 11.7, by
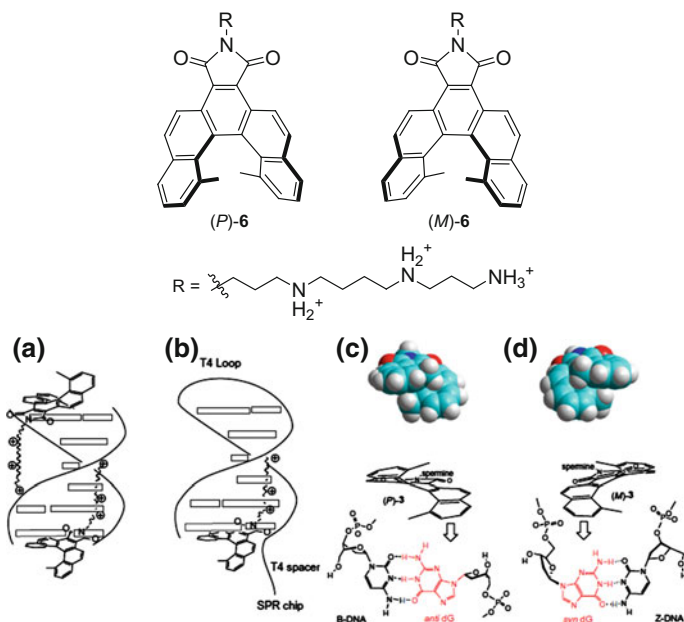
Fig. 11.5 Structures of spermine-functionalized [5]helicene; **a** end-stacking mode with B-DNA; **b** T4-loop and T4-spacer inhibit end-stacking; **c** (*P*)-**6** interacting with a dG of B-DNA in *anti*-conformation; **d** (*M*)-**6** binding to a dG of Z-DNA in *syn*-conformation. Reprinted with the permission from Ref. [7]. Copyright 2013 Elsevier
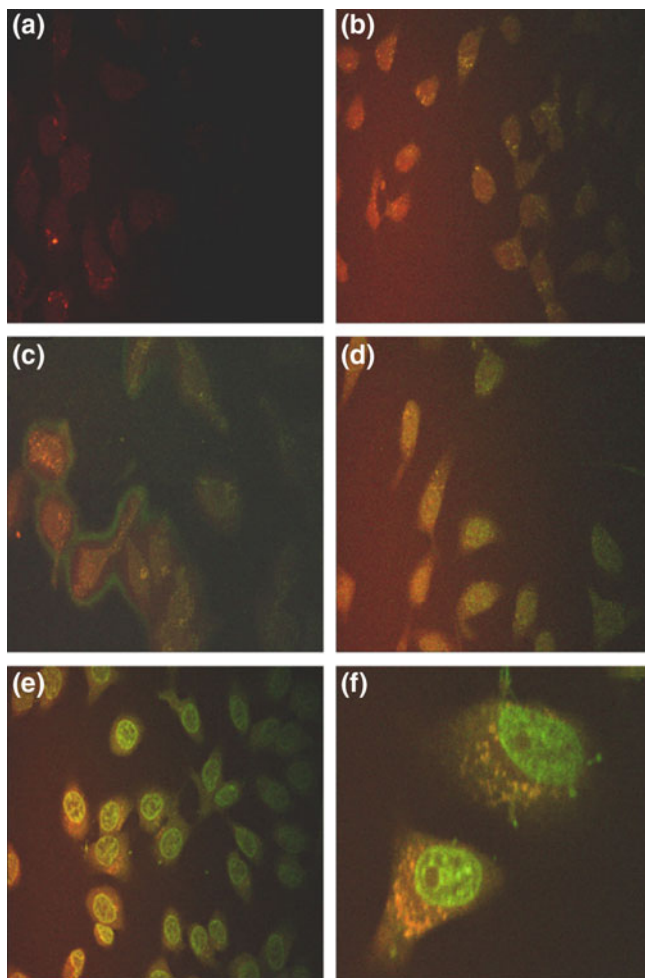
Fig. 11.6 Confocal fluorescence images of Hude-cells (**a**, control) incubated with **4b** for **b** 1, **c** 5, **d** 20, and **e** 60 min. Reprinted with the permission from Ref. [8]. Copyright 2011 Elsevier

incorporation of different functionalities, dye nanoparticles (DNP) could be obtained by precipitation with low cytotoxicity, of which the emission bands were in red (**7**), green (**8**), cyan (**9**), and blue (**10**). Furthermore, the dyes with emission band in orange-yellow (**7/8**) and covering 400–700 nm (**7/8/10**) were easily prepared. Interestingly, according to the fluorescence images, the distribution of the DNP was structure-dependent, which provided a new perspective for the design of the fluorescence probes.

Cauteruccio, Chiellini, and co-workers investigated the cell delivery of thiahelicene, which was loaded in a nanostructured poly(lactic-co-glycolic acid), PLGA, system [10]. The helicene was labeled by rhodamine probe to visualize the loaded
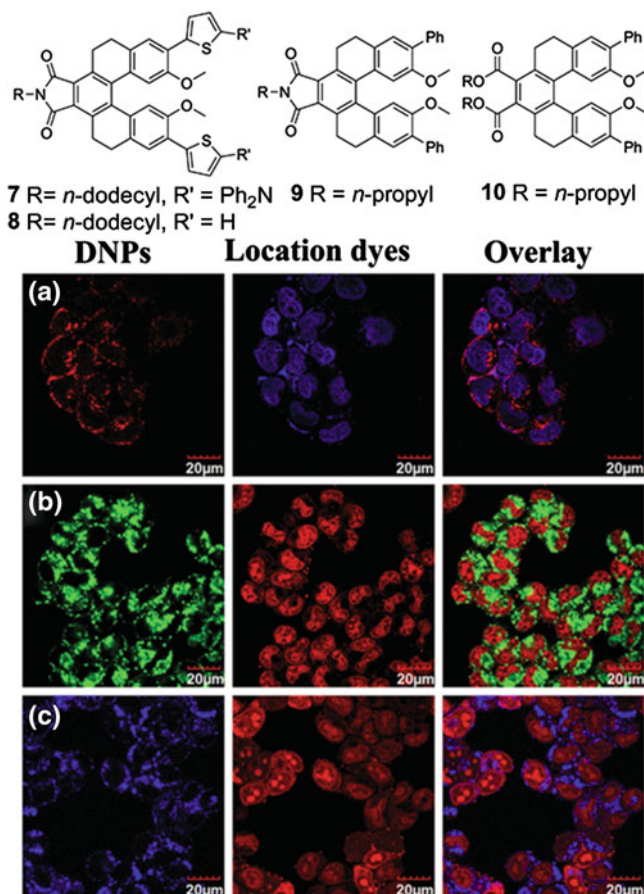
Fig. 11.7 Confocal fluorescence images of Hela cell with tetrahydrohelicenes: **a** DNP of **7** (the corresponding located dye, hochest 33342), **b** DNP of **9** (the corresponding located dye, propdium iodide), and **c** DNP of **10** (the corresponding located dye, propdium iodide). Reprinted with the permission from Ref. [9]. Copyright 2014 John Wiley and Sons

nanoparticles (NPs) in cell, prepared by nanoprecipitation technique. As shown in Fig. 11.8, the confocal laser scanning microscopy (CLSM) images suggested that the **11**-NPs were delivered into the cell and had low cytotoxicity. By preincubating the cells with clathrinmediated endocytosis-chlorpromazine, caveolae-mediated endocytosis-filipin, and macropinocytosis-amiloride, followed by the uptake of **11**-NPs, it was proved that the **11**-NPs were delivered by constitutive macropinocytosis.

In addition, the cytotoxicity of dipyridium dihydro[4]helicenes were examined by Santoro et al. [11]. These types of compounds, with moderate to good cyto-toxicity, displayed high quantum yields as high as 60 % in the visible light region (Fig. 11.9).
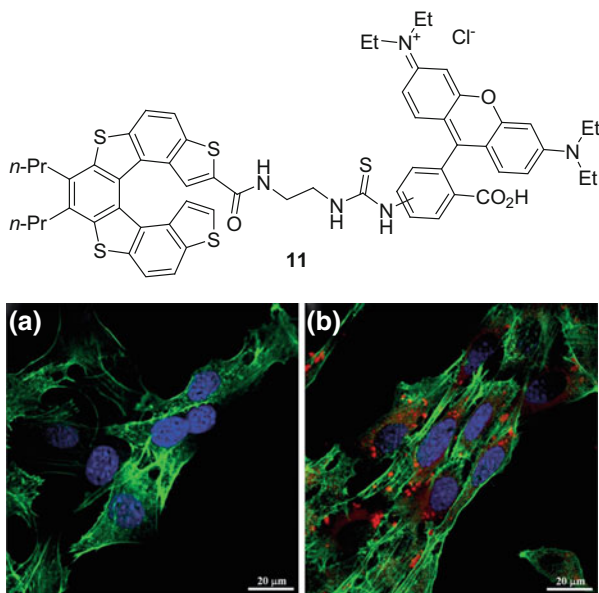
Fig. 11.8 CLSM images of Balb/3T3 clone A31 cells that were **a** untreated, **b** treated with **11**-NPs. Reprinted with the permission from Ref. [10]. Copyright 2014 John Wiley and Sons

Compounds	12a	12b	13	14	cisplatin
IC$_{50}$ (μM)	107 ± 3	110 ± 2	64 ± 1	44 ± 1	3.6 ± 2

* against HT-29 cancer cells
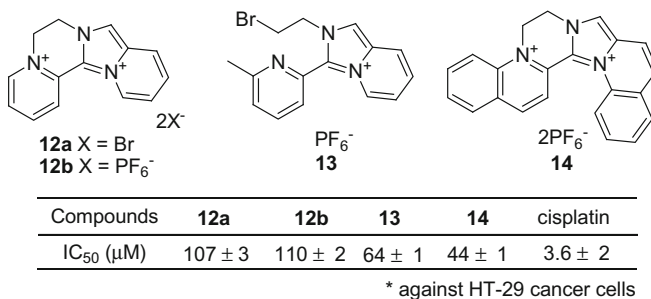
Fig. 11.9 Cytotoxicity data for the dipyridium dihydrohelicenes

References

1. Nakagawa H, Kobori Y, Yoshida M, K-i Yamada (2001) Chiral recognition by single bilayered phosphatidylcholine vesicles using [5]thiaheterohelicene as a probe. Chem Commun (Camb) 24:2692–2693
2. Nakagawa H, Yoshida M, Kobori Y, Yamada KI (2003) Study of chiral recognition of bilayered phosphatidylcholine vesicles using a helicene probe: characteristic function of cholesterol. Chirality 15(8):703–708

3. Honzawa S, Okubo H, Anzai S, Yamaguchi M, Tsumoto K, Kumagai I (2002) Chiral recognition in the binding of helicenediamine to double strand DNA: interactions between low molecular weight helical compounds and a helical polymer. Bioorg Med Chem 10 (10):3213–3218

4. Xu Y, Zhang YX, Sugiyama H, Umano T, Osuga H, Tanaka K (2004) (P)-helicene displays chiral selection in binding to Z-DNA. J Am Chem Soc 126(21):6566–6567

5. Passeri R, Aloisi GG, Elisei F, Latterini L, Caronna T, Fontana F, Sora IN (2009) Photophysical properties of N-alkylated azahelicene derivatives as DNA intercalators: counterion effects. Photochem Photobiol Sci 8(11):1574–1582

6. Shinohara K, Sannohe Y, Kaieda S, Tanaka K, Osuga H, Tahara H, Xu Y, Kawase T, Bando T, Sugiyama H (2010) A chiral wedge molecule inhibits telomerase activity. J Am Chem Soc 132(11):3778–3782

7. Tsuji G, Kawakami K, Sasaki S (2013) Enantioselective binding of chiral 1,14-dimethyl[5] helicene–spermine ligands with B- and Z-DNA. Bioorg Med Chem 21(19):6063–6068

8. Latterini L, Galletti E, Passeri R, Barbafina A, Urbanelli L, Emiliani C, Elisei F, Fontana F, Mele A, Caronna T (2011) Fluorescence properties of aza-helicenium derivatives for cell imaging. J Photochem Photobio A: Chem 222(2–3):307–313

9. Li M, Feng L-H, Lu H-Y, Wang S, Chen C-F (2014) Tetrahydro[5]helicene-based nanoparticles for structure-dependent cell fluorescent imaging. Adv Funct Mater 24 (28):4405–4412

10. Cauteruccio S, Bartoli C, Carrara C, Dova D, Errico C, Ciampi G, Dinucci D, Licandro E, Chiellini F (2015) A nanostructured PLGA system for cell delivery of a tetrathiahelicene as a model for helical DNA intercalators. ChemPlusChem 80(3):490–493

11. Santoro A, Lord RM, Loughrey JJ, McGowan PC, Halcrow MA, Henwood AF, Thomson C, Zysman-Colman E (2015) One-Pot synthesis of highly emissive dipyridinium dihydrohelicenes. Chem Eur J 21(19):7035–7038

Chapter 12
Circularly Polarized Luminescence and Organic Electronics

Abstract Circularly polarized luminescence (CPL) represents the differential emission of left- and right-handed circularly polarized light, which gives information of the excited states of the chiral systems. Because of the combination of specific helical chirality and polycyclic aromatic hydrocarbons (PAH), most helicenes show CPL properties. And supramolecular structures self-assembled by helicenes give relatively higher g_{lum} values than single helicenes. Due to the good thermal and chemical stability, strong intensity and good quantum yields of fluorescence or phosphorescence, helicenes with π-conjugated skeletons are also good candidates for organic electronics. Especially, it was found that helicenes, aza [6]helicene and boron-embedded [4]helicenes can be used as emitting materials in organic light emitting diodes, while thiahelicenes, azaborahelicene, and highly contorted PAH bearing four [4]helicene and two [5]helicene units can be applied in organic field-effect transistor devices. In addition, some helicenes are also utilized in the organic photovoltaic devices, optical waveguides, and organic spintronic devices.

Keywords Circularly polarized luminescence · Organic electronics · Organic field-effect transistor · Organic light emitting diode · Organic photovoltaics · Organic spintronics · Optical waveguides

12.1 Circularly Polarized Luminescence

Circular dichroism (CD) has been extensively utilized to investigate the ground states of chiral systems, including single molecules, supramolecular assemblies, polymers, which measures the differential absorption of left- and right-handed circularly polarized light. However, circularly polarized luminescence (CPL) measures the differential emission of left- and right-handed circularly polarized light, such as fluorescence and phosphorescence, which gives information of the excited states of the chiral systems [1, 2].

The dissymmetric extent of emission was quantified by dissymmetric factor, g_{lum}, which was given by

$$g_{lum} = \frac{2 \times (I_L - I_R)}{(I_L + I_R)},$$
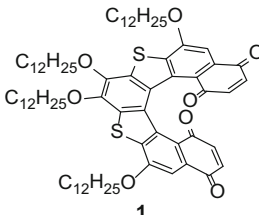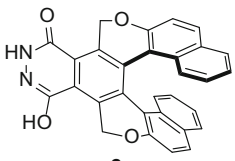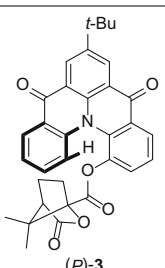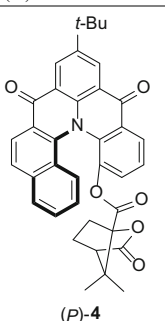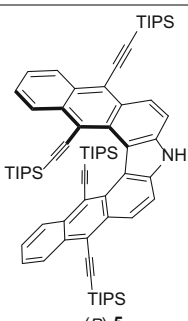
where I_L and I_R are the intensities of the circularly polarized emission or the corresponding quantum yields. The value of g_{lum} is within the range from −2 to +2, in which 0 stands for the unpolarized emission, while +2(−2) means purely left-handed (right-handed) polarized emission.

Generally, the molecules that displayed high activity of CPL based on magnetic dipole-allowed and electronic dipole-forbidden transitions. For example, lanthanide complexes usually exhibit excellent activities (0.05–0.5) than others by the virtue of favorable transitions. The largest g_{lum} was observed as +1.38 (λ = 595 nm) by Muller group, when cesium tetrakis(3-heptafluoro-butylryl-(+)-camphorato) Eu(III) complexes in CHCl$_3$ was excited [3]. In contrast, single organic molecules show lower activity (10^{-4}–10^{-2}) due to the unfavorable transitions, among which helicenes are good candidates for the application in CPL (good quantum yields, structure variation). The chiral polymers and supramolecular assemblies usually showed higher g_{lum} values than single organic molecules (10^{-3}–10^{-1}).

The CPL properties of selected helicenes are listed in Table 12.1. Helicenes self-assembled to give supramolecular structures by π-π stacking (Entry 1) [4] or hydrogen bonds (Entry 2) [5], the assemblies gave relatively higher g_{lum} values than single helicenes. For example, (M)-**2** showed g_{lum} value of −0.021 in dispersed state and −0.035 for the assembly state. Entries 3–22 showed enantioenriched helicene molecules, while the metal-helicene complexes were summarized in Entries 23–36. According to the experimental results, (P)-helicenes generally emitted left-handed circularly polarized light, giving the positive g_{lum} values, whereas (M)-helicenes, with negative values, yielded right-handed circularly polarized light.
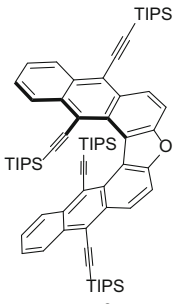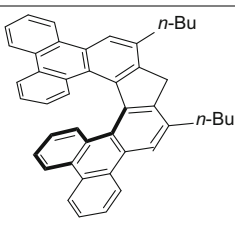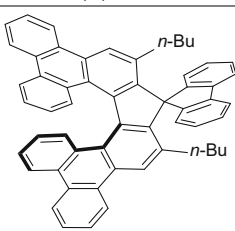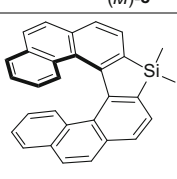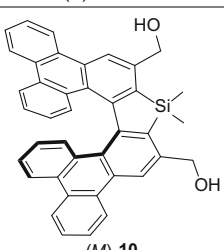
Venkataraman and colleagues prepared azahelicenes, **3** and **4**, and the diastereomers were successfully resolved. [4]Helicene displayed similar activity as [5]helicene with g_{lum} of *ca.* 0.001 [6]. Shinokubo, Hiroto, and co-workers utilized oxidative coupling of 2-aminoanthracene and 2-hydroxyanthracene to construct aza [5]helicene **5** [7] and oxa[5]helicene **6** [8]. The optical resolution was achieved by HPLC, and the dissymmetric factor was observed to be 0.003 and 0.0012, respectively. In addition, Tanaka and colleagues utilized asymmetric Rh-catalyzed [2+2+2] and synthesized (M)-**7** and (M)-**8** in 70–71 % yields and 91–93 % ee [9]. These compounds with triphenylene units displayed very high quantum yields (32 and 29.6 %) and g_{lum} values (−0.030 for (M)-**7** and −0.032 for (M)-**8**). Moreover, sila[7]helicenes have also been investigated. In comparison, dibenzosila[7]helicene (M)-**10** [10] with two triphenylene units showed larger g_{lum} value than sila[7] helicene (P)-**9** [11]. Enantioselective Au-mediated synthesis of helicenes was prepared by Tanaka group, and it was found that the S-shaped amide (P,P)-**13** exhibited a g_{lum} value of +0.028, whereas S-shaped azahelicene (M,M)-**14** displayed a weaker activity of −0.011 [12]. However, the relative [6]helicene (P)-**11**

Table 12.1 CPL properties of helicene-based molecules

Entry	Molecule	ϕ (%)	Solvent (concentration, M^{-1})	CPL λ_{ex} (nm)	g_{lum}	Refs.
1	 **1**	NA[a]	Dodecane (1×10^{-3})	325	0.01[b,c]	[4]
2	 **2**	NA	CHCl₃ (4×10^{-4})	375	−0.021 −0.035[c]	[5]
3	 (*P*)-**3**	NA	CHCl₃ (NA)	NA	+0.0009	[6]
4	(*M*)-**3**				−0.0011	
5	 (*P*)-**4**	NA	CHCl₃ (NA)	NA	+0.0008	[6]
6	(*M*)-**4**				−0.0007	
7	 (*P*)-**5**	36[d]	DCM (NA)	400	0.003[b]	[7]

Table 12.1 (continued)

Entry	Molecule	ϕ (%)	Solvent (concentration, M^{-1})	CPL λ_{ex} (nm)	g_{lum}	Refs.
8	(P)-**6**	66[d]	DCM (1×10^{-5})	NA	0.0012[b]	[8]
9	(M)-**7**	32[d]	CHCl$_3$ (2×10^{-5})	428	−0.030	[9]
10	(M)-**8**	29.6[d]	CHCl$_3$ (2×10^{-5})	449	−0.032	[9]
11	(P)-**9**	23[d]	DCM (6.8×10^{-6})	320	+0.0035	[10]
12	(M)-**10**	15[d]	CHCl$_3$ (NA)	482	−0.016 [g]	[11]
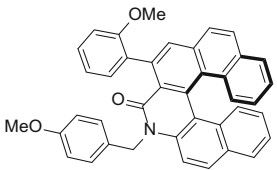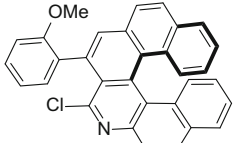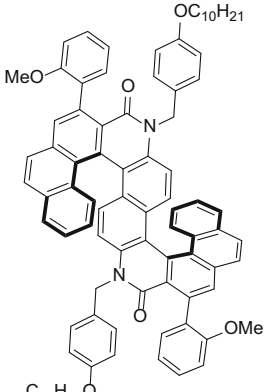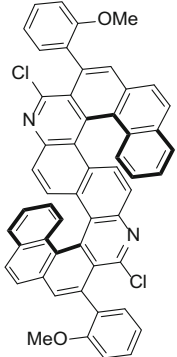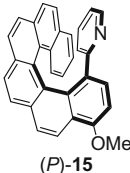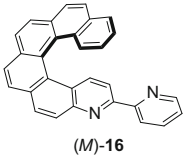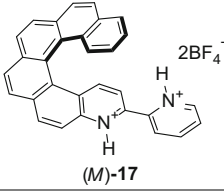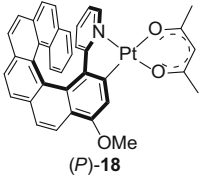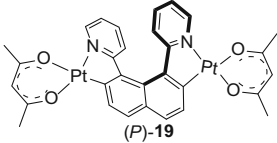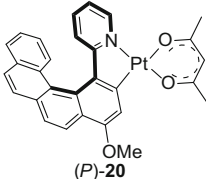
(continued)

Table 12.1 (continued)

Entry	Molecule	ϕ (%)	Solvent (concentration, M^{-1})	CPL λ_{ex} (nm)	g_{lum}	Refs.
13	 (M)-**11**	5.1^d	CHCl$_3$ (1 × 10^{-5})	375	<−0.001^f	[12]
14	 (M)-**12**	2.1^d	CHCl$_3$ (1 × 10^{-5})	375	<−0.001^f	[12]
15	 (P,P)-**13**	19.0^d	CHCl$_3$ (1 × 10^{-6})	375	+0.028	[12]
16	 (M,M)-**14**	9.4^d	CHCl$_3$ (1 × 10^{-6})	375	−0.011	[12]

Table 12.1 (continued)

Entry	Molecule	ϕ (%)	Solvent (concentration, M^{-1})	CPL λ_{ex} (nm)	g_{lum}	Refs.
17	(P)-**15**	3.3^d	DCM (NA)	371–382	+0.0008	[13]
18	(M)-**15**				−0.0008	
19	(M)-**16**	8.4^d	DCM (NA)	400	−0.003	[14, 15]
20	(P)-**16**				+0.0034	
21	(M)-**17**	8.2^d	DCM (NA)	NA	−0.0025	[14]
22	(P)-**17**				+0.0032	
23	(P)-**18**	5.6^e	DCM (NA)	452	+0.0050	[13]
24	(M)-**18**				−0.0040	
25	(P)-**19**	13^e	DCM (NA)	459–469	+0.0005	[13]
26	(M)-**19**				−0.0005	
27	(P)-**20**	10^e	DCM (NA)	452	+0.013	[13]
28	(M)-**20**				−0.011	

Table 12.1 (continued)

Entry	Molecule	ϕ (%)	Solvent (concentration, M^{-1})	CPL λ_{ex} (nm)	g_{lum}	Refs.
29	 (*M*)-**21**	0.38[e]	Acetone (NA)	NA	−0.0011	[14]
30	(*P*)-**21**				+0.0010	
31	 (*M*)-**22**	2.7[e]	Acetone (NA)	NA	−0.0022	[14]
32	(*P*)-**22**				+0.0018	
33	 (*M*)-**23**	0.16[e]	DCM (1×10^{-3})	456–461	−0.0028	[15]
34	(*P*)-**23**				+0.0031	
35	 (*M*)-**24**	6[e]	DCM (1×10^{-3})	458–468	−0.0015	[15]
36	(*P*)-**24**				+0.0013	

[a]*NA* not available

[b]Absolute value, (*P*)-helicene gave positive value, (*M*)-helicene gave negative value

[c]The molecules formed supramolecular assemblies under the testing conditions

[d]Quantum yield of fluorescence

[e]Quantum yield of phosphorescence

[f]74 % ee

[g]91 % ee

and (*P*)-**12** showed the absolute value of g_{lum} smaller than 0.001. Crassous, Autschbach, and co-workers reported the CPL properties of pyridyl helicenes and transition metal-helicene complexes [13–15]. The absolute values of g_{lum} were found to be less than 0.004 for 1-(2-pyridyl)-[6]helicene **15**, 3-(2-pyridyl)-4-aza[6] helicene **16** and [**16**-2H$^+$][2BF$_4^-$]. In some cases, the CPL activity could be enhanced (Entry 17 vs. Entry 23) or weakened (Entry 19 vs. Entry 29) after coordination with metal centers. The g_{lum} value of complexes could be promoted to the order of 10^{-2} (Entry 27), which was comparable to single organic molecules. Because only preliminary studies were reported, the structure-CPL activity relationship of helicenes was unclear.

12.2 Organic Electronics

Due to good thermal and chemical stability, strong intensity and good quantum yield of fluorescence or phosphorescence, helicenes with π-conjugated skeletons are good candidates for organic electronics. The applications in organic light emitting diodes (OLEDs) and transistors will be discussed in this section.

12.2.1 Helicenes in OLEDs

In 2010, Sooksimuang group reported an OLED with the configuration of ITO/PEDOT:PSS (35 nm)/**25**/Ca (10 nm)/Al (100 nm). Helicene **25** (Fig. 12.1) with a HOMO/LUMO energy gap of 2.6 eV had T_m (melting temperature) of 307 °C, T_g (glass-transition temperature) of 130 °C, and T_d (decomposition temperature) of 330 °C. The best result was obtained with turn-on voltage of 3.7 V, the maximum current ($\eta_{c,max}$) and power ($\eta_{p,max}$) efficiency of 0.64 cd/A and 0.29 lm/W, and the maximum brightness (B_{max}) of 1587 cd/m^2 at 8.0 V and 281 mA/cm^2 with CIE coordinates of (0.51, 0.44), when the thickness of **25** was 100 nm [16].

A deep blue-emitting OLED was described by Liu and co-workers [17]. Aza[5] helicene **26** showed good thermal stability (T_g of 203.0 °C, T_d of 372.1 °C) with optical quantum yield of 9–10 %, and the HOMO/LUMO gap was determined as 2.79 eV. The OLED was fabricated as the following configuration: ITO/NPB (50 nm)/CBP:5 % **26** (30 nm)/BCP (20 nm)/Mg:Al (100 nm)/Ag (50 nm). The device, emitting blue light with CIE coordinates of (0.15, 0.10), had turn-on voltage of 5.30 V with B_{max} of 2365 cd/m^2 at 14.6 V, $\eta_{c,max}$ of 0.22 cd/A at 11.8 V, and $\eta_{p,max}$ of 0.09 lm/W, respectively.

Recently, Liu and co-workers prepared aza[6]helicene **27**, and investigated its electroluminescence property [18]. The molecule had a HOMO/LUMO gap of 2.92 eV, and exhibited excellent stability (T_m of 130.9 °C, T_d of 297.0 °C) and the quantum yield was determined to be 4 % in neat films. Two devices were
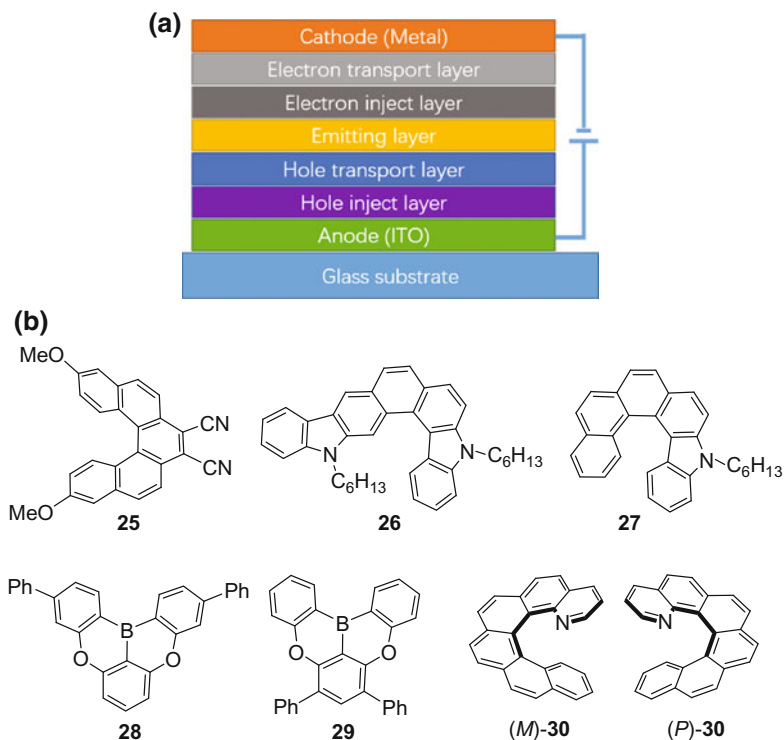
Fig. 12.1 a A general device configuration for OLED; **b** reported helicenes utilized as emitting material

manufactured: A) ITO/NPB (50 nm)/**27** (30 nm)/Bphen (20 nm)/Mg:Ag (150 nm)/ Ag (50 nm) and B) ITO/NPB (50 nm)/CBP:10 % **27** (30 nm)/Bphen (20 nm)/Mg: Ag (150 nm)/Ag (50 nm). Device B exhibited superior electroluminescence properties with turn-on voltage of 5.1 V, B_{max} of 3245 cd/m^2 at 18 V, $\eta_{c,max}$ of 0.68 cd/A at 14.0 V, and $\eta_{p,max}$ of 0.17 lm/W at 14.0 V, respectively. Both of the devices emitted blue lights of CIE coordinates of (0.15, 0.09) for A and (0.15, 0.10) for B.

In addition, Hatakeyama and co-workers investigated the performance of boron-embedded [4]helicenes, **28** and **29**, as the host material with [Ir(ppy)$_3$] (ppy = 2-(2-phyidino)phenyl) as a green dopant for phosphorescent OLED (PHOLED) [19]. The quantum yields on PMMA films and energy gaps were 0.60 and 0.57, 3.10, and 3.03 eV, respectively. The green OLEDs was manufactured as ITO/HAT-CN/TBBD/TCTA/**28** or **29**:5 % [Ir(ppy)$_3$]/TPBi/LiF/Al. The lifetime, from an initial brightness from 2000 to 1600 cd/m^2, was determined to be 1000 h for **28** and 383 h for **29**, respectively, which was much longer than that using CPB as the host material (95 h). The device using **28** as the host showed a turn-on voltage of 5.2 V with $\eta_{c,max}$ of 72.1 cd/A, and $\eta_{p,max}$ of 42.5 lm/W. This was resulted from the localization the SOMOs, induced by the boron and oxygen atoms, displaying a small difference between the S_1 and T_1 states.
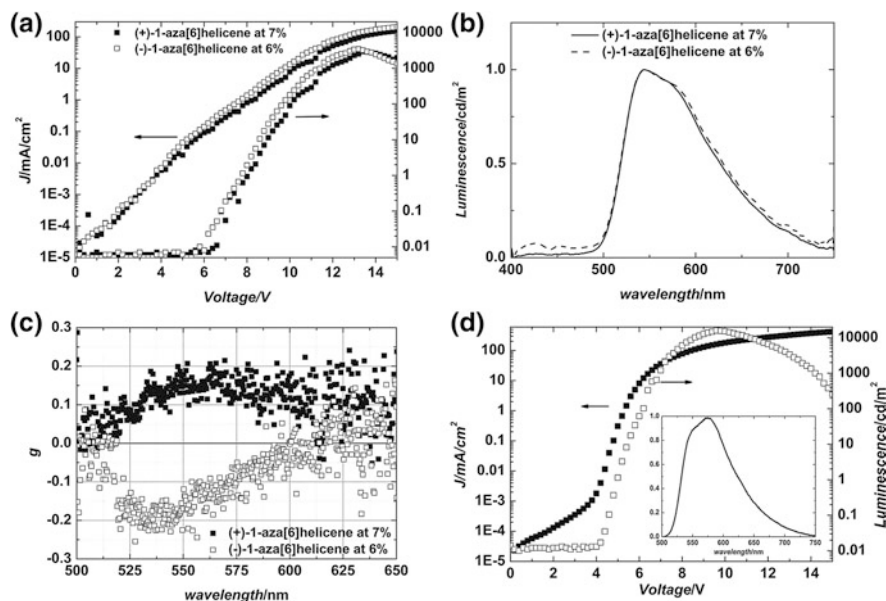
Fig. 12.2 a Variation of current *J* (*circles*) and luminosity *L* (*squares*) with applied voltage *V*. **b** EL spectra and **c** CP-EL spectra of the PLED device containing a light-emitting layer of F8BT doped with 7 % (by weight) of (+)-(*P*)-1-aza[6]helicene (*solid symbols*) and 6 % (by weight) (−)-(*M*)-1-aza[6]helicene (*open symbols*). **d** *J–V–L curves* of an undoped F8BT PLED with EL spectrum as the inset. Reprinted with the permission from Ref. [20]. Copyright 2013 John Wiley and Sons

Moreover, Fuchter, Campbell, and co-workers utilized 1-aza[6]helicene **30** as a chiral dopant in light-emitting polymer to construct an CP-PLED, which exhibited circularly polarized (CP) electroluminescence (EL) [20]. The device was manufactured with a configuration of ITO/PEDOT:PSS (50 nm)/F8BT:6–7 % **30**/Ca (20 nm)/Al (100 nm). The characterization of EL performance is shown in Fig. 12.2. Similar results, including current efficiency, brightness, were observed for (*M*)- and (*P*)-**30**, but the dissymmetric factor was opposite, 0.10–0.20 (at λ_{max} from 550 to 575 nm) for (*P*)-**30**, 0.15-0.25 (at λ_{max} from 525 to 550 nm) for (*M*)-**30**.

12.2.2   Helicenes in Transistors

Facchetti, Licandro, Muccini, and co-workers reported the preliminary investigation of the transistor responses of the thia [7]helicenes (Fig. 12.3) [21]. It was found that **31** (E_g = 2.9 eV) and **32** (E_g = 3.0 eV) showed poor (μ = 1.7 × 10^{-7} cm^2/(V · s), I_{ON}/I_{OFF} = 10^2) and no thin film transistor activity, respectively.
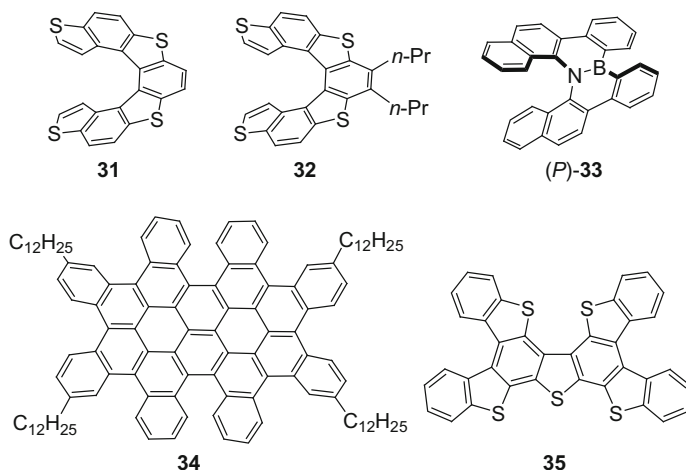
Fig. 12.3 Helicenes for the utilities in transistors
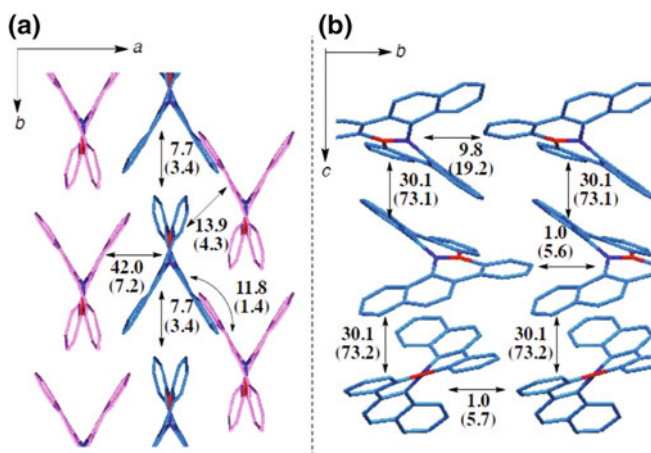
Fig. 12.4 Electronic coupling (in meV) between the HOMOs and LUMOs (in parentheses) of the neighboring helicenes in crystal states of **a** (*rac*)-**33** (*M* in *pink* and *P* in *blue*) and **b** (*P*)-**33**. Reprinted with the permission from Ref. [22]. Copyright 2012 American Chemical Society

In 2012, Hatakeyama, Nakamura, and co-workers reported an unprecedented carrier inversion phenomenon, in which azaborahelicene **33** displayed p-type semiconductivity (hole mobility, $\mu_h = 1.7 \times 10^{-7}$ cm^2/(V · s); electron mobility, μ_e, was not detected) used as the racemate and n-type semiconductivity ($\mu_h = 7.9$ 10^{-4} cm^2/(V · s), $\mu_e = 4.5 \times 10^{-3}$ cm^2/(V · s)) utilized as the single enantiomer state [22]. This was resulted from the different packing in crystals. As Fig. 12.4 shows, the electronic couplings between HOMOs and LUMOs were calculated from their crystal structure. For (*rac*)-**33**, the coupling for HOMOs was at least
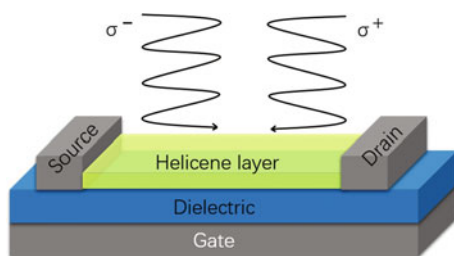
Fig. 12.5 Configuration of circularly polarized light-detecting helicene OFET. σ^- and σ^+ indicated the *left-* and *right*-circularly polarized light, respectively. Reprinted with the permission from Ref. [25]. Copyright 2013 Nature Publishing Group

twice as large as that of LUMOs; in contrast, for (*P*)-**33**, the coupling for LUMOs was at least twice as large as that of HOMOs.

Yang and Si reexamined the compound by DFT calculations and found that the photophysical properties of **33** could be tuned upon substitution [23]. The substituted helicenes were good candidates for nonlinear optical applications.

In addition, Nuckolls, Li, and co-workers prepared highly contorted PAH **34**, bearing four [4]helicene and two [5]helicene units, and examined the electronic properties in an organic field-effect transistor (OFET) device [24]. The graphene source and drain, providing very low contact resistence, were first printed to a silicon wafer, beyond which active layer was transferred and located between the electrodes. **34** was found to be a hole transporting semiconductor with the mobility of 0.002 cm^2/(V · s).

Fuchter, Campbell, and co-workers fabricated OFETs to detect circularly polarized lights by using the enantiomers of 1-aza[6]helicene **30** as responsive hole-transporting material [25]. As depicted in Fig. 12.5, optically pure helicene layer was prepared by spin coating and annealing. Regardless of the helicity, both the OFETs with (*P*)- or (*M*)-[6]helicene exhibit similar output and transfer characteristics ($\mu = 1 \times 10^{-4}$ cm^2/(V · s), $I_{ON}/I_{OFF} = 1 \times 10^3$). The responsive variation between the drain current (I_D) and gate voltage (V_g) was shown in Fig. 12.6. Compared with the results under different CP lights, (*P*)-**30** OFET displayed selective response to the right-CP light, whereas (*M*)-**30** OFET was responsive to left-CP light. As a control, a (*rac*)-**30** OFET was fabricated and found that the off current increase under either left- or right-CP light. Therefore, the change of the off current should be attributed to the absorption of the CP photons by enantiopure helicene layers. For example, by monitoring I_D under a constant drain and gate voltage of −60 and −10 V, respectively, the current varied between 1×10^{-9} A and 5×10^{-10} A with or without the right-CP light irradiation for (*P*)-**30** OFET.

Gao et al. reported a high performance, solution-processed OFET based on thiahelicene **35** [26]. The OFET was fabricated using Au as the source and drain electrodes, *n*-octadecyltrichlorosilane-modified SiO$_2$ as the dielectric layer, and the n-type Si as the gate electrode, providing the mobility of 2.12 cm^2/(V · s) and the on–off ratio greater than 10^5.
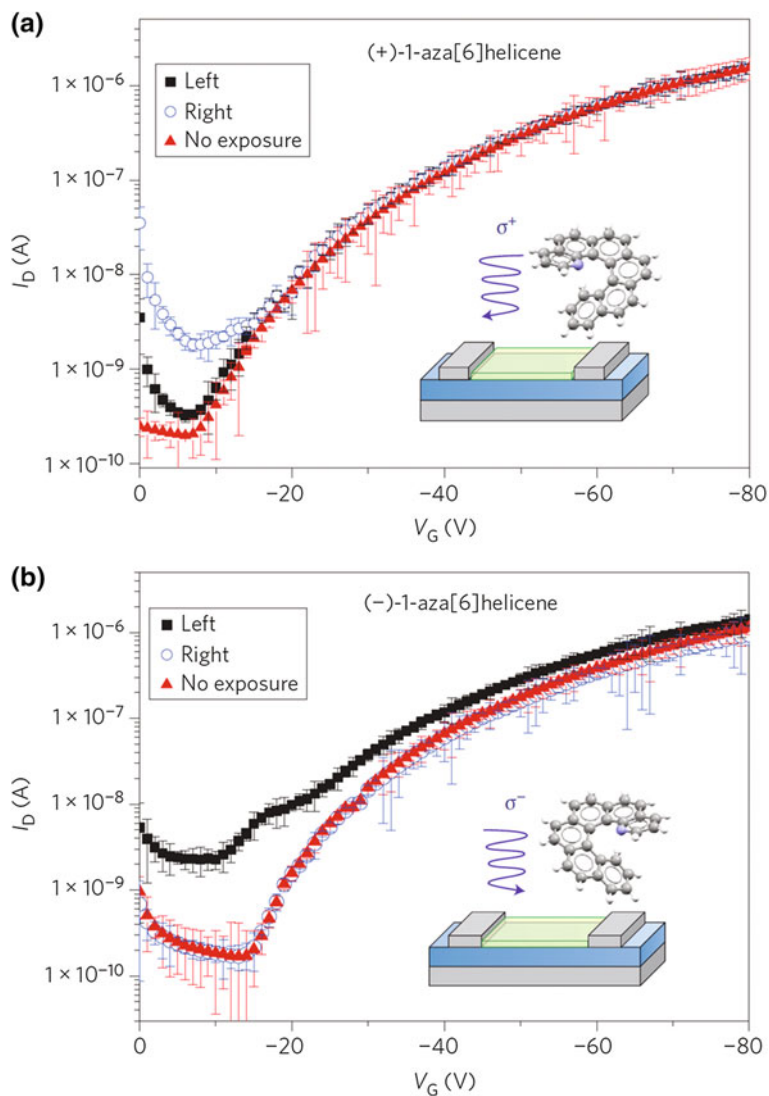
Fig. 12.6 The I_D-V_G curves for the (+)-(P)-1-aza[6]helicene (**a**) and (−)-(M)-1-aza[6]helicene (**b**) OFETs upon exposure towards *left-* (*black squares*) and *right*-circularly polarized light (*blue circles*). Reprinted with the permission from Ref. [25]. Copyright 2013 Nature Publishing Group

12.2.3   Miscellaneous

Nuckolls et al. utilized PAH **34** to form a heterojunction with phenyl-C_{70}-butyric acid methyl ester ($PC_{70}BM$), where they self-assembled with an association constant of *ca.* 5×10^{-4} M^{-1} [24]. The organic photovoltaic (OPV) device was
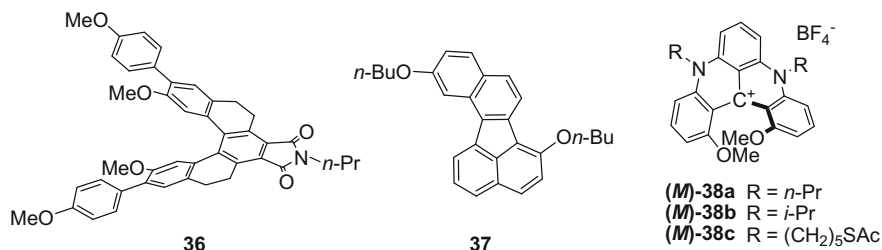
Fig. 12.7 Other helicenes utilized in organic electronics

fabricated as ITO/PEDOT:PSS (30 nm)/**34**:$PC_{70}BM$/TiO_x/Al (60 nm). The optimal performance was observed when the weight ratio between **34** and $PC_{70}BM$ was 1:4, with a power conversion efficiency of 2.88 %, a short circuit current of 7.9 mA/cm^2, and an open circuit voltage of 0.98 V.

Recently, Chen and co-workers investigated the application in optical waveguides [27, 28]. By the systematic survey of a series of tetrahydro[5]helicene imides, it was found that this type of compounds displayed intense fluorescence in solid state and could be easily crystallized. For example, microrods of **36** (Fig. 12.7) could be obtained by antisolvent diffusion and solvent evaporation-induced self-assembly. The intensity of the emission decreased exponentially along the microrod with the optical loss coefficient of 31.13 dB mm^{-1} (Fig. 12.8) [27]. This good activity might be resulted from the large Stokes shift that avoided self-absorption and the smooth surface that inhibited scattering. Very recently, the optical waveguide behavior of [4]helicene **37** was investigated and showed the optical loss coefficient of 18.84 dB mm^{-1} (Fig. 12.9) [28].
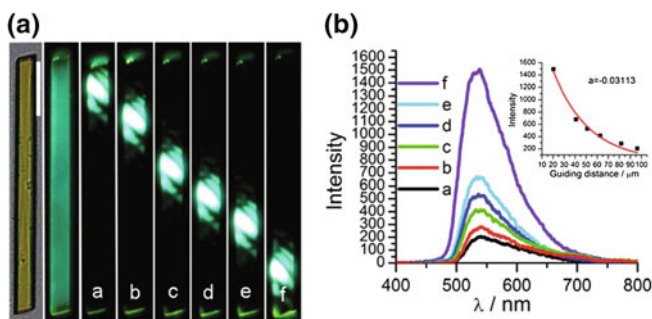
Fig. 12.8 The waveguide behavior of **36**. **a** *Bright-field image* (excited by a focused 351 nm laser beam): the *yellow* microrod (*left*) was 107 μm long. **b** Spatially resolved emission spectra collected from the tip of the microrod for different separation distances between the excitation spot and the tip of the rod as shown in (**a**). The inset showed the peak intensity at 530 nm versus the change of propagation distance. Reprinted with the permission from Ref. [27]. Copyright 2014 Royal Society of Chemistry
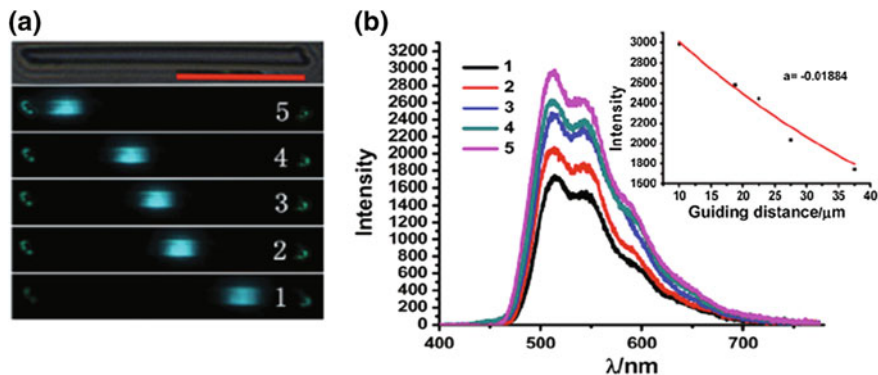
Fig. 12.9 The waveguide behavior of **37**. **a** *Bright-field image* (excited by a focused 351 nm laser beam): the microrod (*top*) was 43 μm long. **b** Spatially resolved emission spectra collected from the tip of the microrod for different separation distances between the excitation spot and the tip of the rod as shown in (**a**). The inset showed the peak intensity at 512 nm versus the change of propagation distance. Reprinted with the permission from Ref. [28]. Copyright 2015 Royal Society of Chemistry

Very recently, Naaman and co-workers applied helicenium cations (*M*)- and (*P*)-**38a-c** in organic spin filters, namely spintronic devices [29]. To investigate the chirality-induced spin selectivity (CISS), monolayer helicene films were first deposited on an atomically flat HOPG substrate with a thickness of 1.2–2.5 nm. It was found that the spin selectivity was opposite for (*M*)- and (*P*)-helicene of the same magnitude measured under the down or up magnetic field by magnetic conductive probe AFM. The spin polarization was determined later to be +49 % ± 3 % and −45 % ± 3 % for (*P*)- and (*M*)-enantiomers, respectively. In addition, the spin filter devices were fabricated as glass/Cr (8 nm)/Au
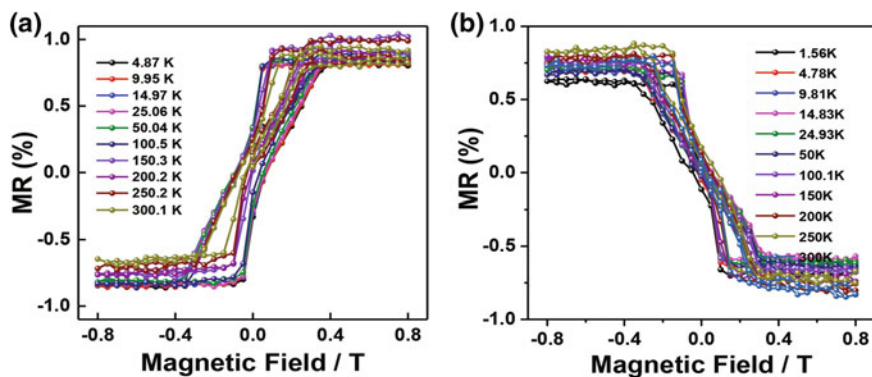
Fig. 12.10 Magnetoresistence−magnetic field curves for (A) (*P*)-**38c** and (B) (*M*)-**38c** up to 0.8 T at different temperatures with a constant current of 10 μA. Reprinted with the permission from Ref. [29]. Copyright 2016 John Wiley and Sons

(60 nm)/monolayer film/Al_2O_3 (2 nm)/Ni(120 nm) and the magnetoresistence was measured as *ca.* 2 % for both the enantiomers (Fig. 12.10). This result complemented the magnetic conductive probe AFM experiment and proved that the spin of electron transferred through the film composed by (*P*)- and (*M*)-helicene was opposite.

References

1. Kumar J, Nakashima T, Kawai T (2015) Circularly polarized luminescence in chiral molecules and supramolecular assemblies. J Phys Chem Lett 6(17):3445–3452
2. Sánchez-Carnerero EM, Agarrabeitia AR, Moreno F, Maroto BL, Muller G, Ortiz MJ, de la Moya S (2015) Circularly polarized luminescence from simple organic molecules. Chem Eur J 21(39):13488–13500
3. Lunkley JL, Shirotani D, Yamanari K, Kaizaki S, Muller G (2008) Extraordinary circularly polarized luminescence activity exhibited by cesium Tetrakis(3-heptafluoro-butylryl-(+)-camphorato) Eu(III) complexes in EtOH and $CHCl_3$ Solutions. J Am Chem Soc 130 (42):13814–13815
4. Phillips KES, Katz TJ, Jockusch S, Lovinger AJ, Turro NJ (2001) Synthesis and properties of an aggregating heterocyclic helicene. J Am Chem Soc 123(48):11899–11907
5. Kaseyama T, Furumi S, Zhang X, Tanaka K, Takeuchi M (2011) Hierarchical assembly of a phthalhydrazide-functionalized helicene. Angew Chem Int Ed 50(16):3684–3687
6. Field JE, Muller G, Riehl JP, Venkataraman D (2003) Circularly polarized luminescence from bridged triarylamine helicenes. J Am Chem Soc 125(39):11808–11809
7. Goto K, Yamaguchi R, Hiroto S, Ueno H, Kawai T, Shinokubo H (2012) Intermolecular oxidative annulation of 2-Aminoanthracenes to Diazaacenes and Aza[7]helicenes. Angew Chem Int Ed 51(41):10333–10336
8. Matsuno S, Koyama Y, Hiroto S, Kumar J, Kawai T, Shinokubo H (2015) Isolation of a 1,4-diketone intermediate in oxidative dimerization of 2-hydroxyanthracene and its conversion to oxahelicene. Chem Commun (Camb) 51(22):4607–4610
9. Sawada Y, Furumi S, Takai A, Takeuchi M, Noguchi K, Tanaka K (2012) Rhodium-Catalyzed enantioselective synthesis, crystal structures, and photophysical properties of helically chiral 1,1′-Bitriphenylenes. J Am Chem Soc 134(9):4080–4083
10. Oyama H, Nakano K, Harada T, Kuroda R, Naito M, Nobusawa K, Nozaki K (2013) Facile synthetic route to highly luminescent Sila[7]helicene. Org Lett 15(9):2104–2107
11. Murayama K, Oike Y, Furumi S, Takeuchi M, Noguchi K, Tanaka K (2015) Enantioselective synthesis, crystal structure, and photophysical properties of a 1,1′-Bitriphenylene-Based Sila [7]helicene. Eur J Org Chem 7:1409–1414
12. Nakamura K, Furumi S, Takeuchi M, Shibuya T, Tanaka K (2014) Enantioselective synthesis and enhanced circularly polarized luminescence of *S*-Shaped double azahelicenes. J Am Chem Soc 136(15):5555–5558
13. Shen C, Anger E, Srebro M, Vanthuyne N, Deol KK, Jefferson TD, Muller G, Williams JAG, Toupet L, Roussel C, Autschbach J, Reau R, Crassous J (2014) Straightforward access to mono- and bis-cycloplatinated helicenes displaying circularly polarized phosphorescence by using crystallization resolution methods. Chem Sci 5(5):1915–1927
14. Saleh N, Moore B, Srebro M, Vanthuyne N, Toupet L, Williams JAG, Roussel C, Deol KK, Muller G, Autschbach J, Crassous J (2015) Acid/Base-Triggered switching of circularly polarized luminescence and electronic circular dichroism in organic and organometallic helicenes. Chem Eur J 21(4):1673–1681

15. Saleh N, Srebro M, Reynaldo T, Vanthuyne N, Toupet L, Chang VY, Muller G, Williams JAG, Roussel C, Autschbach J, Crassous J (2015) Enantio-enriched CPL-active helicene-bipyridine-rhenium complexes. Chem Commun (Camb) 51(18):3754–3757

16. Sahasithiwat S, Mophuang T, Menbangpung L, Kamtonwong S, Sooksimuang T (2010) 3,12-Dimethoxy-7,8-dicyano-[5]helicene as a novel emissive material for organic light-emitting diode. Synth Met 160(11–12):1148–1152

17. Shi L, Liu Z, Dong G, Duan L, Qiu Y, Jia J, Guo W, Zhao D, Cui D, Tao X (2012) Synthesis, structure, properties, and application of a carbazole-based Diaza[7]helicene in a deep-blue-emitting OLED. Chem Eur J 18(26):8092–8099

18. Hua W, Liu Z, Duan L, Dong G, Qiu Y, Zhang B, Cui D, Tao X, Cheng N, Liu Y (2015) Deep-blue electroluminescence from nondoped and doped organic light-emitting diodes (OLEDs) based on a new monoaza[6]helicene. RSC Adv 5(1):75–84

19. Hirai H, Nakajima K, Nakatsuka S, Shiren K, Ni J, Nomura S, Ikuta T, Hatakeyama T (2015) One-step borylation of 1,3-Diaryloxybenzenes towards efficient materials for organic light-emitting diodes. Angew Chem Int Ed 54(46):13581–13585

20. Yang Y, da Costa RC, Smilgies D-M, Campbell AJ, Fuchter MJ (2013) Induction of circularly polarized electroluminescence from an achiral light-emitting polymer via a chiral small-molecule dopant. Adv Mater 25(18):2624–2628

21. Kim C, Marks TJ, Facchetti A, Schiavo M, Bossi A, Maiorana S, Licandro E, Todescato F, Toffanin S, Muccini M, Graiff C, Tiripicchio A (2009) Synthesis, characterization, and transistor response of tetrathia-[7]-helicene precursors and derivatives. Org Electron 10(8):1511–1520

22. Hatakeyama T, Hashimoto S, Oba T, Nakamura M (2012) Azaboradibenzo[6]helicene: carrier inversion induced by helical homochirality. J Am Chem Soc 134(48):19600–19603

23. Si Y, Yang G (2013) Photophysical properties of azaboradibenzo[6]helicene derivatives. J Mater Chem C 1:2354–2361

24. Xiao S, Kang SJ, Wu Y, Ahn S, Kim JB, Loo Y, Siegrist T, Steigerwald ML, Li H, Nuckolls C (2013) Supersized contorted aromatics. Chem Sci 4(5):2018–2023

25. Yang Y, da Costa RC, Fuchter MJ, Campbell AJ (2013) Circularly polarized light detection by a chiral organic semiconductor transistor. Nat Photon 7(8):634–638

26. Liu X, Wang Y, Gao J, Jiang L, Qi X, Hao W, Zou S, Zhang H, Li H, Hu W (2014) Easily solution-processed, high-performance microribbon transistors based on a 2D condensed benzothiophene derivative. Chem Commun (Camb) 50(4):442–444

27. Li M, Yao W, Chen J-D, Lu H-Y, Zhao Y, Chen C-F (2014) Tetrahydro[5]helicene-based full-color emission dyes in both solution and solid states: synthesis, structures, photophysical properties and optical waveguide applications. J Mater Chem C 2(39):8373–8380

28. Li X-J, Li M, Yao W, Lu H-Y, Zhao Y, Chen C-F (2015) Dialkoxybenzo[j]fluoranthenes: synthesis, structures, photophysical properties, and optical waveguide application. RSC Adv 5 (24):18609–18614

29. Kiran V, Mathew SP, Cohen SR, Hernández Delgado I, Lacour J, Naaman R (2016) Helicenes—a new class of organic spin filter. Adv Mater 28(10):1957–1962

Chapter 13
Helicene Assemblies

Abstract This chapter describes the assembly behaviors of helicenes and the properties of aggregates. It was found that optically pure helicenes form ordered monolayer on Ni(111), while thia[11]helicene on gold surfaces can form the 2D ordered layer, and structures of the Au surfaces play an important role in the assembly behaviors. The repulsive interactions between (*M*)-[7]helicenes result in supramolecular chirality of the close-packed 2D layer on Cu(111); but for racemic [7]helicene, an unprecedented chirality amplification is observed. Similarly, (*M*)-[7]helicene-2-carboxylic acid self-assembles into island structures, while the racemates give nanowire-like aggregates. Besides the chiral discrimination, the hydrogen bonds, the dispersive forces in the metal surfaces, temperatures, and even substituents can influence the assembly behaviors of helicenes. It was also found that mixing the pseudoenantiomeric oligomers composed by [4]helicene units with the same helicity can result in two-component gel, in which the π-π interactions between the helicenes are the driving force. After ultrasonication, gelation of (*M*)-[4]helicene derivative can occur upon the diffusion of the gelator from THF phase to hexane phase. Moreover, (*P*)-[4]helicene-grafted SiO_2 NPs can capture the hetero-double-helix of ethynylhelicene oligomers from the gelation procedure. Furthermore, it was found that enantiopure helicenebisquinone can self-assemble into fibers or a true hexagonal assembly of right-handed helices. Different linkers in cycloalkyne-[4]helicene oligomers can control the intra- and intermolecular aggregation, and dynamic and reversible polymorphism exists in the cyclic bis (ethynylhelicene) oligomers. In addition, hydrogen bonds can also be utilized for the construction of screw-shaped fibrous assemblies, which exhibit excellent CPL properties.

In this chapter, the assembly behaviors of helicenes and the properties of aggregates will be discussed. It will be classified into three sections, including interfacial self-assembly, organogels, and other selected assemblies.

13.1   Interfacial Self-Assembly

Ernst and colleagues first studied the self-assembly of [7]helicene **1** (Fig. 13.1) in 1999, and they found ordered monolayer was formed by using optically pure helicenes on Ni(111) [1]. In addition, they tried to prepare chiral metal film on the helicene layer by deposition. Near edge X-ray absorption fine structure (NEXAFS) indicated the orientation of the helicene on metal surfaces, which was influenced by the coverage and temperature [2]. For a saturated monolayer, helicene was tilted and formed an angle of $43 \pm 5°$ between the helix axis and the Ni(100) surface.

Taniguchi and co-workers studied the self-assembly of thia[11]helicene **2** (Fig. 13.1) on gold surfaces [3, 4]. According to STM and low-energy electron diffraction, it was found that the 2D ordered layer was observed, and the structures of the Au surfaces played an important role in the assembly behaviors [3]. For instance, on Au(111), helicene molecules were randomly distributed on the wide terraces, and the chiral discrimination, forming enantiomeric arrays of enantiomers, was observed only at narrow steps; on Au(110), helicenes were arranged into helicity sensitive chains; and for polycrystalline gold, arrays of homochiral helicenes were observed [4].

Fasel, Ernst, and Parschau disclosed the chirality transfer phenomenon that supramolecular chirality of the close-packed 2D layer on Cu(111) was observed due to the repulsive interactions between the (*M*)-**1** [5]. Later, they studied the self-assembly behavior of racemic [7]helicene, and an unprecedented chirality
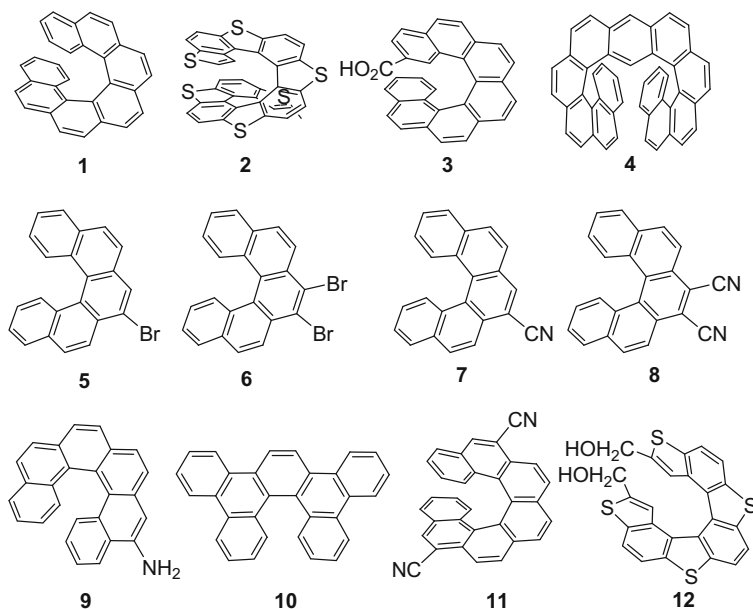
Fig. 13.1 Helicenes investigated in the self-assembly at different surfaces
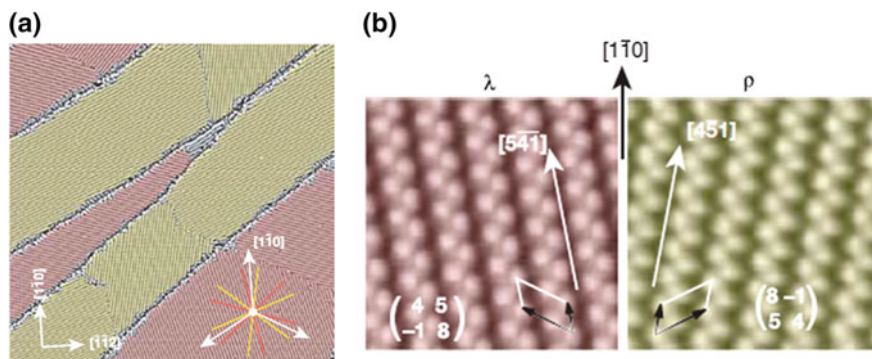
Fig. 13.2 STM images of enantiomorphous domains of racemic heptahelicene on Cu(111): **a** 200 nm × 200 nm, and **b** 10 nm × 10 nm. Left-(λ) and right-handed (ρ) domains were colored red and yellow, respectively. Reprinted with the permission from Ref. [6]. Copyright 2006 Nature Publishing Group

amplification was observed [6]. As Fig. 13.2 shows, (*rac*)-**1** spontaneously formed supramolecular chiral domains, λ and ρ, in equal probability, which were composed by pairs of (*M*)- and (*P*)-enantiomers. If the amount of (*M*)-enantiomer was in excess of 50 %, λ domain was favored and vise versa. It was suggested that the energy of domain boundary and the energy between domain and residue interfaces were two driving forces for this by molecular mechanics calculations.

Kühnle, Stará, and co-workers used insulating substrate, calcite, to investigate the self-assembly of [7]helicene-2-carboxylic acid **3** [7]. The aggregates could be clearly observed in Fig. 13.3 that (*M*)-**3** self-assembled into island structures, while racemic sample gave nanowire-like aggregates. The orientation of helicenes herein
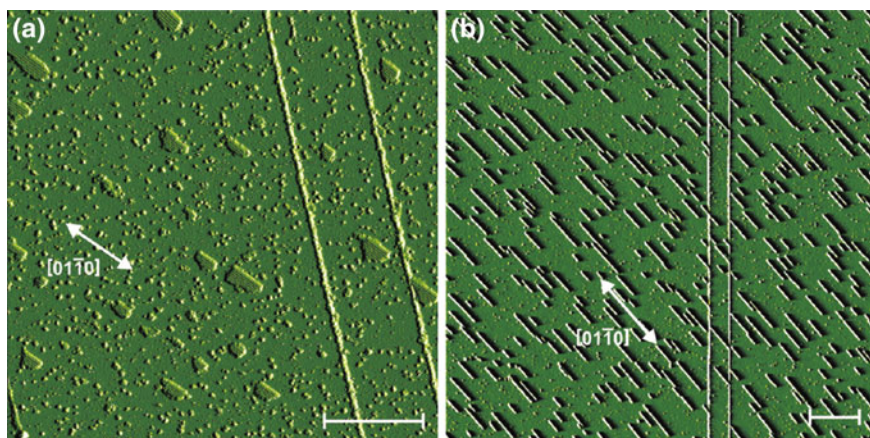
Fig. 13.3 AFM images for **a** (*M*)-**3** and **b** (*rac*)-**3** (scale bars = 100 nm). Reprinted with the permission from Ref. [7]. Copyright 2012 American Chemical Society
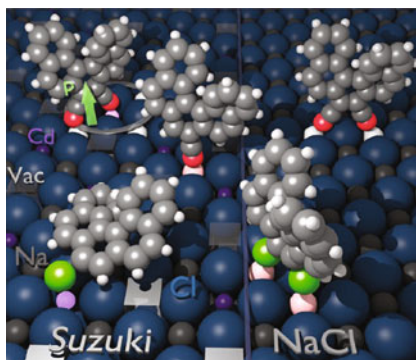
was different from the ones on metal surfaces, where helicenes were standing upright with no aromatic rings in contact with the substrates. This result indicated that the heterochiral recognition was important for row formation in nanowires. Similar orientation was also observed in the self-assembled layers of **4** on InSb (001), but the organization of (*M*)-**4** and (*rac*)-**4** was different at the step edges.

In addition, Barth and colleagues studied the self-assembly behaviors of functionalized [5]helicenes on insulating Suzuki surface of sodium chloride, NaCl:Cd^{2+}(001), in ultra-high vacuum by noncontact AFM and Kelvin probe force microscopy (KPFM). According to the results, monobromo [5]helicene **5** was lying on the Suzuki surfaces [8], while dibromo [5]helicene **6**, monocyano [5]helicene **7**, and dicyano[5]helicene **8** were standing perpendicularly to the surfaces due to the charge matching between the polar functional groups (partially negative charged) and the surface cations (Fig. 13.4) [9]. Helicene **6** could be deposited as wide islands at Suzuki surface and partially in the NaCl domain, but it desorbed with a few hours. Helicenes **7** and **8** could cover the whole Suzuki surface, of which the complete desorption needed about three weeks.

Ivasenko et al. described the impact of chirality and the hydrogen bonds on the self-assembly of amino [7]helicene **9** [10]. (*P*)-**9** self-assembled into a three-dot *p*3-(*P*$_3$) pattern (Fig. 13.5), which was similar to that of (*P*)-**1** on Cu(111) surface [5]. The DFT calculation indicated that the amino group was oriented downwards to the surface of Au substrate. If racemate was deposited, *p*3-(*P*$_3$), *p*3-(*M*$_3$), and *p*6-(*P*$_6$*M*$_6$) regions (Fig. 13.6) were observed, which were composed by (*P*)-, (*M*)-**9**, and (*rac*)-**9**, respectively. The amino group was important for this. If **9** was resolved in octanoic acid, only random distribution was observed.

Besides the chiral discrimination, Ernst and co-workers discovered that the dispersive forces could act as polar forces in the metal surfaces [11]. When (*rac*)-**10** was deposited to the Cu(111), spontaneously resolution was observed in ordered regions, giving enantiomorphs composed by (*P*)- or (*M*)-enantiomer. In addition, if 26 % of (*M*)-**1** was added to the racemate of **10**, monolayer of **10** (80 %) and **1** (20 %) could be obtained. However, only enantiomorph composed by (*M*)-enantiomer was observed, which was attributed to the preferential heterochiral
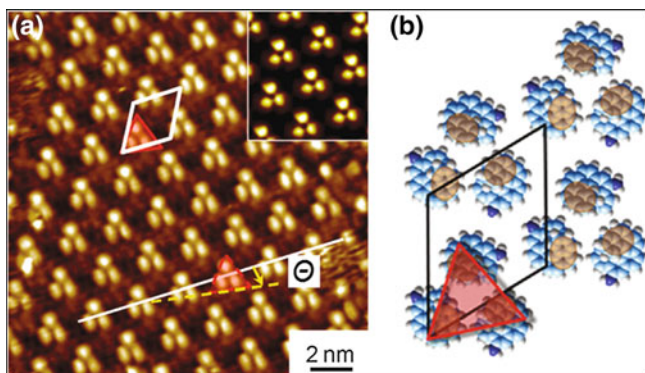
Fig. 13.5 Self-assembly of (*P*)-**9**, p3-(*P₃*), on Au (111). **a** STM images, **b** models for the assembly. Reprinted with the permission from Ref. [10]. Copyright 2013 Royal Society of Chemistry
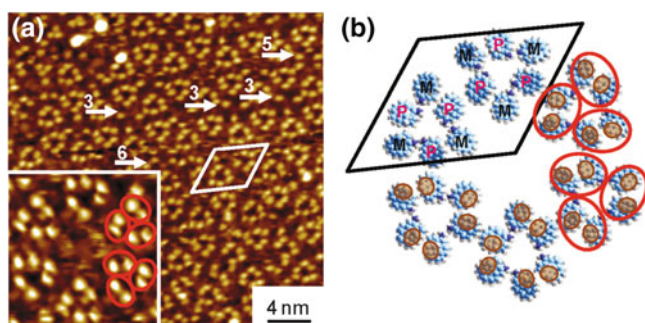
Fig. 13.6 Self-assembly of (*rac*)-**9**, p6-(*P₆M₆*), on Au (111). **a** STM images, **b** models for the assembly. Reprinted with the permission from Ref. [10]. Copyright 2013 Royal Society of Chemistry

interaction between (*P*)-**10** and (*M*)-**1**, suppressing the formation of (*P*)-**10** enantiomorph (Fig. 13.7).

Ernst and Parschau disclosed the chiral amplification in the second layer, when multiple layers of [7]helicene (*rac*)-**1** were deposited to Cu(111) [12]. When the first not-well-ordered layer was saturated (Fig. 13.8a), the second layers was observed with supramolecular chirality (Fig. 13.8b-d). The STM results indicated that (*M*)-**1** was located in the second layer of ρ domains (ρ^{2nd}), whereas (*P*)-**1** was located in λ^{2nd} domains. If the amount of one enantiomer exceeded the other in the double-layer system, the minority enantiomer was found in the second layer and the majority enantiomer was arranged in the first layer, which was attributed to the energetically unfavorable interactions between the mirror-domain boundaries.
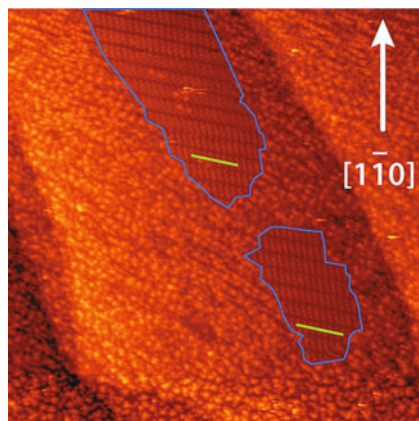
Fig. 13.7 STM image of monolayer of 80 % (*rac*)-**10** and 20 % (*M*)-**1** on Cu(111). Reprinted with the permission from Ref. [11]. Copyright 2013 American Chemical Society
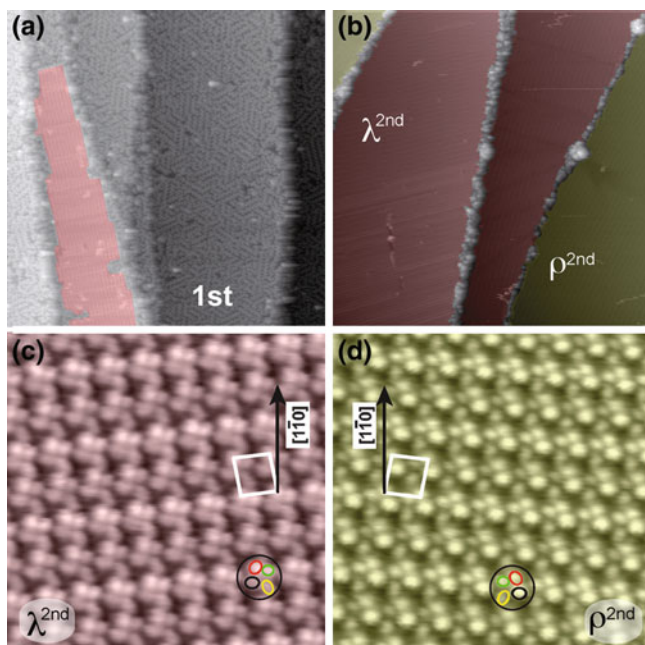
Fig. 13.8 STM images of **a** first layer, **b** second layer, **c** λ domain in second layer (*red*), and **d** ρ domain in second layer (*yellow*) of **1**. Reprinted with the permission from Ref. [12]. Copyright 2015 John Wiley and Sons

However, if two cyano groups was introduced, the self-assembly behavior of [7]helicene differed from the above results. Jung and colleagues studied the chiral transfer in 1D self-assemblies of **11** via hydrogen bonds and metal coordinations
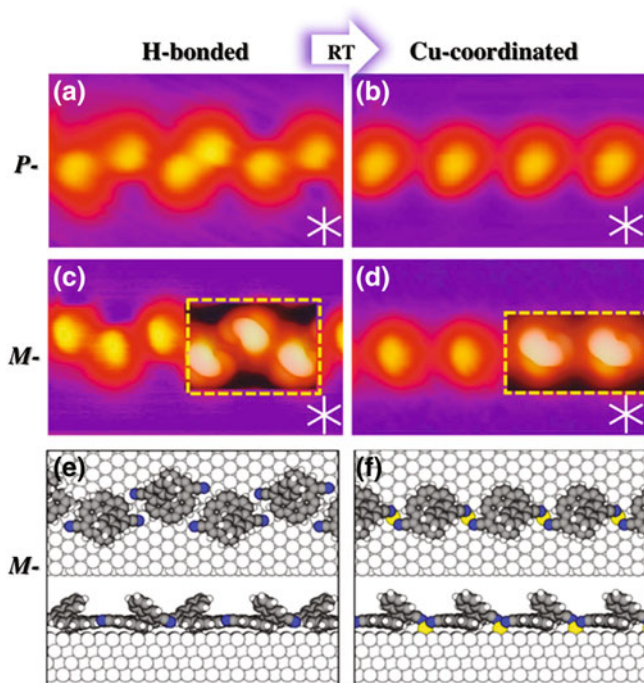
Fig. 13.9 STM images of chains of (*P*)-**11** connected by **a** hydrogen bonds and **b** Cu-coordination, and (*M*)-**11** connected by **c** hydrogen bonds and **d** Cu-coordination on Cu (111). DFT models for **e** H-bonded and **f** Cu-coordinated chains of (*M*)-**11**. The transition from H-bonded chain to Cu-coordinated chain was achieved by annealing at 300 K. Reprinted with the permission from Ref. [13]. Copyright 2013 American Chemical Society

[13]. For the H-bonded chains, mirrored zigzag structures for enantiomers were obtained via head-to-head and tail-to-tail connections (Fig. 13.9a, c). However, linear chains via Cu-coordination for both enantiomers were observed, and no mirrored pattern was formed (Fig. 13.9b, d), where helicene **11** was randomly oriented.

Kuwahara and co-workers investigated the self-assembly of diol **12** at different temperatures [14]. At low temperature, (*M*)-**12** preferentially adsorbed at the step edges, face-centered cubic (fcc) regions, and fcc elbow regions for the submonolayer coverage. For higher coverage, disordered layers were formed with short twin rows. The complete coverage was achieved by increasing the temperature of substrate during the deposition, in which the formation of the whole monolayer was controlled thermodynamically. The layer was composed by ordered islands comprised of twin rows (Fig. 13.10a), surrounded by the disordered domains. According to the results of current imaging tunneling spectroscopy (CITS), it was indicated that (*M*)-**12** had two azimuthal orientations, which was depicted in Fig. 13.10b.
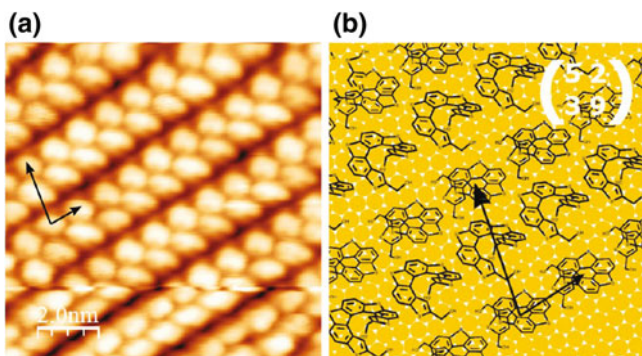
Fig. 13.10 a STM images and **b** molecular model for the twin rows of (*M*)-**12** on Au(111). Reprinted with the permission from Ref. [14]. Copyright 2015 American Chemical Society

13.2 Organogels

In 2010, Yamaguchi group reported the first example of helicene-based organogels (Fig. 13.11) [15]. By mixing the pseudoenantiomeric oligomers **13–16**, which were composed by [4]helicene units with the same helicity, two-component gel could be obtained. For instance, (4*P*)-**14** and (5 *M*)-**15** (1:1) in toluene gave the gel with minimal gelation concentration of 0.05 mM. The π-π interactions between the helicenes were thought to be the driving force. If two oligomers bore the same enantiomer, no gelation was observed. This two-component sol-gel process could provide a variety of organogels with different chiroptical properties by changing the length and ratio of the oligomers. Compared with the transparent gels (Type I) formed by the oligomers with comparable numbers of [4]helicene units, like

13 (n = 3), **14** (n = 4), **15** (n = 5), **16** (n = 6), **17** (n = 7), **18** (n = 8)
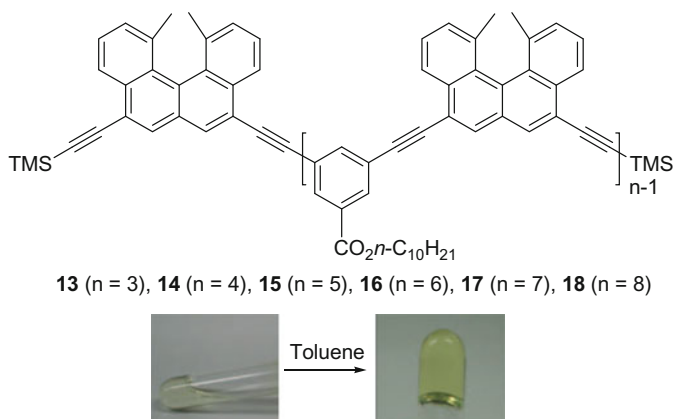
Fig. 13.11 The structures of ethynylhelicene oligomers and images of the sol-gel transformation
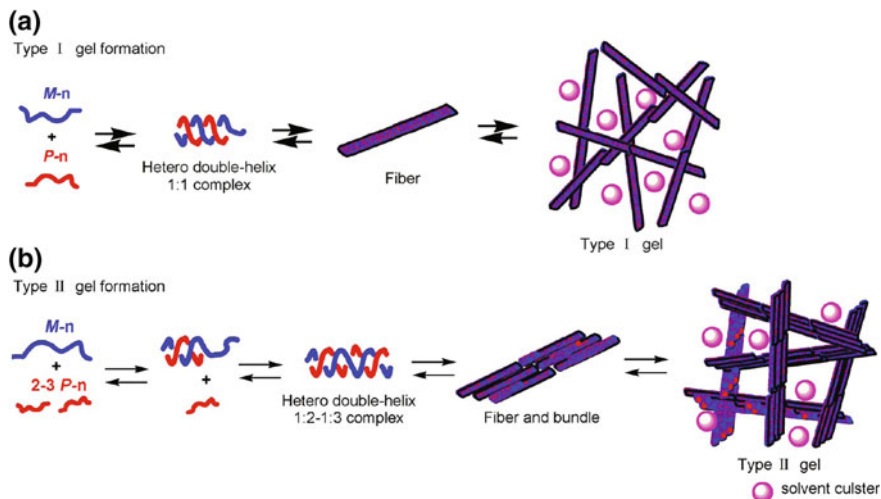
Fig. 13.12 **a** Type I and **b** Type II gel formed by oligomers with different lengths. For, *M*-n and *P*-n, *M*, *P*, and n indicated the helicity and the number of the [4]helicene units in oligomers. Reprinted with the permission from Ref. [16]. Copyright 2012 American Chemical Society

(4*P*)-**14**/(5 *M*)-**15**, the gels formed by one long oligomer ($n = 6$–8) and one short oligomer ($n = 2$–3) was turbid [16]. According to AFM studies, in the turbid Type II gels bundles of 100–150 nm diameter were discovered, whereas the transparent Type I gels only bore fibers with 25–50 nm diameter (Fig. 13.12). In addition, two-layered gel systems could be prepared by Type I and II gels.

Yamaguchi and Shigeno utilized optical pure (*M*)-**19** to construct multilayer systems, achieved by a three-step procedure [17]. As depicted in Fig. 13.13, hexane was added slowly to the top of the THF solution of (*M*)-**19**. After ultrasonication, gelation occurred upon the diffusion of gelator (*M*)-**19** from the THF phase to hexane phase. Therefore, the sol-gel transformation started from the interfaces with the mixing of THF solution and hexane. The final two-layer system was formed and proved by the motion of blue silica gel in THF. Even a six-layer system (water-liquid-gel-water-liquid-gel) could be easily constructed based on this novel method.

Later, the same group investigated the assembly behavior of block copolymer in solutions. For example, tetrameric ααββ aggregates could be obtained by mixing (4 *M*,5 *M*)-**20** and (4 *M*,4*P*)-**21** (Fig. 13.14a) [18]. The stabilities of the assemblies of different domains were determined as amido domain/amido domain (red/red) > heterochiral ethynyl domains (green/blue) > homochiral ethynyl domains (green/green or blue/blue) (Fig. 13.14b). When 1:1 ratio of (4 *M*,5 *M*)-**20** (α-subunit) and (4 *M*,4*P*)-**21** (β-subunit) was added to CHCl$_3$ in a total concentration of 2×10^{-4} M, dimeric αα- and ββ- aggregates, tetrameric ααββ-aggregates were found in 1:1 ratio. When toluene was used as solvent, the sol-gel transformation could be observed, in which the minimum gelation concentration was
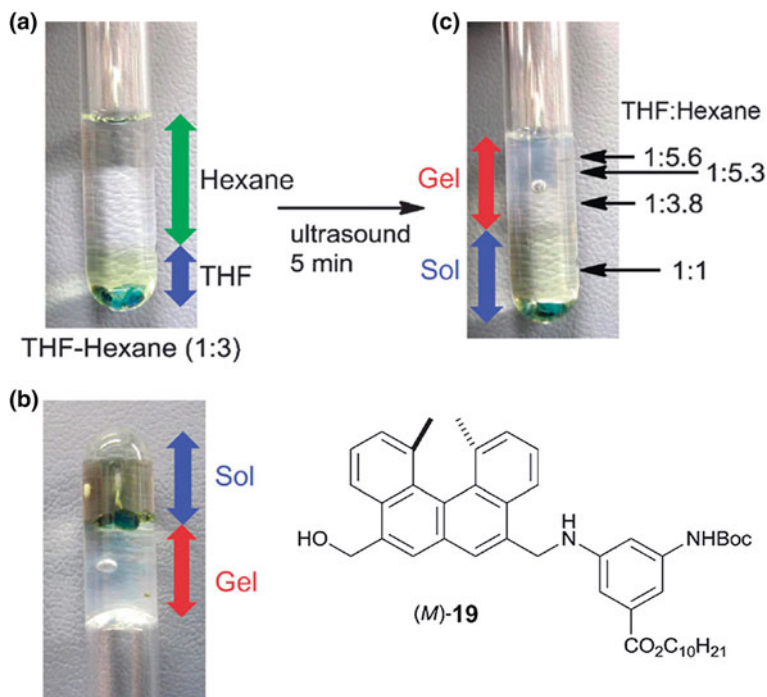
Fig. 13.13 The two-layer organogel-liquid system. **a** The liquids were added one by one, **b** gelation was achieved by ultrasonication, and **c** the system was turned upside down, and the green silica gel fell to the top of the gel layer. Reprinted with the permission from Ref. [17]. Copyright 2012 Royal Society of Chemistry

determined as 6×10^{-3} M. If the amido domain of (4 M,5 M)-**20** was removed, namely the structure as (5 M)-**22**, a lithium ion responsive organogel was prepared with (4 M,4P)-**21** (Fig. 13.14c) [19]. The (4 M,4P)-**21**/(5 M)-**22** organogel could be obtained in pyridine with a minimum gelation concentration of 2×10^{-3} M, and the sol state transformed into gel state reversibly by cooling to 25 °C and heating to 100 °C. In addition, the amido domain was in random coil state and could interact with lithium ions. Therefore, lithium perchlorate was added to the gel system, and the shrinkage of the gel volume was discovered, which could be expanded by removing the supernatant, adding solvent, and the subsequent heating and cooling the mixture. Similar reversible shrinkage was observed when the solvent was piperidine, cyclohexanone, 1,2-dimethoxybenzene. If toluene and anisole were used as solvent, no shrinkage of the gel volume was detected, which was attributed to the aggregation of amido domains in such solvents.
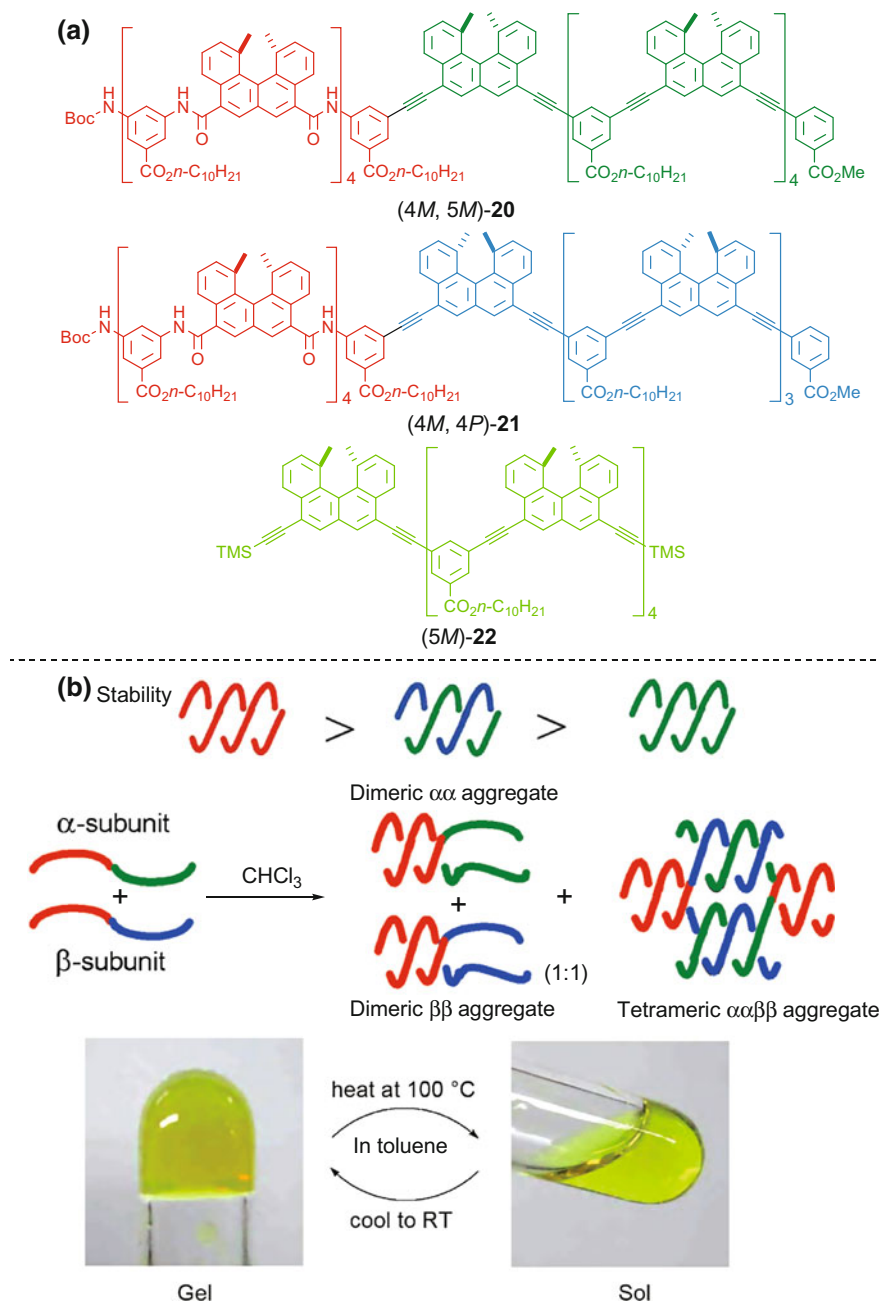
Fig. 13.14 a Structures of [4]helicene-based block copolymers and oligomer; **b** schematic representation and images of interactions between (4 *M*,5 *M*)-**20** and (4 *M*,4*P*)-**21**; **c** schematic representation and images of interactions between (4 *M*,4*P*)-**21** and (5 *M*)-**22**. Reprinted with the permission from Ref. [18, 19]. Copyright 2013 John Wiley and Sons and 2013 American Chemical Society
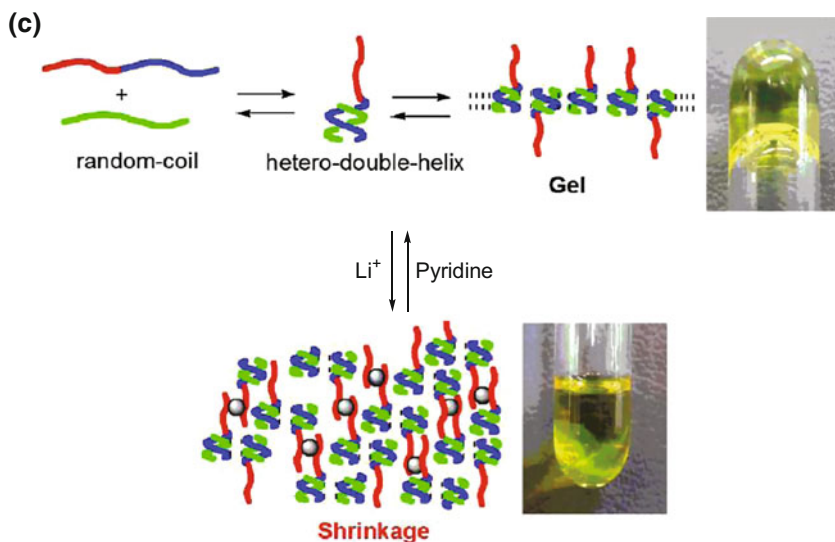
◀ **Fig. 13.14** (continued)

Recently, they utilized (P)-[4]helicene-grafted SiO_2 nanoparticles to capture the hetero-double-helix of ethynylhelicene oligomers from the gelation procedure via adsorption, aggregation, precipitation, and finally liberation [20]. Moreover, crystals of hetero-double-helices could be isolated.

13.3   Other Assemblies

Helicenes functionalized with alkoxyl groups were extensively studied for their assembly behaviors and the properties of the assemblies. In 1996, Katz and co-workers reported the first example of the spontaneous assembly of optically pure helicenebisquinone **23** (Fig. 13.15) [21]. The chiroptical properties were greatly enhanced as the concentration increased, where supramolecular assemblies were formed [22]. However, compared with **23**, helicene **24** would not undergo aggregation even in concentrated solutions. When optically pure **23** was cooled from the melt, liquid crystal fibers could be even clearly resolved by optical microscope (Fig. 13.16), which were comprised of lamellae (50–200 nm wide, 10 nm high) [22]. The Langmuir−Blodgett films of optically pure **23** could also be prepared, where helicenes, perpendicular to the substrate, aggregated into parallel columns and the lamellae afterwards [23]. Such columnar aggregates displayed a susceptibility value of 50 pm/V and a second-order nonlinear optical response ca. 30 times larger than that of the assemblies formed by racemates [24]. In addition, Katz and
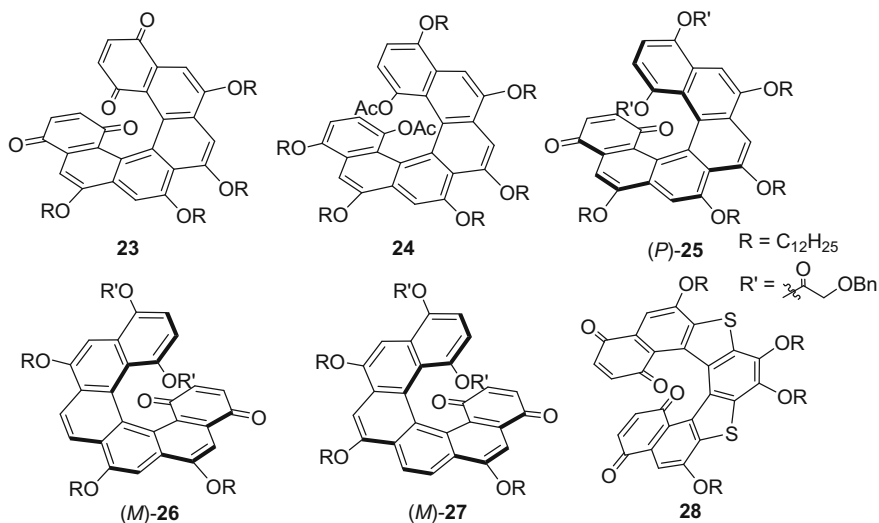
Fig. 13.15 Structures of helicenes for assemblies

Fig. 13.16 Schematic representation of fibers formed by self-assembly of optically pure **23**. Reprinted with the permission from Ref. [22]. Copyright 1998 American Chemical Society
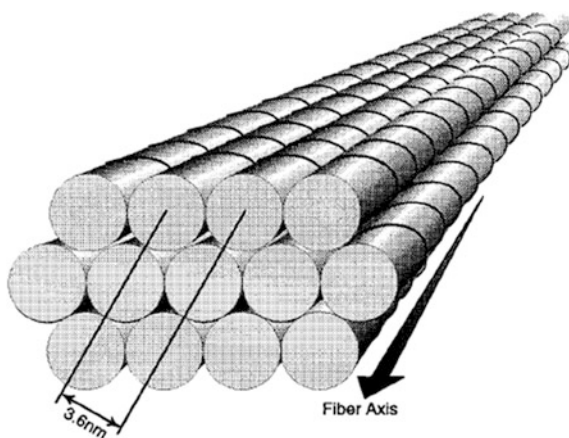
Nuckolls disclosed that helicene (*P*)-**25** showed concentration-dependent aggregation behaviors [25]. Nematic liquid crystalline phase was observed when the concentration of dodecan was higher than 30 vol.%, whereas a hexagonal columnar phase was exhibited when the concentration was less than 5 vol.%. The effect of side chains on C(6), C(8), C(9), and C(11), was investigated as well. It was found that three unsymmetrically functionalized side chains, such as **26** and **27**, were required for the formation of liquid crystalline mesophases [26].
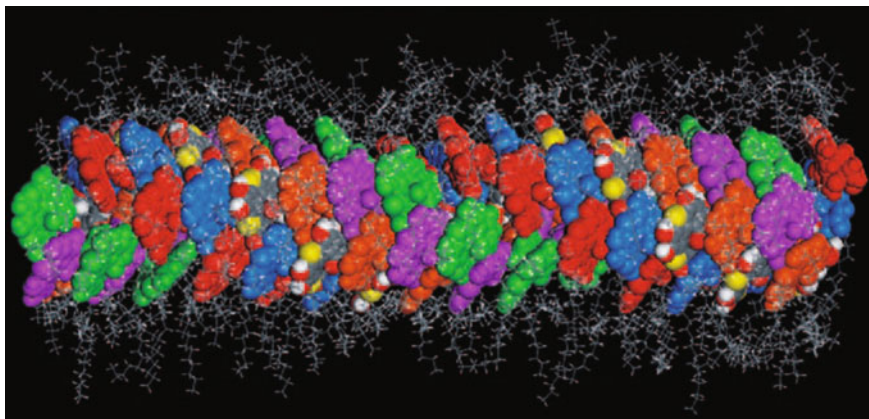
Fig. 13.17 Schematic representation of 13_2 six-stranded helical column of (*M*)-**28**. Reprinted with the permission from Ref. [27]. Copyright 2009 John Wiley and Sons

Ungar and co-workers described a novel structure, hollow 13_2 six-strand helical columns with a six-molecule repeated units and 11.2 nm period, which was assembled by **28** [27]. Enantiopure (*M*)-**28** formed a true hexagonal assembly of right-handed helices (Fig. 13.17), while (*rac*)-**28** would undergo spontaneously optical resolution and form segregated right- and left-handed helices by (*M*)-**28** and (*P*)-**28**, respectively.

Yamaguchi and colleagues investigated effect of different linkers for the self-assembly of [4]helicene oligomers [28, 29]. As depicted in Fig. 13.18, if the linker was flexible, intramolecular interaction was dominated (*a*), where two macrocycles, shown as blue squares, of bis[(3*P*)-cycle] connected by an alkyl chain interacted with each other to give a double layered structure via π-π interaction. If linkers were rigid, the intermolecular aggregation was dominated. For example, when two macrocycles were attached with *cis*-azo groups, 1D polymer chains via π-π interactions were observed (*b*), in which each macrocycle interacted with another molecules; while azo groups were in *trans*-conformation, intermolecular dimers, depicted as (*c*), were preferentially obtained that the cooperation made the system thermodynamically stable. Similarly, when the molecules contain other rigid (*d*, like buta-1,3-diyne-connected bis[(3*P*)-cycle]) and planar (*e*, like 1,3,5-tri-ethynylbenzene-connected tris[(3*P*)-cycle]) linkers, intermolecular dimeric assemblies were formed with the enhanced binding constant with help of cooperation.

Recently, a dynamic and reversible polymorphism was described by Yamaguchi and colleagues [30]. The macrocycle (4 *M*, 4 *M*)-**29** (Fig. 13.19) was found to be random coil in toluene and homo-double-helix in trifluoromethyl benzene. When (5*P*)-**22** was added to the macrocycles in a ratio of 2:1, the trimer complex was
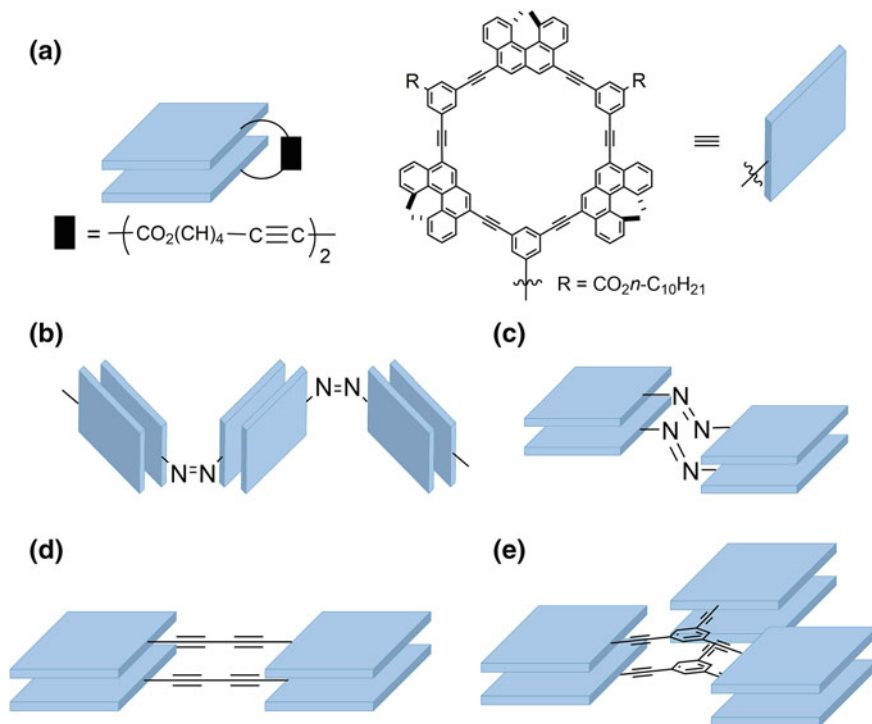
Fig. 13.18 Different types of self-assemblies from cyclic helicene oligomers connected by **a** flexible alkyl; **b** *cis*-azo; **c** *trans*-azo; **d** buta-1,3-diyne; **e** 1,3,5-triethylnylbenzene linkers. Reprinted with the permission from Ref. [29]. Copyright 2003 American Chemical Society

formed via the interaction between the hetero-ethynylhelicene units, which was indicated by Job plot. As the increase of the concentration, lyotropic liquid crystalline (LLC) with a polydomain texture typical of nematic phase was formed. According to AFM studies, the diameter (7–8 nm) of aligned fibers was larger than that of trimolecular complex (4.8 nm). When the nematic LLC phase was cooled to −60 °C, the birefringence disappeared, and turbid gels was observed. This transition was reversibly achieved by changing the temperature.

Besides the above examples, hydrogen bonds were also utilized for the construction of ordered supramolecular structures. Two pyridin-2(1*H*)-one units were fused to the skeleton of helicenes **30** by Branda group [31]. Both in solution and crystals, chiral discrimination was observed that only homochiral dimers were formed via the hydrogen bonds (Fig. 13.20). The driving force for self-assembly behavior was the cooperativity. Moreover, Takeuchi and colleagues reported the hierarchical assembly of phthalhydrazide-functionalized helicene **31** (Fig. 13.21) [32]. Helicenes first self-assembled into trimer disks by hydrogen bonds. Then, in
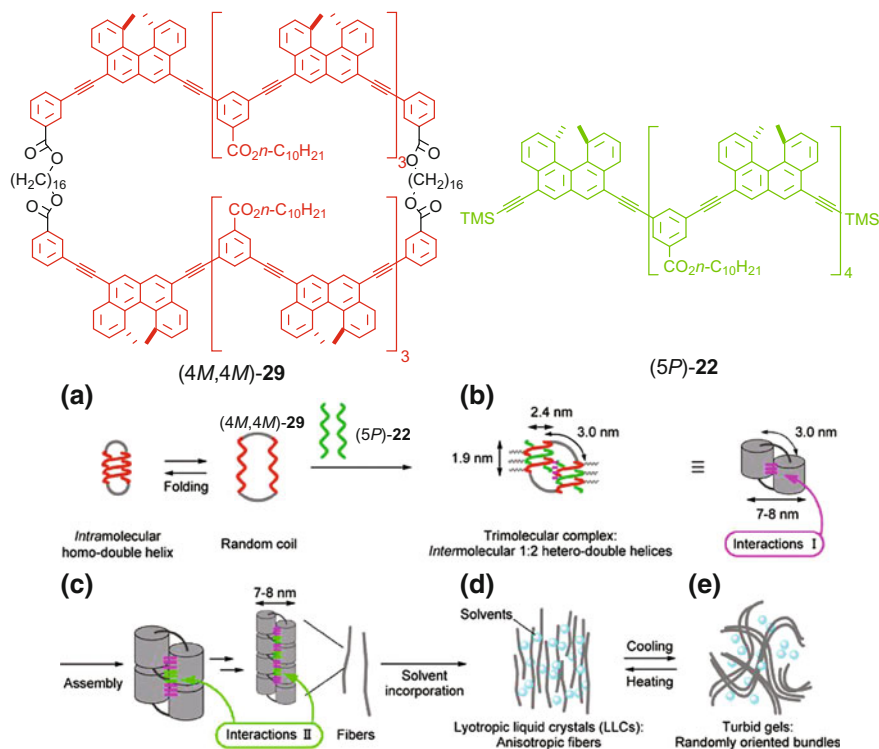
Fig. 13.19 Dynamic and reversible polymorphism of self-assembled lyotropic liquid crystalline systems. **a** Reversible transformation between random coil and homo-double-helix; **b** formation of trimolecular complex; **c** formation of fibers; and the reversible transformation between LLCs (**d**) and turbid gels (**e**). Interactions I showed the interaction between (4 *M*,4 *M*)-**29** and (5*P*)-**22**; Interactions II represented the interaction between the trimolecular complexes. Reprinted with the permission from Ref. [30]. Copyright 2015 American Chemical Society
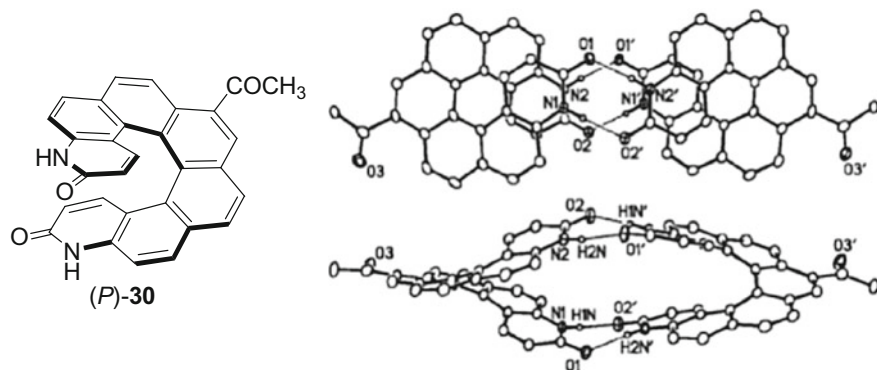
Fig. 13.20 Structure of (*P*)-**30** and its crystal packing (*top-view* and *side-view*). Reprinted with the permission from Ref. [31]. Copyright 2000 American Chemical Society
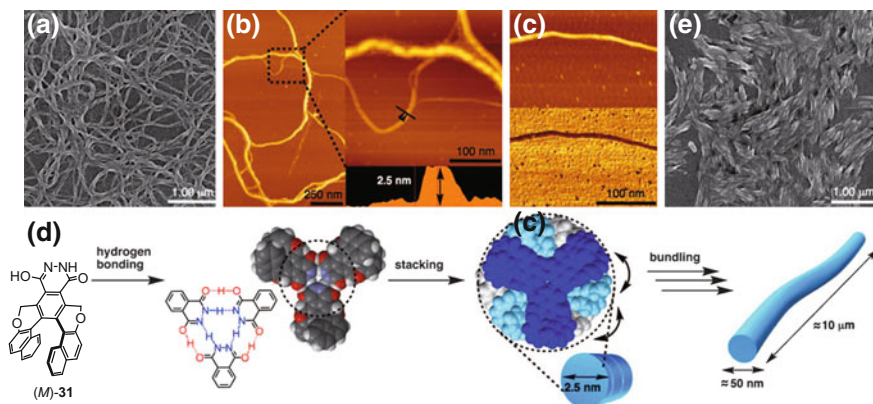
Fig. 13.21 a SEM image of (*M*)-**31** (0.5 mM) prepared in toluene; (**b, c**) AFM images of (*M*)-**31** prepared in toluene; **d** plausible mechanism for the formation of fibers; and **e** SEM image of (*rac*)-**31** (0.5 mM) prepared in toluene. Reprinted with the permission from Ref. [32]. Copyright 2011 John Wiley and Sons

nonpolar solvents, the disks would aggregate to form screw-shaped fibrous assemblies, which exhibited excellent CPL properties with the dissymmetric factor (g_{lum}) of 0.035.

References

1. Ernst KH, Bohringer M, McFadden CF, Hug P, Muller U, Ellerbeck U (1999) Nanostructured chiral surfaces. Nanotechnology 10(3):355–361
2. Ernst KH, Neuber M, Grunze M, Ellerbeck U (2001) NEXAFS study on the orientation of chiral P-heptahelicene on Ni(100). J Am Chem Soc 123(3):493–495
3. Taniguchi M, Nakagawa H, Yamagishi A, Yamada K (2000) Molecular chirality on a solid surface: thiaheterohelicene monolayer on gold imaged by STM. Surf Sci 454:1005–1009
4. Taniguchi M, Nakagawa H, Yamagishi A, Yamada K (2003) STM observation of molecular chirality and alignment on solid surface. J Mol Catal Chem 199(1–2):65–71
5. Fasel R, Parschau M, Ernst KH (2003) Chirality transfer from single molecules into self-assembled monolayers. Angew Chem Int Ed 42(42):5178–5181
6. Fasel R, Parschau M, Ernst KH (2006) Amplification of chirality in two-dimensional enantiomorphous lattices. Nature 439(7075):449–452
7. Hauke CM, Rahe P, Nimmrich M, Schütte J, Kittelmann M, Stará IG, Starý I, Rybáček J, Kühnle A (2012) Molecular self-assembly of enantiopure heptahelicene-2-carboxylic acid on calcite (10$\bar{1}$4). J Phys Chem C 116(7):4637–4641
8. Barth C, Gingras M, Foster AS, Gulans A, Félix G, Hynninen T, Peresutti R, Henry CR (2012) Two-dimensional nanostructured growth of nanoclusters and molecules on insulating surfaces. Adv Mater 24(24):3228–3232
9. Hoff B, Gingras M, Peresutti R, Henry CR, Foster AS, Barth C (2014) Mechanisms of the adsorption and self-assembly of molecules with polarized functional groups on insulating surfaces. J Phys Chem C 118(26):14569–14578

10. Balandina T, van der Meijden MW, Ivasenko O, Cornil D, Cornil J, Lazzaroni R, Kellogg RM, De Feyter S (2013) Self-assembly of an asymmetrically functionalized [6] helicene at liquid/solid interfaces. Chem Commun (Camb) 49(22):2207–2209

11. Seibel J, Allemann O, Siegel JS, Ernst K-H (2013) Chiral conflict among different helicenes suppresses formation of one enantiomorph in 2D crystallization. J Am Chem Soc 135 (20):7434–7437

12. Parschau M, Ernst K-H (2015) Disappearing enantiomorphs: single handedness in racemate crystals. Angew Chem Int Ed 54(48):14422–14426

13. Shchyrba A, Nguyen M-T, Wäckerlin C, Martens S, Nowakowska S, Ivas T, Roose J, Nijs T, Boz S, Schär M, Stöhr M, Pignedoli CA, Thilgen C, Diederich F, Passerone D, Jung TA (2013) Chirality transfer in 1D self-assemblies: influence of H-bonding vs metal coordination between dicyano[7]helicene enantiomers. J Am Chem Soc 135(41):15270–15273

14. Chaunchaiyakul S, Krukowski P, Tsuzuki T, Minagawa Y, Akai-Kasaya M, Saito A, Osuga H, Kuwahara Y (2015) Self-assembly formation of M-type enantiomer of 2,13-Bis (hydroxymethyl)[7]-thiaheterohelicene molecules on Au(111) surface investigated by STM/CITS. J Phys Chem C 119(37):21434–21442

15. Amemiya R, Mizutani M, Yamaguchi M (2010) Two-component gel formation by pseudoenantiomeric ethynylhelicene oligomers. Angew Chem Int Ed 49(11):1995–1999

16. Yamamoto K, Oyamada N, Mizutani M, An Z, Saito N, Yamaguchi M, Kasuya M, Kurihara K (2012) Two types of two-component gels formed from pseudoenantiomeric ethynylhelicene oligomers. Langmuir 28(32):11939–11947

17. Shigeno M, Yamaguchi M (2012) Formation of organic gel-liquid two-layer systems using diffusion-controlled gelation with a helicene derivative. Chem Commun (Camb) 48 (49):6139–6141

18. Ichinose W, Ito J, Yamaguchi M (2013) Tetrameric ααββ aggregate formation by stereoisomeric bidomain helicene oligomers. Angew Chem Int Ed 52(20):5290–5294

19. Ichinose W, Miyagawa M, Yamaguchi M (2013) Reversible shrinkage of self-assembled two-component organogels by lithium salts: synthesis of gelation property and lithium salt response using bidomain helicene oligomer. Chem Mater 25(20):4036–4043

20. Miyagawa M, Yamaguchi M (2015) Helicene-grafted silica nanoparticles capture hetero-double-helix intermediates during self-assembly gelation. Chem Eur J 21 (23):8408–8415

21. Nuckolls C, Katz TJ, Castellanos L (1996) Aggregation of conjugated helical molecules. J Am Chem Soc 118(15):3767–3768

22. Lovinger AJ, Nuckolls C, Katz TJ (1998) Structure and morphology of helicene fibers. J Am Chem Soc 120(2):264–268

23. Nuckolls C, Katz TJ, Verbiest T, Van Elshocht S, Kuball HG, Kiesewalter S, Lovinger AJ, Persoons A (1998) Circular dichroism and UV-visible absorption spectra of the Langmuir-Blodgett films of an aggregating helicene. J Am Chem Soc 120(34):8656–8660

24. Verbiest T, Van Elshocht S, Kauranen M, Hellemans L, Snauwaert J, Nuckolls C, Katz TJ, Persoons A (1998) Strong enhancement of nonlinear optical properties through supramolecular chirality. Science 282(5390):913–915

25. Nuckolls C, Katz TJ (1998) Synthesis, structure, and properties of a helical columnar liquid crystal. J Am Chem Soc 120(37):9541–9544

26. Vyklicky L, Eichhorn SH, Katz TJ (2003) Helical discotic liquid crystals. Chem Mater 15(19):3594–3601

27. Shcherbina MA, Zeng XB, Tadjiev T, Ungar G, Eichhorn SH, Phillips KES, Katz TJ (2009) Hollow six-stranded helical columns of a helicene. Angew Chem Int Ed 48(42):7837–7840

28. Saiki Y, Nakamura K, Nigorikawa Y, Yamaguchi M (2003) [3+3]Cycloalkyne oligomers: linking groups control intra- and intermolecular aggregation by π–π interactions. Angew Chem Int Ed 42(42):5190–5192

29. Saiki Y, Sugiura H, Nakamura K, Yamaguchi M, Hoshi T, Anzai J (2003) [3+3]Cycloalkyne dimers linked by an azo group: a stable cis-azo compound forms polymeric aggregates by nonplanar pi-pi interactions. J Am Chem Soc 125(31):9268–9269

30. Saito N, Kanie K, Matsubara M, Muramatsu A, Yamaguchi M (2015) Dynamic and reversible polymorphism of self-assembled lyotropic liquid crystalline systems derived from cyclic bis (ethynylhelicene) oligomers. J Am Chem Soc 137(20):6594–6601
31. Murguly E, McDonald R, Branda NR (2000) Chiral discrimination in hydrogen-bonded [7] helicenes. Org Lett 2(20):3169–3172
32. Takahiro K, Seiichi F, Zhang X, Ken T, Masayuki T (2011) Hierarchical assembly of a phthalhydrazide-functionalized helicene. Angew Chem Int Ed 50(16):3684–3687

Appendix
Important Helicene Compounds

[5]Helicenes
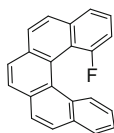
JOC, **1983**, 521
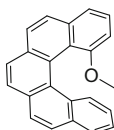
OL, **2013**, 1806
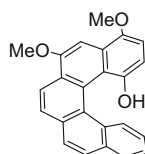
JOC, **2000**, 806
(optical resolution)
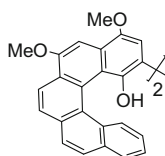
JOC, **2000**, 815
(Asymmetric Catalysis)
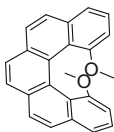
JOC, **1991**, 3769
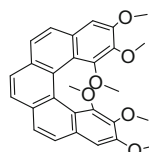
TL, **2002**, 3189 & 7345
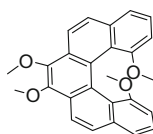
ACIE, **2006**, 2242
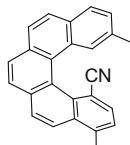
EJOC, *1999*, 1709
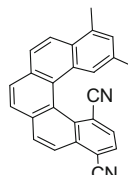
EJOC, **1999**, 1709
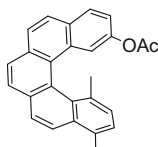
TL, **2003**, 2167
(enantioselective synthesis)
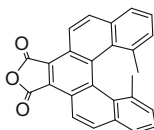
BMC, **2013**, 6063
(selective binding with DNA)
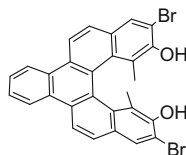
ACIE, **2014**, 4648
(optical resolution)

ACIE: Angew Chem Int Ed
AFM: Adv Fun Mater
BMC: Bioorg Med Chem
EJOC: Eur J Org Chem
JCS PT1: J Chem Soc Perkin Trans 1

JOC: J Org Chem
JPP: J Phorphyr Phthalocya
OL: Org Lett
SM: Syn Metals
TL: Tetrahedron Lett
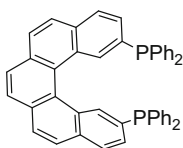
Synthsis, **1997**, 79
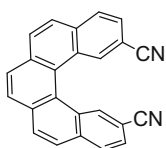
EJOC, **1999**, 1709
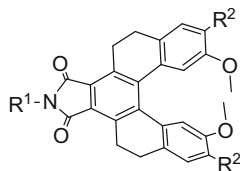
AFM, **2014**, 4405
(cell imaging)
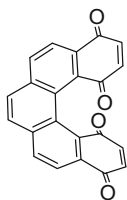
TL, **1990**, 3983
JOC, **1999**,1387
(enantioselective synthesis)
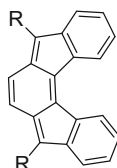
OL, **2013**, 1362
(electron accepting)
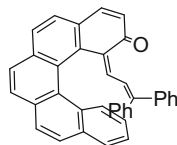
JACS, **2013**, 6872
(photochromism & logic gate)
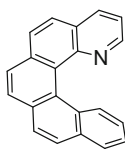
ACIE, **2008**, 9708
(Asymmetric Addition)
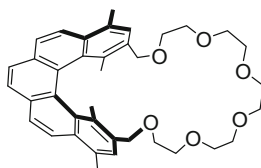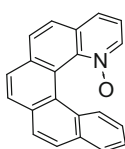
JCS PT1, **1990**, 271
(chiral recognition)
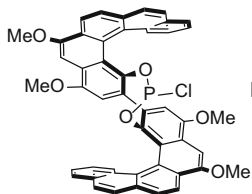
JACS, **2000**, 10027
JOC, **2005**, 8497
(chiral recognition)
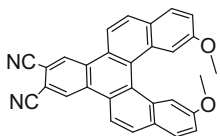
JOC, **2003**, 652
(Dye)
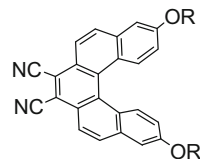
SM, **2010**, 1148
(OLED)
JPP, **2002**, 66
(Dye)

[6]Helicenes
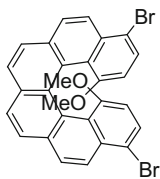
JOC, **1991**, 3769
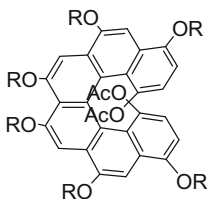
JACS, **1999**, 79
(optical resolution)
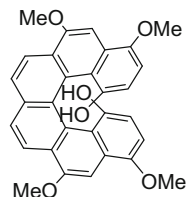
JOC, **2000**, 1850 & 8539
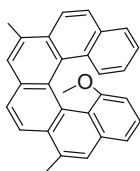
JOC, **2009**, 3090
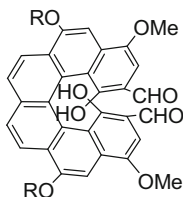
*ACIEE, **1996**, 2109*
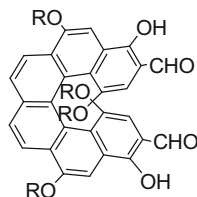
*JOC, **1997**, 1274*
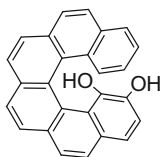
JACS, **2014**, 13045
(Chiroptical switch)
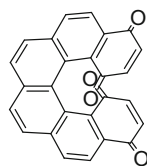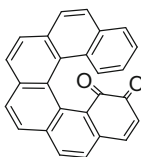
ACIEE, **1992**, 1093
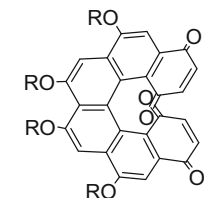
Science, **1998**, 913
(nonlinear optical properties)
JACS, **1998**, 8656
(LB film)
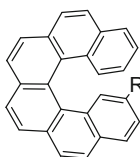
R = F, Cl, Br, Me
JACS, **1973**, 527
R = OH
EJOC, **2007**, 4244 & **2011**, 853
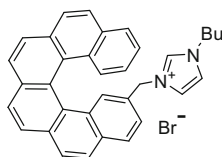
CEJ, **2015**, 2343
(semiconductor)

ACIEE: Angew Chem Int Ed Engl   *CEJ: Chem Eur J*
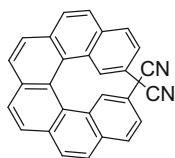
JACS, **2000**, 1717
EJOC, **2007**, 4244
(crystal Structure)
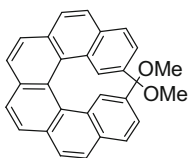
EJOC, **2003**, 2863
(optical resolution & crystal structure)
JCS CC, **1983**, 787
JCS PT1, **1990**, 271
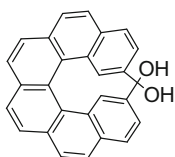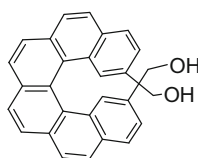
TL, **1981**, 4867
T, **2001**, 2515
(enantioselective sensor)
EJOC, **2007**, 4244
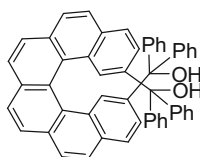
EJOC, **2003**, 2863
(crystal structure)
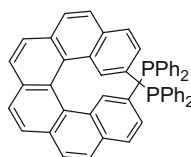
TL, **1997**, 3211
(crystal structure & Rh-
catalyzed asymmetric
hydrogenation)
Synthesis, **1997**, 79
JOmC, **2000**, 105
(Pd-mediated allylic
substitution & crystal structure)
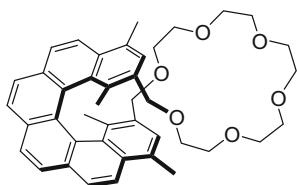
JCS PT1, **1990**, 271
(chiral recognition)
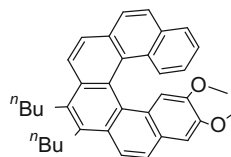
JACS, **2002**, 9175

JCS CC: J Chem Soc Chem Commun
JOmC: J Organomet Chem
T: Tetrahedron
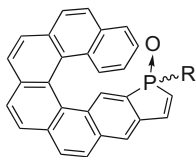
ACIE, **2012**, 695 & **2014**, 861
& **2015**, 5470
(crytal structures &
asymmetric catalysis,
complexes)
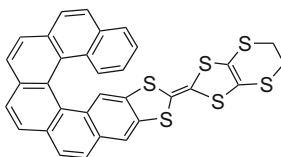
CEJ, **2013**, 13160
(chiroptical switch)
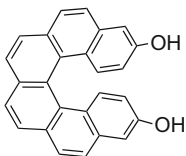
CR Chimie, **2009**, 284
(optical resolutioni)
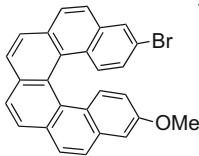
TL, **2007**, 2017
(crystal structure)
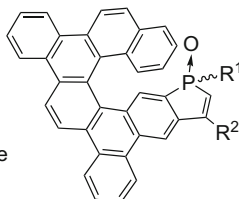
CEJ, **2015**, 11989
(stereoselective synthesis)
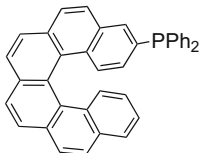
TL, **2009**, 4321
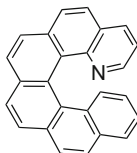
ACIE, **2008**, 3188
(crystal structure)
Nat. Photonics, **2013**, 634
(semiconductor)
OL, **2013**, 1706
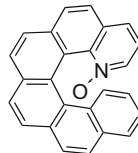
ACIE, **2008**, 9708
(crystal structure &
asymmetric catalysis)
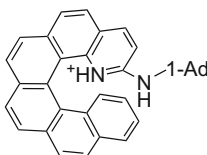
JACS, **2010**, 4536
(crystal structure &
asymmetric catalysis)
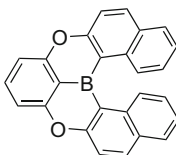
ACIE, **2015**, 13581
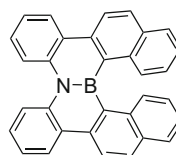
JACS, **2012**, 19600
(semiconductor)

[7]Helicenes
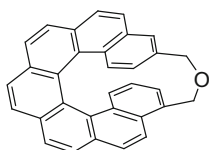
HCA, **1997**, 537
(crystal structure)
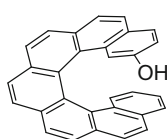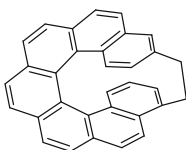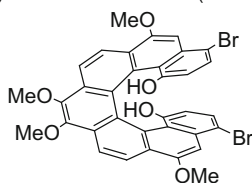
EJOC, **2004**, 1517
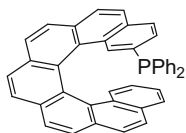
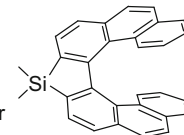*JOmC*, **2007**, 1156
(optical resolution)
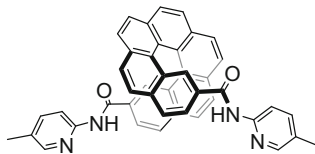
HCA, **1993**, 2757
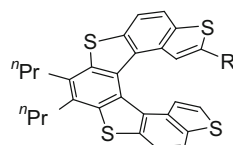(chiral recognition)
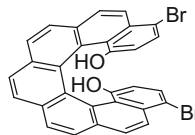
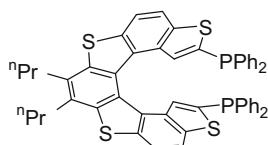
JOC, **1991**, 3769

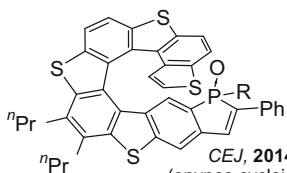*JOC*, **2000**, 1850 & 7602
& 2003, 8539

OL, **2013**, 2104

CPC, **2015**, 490
(Cell delivery)

JOC, **2015**, 3921
(allene hydroarylation)

CEJ, **2014**, 12373
(enynes cycloisomerization)

CPC: ChemPlusChem
HCA: Helv Chim Acta